Universitat Autònoma de Barcelona

Etiopathogenic relevance of CD8+ T cells in Parkinson's disease

Jordi Galiano Landeira

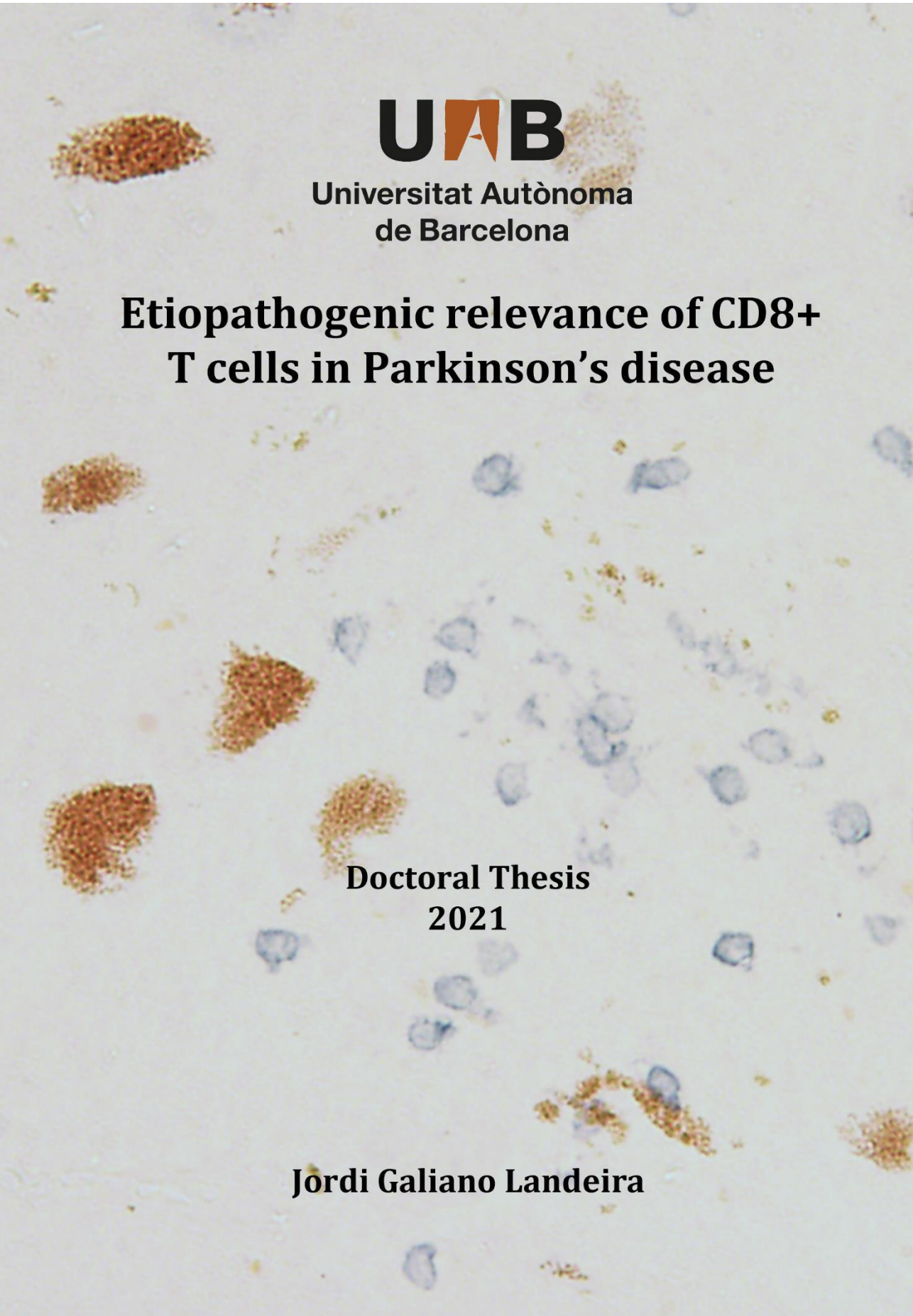

Universitat Autònoma de Barcelona

Etiopathogenic relevance of CD8+ T cells in Parkinson's disease

Doctoral Thesis
2021

Jordi Galiano Landeira

Universitat Autònoma de Barcelona

Etiopathogenic relevance of CD8+ T cells in Parkinson's disease

TESI DOCTORAL

2021

Programa de Doctorat en Neurociències

Institut de Neurociències

Tesi realitzada al laboratori de Malalties Neurodegeneratives de l'Institut de Recerca de la Vall d'Hebron (VHIR) a Barcelona amb el suport de la beca predoctoral en Neurociències de la Fundación Tatiana Pérez de Guzmán el Bueno

Doctorand

Jordi Galiano Landeira

Director

Dr. Jordi Bové Badell

Tutor

Dr. José Rodríguez Álvarez

El conocimiento es solo una de las representaciones de la existencia
-José Vasconcelos-

Natura semina scientiæ nobis dedit, scientiam non dedit
(Nature has given us the seeds of knowledge, not knowledge itself)
-Seneca-

Good life is like a solved knot: you cannot unravel it until you know how it was tangled.
-Adapted from Aristotle-

AGRAÏMENTS

Agraïments

En primer lloc voldria agrair al meu director de tesi Jordi Bové. Evidentment, has estat una peça fonamental per aquesta tesi sent director i *coach* al mateix temps. Com tota relació director-estudiant, hem tingut les nostres desavinences ja que ha estat un estira-arronsa fins al final. Junts hem pogut tirar endavant el projecte i publicar un *Brain* del qual estem els dos molt orgullosos (que sí home, que sí). Tota la tesi ha estat extremadament intensa, fins a un punt on jo vaig haver de baixar el ritme. En tot moment ho vas entendre i em vas ajudar, no només científicament però també personalment. Ets un incomprès, això ja ho saps. El nou Da Vinci de la ciència diuen (tan debò puguis seguir amb el teu projecte-hobby en un futur no molt llunyà). Sé que els dos ens hem sincerat l'un amb l'altre i hem compartit pensaments i discussions com amics. I això és el que m'emporto: un bon amic.

Esta tesis no habría sido posible sin la Fundación Tatiana Pérez de Guzmán el Bueno que confiaron en mí y creyeron en este proyecto cuando ninguna otra beca lo hizo. Más allá de la parte institucional, que ha sido muy placentera por todas las facilidades que otorgáis, ha sido un placer poder participar en todas las jornadas de investigadores. La labor que hacéis dando soporte a la comunidad científica y artística de este país es impresionante y hasta indispensable en los tiempos que corren. Solo deciros que os estoy inmensamente agradecido.

També voldria donar les gràcies a la meva família, especialment als meus pares Margarita i Rafel, i a les meves tietes Pilar i Sandra, qui han estat un recolzament constant per a la meva educació des del minut zero passant pel grau i màster i acabant, per ara, amb el doctorat. Sé que sempre sereu allà per tot allò que

necessiti i això és una de les comoditats més dolces que una persona pot tenir. Moltíssimes gràcies ja que, evidentment, no es podria entendre qui i com sóc sense vosaltres.

Durant tots aquests anys (no només de la tesi) he tingut l'oportunitat de conèixer a moltes persones, i algunes d'elles s'han quedat a la meva vida per compartir un camí amb mi. Moltes gràcies Martí per compartir pam-a-pam aquest camí científic. Des que ens vam conèixer en el grau que la meva vida va fer una inflexió. Vaig poder emmirallar les aspiracions i les ganes de conèixer en la teva persona i això m'ha ajudat moltíssim a arribar a on sóc ara. Vam tenir la sort de viure junts durant un any MOLT intens, però que vam gaudir moltíssim. T'he trobat a faltar aquests anys que has estat a Londres fent la tesi. Però hem pogut fer algun que altre viatge (Finlàndia, Madrid, Londres) que ens ha permès gaudir d'aquest moment de la vida en part junts. Moltíssimes gràcies per tots aquests bonics records. Tu Sergi vas bastant tard començant la tesi a destemps, però què hi farem, sempre has volgut donar bastant la "nota". Ens coneixem des de fa 25 anys i encara ens queden bastants. Moltes gràcies pel suport en els moments més difícils i per discutir amb mi tots els pensaments i idees de llibres. Encara et queda bastant de camí per acabar la tesi, serà dur, molt dur, però gaudeix-lo el màxim que puguis (i jo estaré aquí per burxar-te i recolzar-te). Moltes gràcies a la colla de Palafrugell Joan, Albert, Emma, Martí, Marina, Edu i en especial a en Gerard Ros qui és una gran persona i un amic incondicional. Rammstein va ser el millor concert que he anat mai. Finalment, moltes gràcies a les amistats del grau i en especial a en Gerard Funosas. Hem tingut els nostres pics de veure'ns però crec que hem aconseguit un bon ritme ara. Aventures, excursions, treballs, cerveses i discussions són unes de les moltes coses que hem compartit durant aquests anys. Crec que has pres moltes decisions molt difícils durant aquests anys però el temps ha demostrat que les

vas escollir molt bé. Sempre recordaré el Gallinago que em vas dibuixar al principi del grau. Aquell va ser el principi d'una gran amistat.

Arnau i Samuel, heu estat uns grans companys de pis durant tota la tesi. No hem estat el pis exemplar, no hem fet molta convivència junts però simplement ens ho hem passat bé. Moltes gràcies per totes les intervencions i les reunions de "los Sabios". Jo he estat el primer dels tres en escriure la tesi però a vosaltres us queda ben poc.

També voldria agrair als nostres labo-veïns de mitocondrials per tots els cafès conjunts, cerveses/sopars compartits i per ser un grup d'allò més eixerit.

L'últim paràgraf el volia reservar pel VilaLab. No exagero ni menteixo quan dic que és el millor laboratori que he estat (i que presumiblement estaré). Citant a en Quim Masferrer: "Sou molt bona gent!". Potser no som el grup que publica més, però tan pel rigor científic com pel caire personal, sou espectaculars. Gràcies a vosaltres la tesi ha estat molt més lleugera. Ajuda, mentoria, rialles, experiències i amistats són unes poques paraules que resumeixen el meu camí pel laboratori. Evidentment vull començar agraint a en Miquel Vila per permetre'm fer la tesi en el seu laboratori i entrar a formar part d'aquest grup. A més, ha estat un plaer compartir discussions al despatx durant les hores de microscopi. Moltíssimes gràcies a "la Jefa" Ariadna per tota la feina que fas i per ser una grandíssima científica. T'estaré eternament agraït pel teu suport durant la tesi i, sobretot, en el viatge a Chicago. Més enllà de passar-nos-ho molt bé conjuntament, vaig poder anar al millor congrés que he anat gràcies a tu. A l'*Autophagy Team*, Jordi Riera i Marta Martínez per compartir taula, despatx i laboratori amb mi. Especialment voldria mencionar a la Marta Montpeyó per totes les discussions *freaks* i pel llibre preciós d'*Odonata*, a l'Alba Navarro per compartir el millor *workshop* de la història i discussions de llibres i feminisme y a la Irene por hacernos vivir muy intensamente la vida des del momento en

que entraste, confiando plenamente en mí. Mucha suerte en tu tesis y sabes que siempre puedes contar con mi hacha. Moltes gràcies a en Jordi Romero per l'ajuda al microscopi i insistir en el punt d'inflexió perfecte a fer cerveses. A l'Helena pel viatge a Viena i ajudar-me amb problemes bioinformàtics. A la Iria por tu *fact checking* y esos Margaritas que compartimos. A la Camille per compartir amb mi aficions tant de lectura com *freaks*. A la Júlia que tot i que ja no hi ets al lab, de la intensitat com vius la vida, has deixat petjada. A l'Annabelle por ser la mejor *lab manager* que un laboratorio puede pedir. Contigo he pasado algunos de los momentos más graciosos en el laboratorio. A la Marina per ser una gironina-canadenca de valors. Encara espero que ens convidis a Camprodon… A l'Alba Nicolau alias "la lesionada" per portar "vidilla" al laboratori i ser única en fer que preguntes incòmodes siguin fàcils de respondre. A la Thaïs per ser el sinònim de *poiata machine*. Sigui quina sigui la tècnica, tu la coneixes i l'has optimitzat. Ets el pivot que tot equip necessita. A vegades fas feina bruta, però absolutament essencial. Gràcies per venir amb nosaltres, ets un gran fitxatge per qualsevol grup d'amics i laboratori. A la Marta González por confiar en mi cuando más lo necesitaba y dándome horas de docencia (mi pasión), haciéndome partícipe de tu proyecto y leyendo todas mis historias e hilos. Llegaste de las últimas, però te hiciste un pilar en el laboratorio. Voldria agrair sincerament a en Joan pel millor *workshop* de la història, per unes grans discussions microglials, pel viatge a Viena, per ser dels millors "barbacoa lad" que he vist mai i pels valors que tens que et defineixen com una bellíssima persona. Ets el messies científic. Voldria esmentar a tots els estudiants que han passat pel laboratori i, especialment, aquells que he fet de mentor: Alexandra, Xavier i Marc. Em vau fer créixer com a científic permetent-me ensenyar-vos el poc que sé. A l'Albert per incomptables fites conjuntament. Vam començar compartint un supervisor però vam acabar anant de cerveses artesanes, viatjant junts (Viena i Firenze) i fent-nos grans amics. Has estat un company

doctoral impressionant i m'has mostrat i ensenyat que la vida a vegades no és fàcil però si és difícil és perquè ens la fem nosaltres. En Kulchitsky encara ens espera per respondre-li el 15% jeje. Finalment, voldria agrair amb totes les meves forces a la Núria amb qui he compartit hores de microdissecció, viatges, congressos, sopars, dinars i *retreats*. Moltíssimes experiències inoblidables. Gran científica i millor persona. Treballadora i intel·ligent, he compartit amb tu les millors discussions de la meva vida. Amb tu he après moltíssim i he millorat com a persona i científic. El teu recolzament durant els moments més durs de la tesi van ser essencials per arribar on sóc ara. Arribaràs on vulguis arribar, la teva projecció i representació de la voluntat són infinites. *In essentia,* YAAMR de l'equilibri de Nash.

TABLE OF CONTENTS

AGRAÏMENTS ..... **iii**

TABLE OF CONTENTS ..... **xiii**

LIST OF TABLES ..... **xix**

LIST OF FIGURES ..... **xxi**

LIST OF ABBREVIATIONS ..... **xxvii**

ABSTRACT **1**

INTRODUCTION **7**

1.1 Parkinson's disease 9

1.1.1 Pathophysiology 10

1.1.1.1 Brain pathology staging 13

1.1.2 Clinical motor symptoms and management 18

1.1.3 Etiology and risk factors 21

1.1.3.1 Environmental factors 22

1.1.3.2 Genetic factors 28

1.1.4 Experimental animal models 30

1.1.4.1 Toxin models 32

1.1.4.1.1 The MPTP animal model 33

1.1.4.2 Genetic models 36

1.1.4.2.1 α-synuclein (*SNCA*) 37

1.2 Immune system 43

1.2.1 Innate immune system 45

1.2.2 Adaptive immune system 49
1.2.2.1 B cells 51
1.2.2.2 T cells 52
1.2.2.2.1 CD4+ helper T lymphocytes 53
1.2.2.2.1.1 Regulatory T lymphocytes 55
1.2.2.2.2 CD8+ cytotoxic T lymphocytes 56
1.2.2.2.2.1 Tissue resident memory CD8+ T cells 57
1.2.2.2.2.2 CD8+ T cell cytotoxic mechanisms 58
1.2.3 Immune system in the central nervous system 60
1.2.3.1 Meninges, cerebro-spinal fluid and glymphatic system 62
1.2.3.2 Innate immune system: Microglia and monocyte-derived macrophages 65
1.2.3.3 Adaptive immune system in the CNS under physiological conditions 72
1.3 Neuroinflammation in Parkinson's disease 75
1.3.1 Human tissue and fluids 76
1.3.1.1 Cerebrospinal fluid and blood 76
1.3.1.1.1 Cerebrospinal fluid 76
1.3.1.1.2 Blood 77
1.3.1.2 Human post-mortem tissue 81
1.3.2 Experimental animal models 86
1.3.2.1 MPTP 87
1.3.2.2 Overexpression of α-synuclein 89

HYPOTHESES AND AIMS **97**

MATERIALS AND METHODS **103**

3.1 Animals 105

3.2 MPTP intoxication 105

3.3 FoxP3.LuciDTR transgenic mice and Treg depletion 106

3.3.1 Flow cytometry 107

3.3.2 Bioluminescence imaging 108

3.4 Adeno-associated viral vectors 108

3.5 Surgical procedures for stereotaxic delivery of adeno-associated viral vectors 109

3.6 Euthanasia and animal brain processing for histological analyses 109

3.7 Human post-mortem brain tissue 110

3.8 Immunohistochemistry/immunofluorescence 111

3.9 Antibodies 112

3.10 Quantitative analyses 115

3.10.1 Rodent tissue 115

3.10.1.1 Striatal optical densitometry analysis 115

3.10.1.2 Dopaminergic neuron counts 116

3.10.1.3 T cell counts 116

3.10.2 Human tissue 117

3.10.2.1 T cell density 117

3.10.2.2 Dopaminergic neuron density 117

3.10.2.3 MHC class-II+ microglial morphologies 118

3.10.2.4 Phenotypic characterization of CD8+ T cells 118

3.10.2.5 Density of synucleinopathy-related aggregates 119

3.11 Laser capture microdissection 119
3.12 RNA extraction and gene expression analysis by qPCR 120
3.12.1 RNA extraction 120
3.12.2 cDNA synthesis 122
3.12.3 cDNA Preamplification 122
3.12.4 qPCR analyses 122
3.13 Statistical analyses 124
RESULTS 127
4.1 T cell infiltration in Parkinson's disease animal models 129
4.1.1 Not consistent SN*pc* T cell infiltration in acute MPTP treated C57BL/6Ncrl mice 130
4.1.2 T cells transiently infiltrate SN*pc* of subacute MPTP treated C57BL/6Ncrl mice 133
4.1.3 Systemic Treg depletion in C57BL6/Ncrl mice does not exacerbate nigrostriatal degeneration in the subacute MPTP model 137
4.1.4 Overexpression of human wild-type α-synuclein in Sprague-Dawley rats SN*pc* induces behavioural motor changes and striatal tyrosine hydroxylase depletion but no dopaminergic cell loss. Non-conclusive results on T cell infiltration due to distinct status of purification between EV and α-synuclein vector. 141
4.1.5 Overexpression of α-synuclein in Lewis rats SN*pc* induce T cell brain infiltration which is not accompanied with motor impairment and nigrostriatal damage 146
4.2 T cell infiltration in human post-mortem tissue 150
4.2.1 Density of CD8+ T cells but not CD4+ T cells is increased in SNpc of Parkinson's disease cases 151

4.2.2 Infiltrating CD8+ T cells contact with dopaminergic neurons and their densities correlate with dopaminergic neuronal death in Parkinson's disease SN*pc* 153

4.2.3 CD8+ T cell infiltration is an early event of the disease occurring in absence of neuronal death and synucleinopathy in SN*pc* of incidental Lewy body disease cases 155

4.2.4 SN*pc* dopaminergic cell loss appears simultaneously with nigral synucleinopathy 157

4.2.5 Total MHC class-II+ microglial cells are decreased in early stages of the disease and low densities of ameboid microglia correlate with higher neuronal loss 159

4.2.6 A high proportion of SNpc CD8+ T cells express CD103 tissue-resident memory T cell marker 163

4.2.7 SN*pc* CTLs display IFNγ and several granzymes to potentially induce dopaminergic cell death 166

4.2.7.1 Half of CD8+ T cells in human SN*pc* express IFNγ but not TNFα 166

4.2.7.2 Granzymes but no FasL are present in SN*pc*-infiltrating CTLs 168

4.2.8 SN*pc* CTLs express distinct T cell receptors indicating the presence of heterogeneous subpopulations of CD8+ T cells 174

4.2.9 SN*pc* dopaminergic neurons express HLA class-I but not CD1 molecules 176

4.2.10 SN*pc* CTLs increase their densities in parallel with synucleinopathy and dopaminergic cell loss 177

4.2.11 CTLs also infiltrate locus coeruleus in early and late stages of Parkinson's disease 180

DISCUSSION 187

5.1 Parkinson's disease experimental animal models 189

5.2 Parkinson's disease post-mortem human tissue 197

CONCLUSIONS 213

REFERENCES 219

ANNEX I 267

ANNEX II 293

1. Scientific articles belonging to my PhD thesis 295

2. Participation in other published articles 295

3. Participation in congresses as a first and presenting author 296

4. Participation in other studies presented in congresses 297

LIST OF TABLES

Table 1. Gliosis in overexpression of α-synuclein PD animal model.....90

Table 2. List of primary antibodies for human tissue.....112

Table 3. List of primary antibodies for mouse tissue.....113

Table 4. List of primary antibodies for rat tissue.....114

Table 5. List of secondary antibodies.....114

Table 6. List of human Taqman gene expression assays.....123

Table 7. Adaptive immunity in MPTP and OE of α-synuclein models.....190

Annex Table 1. Donor sample information.....269

Annex Table 2. Clinical and autopsy information.....275

LIST OF FIGURES

Figure 1. Neuropathology of Parkinson's disease. 10

Figure 2. Cell loss in Parkinson's disease. 11

Figure 3. Clinical motor and non-motor symptoms associated with Parkinson's disease throughout all stages of the disorder. 12

Figure 4. Braak Lewy Body staging and Unified Systematic Staging of Lewy body disorders. 15

Figure 5. Overview representation of the PD risk factor genes and the molecular pathways in which they participate.....30

Figure 6. Functions and distribution of α-synuclein 38

Figure 7. Antigen recognition by T cells 50

Figure 8. CD4+ Helper T lymphocyte subsets 54

Figure 9. Cytotoxic interaction of a CD8+ T lymphocyte with a target cell 60

Figure 10. Immune trafficking through the central nervous system 64

Figure 11. Microglial morphology in adult human brain 68

Figure 12. Microglial phenotypes.....71

Figure 13. T cell immunity in the central nervous system 72

Figure 14. Evidence for the involvement of the immune system in PD 75

Figure 15. Mechanisms of microglial involvement in dopaminergic neuronal damage and death 84

Figure 16. Immune response to α-synuclein induced neurodegeneration 93

Figure 17. FoxP3.LuciDTR transgenic construct 106

Figure 18. Laser capture microdissected SNpc dopaminergic neurons 120

Figure 19. TH+ axon terminal and dopaminergic cell losses in acute MPTP treated C57BL/6Ncrl mice 131

Figure 20. CD3+ T cell infiltration in the SNpc of MPTP treated C57BL/6Ncrl mice 133

Figure 21. Dopaminergic cell loss and CD3+ T cell brain infiltration in the subacute MPTP treated C57BL/6Ncrl FoxP3.LuciDTR transgenic mice 134

Figure 22. Number of SNpc T lymphocytes correlates with TH+ immunostaining in the striatum at d1 137

Figure 23. Systemic Treg depletion injecting diphtheria toxin in C57BL/6Ncrl FoxP3.LuciDTR transgenic mice 138

Figure 24. Loss of TH+ striatal axon terminal and dopaminergic cell losses in subacute MPTP treated C57BL/6Ncrl FoxP3.LuciDTR transgenic mice after Treg depletion 139

Figure 25. Overexpression of h-WT-α-synuclein in Sprague-Dawley strain rat SNpc induces motor asymmetry and loss of striatal TH+ axon terminals without SNpc dopaminergic cell loss 142

Figure 26. Empty vector and overexpression of h-WT-α-synuclein in Sprague-Dawley strain rat SNpc trigger both CD4+ and CD8+ T cell infiltration.....145

Figure 27. Overexpression of h-WT-α-synuclein in Lewis strain rat SNpc does not induce motor asymmetry, striatal TH loss and SNpc dopaminergic cell death.....147

Figure 28. Overexpression of h-WT-α-synuclein in Lewis strain rat SNpc does increase both CD4+ and CD8+ T cell brain infiltration.....149

Figure 29. CD4+ T cell densities in control and Parkinson's disease SNpc 151

Figure 30. CD8+ T cell densities in control and Parkinson's disease SNpc 152

Figure 31. CD8+ T cells make contact/appositions with dopaminergic neurons and their density correlate with dopaminergic cell loss.....153

Figure 32. CD4+ and CD8+ T cell densities in iLBD cases with or without nigral synucleinopathy.....156

Figure 33. Dopaminergic cell densities in control, iLBD SN syn-/+ and PD cases and its correlation with UPDRS Off motor score.....158

Figure 34. Low magnification analysis of MHC class-II+ staining in SNpc. 159

Figure 35. Density of SNpc MHC class-II+ glia morphologies.....161

Figure 36. Correlation between MHC class-II+ ameboid glia and dopaminergic neuronal density.....162

Figure 37. CD8+ CD103+ T cells in SNpc of control, iLBD and PD cases.....164

Figure 38. CD8+ IFNγ+ T cells in SNpc of control, iLBD and PD cases 167

Figure 39. CD8+ Granzyme B+ T cells in SNpc of control, iLBD and PD cases 169

Figure 40. CD8+ Granzyme A+ T cells in SNpc of control, iLBD and PD cases 171

Figure 41. CD8+ Granzyme K+ T cells in SNpc of control, iLBD and PD cases 172

Figure 42. Expression of TCR genes in fresh frozen post-mortem SNpc of control, iLBD SN syn-/+ and PD cases 175

Figure 43. HLA class-I and CD1 genes expression in SNpc microdissected dopaminergic neurons of four control cases 176

Figure 44. Density of distinct phospho-serine129-α-synuclein aggregates at distinct stages of the unified scale for Lewy body disorders 178

Figure 45. Relationship between CD8+ T cells, dopaminergic neurons and synucleinopathy.....179

Figure 46. Locus coeruleus CD8+ T cell infiltration in control, iLBD LC syn-/+ and PD cases.....181

Figure 47. Norepinephrinergic neuronal loss in LC of control, iLBD LC syn-/+ and PD cases.....182

Figure 48. Correlation between infiltrating CD8+ T cells in both LC and SNpc of control and PD cases.....183

Figure 49. CD8+ T cell SNpc infiltration precedes both synucleinopathy and dopaminergic cell loss and express markers of cytotoxic machinery and tissue resident memory T cells.....208

Figure 50. Foreseeable open questions about adaptive immunity in PD...210

Annex Figure 1. Immunohistochemical images of human positive control tissues to detect T cell markers.....287

Annex Figure 2. Representative immunofluorescence images of perivascular and parenchymal CD8+ CD69+ T cells in the SNpc.....290

LIST OF ABBREVIATIONS

Only those appearing more than once in the text. The rest are indicated in their first appearance in the text.

6-OHDA	6-hydroxydopamine
AAV	adeno-associated virus
APC	antigen presenting cell
BBB	blood-brain barrier
BCR	B-cell receptor
BSA	bovine serum albumin
CC	*corpus callosum*
CCR	C-C chemokine receptor
CD	cluster of differentiation
cDNA	complementary deoxyribonucleic acid
CNS	central nervous system
COMT	cathecol-o-methyltransferase
COPD	chronic obstructive pulmonary disease
CSF	cerebro-spinal fluid
C_t	threshold cycles
CTL	cytotoxic T lymphocyte
CTLA-4	cytotoxic T lymphocyte antigen 4
CXCR/CXCL	C-X-C chemokine receptor/ligand

d	days
DA	dopamine
DAT	dopamine transporter
DLB	dementia with Lewy bodies
DT	diphtheria toxin
EAE	experimental autoimmune encephalomyelitis
EBV	Epstein-Barr virus
ER	endoplasmic reticulum
EV	empty vector
FFPE	formalin-fixed paraffin-embedded
FoxP3	forkhead box P3
GBA	glucocerebrosidase
GFAP	glial fibrillar acidic protein
GFP	green fluorescent protein
GrzA/B/K	granzyme A/B/K
GWAS	genome wide association
HC	healthy control
HLA	human leukocyte antigen
HPRT1	hypoxhanthine phosphoribosyltransferase 1
HSV	herpes simplex virus
HTL	helper T lymphocyte
HY	Hoehn & Yahr

Iba-1	ionized calcium-binding adapter molecule 1
IFNγ	interferon-γ
Ig	immunoglobulin
IL/IL-R	interleukin/interleukin receptor
ILC	innate lymphoid cell
iLBD	incidental Lewy body disease
iNOS	inducible nitric oxide synthase
ip	intraperitoneal
ISF	interstitial fluid
KLRB1	killer cell lectin-like receptor subfamily B 1
LB	Lewy body
LC	locus coeruleus
LN	Lewy neurite
LRRK2	leucine rich repeat kinase 2
MAO	monoamine oxidase
MHC	major histocompatibility complex
MPP+	1-methyl-4-phenylpyridinium ion
MPPP	1-methyl-4-phenyl-4-propionoxy-piperidine
MPTP	1-methyl-4-phenyl-1,2,3,6-tetrahydropyridine
MS	multiple sclerosis
NGAL	neutrophil gelatinase-associated lipocalin
NM	neuromelanin

NK	natural killer
NSAID	nonsteroidal anti-inflammatory drugs
Ob	olfactory bulb
PBS	phosphate buffered saline
PD	Parkinson's disease
PRF-1	perforin-1
PD-1/-L1	programmed cell death protein 1/ligand protein 1
qPCR	quantitative polymerase chain reaction
ROS	reactive oxygen species
rpm	rotations per minute
SN*pc*	substantia nigra *pars compacta*
Str	striatum
TBI	traumatic brain injury
Tc	T cytotoxic
T_{CM}	T central memory
TCR	T-cell receptor
T_{EM}	T effector memory
TGFβ	transforming growth factor-β
TH	tyrosine hydroxylase
Th	T helper
Tr	T regulatory
TRAC	T cell receptor alpha constant

TRBC1	T cell receptor beta constant 1
TRDV3	T cell receptor delta variable 3
T_{RM}	tissue resident memory
TNFα	tumor-necrosis factor-α
UPDRS	unified Parkinson's disease rating score
USSLBD	unified staging system for Lewy body disorders
VMAT2	vesicular monoamine transferase 2

ABSTRACT

Abstract

Mounting evidence has pointed out that the adaptive immune system has an important role in Parkinson's disease (PD) etiopathogenesis. T cell infiltration has been described in both PD experimental animal models and post-mortem human tissue. Some authors have proposed α-synuclein posttranslational modifications as the antigen eliciting this adaptive immune response. Thus, the main goal of this thesis was to determine whether T cells participate in the onset and progression of the disease. Moreover, we wanted to know whether α-synuclein behaved as a neoantigen. In order to overcome this, we analyzed and phenotypically characterized substantia nigra *pars compacta* (SN*pc*) infiltrating T cells in post-mortem human tissue at distinct disease stages. PD and incidental Lewy Body disease (iLBD) cases, which are considered to be an early pre-motor stage of the disorder, were analyzed. We studied the relationship between T cell infiltration with dopaminergic cell loss and synucleinopathy, two hallmarks of the disorder. We found a biphasic SN*pc* CD8+ cytotoxic T lymphocyte (CTL) infiltration. Strikingly, the first and highest peak was found when synucleinopathy and dopaminergic cell loss were not established. SN*pc* CTL infiltration subsided when synucleinopathy and dopaminergic cell loss started. SN*pc* CTL infiltration again increased in PD cases where CD8+ T cell densities correlated with neuronal death. Similar results were also obtained in another PD brain affected area such as locus coeruleus (LC). The fact that SN*pc* CTL*s* made contact with dopaminergic neurons and correlated with dopaminergic cell loss, suggests a likely role in dopaminergic cell death. To delve further into this concept, we found that SN*pc* CTL*s* expressed cytotoxic machinery *i.e.* granzymes and interferon-γ. Infiltrating SN*pc* granzyme+ CTL*s* were found increased in iLBD cases indicating an acute

adaptive immune response in early stages of the disease. A high percentage of SN*pc* CTLs were tissue resident memory T cells identified by CD103 expression. Antigen presentation by means of MHC class-II+ microglia was reduced in early stages of the disease. Low densities of ameboid/activated MHC class-II+ microglial cells correlated with higher dopaminergic cell loss, suggesting a positive role of MHC class-II+ microglia in the disease. To determine the best rodent model to assess the T cell role in PD, we characterized the immune response in MPTP injected mice and rats overexpressing α-synuclein. We found a transient CD4+ and CD8+ T cell infiltration preceding dopaminergic cell death in the subacute MPTP injected mice which correlated with striatal damage. Nonetheless, breaking immune tolerance through systemic Treg depletion did not increase nigrostriatal damage. Finally, we also observed CD4+ and CD8+ T cell SN*pc* infiltration in rats overexpressing α-synuclein. However, these rats did show neither behavioural motor changes nor nigrostriatal damage. To conclude, human PD-specific brain adaptive immune response reported in our study is different to the one observed in PD experimental animal models. In SN*pc* human tissue CD4+ T cells were not elevated, and CTL infiltration preceded synucleinopathy. These results point out the fact that α-synuclein seems not to be the antigen for the cytotoxic attack elicited by CD8+ T cells. Overall, this thesis demonstrated that CTL infiltration is an early event of the disease preceding both α-synuclein deposition and dopaminergic cell loss. Thus, targeting the adaptive immune response in both early and late stages of the disease may have beneficial effects. Nevertheless, there is a need to establish new PD experimental animal models which recapitulate the human adaptive immune response.

INTRODUCTION

1. Introduction

1.1 Parkinson's disease

Parkinson's disease (PD) was initially described as *paralysis agitans* (also known as "shaking palsy") by Dr. James Parkinson (1775-1824) two hundred years ago (Parkinson, 1817). However, some medical texts from before Parkinson's work reported Parkinsonism symptoms like resting tremor (Goetz, 2011). Parkinson described a disease of late but variable onset and a progressive, disabling course. Some of the motor symptoms of the disease were described at that moment such as resting tremor and flexed posture. However, bradykinesia or rigidity were not reported (Obeso *et al.*, 2017). Parkinson considered patients to be weak but this impairment was related with an "interruption of the flow of the nervous influence to the affected parts" making an inference of the importance of the central nervous system in the disease (Obeso *et al.*, 2017). Some years later, Parkinson's work was reviewed by Jean-Martin Charcot, premier 19th-century clinical neurologist, who emphasized the importance and acuteness of the study. Afterwards, Charcot added extensive details to Parkinson's observations identifying bradykinesia and rigidity. These two symptoms were key for disease diagnosis and tremor was shown as just typical. After some studies and work in the disease, Charcot was the first to suggest the use of the term "Parkinson's disease" rejecting *paralysis agitans* or shaking palsy recognizing Parkinson's contribution and extracting some importance of the tremor symptom and lack of muscle weakness in patients (Goetz, 2011; Obeso *et al.*, 2017).

1.1.1 Pathophysiology

PD is considered a chronic neurodegenerative disorder mainly characterized by the loss of dopaminergic neurons located in the substantia nigra *pars compacta* (SN*pc*) (Lewy, 1912; Tretiakoff, 1919; Fearnley and Lees, 1991; Ma *et al.*, 1997; Dauer and Przedborski, 2003; Cheng *et al.*, 2010; Poewe *et al.*, 2017; Giguère *et al.*, 2018), which project their axons to the basal ganglia constituting what is known as nigrostriatal pathway (Goedert, 2001) (**Figure 1A-D and I-J**).

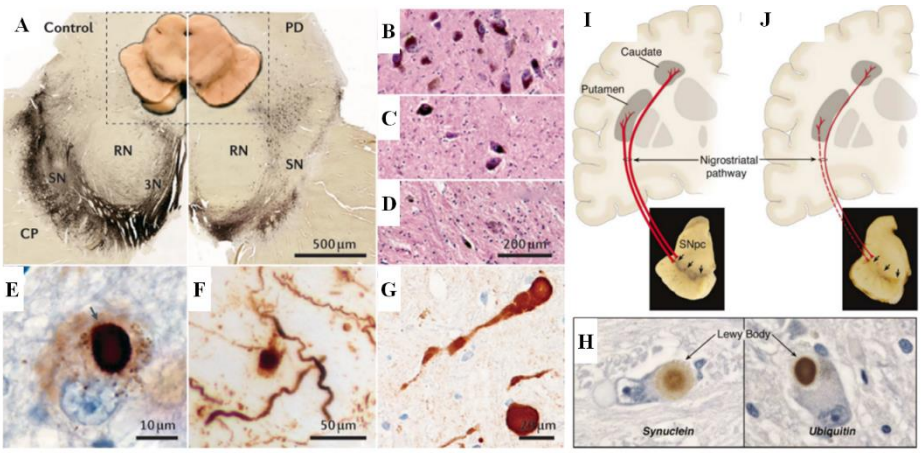

Figure 1. Neuropathology of Parkinson's disease. (**A**) Two macroscopically visions of *post-mortem* midbrains which exhibit loss of SN*pc* dopaminergic neurons upon immunohistochemical staining for tyrosine hydroxylase. (**B-D**) Haematoxylin and eosin staining of the SN*pc* showing a normal distribution of neuromelanin-containing dopaminergic neurons in a healthy control (**B**) and moderate (**C**) or severe neuronal loss (**D**) of PD cases. (**E-H**) Immunohistochemical staining of α-synuclein, with Nissl as counterstaining, which can have several forms as typical intracytoplasmic round Lewy Bodies (**E** & **H** with arrows), more diffuse and punctuate staining (part **E** & part **F**), intracytoplasmic lineal Lewy neurites (**F**) and α-synuclein spheroids in axons (**G**). (**H**) Both α-synuclein and ubiquitin may be found in Lewy Bodies. (**I-J**) Schematic representation of the normal nigrostriatal pathway (**I**) comprised by dopaminergic neurons located in the SN*pc* which project their axons to the caudate-putamen region and a degenerated nigrostriatal pathway due to the loss of these

dopaminergic neurons (**J**). *CP* cerebral peduncle; *RN* red nucleus. Adapted from Dauer and Przedborski, 2003; Poewe *et al.*, 2017.

Dopaminergic neurons contain and accumulate neuromelanin (NM) during the whole human lifespan, which is a dark-brown pigment created due to the oxidative metabolism of dopamine (Carballo-Carbajal *et al.*, 2019). The loss of these dopaminergic neurons explains mainly the motor symptoms like resting tremor, rigidity, bradykinesia and postural instability as the nigrostriatal pathway is involved in motor regulation releasing dopamine (DA) in the caudate-putamen region (Molinoff and Axelrod, 1971; Björklund and Dunnett, 2007). NM pigment can also be detected in other PD affected brain areas such as locus coeruleus (LC). Other brain areas are also vulnerable in PD such as dorsal motor nucleus of vagus (DMV), ventral tegmental area (VTA), retrorubral field (RRF), red nucleus (RN), pedunculopontine nucleus (PPN), nucleus basalis of Meynert (NBM) and olfactory bulb (Ob) (Sulzer and Surmeier, 2013; Butkovich *et al.*, 2018; Giguère *et al.*, 2018; Carballo-Carbajal *et al.*, 2019) (**Figure 2**).

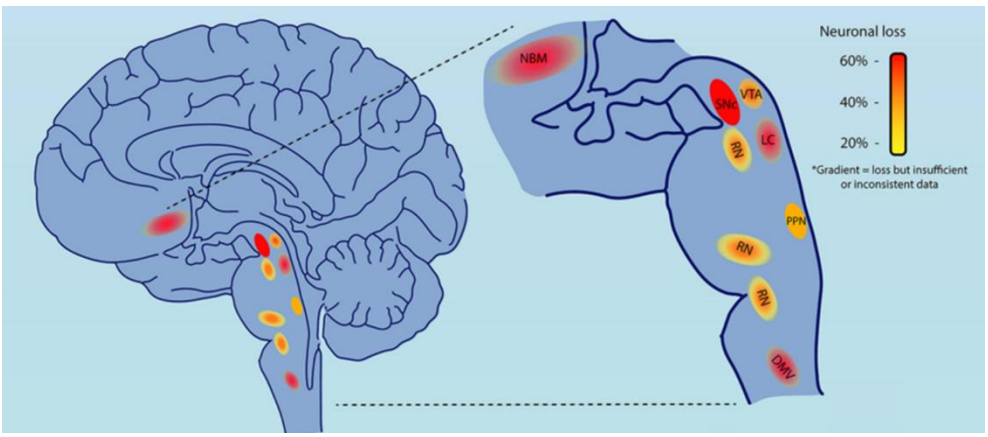

Figure 2. Cell loss in Parkinson's disease. Schematic representation of brain regions which present cell loss in PD. Yellow-red colour code indicates the evidence of cell loss according to the meta-analysis. Colour gradients denote uncertainty in the extent of this cell loss. Adapted from Giguère *et al*., 2018.

Furthermore, PD patients also present a wide variety of non-motor symptoms related with these non-dopaminergic regions, including autonomic dysfunction (e.g. constipation, urogenital dysfunction and orthostatic hypotension), sleep disorders (e.g. insomnia, rapid eye movement sleep behavior disorder and insomnia), neuropsychiatric dysfunction (e.g. cognitive impairment, anhedonia, apathy, anxiety, psychosis, social phobia, depression and dementia) and in some cases sensory symptoms (e.g. hyposmia, abnormal sensations, pain and fatigue) (Kalia and Lang, 2015; Doppler *et al.*, 2017; Obeso *et al.*, 2017). Many of these non-motor symptoms appear in early stages of the disease when patients are not still diagnosed (**Figure 3**). It is important to note that neuronal loss has been detected in several regions of "healthy" (with no brain-related disorders) aged brains (Giguère *et al.*, 2018). This aging-induced neuronal loss is a confounding factor in post-mortem human studies as not always dissecting between aging and pathology specific mechanisms is a feasible task.

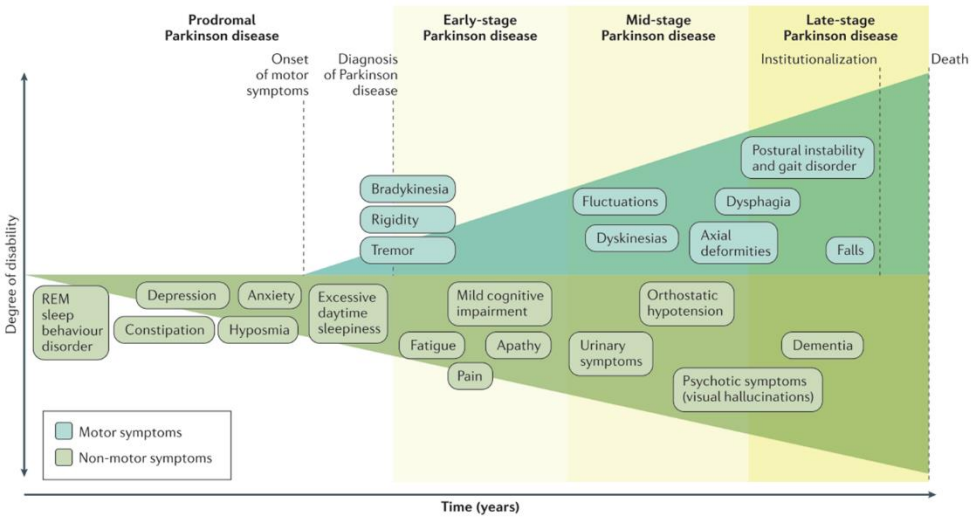

Figure 3. Clinical motor and non-motor symptoms associated with Parkinson's disease throughout all stages of the disorder. Before onset of motor symptoms, which are currently essential for PD diagnosis, there are several non-motor symptoms in what is known the PD prodromal phase. Although these non-motor symptoms become increasingly prevalent over the course of the illness, they can be present to a variable degree according to each individual. Both non-motor and motor symptoms finally induce a progressive disability for the patient. From Poewe *et al.*, 2017.

1.1.1.1 Brain pathology staging

Histologically, one of the hallmarks of the disease is the accumulation and aggregation of eosinophilic inclusions called Lewy bodies (LBs) and Lewy neurites (LNs) in the soma or neuronal branches, respectively (Spillantini, Schmbidt, Lee, & Trojanowski, 1997) (**Figure 1E-G**). LBs and LNs can be found in many regions including SN*pc*, LC, NBM, hypothalamus, cerebral cortex, dorsal motor nucleus of the glossopharyngeal vagal nerves, raphe system, subnuclei of the thalamus and amygdala, Ob or anterior olfactory areas and central and peripheral divisions of the autonomic system (Beach et al., 2009; H. Braak, Rüb,

Gai, & Del Tredici, 2003; de Vos, Jansen, Stam, Ravid, & Swaab, 1995; Polymeropoulos et al., 1997; Rüb et al., 2002). These aggregates are constituted by several lipids and proteins but one of the most abundant is α-synuclein (Spillantini *et al.*, 1997; Hashimoto and Masliah, 1999; Wakabayashi *et al.*, 2007) (**Figure 1H**). Moreover, α-synuclein positive aggregates can also be observed in peripheral organs like the gut (Borghammer and Van Den Berge, 2019; Leclair-Visonneau *et al.*, 2020), salivary glands (Beach *et al.*, 2013) and skin (Doppler *et al.*, 2017). Familial forms of the disease have been linked with point mutations or increase in number of α-synuclein gene (*SNCA*) copies (Polymeropoulos *et al.*, 1997).

Several authors have built hypotheses around aggregates appearance and pathology evolution but they still remain controversial (Burke *et al.*, 2008). Braak LB staging (Braak *et al.*, 2003*a*; Braak and Del Tredici, 2017) and dementia with Lewy Bodies (DLB) guidelines (McKeith *et al.*, 1996, 2005) were the first ones to classify histopathologically both PD and DLB, respectively. Braak and Braak tried to answer the question as to whether pathology in different areas evolves simultaneously or they follow a specific temporal pattern (**Figure 4A**). In order to answer this, they assumed that both symptomatic and non-symptomatic cases, which had brain synucleinopathy, could be ordered in a sequence. Cases with mildest pathology represented the starting point, while the ones with more severe pathology were in a terminus of the disease spectrum. They reported a total of 6 stages which each of them had features of the previous stage plus some new ones: stage 1 *medulla oblongata* affectation, stage 2 *medulla oblongata* and pontine tegmentum affectation, stage 3 midbrain affectation, stage 4 basal prosencephalon and mesocortex affectation, stage 5 neocortex affectation and stage 6 more broadly neocortex affectation (sensory associated and premotor areas) (Braak and Del Tredici, 2017). In general terms, LBs and LNs appear initially in some brain

areas such as Ob and dorsal motor nucleus of the glossopharyngeal and vagal nerves. In late Braak's stages, LBs and LNs appear in other brain areas supposed to be less vulnerable such as SN*pc* and finally cerebral cortex. These two brain areas are related with motor and dementia symptoms, *ergo*, typical motor PD is normally diagnosed when SN*pc* is affected and its dementia variations when cerebral cortex is also affected. In a more adventurous way, they also proposed the dual-hit hypothesis of synucleinopathy. Accumulating evidence has demonstrated that PD has a long prodromal period in which olfactory dysfunction, constipation and sleep disorders are its main symptoms. These clinical manifestations and the presence of peripheral synucleinopathy (salivary glands, gut and olfactory areas) made Braak and collaborators (Hawkes *et al.*, 2007) hypothesize that α-synuclein pathology may be provoked by an unknown insult which, in fact, would cause subsequently the accumulation of α-synuclein aggregates. They proposed a neurotropic pathogen, probably viral, which can enter the brain by two distinct routes: 1) nasal, with anterograde progression to the temporal lobe and 2) gastric, reaching parasympathetic motor neurons of the vague nerve.

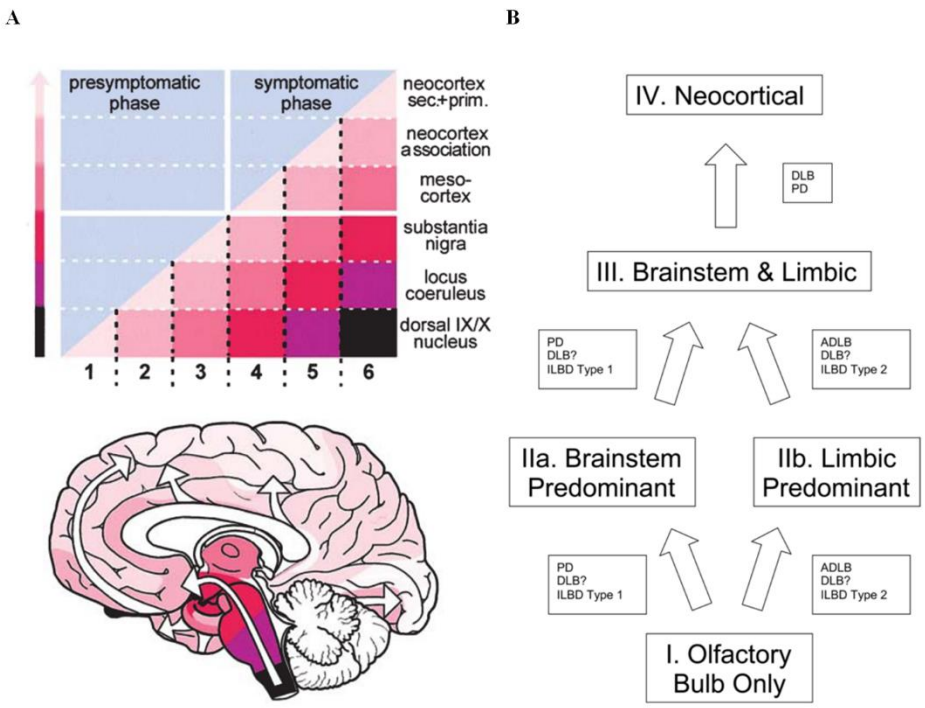

Figure 4. Braak Lewy Body staging and Unified Systematic Staging of Lewy body disorders. (**A**) Schematic representation of progression pathways and stages (from 1 to 6) for PD synucleinopathies regarding Braak Lewy Body staging. Synucleinopathy burden is shown by increasing degrees of shading (red, violet, black). Adapted from Braak *et al*., 2003. (**B**) Schematic representation of progression pathways and stages for Lewy Body disorders regarding USSLBD staging. Two types of iLBD stage II are designed. It is presumed that stage IIa iLBD leads to PD and stage IIb leads to AD with LBs and possible DLB. Only PD and DLB progress to the neocortical stage. Adapted from Beach *et al*., 2009.

Braak LB staging raised some criticism (Parkkinen *et al.*, 2005, 2008; Linazasoro, 2007; Burke *et al.*, 2008; Fujimi *et al.*, 2008; Kalaitzakis *et al.*, 2008; Leverenz *et al.*, 2008; Jellinger, 2009). Patterns of synucleinopathy described by Braak were often not observed in DLB cases neither when synucleinopathy

occured in the absence of neurological manifestations (iLBD cases). Braak and colleagues presumed that brainstem synucleinopathy represented early stages of PD as these cases had a potential likelihood to increase and spread α-synuclein to other brain areas. However, this was an assumption because conclusions were not drawn from longitudinal studies. Between 6.3 and 43% of cases did not follow rostro-caudal synucleinopathy brain progression. Moreover, there was no correlation between Braak stages and clinical PD severity although, mentioned by Braak himself, this was not the aim of the study.

Unified Staging System for Lewy Body disorders (USSLBD) surged as an attempt to improve these aforementioned flaws of Braak LB staging (Beach *et al.*, 2009*b*, *a*) (**Figure 4B**). First of all, USSLBD can be applied to all of the major Lewy body disorders including PD, DLB, AD with sparse Lewy pathology and incidental with Lewy Body disease (iLBD) cases. USSLBD also takes into account subjects who have Lewy pathology confined to the Ob or who pass through a limbic-predominant pathway that initially bypasses the brainstem. Its authors proposed the following staging similar to Braak's one: stage I Ob only, stage IIa brainstem predominant, stage IIb limbic predominant, stage III brainstem and limbic, stage IV neocortical. Not only α-synuclein pathology spread to different brain areas through stages but it was also accompanied by a worsening of striatal tyrosine hydroxylase staining and dopaminergic SN*pc* neuronal loss. Altogether, USSLBD allowed the classification of a much greater proportion of Lewy pathology cases than Braak score (Adler *et al.*, 2019).

One of the most important points drawn from these staging analyses was the existence of iLBD cases. iLBD cases are healthy donors which after a neuropathological analysis of their brains α-synucleinopathy is found. Regarding to USSLBD staging, they would be considered between stage I (Ob)

or II (brainstem or limbic predominant). Some critics opposed to the idea of considering iLBD a premotor early stage of PD (Burke *et al.*, 2008; Figerio *et al.*, 2011). It is certain that it is an assumption to believe that a high percentage of iLBD cases would evolve to some type of clinical synucleinopathy. Nonetheless, mounting evidence has shed light on this issue. SN*pc* of iLBD cases presented variable dopaminergic cell death in comparison with age-matched healthy controls but less than PD cases (Beach *et al.*, 2009*a*; Cheng *et al.*, 2010; Dijkstra *et al.*, 2014; Iacono *et al.*, 2015). This was also accompanied by a reduction of striatal TH and VMAT2 immunostaining in both iLBD and PD cases (DelleDonne *et al.*, 2008; Dickson *et al.*, 2008). Patterns of expression of T cell-related cytokines, vascular changes and loss of certain growth factors correlated with disease progression considering iLBD an early stage of the disease (Walker *et al.*, 2016). However, iLBD cases are a mixture of different USSLBD or Braak stages provoking high variability in the obtained results. More work needs to be performed classifying separately iLBD cases according to synucleinopathy stages.

1.1.2 Clinical motor symptoms and management

As it was mentioned in the first section, PD is comprised by motor and non-motor symptoms. Hoehn and Yahr (HY) scale appeared as a clinical staging system for severity of PD (Hoehn and Yahr, 1967). It significantly correlated with neuroimaging studies of dopaminergic cell loss (Staffen *et al.*, 2000). Even though HY is considered the reference standard staging for PD disability, it presents some limitations such as mixing impairment and disability, nonlinear character between the five stages and it is more weighted towards postural instability and mobility problems (Skorvanek *et al.*, 2017). Unified Parkinson's Disease Rating Scale (UPDRS) was initially developed to comprehensively

assess the main symptoms of PD and to monitor severity as HY staging (Fahn *et al.*, 1987). Since its creation it has been reviewed by Movement Disorder Society Task Force on Rating Scales (Movement Disorder Society Task Force on Rating Scales for Parkinson's Disease, 2003). The new MDS-UPDRS covers a greater number of PD symptoms, including non-motor ones and better discriminates mild manifestations. In this sense is more sensitive than HY scale and accepts PD as a systemic disease (Skorvanek *et al.*, 2017).

All available PD treatments are symptomatic, *ergo*, there is no treatment which stops or, at least, reduces the progression of the neurodegenerative process as no drug has been proven to be neuroprotective in clinical trials (Athauda and Foltynie, 2014; Kalia and Lang, 2015). Understanding the mechanisms which are involved in disease progression and dopaminergic cell loss are important to create new therapeutic strategies. Practically all symptomatic treatments focus on motor symptoms. Loss of dopaminergic neurons in the SN*pc* leads to striatal DA depletion in PD (Ehringer and Hornykiewicz, 1960). Initially DA was described as an intermediate product of norepinephrine synthesis from tyrosine but it was not until 1950 decade when it was recognized as a neurotransmitter itself (Carlsson *et al.*, 1957, 1958; Montagu, 1957). DA is synthesized through DOPA-decarboxylase enzyme from L-3,4,-dihydroxyphenylalanine (L-DOPA). The latter is obtained from the hydroxylation of the amino acid L-tyrosine by tyrosine hydroxylase enzyme (TH) (Molinoff and Axelrod, 1971; Barron *et al.*, 2010; Gonzalez-Sepulveda *et al.*, 2020). Drugs that enhance intracerebral dopamine concentrations or stimulate dopamine receptors are the main strategy to reduce PD motor symptoms. Treatment normally starts when symptoms cause patient disability, trying to improve its quality of life. Normally, these treatments act on rigidity and bradykinesia symptoms. For tremor, some anti-cholinergic drugs can also be useful (Kalia and Lang, 2015).

3,4-dihydroxyphenylalanine, L-DOPA or Levodopa is the most effective treatment for PD-related motor symptoms and it was described by Cotzias and colleagues in 1967 and its beneficial effects were confirmed two years later by Yahr and coworkers in a double-blind, placebo-controlled trial reaching 81% of "significant overall improvement" in 60 patients with parkinsonism. Levodopa treatment is aimed to replenish DA levels in the caudate-putamen nucleus (Kalia and Lang, 2015). It can go through the blood-brain barrier (BBB), in contrast with DA, and then by DOPA decarboxylase it is decarboxylated yielding DA (Gonzalez-Sepulveda *et al.*, 2020). Co-administration of Levodopa with carbidopa or benserazide, which are dopa-decarboxylase inhibitors, reduces the peripheral conversion of levodopa to DA, increasing the bio-availability of levodopa in the brain and reducing its total dosage (Nagatsu and Sawada, 2009; Salat and Tolosa, 2013). Both dopamine agonists and levodopa are associated with side-effects such as nausea, oedema, daytime somnolence, impulse control disorders, hallucinations and psychiatric side-effects although they are more frequently observed with dopamine agonist treatment. However, Levodopa use is also associated with motor complications such as dyskinesias (hyperkinetic involuntary movements) and motor fluctuations (Kalia and Lang, 2015; Obeso *et al.*, 2017).

In order to alleviate PD-associated motor symptoms monoamine oxidase (MAO) or cathecol-o-methyltransferase (COMT) inhibitors have been used as both of them are enzymes which degrade DA into its final precursors 3,4-dihydroxyphenylethanol (DOPE) and 3,4-dihydroxyphenylacetic (DOPAC) for MAO and 3-methoxytyramine (3-MT) for COMT (Gonzalez-Sepulveda *et al.*, 2020). This strategy keeps higher level of DA in the caudate-putamen region. With similar results, DA receptor agonists are used to activate striatal neurons such as medium spiny neurons which they present dopaminergic receptors. However, many of these dopaminergic agonists have similar side effects to

Levodopa but with higher frequencies and other ones such as retroperitoneal and pleuropulmonary fibrosis up to 30% of treated patients although this remains controversial (Reichmann *et al.*, 2006).

1.1.3 Etiology and risk factors

PD is recognized as the second most common neurodegenerative disorder just after Alzheimer's disease and the most common motor one. Prevalence of PD in our society is increasing in the same way as ageing, the most important risk factor. It was estimated that in 1990, 2.5 million individuals had PD and it was increased to 6.1 million in 2016. This increase was due to increasing numbers of older people but also due to longer disease duration and environmental factors. Thus, total economic and social burden are also increasing (Ray Dorsey *et al.*, 2018). This ageing of the society in part would also explain why prevalence of PD is higher in Europe, North America and South America in contrast with African, Asian and Arabic countries (Kalia and Lang, 2015; Ascherio and Schwarzschild, 2016). Nonetheless, this is not totally consistent as socio-economic factors are also important explaining these prevalence differences (Ascherio and Schwarzschild, 2016). Its incidence ranges from 10-18 per 100000 person-years (Kalia and Lang, 2015) although it is low before the age of 50 years and it increases up to 160 per 100000 person-years after this age threshold (Ascherio and Schwarzschild, 2016).

Thus, the most important risk factor to develop PD is age. However, there are other risk factors associated with the disorder. Sex is an established risk factor as male to female incidence ratio ranges from around 1.3 to 2 in most studies but rates as low as 0.95 can also be observed in different regions reflecting possible behavioural sex differences (Kalia and Lang, 2015; Ascherio and Schwarzschild, 2016). However, it is generally hypothesized that estrogen

activity could protect women from developing PD (Haaxma *et al.*, 2007; Shulman, 2007; Meoni *et al.*, 2020). Male sex variable is not only associated with higher incidence rates and prevalence but also with earlier onset, more severe motor symptoms and progression and faster cognitive decline (Meoni *et al.*, 2020).

Overall, although there are many groups which have focused on studying PD epidemiology, there are some difficulties which need to be addressed to make them more consistent. Size of these studies and an accurate diagnostic test are the most important ones. PD diagnosis is based on clinical accuracy which is around 80-90% of efficacy after post-mortem confirmation (de Lau and Breteler, 2006). A reliable and easily applicable diagnostic test or marker would improve the classification of parkinsonisms and it would detect the onset in earlier stages of the disease (de Lau and Breteler, 2006).

1.1.3.1 Environmental factors

Environmental factors are believed to contribute at some extent to the vast majority of late-onset sporadic PD cases (Chen and Ritz, 2018). These environmental factors can be classified according to its increasing or decreasing effect in the risk of developing PD. Among the former, it can be found dairy products, pesticides, methamphetamine, cancer, and traumatic brain injury (TBI). Dairy products are believed to increase the risk (Ascherio and Schwarzschild, 2016) by decreasing urate levels (Choi *et al.*, 2004), which is associated as protective for PD (Guerreiro *et al.*, 2009). Consequences of pesticide exposure causing PD (Dick *et al.*, 2007) started to see the light when neurotoxic effects of a metabolite of 1-methyl-4-phenyl-1,2,3,6-tetrahydropyridine (MPTP), a by-product in the synthesis of 1-methyl-4-phenyl-4-propionoxy-piperidine (meperidine or MPPP), were discovered.

MPTP has a structure similar to the herbicide paraquat (Langston, 2017; Vaccari *et al.*, 2019). Epidemiological works showed how long exposures to paraquat due to work in plantations, increased the relative risk of developing PD (Dinis-Oliveira *et al.*, 2006; Zhang *et al.*, 2016; Vaccari *et al.*, 2019). Since then, other pesticides such as rotenone which affects the mitochondrial complex I have been found to also increase the relative risk. Overall, they normally have oxidative effects increasing reactive oxygen species (ROS). These ROS then can increase protein (Singh *et al.*, 2019) and lipid peroxidation (Shichiri, 2014), α-synuclein aggregation/deposition (Scudamore and Ciossek, 2018; Musgrove *et al.*, 2019; Angelova *et al.*, 2020) and activate immune system (Solleiro-Villavicencio and Rivas-Arancibia, 2018) among other detrimental effects (Vaccari *et al.*, 2019).

Other drugs such as methamphetamine and derivates have also been related with an increase in the relative risk (Callaghan *et al.*, 2010). Due to the fact that methamphetamine binds to the presynaptic dopamine transporter (DAT), it increases extracellular concentrations of DA which its metabolism is highly oxidative damaging dopaminergic neurons as it has been demonstrated in PD experimental animal models (Guilarte *et al.*, 2003). For cancer, it has been reported an increase of relative risk of PD among individuals with melanoma (Constantinescu *et al.*, 2007, 2014; Liu *et al.*, 2011). Reciprocally, there is an increased risk of melanoma among individuals in early stages of PD.

As it will be discussed in further sections, neuroinflammation is one of the hallmarks of PD. TBI can cause neuroinflammation, breakdown of the BBB, excitotoxicity, oxidative stress and, associated with all these events, accumulation of α-synuclein. Observably, TBI direct or indirect effects are related with PD pathophysiology. However, results are controversial and

contradictory and more research on the topic needs to be performed before drawing conclusions (Tsai *et al.*, 2002; Marras *et al.*, 2014).

Viral infections have also been linked with PD (Caggiu *et al.*, 2019; Sulzer *et al.*, 2020). After viral infection, numerous cases of post-encephalitic parkinsonism have been reported. Nonetheless, these parkinsonism are suggested to be "phenocopies" of PD as they do not exhibit the same cellular or molecular pathologies (Olsen *et al.*, 2018). Afterwards, case-control epidemiological studies showed an increase of PD incidence in patients which had undergone viral infections mediated by herpes simplex virus (HSV), influenza virus A and mumps (Marttila, 1981; Marttila *et al.*, 1982; Vlajinac *et al.*, 2013). Other studies found no associations with these aforementioned viruses or even decrease of incidence when viral infections were mediated by measles, cytomegalovirus and coronavirus (Marttila, 1981; Marttila *et al.*, 1982; Fazzini *et al.*, 1992). However, these studies presented some downsides as it was difficult to control for side-effects of anti-viral treatments such as IFNγ or they relied on accurate patient memory and interpretation of their condition (Olsen *et al.*, 2018). It is believed that viral infections most likely are not the primary cause, but they may act as triggers to induce a cytotoxic attack to neurons. Several authors have suggested that some viruses present mimicry with some proteins expressed in PD affected neurons. It has been found immunological cross-reactivity between HSV-1 and α-synuclein (Caggiu *et al.*, 2016). Molecular mimicry has also been observed between latent membrane protein 1 (LMP1) of Epstein-Barr virus (EBV) and the C-terminal region of α-synuclein (Woulfe *et al.*, 2014, 2016). All these results were in line with the dual-hit hypothesis described by Hawkes, del Tredici and Braak (Hawkes *et al.*, 2007).

Among protective factors which have been related with a decrease in relative risk of PD we can find tobacco, coffee and caffeine intake, urate, non-steroidal

anti-inflammatory drugs (NSAIDs), calcium channel blockers and physical activity (Ascherio and Schwarzschild, 2016). In late 90s, an inverse correlation between coffee intake and caffeine consumption with relative risk of PD was reported (Hellenbrand *et al.*, 1997; Fall *et al.*, 1999; Ross *et al.*, 2000; Ascherio *et al.*, 2001; Hu *et al.*, 2007; Sääksjärvi *et al.*, 2008; Buchwalow *et al.*, 2011). Although initially was thought niacin had a positive effect, it seemed that the positive effect was due to caffeine mainly (Ross *et al.*, 2000). Its inverse association with the disorder was a clear dose-response and it passed a multivariate adjustment with other confounding parameters such as smoking routines. More case-control and prospective studies reinforced the conclusions (Liu *et al.*, 2012).

Although cigarette smoking is an established risk factor for various diseases such as lung cancer, heart disease and chronic obstructive pulmonary disease (COPD), in late 1950s some studies reported an inverse association between tobacco use (independently of smoking or chewing tobacco) and PD (Dorn, 1959; Miller & Das, 2007). Afterwards, longitudinal and case-control studies confirmed these previous results (Morens *et al.*, 1995; Hellenbrand *et al.*, 1997; Wirdefeldt *et al.*, 2005; Miller and Das, 2007). Likelihood to develop PD decreases with increasing duration of smoking and it increases with time since quitting in ex-smokers (Hernán *et al.*, 2001; Thacker *et al.*, 2007). In some reports, examination of smoking behaviours in early life showed how PD patients were less prone to be smokers (Chen *et al.*, 2010). Robustness of reproducibility, strong association, low odd-ratios, clear dose-response and clean multivariate adjustments made confounding by known risk factors for PD a highly unlikely explanation for this decrease in risk (Ascherio and Schwarzschild, 2016).

Antioxidants such as urate, which is an end product in the metabolism of adenosines, can have beneficial effects in PD as it has been suggested by several PD experimental animal models and prospective human studies (Filograna *et al.*, 2016; Yang *et al.*, 2017). In the same sense as tobacco, high serum urate concentrations have been linked to several diseases such as gout, hypertension, cardiovascular disease, and renal disease (Gong *et al.*, 2012). However, a reduction of urate concentration in SN*pc* of PD patients compared with age-matched healthy controls was observed (Church and Ward, 1994). Some years later, it was reported that high serum uric acid levels were associated with a reduced risk of idiopathic PD (Davis *et al.*, 1996). These results were again confirmed by several independent labs although some controversy was found in women, which this association was not reported (de Lau *et al.*, 2005; O'Reilly *et al.*, 2010; Jain *et al.*, 2011; Gao *et al.*, 2016). In PD animal models, this association has been strengthen due to the fact that increased levels of urate in the brain by several mechanisms induce neuroprotection of dopaminergic neurons (Gong *et al.*, 2012; Chen *et al.*, 2013; Bakshi *et al.*, 2015).

Physical therapy was proposed as a treatment for PD in order to try to increase brain DA levels hampering the progression of motor symptoms (Sasco *et al.*, 1992). Initially, physiotherapy and occupational therapy did not get positive results (Gibberd *et al.*, 1981) although some years later a more detailed program found an improvement in gait, tremor and motor coordination tasks (Palmer *et al.*, 1986). A case-control study reinforced this idea showing an association between physical activity at the time of college and the relative risk of PD (Sasco *et al.*, 1992). These results were confirmed in other case-control studies and in PD animal models with exercise treatments (Tsai *et al.*, 2002; Cohen *et al.*, 2003; Zigmond and Smeyne, 2014; Yang *et al.*, 2015). Among the mechanisms, neuroplasticity, increase of DA levels and also an increase of GDNF concentrations have been proposed (Cohen *et al.*, 2003).

As it will be commented in more detail in the following sections, neuroinflammation is a hallmark of PD. Many studies have demonstrated how both innate and adaptive immune systems play a role in the disease (Croisier *et al.*, 2005; Brochard *et al.*, 2009; Hirsch and Hunot, 2009; González and Pacheco, 2014; Chen *et al.*, 2016). Thus, it has been hypothesized that anti-inflammatory treatments could be beneficial for PD (Asanuma and Miyazaki, 2008; Hirsch and Hunot, 2009). In this sense, analyzing the impact of NSAIDs in the incidence of PD could be useful to obtain more evidence for beneficial effects of anti-inflammatory treatments. Consumption of NSAID ibuprofen has been associated with a decline in relative risk of PD but, in these same studies, no associations were found for other NSAIDs such as aspirin or aminophen (Chen *et al.*, 2005; Gao *et al.*, 2011). However, independent groups found some discrepancies observing a slight decrease in relative risk only for aspirin (Ton *et al.*, 2006; Chen *et al.*, 2007) and others reported no associations in any of the NSAIDs commented above (Hernán *et al.*, 2006; Becker *et al.*, 2011). A recent meta-analysis showed that the link between NSAIDs consumption and incidence of PD is weaker than previously thought and many of the NSAIDs which were addressed had no association with PD (Ren *et al.*, 2018).

One of the hypotheses which tries to explain the selective vulnerability of dopaminergic neurons is their increasing reliance on Ca^{2+} channels (Surmeier, 2007). With these, dopaminergic neurons maintain autonomous activity with age, generating action potentials in the absence of synaptic input (Ping and Shepard, 1996; Bonci *et al.*, 1998; Puopolo *et al.*, 2007). This dependency on Ca^{2+} could pose a sustained metabolic stress on oxidative processes in the mitochondria, accelerating cellular ageing and death. Thus, with these previous results, epidemiological studies about calcium channel blockers consumption and incidence of PD were worthy to be performed (Ascherio and Schwarzschild, 2016). Use of calcium channel blockers of the dihydropyridine class was

associated with reduced PD relative risk (Ton *et al.*, 2007; Ascherio and Tanner, 2009; Pfeiffer, 2010; Ritz *et al.*, 2010; Lee *et al.*, 2014). Notwithstanding these positive results, other studies did not find this positive association (Simon *et al.*, 2010). Other drugs treating hypertension were not linked with PD relative risk.

1.1.3.2 Genetic factors

Although initially PD was thought to be primarily caused by environmental factors, currently it is widely accepted that is an interaction between those and genetic ones (Hardy, 2010). Monogenic causes only explain a low percentage of PD cases in our society (de Lau and Breteler, 2006) although it seems clear that a familial history of PD increases the relative risk of developing the disorder (Hardy *et al.*, 2003; Noyce *et al.*, 2012). Some familial forms of PD are clinically equal to typical PD although histologically there are clear differences such as absence of α-synuclein accumulation and aggregation in some *LRRK2* mutated cases (Rodríguez-Moreno *et al.*, 2010; Corti *et al.*, 2011). Nonetheless, many of the familial forms of PD display parkinsonism symptoms and other ones that are atypical such as dystonia, young onset and early occurrence of dementia (de Lau and Breteler, 2006; Blauwendraat *et al.*, 2020). All causal and genetic risk factors can be classified as *PARK* and non-*PARK* loci as many of them, which were initially described, were of the *PARK* loci (*i.e. SNCA, PRKN, PINK1, DJ-1* and *LRRK2*) (Gubellini and Kachidian, 2015).

The first gene to be associated as a monogenic form of PD was *SNCA* (PARK1 and 4) which encodes the protein α-synuclein (Polymeropoulos *et al.*, 1997). Mutations in *SNCA* gene which cause PD are missense mutations, amino acid substitutions and multiplications of the gene locus (Kalia and Lang, 2015), which make α-synuclein more prone to aggregate (Devine *et al.*, 2011). However, mutations in *LRRK2* (PARK8) and *PRKN* (PARK2) genes are the most

abundant causes of dominantly and recessively inherited PD, respectively (Corti *et al.*, 2011). *LRRK2* function is tissue dependent as it is expressed in several cell types but a toxic gain-of-function has been proposed to explain the negative effects for PD (Thomas and Flint Beal, 2007). Mutantions in *GBA* gene, which encodes β-glucocerebrosidase, that is a lysosomal enzyme deficient in Gaucher disease, are common genetic factors for developing PD (Sidransky and Lopez, 2012; Xicoy and Peñuelas *et al.*, 2019). Overall, to date mutations in more than 20 genes have been identified to cause Parkinson's disease with different penetrance (Blauwendraat *et al.*, 2020).

Thanks to genome-wide association studies (GWAS) 90 independent risk signals have been identified in sporadic PD. A large proportion of PD cases are affected by these genetic risk factors altogether with environmental factors (Blauwendraat *et al.*, 2020). GWAS allowed, in a hypothesis-free manner, to evaluate the majority of common variations in all the genome, not focusing on candidate-based single variants. Heritable component of PD due to this genetic variability is estimated to be around 16-36%. However, current GWAS exposed loci only explain a part of this heritability (Nalls *et al.*, 2019). GWAS studies also show how some pathways contribute to accelerate PD as variants in these pathways have been identified in early age onset of the disorder (Blauwendraat *et al.*, 2019). Several GWAS have identified variants in the human leukocyte antigen (HLA) region, a locus encoding for major histocompatibility human proteins, to be associated with PD (Hamza *et al.*, 2010; Hill-Burns *et al.*, 2011; Holmans *et al.*, 2013; Wissemann *et al.*, 2013; Chang *et al.*, 2017; Nalls *et al.*, 2019). It has been suggested that the hits at HLA-DRB6 and HLA-DQA1 could implicate regulation of antigen presentation (Kannarkat *et al.*, 2015). Other gene variants implicated in both innate and adaptive immune systems such as bone marrow stromal cell antigen 1 (BST1) have also been linked with the disorder (Gagliano *et al.*, 2016; Billingsley *et al.*, 2018). Moreover, some of the

genes associated with familial forms of PD are also expressed in immune cells (Shameli *et al.*, 2015; Wallings and Tansey, 2019).

Overall, the identification of gene or locus variant could allow sorting the population for better targeted clinical trial recruitments. Moreover, these novel identified variants may help us to better understand the disease and to find new molecular candidates to develop drug targeting studies (**Figure 5**).

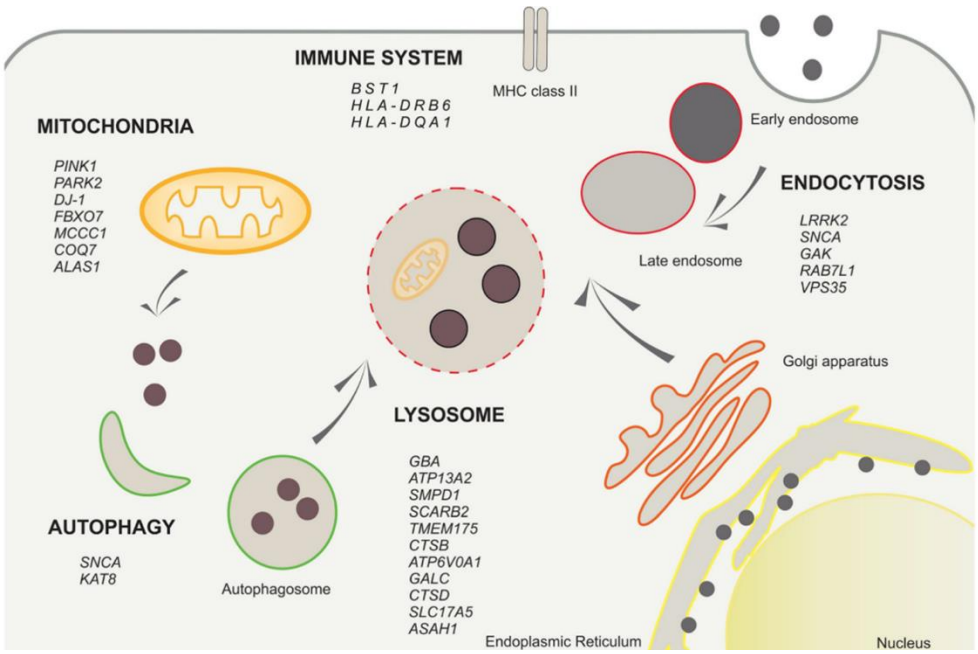

Figure 5. Overview representation of the PD risk factor genes and the molecular pathways in which they participate. Observably, PD risk factor genes encode for proteins that mainly participate in mitochondrial-associated pathways, autophagy, endocytosis, immune system and/or lysosomal function. From Billingsley *et al.*, 2018.

1.1.4 Experimental animal models

In order to find new therapeutic targets to halt the disease progression and, at some point, to stop it, it is totally necessary to deeply understand the

pathophysiology of the disease. It seems obvious that using only human post-mortem tissue and epidemiological analysis is not enough. Experimental animal models enable us to study temporarily the mechanisms which provoke dopaminergic cell death and to test therapeutic targets (Bezard and Przedborski, 2011). Cell disease models also exist such as overexpression of human α-synuclein or cells treated with 1-methyl-4-phenylpyridinium ion (MPP+) or rotenone. However, they lack the complexity of the whole brain tissue (*e.g.* cell-to-cell interactions, non-autonomous cell mechanisms), animal pharmacokynetics, blood-brain barrier permeability and behavioural output (Falkenburger *et al.*, 2016). Furthermore, animal models are normally preferred although cell models are useful to dissect more accurately specific molecular pathways (Le *et al.*, 2014).

Many animal species have been used to model the disease, from invertebrates like nematodes and flies to rodents and non-human primates (Hewitt and Whitworth, 2017; Dun and Thao, 2018; Ünal and Emekli-Alturfan, 2019). Although these animal models try to resemble some aspects of PD pathophysiology, they fail to recapitulate all of them. Nonetheless, this can be somehow overcame combining some of them. Overall, there is no uncertainty that PD experimental animal models have contributed and are actively doing so to a better understanding of PD pathophysiology and their usefulness as a first filter for novel therapies.

Animal models can be divided in two general types according to the mechanism with which they are created.

1.1.4.1 Toxin models

As it has been previously discussed, both genetic and environmental factors play an important role in PD. Toxin-induced PD animal models are the most classical ones. Some of these toxins are pesticides which have been linked with PD such as rotenone and paraquat. Others have similar structures to these pesticides like MPTP. But generally the important aspect of all these toxins is that they provoke a more or less selective neurodegeneration of dopaminergic neurons (Blandini and Armentero, 2012). They may produce motor symptoms to the animals even though they are hard to compare with those observed in the human disease (Gubellini and Kachidian, 2015). Thus, in comparison with genetic ones, toxin-based models are best fitted for studying the neurodegenerative processes and for both symptomatic and preventive treatments (Gubellini and Kachidian, 2015). Nevertheless, the progression of the pathology is very rapid (only a few days or weeks) and synucleinopathy is rarely found [some increases of α-synuclein (Vila *et al.*, 2000)]. Chemically, rotenone and MPTP toxins inhibit the mitochondrial complex I when they accumulate inside the neuron by dopaminergic or noradrenergic membrane transporters (Castello *et al.*, 2007; Gubellini and Kachidian, 2015). This mitochondrial complex I deficiency has also been described in PD human SN*pc* dopaminergic neurons (Mizuno *et al.*, 1989; Schapira *et al.*, 1990; Flønes *et al.*, 2018). Toxins can be administered systemically or intracerebrally according to their BBB permeability. Among all of them, MPTP and 6-hydroxydopamine (6-OHDA) are the most commonly used although more novel models are discovered each year (Simola *et al.*, 2007, Decressac *et al.*, 2012*b*; Carballo-Carbajal *et al.*, 2019; Kin *et al.*, 2019).

1.1.4.1.1 The MPTP animal model

As it has been previously explored in the environmental factors section, MPTP is a byproduct of meperidine (MPPP) production (Langston *et al.*, 1983) which cause parkinsonism symptoms in humans and neurodegeneration of the nigrostriatal pathway years later after last exposure (Langston *et al.*, 1999; Nonnekes *et al.*, 2018). After this discovery in meperidine drug addicts, MPTP was broadly administered in different non-human primate monkey species reporting parkinsonism syndrome in all of them (Kopin and Markey, 1988; Hamadjida *et al.*, 2019). These motor symptoms can be reversed with L-DOPA and dopamine receptor agonist treatments (Shimohama *et al.*, 2003). Due to the lipophilicity of MPTP, it can cross the BBB and enter to the brain parenchyma (Blandini and Armentero, 2012; Le *et al.*, 2014). Once there, enzyme monoamine oxidase B (MAO-B) converts MPTP to 1-methyl-4-phenyl-2,3-dihydropyridinium ion (MPDP+) in astrocytes and then it is oxidized to MPP+ (Heikkila *et al.*, 1985; Gubellini and Kachidian, 2015; Hamadjida *et al.*, 2019). Blocking this conversion protected totally the dopaminergic neurodegeneration (Langston *et al.*, 1984). MPP+ is then taken up by DAT into dopaminergic neurons of SN*pc*. In the same sense as MAO-B blockers, DAT inhibitors also prevent neurodegeneration (Javitch *et al.*, 1985; Madras *et al.*, 2006). Then, it tends to accumulate inside synaptic vesicles (Liu *et al.*, 1992) and mitochondrial matrix by passive transport (Hoppel *et al.*, 1987; Davey *et al.*, 1992) inhibiting the complex I of the respiratory chain. On the one hand, this provokes the activation of inducible nitric oxide synthase (iNOS) and the release of ROS as well as reducing adenosine triphosphate (ATP) production (Liberatore *et al.*, 1999; Le *et al.*, 2014; Gubellini and Kachidian, 2015; Hamadjida *et al.*, 2019). On the other hand, ROS may also be produced by the auto-oxidation of DA resulting from the massive release of synaptic vesicles

induced by MPP+ entrance. Blocking ROS-induced oxidative processes protects dopaminergic neurons in front of MPTP insults (Bové and Perier, 2012).

MPTP is more used in rodents than non-human primates due to costs and reproducibility. It is quite clear that is cheaper to use rodents than non-human primates considering both time and spaces. Moreover, to gain reproducibility non-human primates are injected intra-carotidly low doses of MPTP until motor symptoms are visible (Masilamoni and Smith, 2018). This strategy creates high inter-individual variability (Porras *et al.*, 2012). In rodents, paradigms are established and number, frequency and dosage of injections are validated (Jackson-Lewis and Przedborski, 2007). However, non-human primates are preferred when testing treatment protocols before going to clinical trials as they are more similar to human than rodent species and present clearer motor symptoms (Bové *et al.*, 2005; Porras *et al.*, 2012).

Mice are normally used over rats as the latter are more resistant and need MPP+ to be stereotaxically injected in the brain parenchyma (Giovanni *et al.*, 1994; Bové *et al.*, 2005). On the contrary, mice can be administered subcutaneously, intravenously or intraperitoneally (ip) depending on the paradigm (Jackson-Lewis and Przedborski, 2007). There are differences of susceptibilities among mice strains (Muthane *et al.*, 1994; Hamre *et al.*, 1999; Sedelis *et al.*, 2000; Smeyne *et al.*, 2001; Boyd *et al.*, 2007), some of them having practically full protection while some others present high levels of dopaminergic neurodegeneration. MPTP susceptibility is also age, body weight and sex dependent (Antzoulatos *et al.*, 2010; Bové and Perier, 2012; Le *et al.*, 2014). Normally, female mice are excluded from MPTP treatments as they have high rate of mortality. Male mice weighting at least 22g and aged at least 8 weeks are included (Jackson-Lewis and Przedborski, 2007).

Even though many paradigms or regimens have been validated, acute and subacute ones are the most commonly used and characterized. Paradigms vary according to the magnitude of lesion and the mode of cell death of the dopaminergic neurons (Przedborski and Vila, 2003). Normally intraperitoneal injections are used over subcutaneous ones as the latter produce more severe neurodegeneration due to MPTP avoiding first hepatic pass (Chiba et al 1988). Thus, dose, number of injections and their frequency and route of administration determine the nigrostriatal neurodegeneration. Acute paradigm consists of four intraperitoneal injections of 20 mg/kg MPTP with 2 hour intervals in a single day and it was developed by Jackson-Lewis and colleagues (Jackson-Lewis *et al.*, 1995). Active phase of degeneration starts at 12h post-injection and it follows until 4 days (d). 70% of cell loss is achieved at 7d post-injection when neurodegeneration is stable. Acute MPTP treatment also leads to 90% of dopamine striatal depletion. With this paradigm cell death occurs via non-apoptotic pathways (Jackson-Lewis *et al.*, 1995). Despite this fact, it is still controversial that this 70% of cells are totally lost at 7d post-injection or some of them have merely lost their dopaminergic phenotype (Chandra *et al.*, 2017). Due to the fact that cell death is driven by non-apoptotic pathways, acute MPTP regimen has also been used to study the role of inflammation in dopaminergic neurodegeneration (Bové and Perier, 2012), as it is commented in the next chapter about neuroinflammation in PD. However, this inflammation is a fast event because of the acute impact of MPTP insult. This totally contrasts with the subacute regimen which cell death occurs primarily by apoptotic pathways. Subacute regimen is comprised of one ip injection of 30mg/kg for 5 consecutive days and it was described by Tatton & Kish lab (Tatton and Kish, 1997). In contrast with the MPTP acute treatment, both cell loss and dopamine striatal depletion are lower reaching 30-40% and 40-50%, respectively and they are stabilized at 21d post-injection (Perier *et al.*, 2007). Subacute regimen has

barely been used to study the role of inflammation in PD. Nevertheless, there is enough time to build an adaptive immune response to orchestrate the neuroinflammation as some studies have suggested (Depboylu *et al.*, 2012).

1.1.4.2 Genetic models

Neurotoxin-induced PD animal models have provided invaluable knowledge about disorder pathogenesis and cellular processes related with dopaminergic cell death but the lack of an age-dependent and progressive lesion and the fact that LBs are typically not observed in these models represent a downside (Dawson *et al.*, 2010; Blandini and Armentero, 2012). Despite the fact that only a minority of all PD cases may be fully explained genetically (20% approximately) (Zeitlin *et al.*, 1995; Dawson *et al.*, 2010; Jackson-Lewis *et al.*, 2012; Le *et al.*, 2014; Gubellini and Kachidian, 2015) many of the mutated processes are somehow related with sporadic PD. Genetic models allow us to better understand some processes linked with the disease targeting a mutation or deleting a gene. Many of the *PARK* and non-*PARK* genes associated with PD have been modeled in mice and rats, the most common being *SNCA*, *PRKN*, *PINK1*, *DJ-1* and *LRRK2*. Unfortunately, in general terms they show little or no nigrostriatal neurodegeneration, striatal dopamine depletion and motor behavioural changes but they are still useful to better understand the neuronal effects of these mutations and their functions in physiological conditions (Le *et al.*, 2014; Gubellini and Kachidian, 2015). Even in a triple knock-out of *parkin*/*DJ-1*/*PINK1* there is still no neuronal degeneration (Kitada *et al.*, 2009).

1.1.4.2.1 α-synuclein (*SNCA*)

Alpha-synuclein is a small (140 amino acids) phosphoprotein abundant in both nucleus and presynaptic terminals which, in neurons, participates in membrane protein regulation and vesicular dynamics of synaptic transmitter release (**Figure 6**) (Lavedan, 1998; Murphy *et al.*, 2000; Sharon *et al.*, 2001; Dawson *et al.*, 2010; Miraglia *et al.*, 2018; Kin *et al.*, 2019). More recently, α-synuclein has also been described to play a role in protein trafficking from endoplasmic reticulum to endosomes/lysosomes through Golgi apparatus (Cooper *et al.*, 2006; Gitler *et al.*, 2008; Thayanidhi *et al.*, 2010) and in axonal transport acting as a molecular dynamase (Cartelli *et al.*, 2016). Nonetheless, its exact and complete functions remain unclear and elusive (Miraglia *et al.*, 2018).

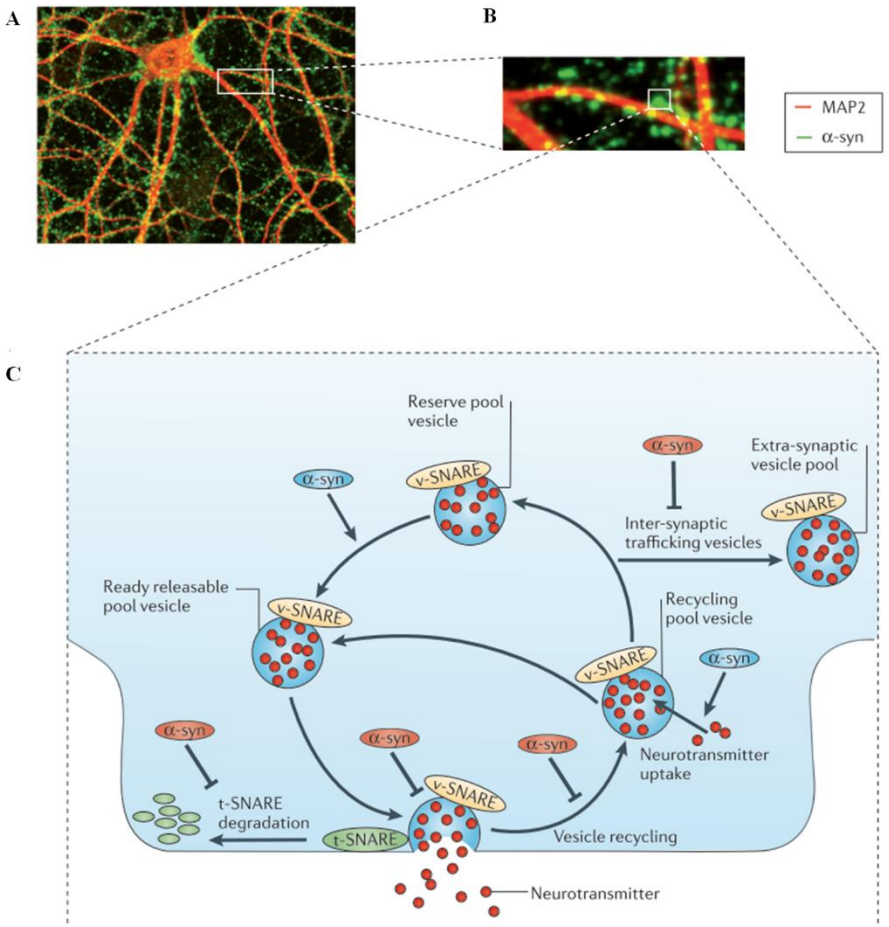

Figure 6. Functions and distribution of α-synuclein. (**A** & **B**) Images of cultured cortical neurons from a postnatal day 1 wild-type mouse. Neuronal dendrites [microtubule-associated protein 2 (MAP2), red] present α-synuclein-positive presynaptic densities (green). (**C**) Scheme representing the known roles of α-synuclein. It participates in the regulation of vesicle trafficking as well as the interactions between target membrane-associated SNARE (t-SNARE) and vesicle-associated SNARE (v-SNARE) proteins and neurotransmitter release. However, many of the functions of α-synuclein remain unknown. From Lashuel *et al.*, 2013.

A link between α-synuclein and PD was found when Golbe and colleagues (Golbe *et al.*, 1990) described an autosomal dominant inherited form of PD in an Italian-American family called Contursi kindred. This was the first familial form of PD in which LBs were found (Polymeropoulos *et al.*, 1996). The penetrance of PD in these kindred was over 90% and accordant with a monogenic inheritance. Subsequently, several more families with Lewy body pathology were found (Degl'Innocenti *et al.*, 1989; Denson *et al.*, 1997; Goedert, 2001). Due to these families, α-synuclein expression was studied in post-mortem tissue of PD cases and it was found to be enriched in LBs and LNs (Spillantini *et al.*, 1997). Thus, these hallmarks of the disease were a connection between familial and sporadic forms of PD. As previously discussed, both point mutations (A30P, A53T and E46K) (Blandini and Armentero, 2012) and increase of the total levels of α-synuclein due to multiplication of the gene rise its tendency to accumulate and aggregate (Polymeropoulos *et al.*, 1997). During pathology, α-synuclein shifts from its monomer form to higher-order structures such as oligomers, protofibrils and finally fibrils which are considered the ones which will build LBs and LNs and that are toxic (Dawson *et al.*, 2010; Lashuel *et al.*, 2013; Koprich *et al.*, 2017). Beyond losing its physiological function, α-synuclein gains some toxic ones such as provoking mitochondria dysfunction leading to ROS creation, endoplasmic reticulum (ER) stress and disrupting ER-Golgi trafficking, neuroinflammation dysregulation and impairment of microtubule formation, axonal transport and proteostasis (Lashuel *et al.*, 2013; Koprich *et al.*, 2017). This gain-of-function leads to a triad of more synthesis, less clearance and more aggregation of α-synuclein which was reported by Lashuel and collaborators (Lashuel *et al.*, 2013).

Until now, several α-synuclein transgenic mice have been developed in which the wild-type (sometimes truncated) or mutated protein is expressed under the tyrosine hydroxylase promoter (selective expression for catecholaminergic neurons). However, no significant and robust nigrostriatal degeneration has been obtained in any of them, only some down-regulation of tyrosine hydroxylase expression (Fernagut and Chesselet, 2004; Blandini and Armentero, 2012; Gubellini and Kachidian, 2015). Some other models combine α-synuclein transgene with other PD-related mutations. But neither of them shows evident nigrostriatal degeneration nor motor symptoms. Some of them show some α-synuclein aggregates which help to understand how LBs and LNs are created and how α-synuclein propagation is done among several brain regions in a prion-like manner (Recasens *et al.*, 2017). Other promoters have been tested (*i.e.* thy-1 and prion) obtaining a broader expression of α-synuclein but similar results about the neurodegeneration (Blandini and Armentero, 2012). These last promoters altogether with an expression of a mutated form of α-synuclein increase motor and cognitive symptoms of these animal models and, until some extent, some neurodegeneration may be observed in different brain areas (Hatami and Chesselet, 2015).

Due to the lack of robust neurodegeneration in α-synuclein transgenic mice, some novel strategies were tried. Inoculation of preformed recombinant human α-synuclein fibrils or human extracted α-synuclein aggregates have also been performed in rodents. They assisted us to map how α-synuclein aggregates spread along neuroanatomical pathways or traffic from the periphery to the central nervous system (CNS) (Luk *et al.*, 2012*a*; Holmqvist *et al.*, 2014). This PD animal model allowed us to test how antibodies can block α-synuclein propagation while it is spreading cell-to-cell (Tran *et al.*, 2014). Despite this utility, neurodegenerative synucleinopathy has only been observed in some studies (Luk *et al.*, 2012*b*; Mougenot *et al.*, 2012). Thus, in order to detect

neuropathological changes, it seems more important the mutant transgene *per se* or the total increase of α-synuclein quantity.

Viral vector-mediated α-synuclein overexpression strategy appeared as an intention to solve the issues presented before (Albert *et al.*, 2017). This system allowed producing high quantities of wild-type or mutated α-synuclein selectively in dopaminergic neurons but not during developmental stages. Lentiviral and adeno-associated virus (AAV) are the ones mainly used and they are normally injected in one of the two hemispheres using the other as a control. Both rodents and non-human primates can be employed. In general terms, they are able to induce α-synuclein accumulation and dopaminergic neurodegeneration (Klein *et al.*, 2002; Yamada *et al.*, 2004; Gorbatyuk *et al.*, 2008, McFarland *et al.*, 2009*b*, *a*; Chung *et al.*, 2009; da Silveira *et al.*, 2009; Cao *et al.*, 2010; Koprich *et al.*, 2010; Sanchez-Guajardo *et al.*, 2010, 2013*a*; Ulusoy *et al.*, 2010; Lam *et al.*, 2011; Taschenberger *et al.*, 2012; Harms *et al.*, 2013; Febbraro *et al.*, 2013; Gombash *et al.*, 2013; Daher *et al.*, 2014, 2015; Davies *et al.*, 2014; Bourdenx *et al.*, 2015; Thome *et al.*, 2015; Van der Perren *et al.*, 2015, Qin *et al.*, 2016*a*; Soria *et al.*, 2017) and some of them behavioural changes too, such as motor asymmetry (*i.e.* cylinder test or apomorphine/amphetamine-induced rotations) or depressive-like symptoms (Decressac *et al.*, 2011, 2012*a*, 2013; Koprich *et al.*, 2011; Gaugler *et al.*, 2012; Lastres-Becker *et al.*, 2012, 2016; Caudal *et al.*, 2015; Daniel *et al.*, 2015; Van der Perren *et al.*, 2015; Soria *et al.*, 2017). Moreover, some studies have reported an immune response mediated by both microglia/monocyte-derived macrophages and lymphocytes (Theodore *et al.*, 2008; Chung *et al.*, 2009; Cao *et al.*, 2010; Sanchez-Guajardo *et al.*, 2010, 2013*a*; Lastres-Becker *et al.*, 2012, 2016; Febbraro *et al.*, 2013; Harms *et al.*, 2013; Daher *et al.*, 2014, 2015; Thome *et al.*, 2015, 2016; Van der Perren *et al.*, 2015; Daniel *et al.*, 2015, Qin *et al.*, 2016*a*; Soria *et al.*, 2017; Thakur *et al.*, 2017; Jimenez-Ferrer *et al.*, 2017). They required shorter timecourses

compared with transgenic mice but similar to α-synuclein inoculation (about 8-16 weeks) (Visanji *et al.*, 2016; Volpicelli-Daley *et al.*, 2016). Nonetheless, factors such as species and subspecies of rodents, timecourse, titration of the viral vector, method of purification, total viral units inoculated, capsid, promoters, enhancers and post-transcriptional regulatory elements, the use of wild-type or mutated α-synuclein and adding a green fluorescent protein (GFP) to tag the overexpression create high variability among studies as there is no gold-standard protocol. Some studies have reported how GFP can elaborate an immune response (Ansari *et al.*, 2016), making empty vectors (EV), altogether with the contralateral side, a current more popular control.

1.2 Immune system

All multicellular organisms need to defend themselves against infections provoked by pathogens (Chaplin, 2010; Marshall *et al.*, 2018). While invertebrates use relatively simple defense strategies including barriers, toxic molecules and phagocytic cells, vertebrates have, in general, a more complex immune system (Rinkevich, 1999; Cooper and Alder, 2006; Boehm, 2011; Gasteiger *et al.*, 2017). It can be classified in two families according to its specificity when getting rid of pathogens: 1) innate immune system and 2) adaptive immune system.

The innate immune system (*i.e.* neutrophils and macrophages) is the first line of defense (Nicholson, 2016). Some authors define it as the 'deployment of germline encoded receptors to identify noxious elements' (Rinkevich, 1999). Adaptive immune system can mount much more sophisticated and specific responses against pathogens compared with the innate immune system. However, it does it in a slower fashion. In contrast with the innate immunity, the adaptive one is based on gene rearrangement processes (Rinkevich, 1999). Both cell families are tightly connected. In front of a pathogen, innate immune system begins to act trying to erase it but at the same time calls the adaptive immune system into play. The latter creates a more specific immune response to eliminate the pathogen from the entire body and it raises long-lasting immune memory. In the case pathogen reenters the body, this immune memory would help to erase it more rapidly and efficiently (Chaplin, 2010; Nicholson, 2016). Due to the fact that these responses are destructive, it is crucial that the adaptive immune response is raised around foreign pathogens but not against the host itself. Immune tolerance, acquired during the development, avoids the recognition of the host's own molecuules (Chaplin, 2010). Occasionally, tolerance can fail and it is then when an autoimmune response happens. Innate immune system does not always call the adaptive immune system when foreign

molecules are found. It is important that this call takes place only when foreign molecules express pathogen-associated immunostimulants which are a typical feature of host-invading pathogens (Chaplin, 2010). An uncontrolled adaptive immune response against non-harmful foreign agents is called allergy.

An adaptive immune response is raised around a pathogen, but more specifically around a pathogen-derived antigen (*anti*body *gen*erator). The adaptive immune system can distinguish between similar antigens (*i.e.* differing in only a single amino acid). Adaptive immune responses are carried out by white blood cells called lymphocytes. Two general processes can be distinguished here: 1) antibody immune responses (mainly B cells) and 2) cell-mediated immune responses (mainly T cells). In the former, B cells are activated differentiating to plasma cells and, then, they secrete antigen-specific antibodies called immunoglobulins which bind specifically to the foreign antigen which stimulated antibody production (Alberts *et al.*, 2002; Murphy, 2011). This binding will provoke the total antibody-dependent opsonization of the pathogen. Opsonized pathogens will not be able to bind to host cell receptors. Moreover, antibody opsonization is a warning mark for the immune system to direct its cells to phagocytose the opsonized pathogen.

In cell-mediated immune responses, activated T cells react directly against a foreign antigen which is presented to them on the surface of a host cell (Chaplin, 2010). Some T cells [*i.e.* CD8+ cytotoxic T lymphocytes (CTLs)] can directly kill the cell which presents the foreign antigen. Other T cells [*i.e.* CD4+ helper T cells (HTLs)] produce signal molecules which regulate the immune response in general. However, this is a generalization as both CD8+ and CD4+ T cells have several subpopulations with a great variety of functions, some of them practically opposite.

A physiological immune response involves many subsets of leukocytes. These subsets can be discriminated morphologically by a combination of histological stains which specifically recognize cell phenotype-determining antigens which are assigned with cluster of differentiation (CD) numbers (Chaplin, 2010). Human Cell Differentiation Molecules (HCDM) is an organization that periodically reviews these cell surface molecules published at http://www.hcdm.org/.

1.2.1 Innate immune system

The innate immune system, firstly described by Novel Prize awarded Ilya Mechnikov (Turvey and Broide, 2010), includes different aspects such as secreted mucus layer in some epithelium and its respective epithelial cilia that seep away this mucus layer refreshing it. It also includes soluble proteins and bioactive small molecules permanently present in biological fluids (*i.e.* complement proteins) or released after cell activation such as cytokines (regulating immune response), chemokines (attracting inflammatory leukocytes) and reactive free radical species among others (Chaplin, 2010; Gasteiger *et al.*, 2017). Some authors consider physical barriers (*i.e.* epithelial cell layers expressing tight cell-cell contacts) a part of the innate immune system meanwhile others do not (Turvey and Broide, 2010). Finally, in order to distinguish immunostimulant pathogen-dependent patterns from host molecules, they express membrane bound receptors and cytoplasmic proteins that bind and recognize them (Chaplin, 2010). This limited repertoire of receptors is compensated with the fact that they target conserved components shared by groups of pathogens (Turvey and Broide, 2010).

Cells which comprise the innate immune system come from both hematopoietic and non-hematopoietic origins (Gasteiger *et al.*, 2017). The former includes

macrophages, dendritic cells, mast cells, neutrophils, eosinophils, natural killer (NK) cells and NK T cells. The latter are epithelial cells from several organic systems such as respiratory, gastrointestinal and genitourinary tracts which are in close contact with the outside (Turvey and Broide, 2010).

Macrophages, as it will be discussed in more detail in following sections, are the main phagocytes of the innate immune system (Turvey and Broide, 2010; Gasteiger *et al.*, 2017). They also scan the tissue in which they reside participating continuously in tissue homeostasis, integrity and development (Lewis and Pollard, 2006; Chovatiya and Medzhitov, 2014; Kotas and Medzhitov, 2015; Okabe and Medzhitov, 2016). Macrophages have both pro-inflammatory and anti-inflammatory roles in an immune response, according to its stage and environmental cues. They express several membrane and intracellular receptors to work properly as environmental scanners (Okabe and Medzhitov, 2016). Macrophages act as antigen presenting cells (APCs) which through major histocompatibility complex (MHC) class-II can present peptide antigens to B lymphocytes and CD4+ T cells. Dendritic cells, as well as macrophages, are APCs (Mellman and Steinman, 2001; Sato and Fujita, 2007). They have important roles in regulating the immune response mediated by T cells, inducing immune tolerance in some occasions (Banchereau *et al.*, 2000; Shortman and Liu, 2002; Wilson and O'Neill, 2003) and work as vigilant for the innate immune system (Rescigno and Borrow, 2001; Iwasaki and Medzhitov, 2004). Mast cells are immune cells of the myeloid lineage and are present in connective tissues throughout the body (da Silva *et al.*, 2014). They participate in allergy reactions. The activation and degranulation of mast cells significantly modulates many aspects of physiological and pathological conditions. With respect to normal physiological functions, mast cells are known to regulate vasodilation, vascular homeostasis, innate and adaptive immune responses, angiogenesis, and venom detoxification (Krystel-Whittemore *et al.*, 2016).

These granules contain several inflammatory mediators (*i.e.,* histamine, heparin, chondroitin sulfate and several cytokines). However, they cannot be found in brain and retina under physiological conditions (da Silva *et al.*, 2014). Bone marrow derived eosinophils work controlling parasitic infections and have some defensive tasks against bacterial and viral pathogens (Ramirez *et al.*, 2018). They act against pathogens releasing their granules which contain several cytotoxic proteins: eosinophil peroxidase, major basic protein, ribonucleases, eosinophil cationic protein and eosinophil-derived neurotoxin among others (Rosenberg *et al.*, 2013). Moreover, they express surface receptors for ligands that support their growth, development, chemotaxis, degranulation and cell-to-cell interactions such as IL-5Rα, CCR3 and some sialic-acid binding immunoglobulin-like receptors (Rosenberg *et al.*, 2013; Klion *et al.*, 2020). Neutrophils present a fast phagocytosis response against small size microbial organisms frequently followed by phagocytosis-induced cell death. For big microbial organisms which cannot be easily phagocytized, neutrophils are induced to release neutrophilic granules (Gasteiger *et al.*, 2017). These granules contain metalloproteases which facilitate cell extravasation and proteases which efficiently degrade bacterial and fungal proteins (Häger *et al.*, 2010). They also release neutrophil extracellular traps (NETs) which are made of chromatin and form sticky fibrils around pathogen (Brinkmann *et al.*, 2004; Yipp and Kubes, 2013) to impede its moving capacities. After long-lasting contact with the foreign pathogen, neutrophils undergo cell death (Gasteiger *et al.*, 2017).

In addition to the myeloid cells presented above, some lymphoid-derived cells have innate immune response roles. In contrast with typical B and T lymphocytes, innate lymphoid cells (ILCs) are CD127- CD90- (Gasteiger *et al.*, 2017). Ostensibly, ILCs mirror CD4+ T lymphocyte functions, meanwhile NK cells do the same with CD8+ T lymphocytes (Vivier *et al.*, 2018). They react by

providing proinflammatory and anti-inflammatory feedbacks through regulatory and effector functions. While T cell-dependent responses take some days to be developed, ILCs are significantly faster. ILCs can be divided into several groups according to cytokines and transcription factors expression but one of them has been largely studied: NK cells. NK cells are cytotoxic cells which circulate through blood stream. Their main function is to direct a cytotoxic attack to kill virus-infected and tumor cells. They generally produce interferon-γ (IFNγ) as their main cytokine. NK cells can recognize stressed cells from normal cells via a cluster of germline-encoded recognition receptors (Vivier and Ugolini, 2011). NK cells express MHC class-I-specific inhibitory receptors to recognize MHC class-I in target cells. Some stressed cells down-regulate MHC class-I avoiding antigen presentation, what is called as "missing self". When MHC class-I is absent, MHC class-I receptors in NK cells cannot send inhibitory signals to hamper NK cell activation (Vivier and Ugolini, 2011). MHC class-I inhibitory receptors include the killer cell immunoglobulin-like receptors (KIRs) in humans, lectin-like Ly49 dimers in mouse and lectin-like CD94-NKG2A heterodimers in both species (Anfossi *et al.*, 2006).

Apart from cellular components, innate immunity also has a humoral component including complement proteins, lipopolysaccharide binding protein, C-reactive protein and other pentraxins, collectins, alarmins, cytokines/chemokines as inflammatory regulators and anti-microbial peptides such as defensins. Some of them circulate in the body fluids working as sensors for microbes or with effector mechanisms to facilitate its clearance (Turvey and Broide, 2010).

NK T cells are situated overlapping both innate and adaptive immune systems. NK T cells co-express typical NK cell receptors with T-cell receptor (TCR) invariant α chain (Godfrey *et al.*, 2004, 2015; Kronenberg, 2005; Balato *et al.*,

2009). However, they are considered part of the innate immune response due to its fast response without the need of clonal expansion and differentiation (Tupin *et al.*, 2007). These T cells recognize antigens presented by CD1d molecules (**Figure 7**). They can be also activated, when there is no TCR-antigen engagement, by cytokines from dendritic cells. After activation they regulate the immune response releasing an array of cytokines from pro-inflammatory to anti-inflammatory ones (Crosby and Kronenberg, 2018). Another subset of T lymphocyte, that overlap between innate and adaptive immunities, expresses γδTCR chains. These so-called γδ T cells recognize antigens presented by CD1 molecules, and MIC (MHC class-I chain-related proteins) A/B. They normally act before αβ T cell responses are completely developed, releasing a myriad of cytokines such as IL-17, IL-4 and IFNγ (Chien *et al.*, 2014).

CD1 proteins are encoded in humans and other mammals by 5 genes (CD1A-E). These have an antigen-binding groove like MHC class-I but more hydrophobic. Contrarily to MHC class-I, they are nearly invariant. CD1 molecules present lipid antigens, mostly glycolipids (Brigl and Brenner, 2004; Moody *et al.*, 2005). In the same way as MHC class-I, CD1 molecules travel through the endolysosomal system, where they bind the lipid antigens, to the plasma membrane (Tupin *et al.*, 2007). Polar lipid groups are located upwards the CD1 molecule and altogether with the CD1 will be recognized by TCRs.

1.2.2 Adaptive immune system

One of the main functions of the adaptive immune system is to screen and eliminate stressed cells such as infected by pathogen microorganisms or mutation-induced malfunctioning. In general terms, one could define two main characteristics of the adaptive immune system in comparison with the innate one: 1) antigen specificity due to gene rearrangements of T and B cell receptors

and 2) creation of immune memory (Bonilla and Oettgen, 2010). T cells can recognize peptide antigens presented by MHC class-I in the surface of nucleated cells or presented by MHC class-II in the surface of APCs like macrophages, dendritic cells and microglia (Chaplin, 2010). MHC molecules, also known as HLA, are cell surface glycoproteins that bind peptide fragments of proteins that either have been synthesized by the same cell (MHC class-I) or that have been previously phagocytosed and proteolytically processed in the case of APCs (MHC class-II).

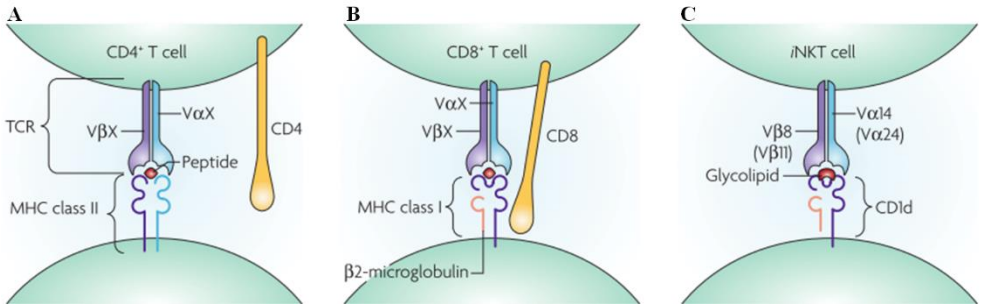

Figure 7. Antigen recognition by T cells. (**A**) Interaction between the complex MHC class-II/peptide and the T cell receptor altogether with CD4 coreceptor. (**B**) Interaction between the complex MHC class-I/peptide and the T cell receptor altogether with CD8 coreceptor. (**C**) iNKT cells recognize glycolipid antigens carried by CD1d with its T cell receptor. "X" indicates variable antigen-receptor chains. Adapted from Tupin *et al.,* 2007.

In humans, there are three major MHC class-I molecules designated as HLA-A, -B, and -C each encoded by distinct genes. They are heterodimers consisting of a polymorphic transmembrane 44kDa α-chain, designated as the heavy chain, associated with the 12kDa non-polymorphic β-2 microglobulin protein (Bjorkman, 1997). The heavy chain determines HLA-A, -B and -C. This complex MHC class-I presents a groove in which antigenic peptides can bind and then be presented in the surface of the cell. This complex MHC class-I and antigen

peptide will be then recognized by their molecular target TCR which contact both components of the complex (Chaplin, 2010) (**Figure 7**). TCR have high affinity for the peptide antigen only when it is carried by MHC class-I and it needs its coreceptor CD8. Thus, not CD4+ helper T lymphocytes (HTLs) but CD8+ cytotoxic T lymphocytes can bind to MHC class-I and peptide antigen complex. This process makes sure that T cells specifically take care of intracellular stressors, leaving extracellular ones for the innate immune system. This selective recognition was named as "MHC restriction" and described by Zinkernagel and colleagues, awarded by the Novel Prize on medicine (Zinkernagel and Doherty, 1997). In contrast with the aforementioned, MHC class-II is recognized by TCR with the CD4 as coreceptor, *ergo*, only CD4+ HTLs can cognate its TCR with MHC class-II (**Figure 7**). Afterwards, HTLs will regulate the immune response releasing a broad variety of cytokines (Bjorkman, 1997).

TCR recognition of its cognate MHC and peptide antigen complex need to work properly and avoid the recognition of self-peptides otherwise autoimmune disease would rise. During T cell maturation in the thymus, TCR are subjected to two processes of quality control: 1) Propensity for binding self MHC molecules (positive selection) and 2) not binding them in extremely high affinities (negative selection) because then self-peptides could be recognized as problematic (Bjorkman, 1997; Marshall *et al.*, 2018).

1.2.2.1 B cells

B cells arise from hematopoietic stem cells in the bone marrow. After maturation, they leave the bone marrow. B cells express B-cell receptor (BCR) and MHC class-II and work as both antibody producers and APCs (Marshall *et al.*, 2018). When BCR encounters its specific antigen, B cells get activated and

start to proliferate and differentiate into antibody-secreting plasma cells or memory B cells. The latter present a long lifespan which would allow a fast response against the same antigen for possible future encounters with it. This activation totally depends on the environmental cues as some of them may provoke B cell apoptosis under antigen encountering (Bonilla and Oettgen, 2010; Tarlinton, 2019).

Five major types of antibodies or immunoglobulins (Ig) can be produced by B cells: IgA, IgD, IgE, IgG and IgM. Each of them has distinct biological functions. IgM is the first immunoglobulin expressed during B cell development which acts opsonizing the antigen and serve for complement fixation. IgG is the second wave of immunoglobulin during the secondary immune response. It helps on neutralizing toxins and viruses in the same way as IgM but with a better outcome due to higher specificities with the antigen. IgA acts on mucosal immune response protecting against toxins, viruses and bacteria through either direct neutralization or preventing them of binding to their receptors. IgE is associated with allergic reactions and parasites. IgD function remains unclear. Overall, antibody response is important in containing virus proliferation during the acute phase of infection. Nonetheless, they alone are not able to eliminate the virus infection and they will require the association of a cell-mediated immune response by T cells (Alberts *et al.*, 2002; Murphy, 2011; Marshall *et al.*, 2018).

1.2.2.2 T cells

T cells arise from hematopoietic stem cells in the bone marrow like B cells (Marshall *et al.*, 2018). Then they migrate to the thymus to finalize its maturation with both positive and negative selections. They express TCRs which are unique for each T cell due to gene rearrangement processes. T cells

get activated after encountering its antigen being presented by MHC class-II+ APCs (CD4+ HTLs) or MHC class-I+ nucleated cells (CD8+ CTLs) and then they proliferate and differentiate. T cells can be sorted out in two general populations, as it has been already mentioned, CD4+ Helper T lymphocytes and CD8+ Cytotoxic T lymphocytes.

1.2.2.2.1 CD4+ helper T lymphocytes

CD4+ HTLs play an important role in regulating the immune response releasing several cytokines once they get activated through recognition of the antigen carried by MHC class-II (Marshall *et al.*, 2018). It is generally accepted that HTLs do not direct cytotoxic attacks to target cells. However, some recent studies have shown that in some scenarios HTLs can express Fas-ligand (FasL) to induce apoptosis in other cells (Brochard *et al.*, 2009; Malyshkina *et al.*, 2017). HTLs are activated through TCR recognition of antigen carried by MHC class-II.

Mossman and colleagues discovered twenty years ago the fact that not all HTLs could express the broad array of cytokines known to be in the T cell repertoire (Mosmann *et al.*, 1986). Some years later, several studies started to describe several subsets of CD4+ HTLs according to their functions and transcription factors expression (Hall, 2015; Goropevšek *et al.*, 2017; Guisier, 2020) (**Figure 8**). T helper 1 (Th1) cells are characterized by thr release of IFNγ and IL-2 which activate macrophages and anti-viral immunity for both extracellular and intracellular pathogens. They also contribute to the differentiation of B cells and, indirectly, antibody production (Marshall *et al.*, 2018). Th2 response is characterized by the production of IL-4, -5 and -13 cytokines involved in IgE production and attraction of eosinophils and mast cells. They have also been reported to express the anti-inflammatory cytokine IL-10 under some scenarios (Bonilla and Oettgen, 2010). As its name indicates, Th17 cells are known for the

release of IL-17 and they have been associated with ongoing inflammatory responses in chronic infection and diseases (Crome *et al.*, 2009). IL-17 induces the production of IL-8 and G-CSF by epithelial cells in order to recruit neutrophils (Weaver *et al.*, 2013). Th17 cells also produce other cytokines such as GM-CSF and IL-22. More recently, other HTL subpopulations have been described: Th9, Th22, follicular T helper (Tfh), regulatory T cell 1 (Tr1) and regulatory T cells (Tregs), the last two showing a pretty similar phenotype. Th9 cells produce IL-9 which acts as a mast cell growth factor. Tfh cells are memory CXCR5+ CD4+ HTLs which reside in follicles (Bonilla and Oettgen, 2010) where they can trigger B-cell activation. Altogether, it seems that each of these HTLs subtypes can regulate several innate immune populations.

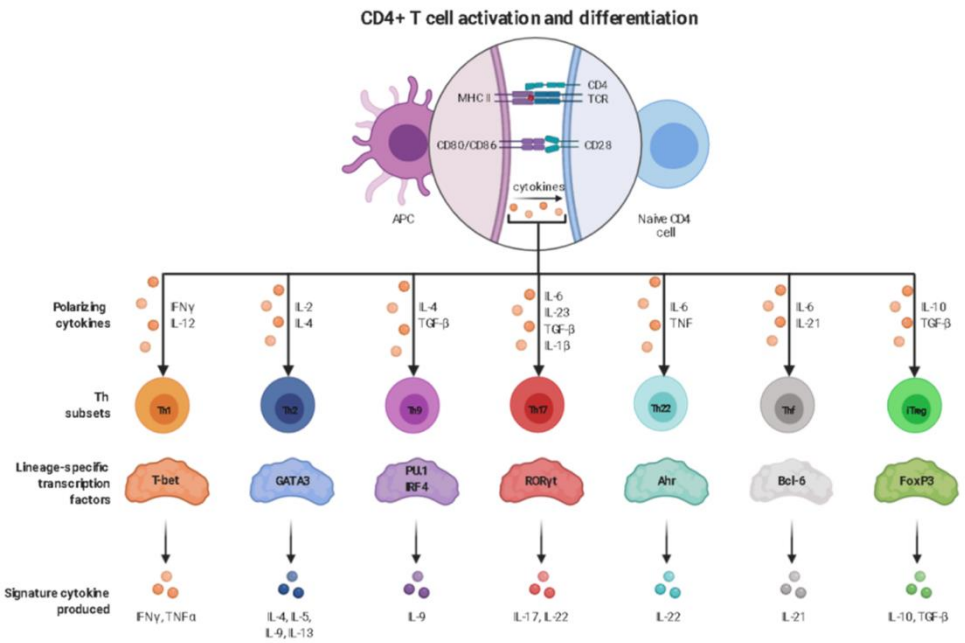

Figure 8. CD4+ Helper T lymphocyte subsets. CD4+ HTLs get activated after recognizing antigen/MHC class-II complex presented by APCs. In this immune synapse, other molecules such as CD80/86 and cytokines are also involved. Depending on the environmental cues and

the polarizing cytokines, CD4+ HTLs can differentiate into several subsets with distinct and sometimes opposite tasks. Adapted from Goropevšek et al., 2017 and Anna Lazaratos according to Hall, 2015 and Guisier, 2020. Created with BioRender.com.

1.2.2.2.1.1 Regulatory T lymphocytes

Naturally occurring CD25+ CD4+ Tregs are a subset of CD4+ HTLs which suppress immune responses and control aberrant immune responses against self-antigens. Thus, they play an important role in developing immune tolerance (Chatila and Angeles, 2005). They also participate during the resolution of an immune response. They constitutively express IL-2Rα, also known as CD25 (Sakaguchi *et al.*, 1995), the transcription factor forkhead box protein 3 (FoxP3), cytotoxic T lymphocyte-associated antigen 4 (CTLA-4) (Read *et al.*, 2000; Takahashi *et al.*, 2000) and glucocorticoid-induced TNF receptor family-related gene (GITR) (McHugh *et al.*, 2002). FoxP3 gene acts as a master switch gene for their development and function (Hori *et al.*, 2017). Absence of FoxP3 gene located in the X-chromosome gives rise to a severe multisystem inflammatory disorder (polyendocrinopathy, X-linked syndrome). According to its role in the immune system, Treg depletion induces autoimmunity against multiple tissues (Sakaguchi *et al.*, 1995). Once Tregs are activated they suppress effector activities of other T cells impeding the release of HTLs conventional cytokines. Tregs typically release IL-10 and transforming growth factor β (TGF-β) as anti-inflammatory cytokines. They can also contact other T cells through CTLA-4 mechanism. Tregs development is still unclear but mounting hypotheses point out the fact that they have high avidity for self-antigens but they are less sensible compared with other T cells to be negatively selected. Their peripheral anti-inflammatory activity is totally dependent on IL-2 and TGF-β, as the latter is necessary for FoxP3 expression. Tr1 cells are a CD4+ T cell population exerting similar functions to Tregs but they secrete IL-10, IL-5

and IFNγ (Groux *et al.*, 1997; Levings *et al.*, 2001). It is thought that they normally participate in diseases in which there is a high antigenic load (O'Garra *et al.*, 2004).

1.2.2.2.2 CD8+ cytotoxic T lymphocytes

Hematopoietic derived CD8+ CTLs have an important role in reacting against pathogens expanding massively their numbers and differentiating into cytotoxic effector cells. They detect stressed cells through complex MHC class-I/antigen in the surface of target cells. However, they first activate in secondary lymphoid organs when they contact with CD4+ T cell-conditioned APCs (Bousso and Robey, 2003; Miller *et al.*, 2003; Mempel *et al.*, 2004). Afterwards, CTLs migrate toward peripheral regions of the lymphoid organ, called T cell zone, close to the subcapsular sinus region and the infected macrophage population (Zhang and Bevan, 2020). In the inflamed tissue they also interact with APCs and other immune cells to orchestrate a combined immune response. With that they further differentiate or clonally expand. At the peak of the primary response to the pathogen, CTL effector population is phenotypically and functionally heterogeneous. The main bulk of CTLs are short-lived effector cells which will die when the infection is cleared. Nonetheless, some CTLs will have differentiated to memory precursor effector cells which will survive and contribute to adaptive immune memory (Mescher *et al.*, 2006; Parish *et al.*, 2013). After recognizing antigen presented by APCs, CD8+ effector CTLs upregulate CXCR3 which will lead them to enter peripheral tissues (Groom and Luster, 2011). In the inflamed tissue, they continue engaging antigen-specific interactions which will cause CTL proliferation and cytokine release (Zhang and Bevan, 2020). CTLs can also produce anti-inflammatory cytokine IL-10 during the acute phase of inflammation. They release it to dampen immunopathology

without reducing viral clearance as they coexpress IL-10 with granzymes and IFNγ (Sun *et al.*, 2009; Palmer *et al.*, 2010; Trandem *et al.*, 2011).

CD8+ CTLs can be classified to several subsets according to the cytokines they express in the same way as CD4+ HTLs (St. Paul and Ohashi, 2020). In general terms, all subsets express, at least, low levels of IFNγ, granzymes, and perforin-1 (PRF-1) which are important to mediate their cytotoxic attack. It is generally believed that memory CD8+ CTLs come from Tc1 subset which, equally to Th1, express high levels of IFNγ (Samji and Khanna, 2017). However, it is unclear whether all CTL subsets can derive to memory CTLs. Currently, Tc17 cells, which express IL-17 (Amancha *et al.*, 2020), have also been observed as memory CTLs. In contrast with Tc1 memory cells, it has been pointed out that Tc17 memory cells express higher levels of tissue resident memory T cells (T_{RM}) marker CD103 (Yen *et al.*, 2009).

1.2.2.2.2.1 Tissue resident memory CD8+ T cells

Tissues which are normally exposed to pathogens are largely surveyed by memory T cells. Until now, memory T cells were thought to be comprised by central memory T cells (T_{CM}) which are restricted to secondary lymphoid tissues and blood, and effector memory T cells (T_{EM}) which migrate through peripheral tissues, the blood and the spleen but they do not stay in any of them. Nonetheless, some years ago, a new group of memory T cells were described called T_{RM} which are normally found in peripheral tissues without migrating. Even though they did not coined the name, T_{RM} cells were firstly described by Kim and Masopust studies (Kim *et al.*, 1999; Masopust *et al.*, 2001). These T_{RM} cells have been described expressing CD44 like both T_{CM} and T_{EM}, lacking CD62L and CCR7 like T_{EM} but, in contrast with both subsets, expressing CD69 and CD103 (αE integrin). After infection, CD69+ CD103+ T_{RM} cells may be found in

several tissues such as skin, gut, vagina, salivary glands, brain and lung airways (Mueller *et al.*, 2013). These tissues share some characteristics such as that they are in contact with the external environment or they are old-typical immunocompetent tissues. Thus, all of them need higher levels of surveillance compared with other tissues. CD69+ CD103- T_{RM} cells may be observed in all tissues but blood (Wong *et al.*, 2016). CD103 is important for T cells residence in peripheral tissues as it is involved in interactions with epithelial cells by binding the ligand E-cadherin. CD69 is believed to play a role in T_{RM} cell retention in peripheral tissues. T_{RM} cells can be maintained in peripheral tissues in absence of the cognate antigen through CD69 upregulation. However, in presence of the antigen, T_{RM} cells upregulate CD103.

1.2.2.2.2.2 CD8+ T cell cytotoxic mechanisms

Initially, due to some *in vitro* experiments, it was thought that CTLs could induce cell apoptosis very efficiently. Their cytotoxic capacity was then coined as "sequential killing", "recycling" or "serial killing" (Halle *et al.*, 2016). CTLs can assemble their cytolytic granule secretion machinery very rapidly and accomplish a target cell lysis with only a few minutes. However, little is known about their cytotoxic capabilities *in vivo*. Some recent microscopy studies have pointed out that "serial killing" in CTLs is not as abundant as previously thought.

CTLs need to detect target cells in a TCR-dependent manner establishing direct cell-to-cell contact. This engagement is known as immunological synapse (Dustin and Long, 2010) (**Figure 9**). CTLs present distinct effector mechanisms to induce a cytotoxic attack to target cells: secretion of PRF-1, granzymes and FasL as death-inducing effector molecules. However, they also secret chemokines and effector cytokines with important effects on the cellular state of the target such as IFNγ, and tumor necrosis factor-α (TNFα).

Perforin-1, at physiological pH and in presence of Ca^{2+}, oligomerizes and creates membrane-spanning pore-like and arcs (Lopez *et al.*, 2013). It is still unclear how this process happens and if it is necessary enough to allow granzymes passage to the target cell cytosol. Some studies have tried to approach this question but it is a topic of debate (Voskoboinik *et al.*, 2015). The target cell then starts repairing the cell membrane to erase these pore-like structures within approximately one minute. Small amounts of granzyme that have been able to enter the target cell in this short timeframe are normally lethal though (Lopez *et al.*, 2013). Granzymes are serine proteases, broadly labelled as trypsin-like or chymotrypsin-like, characterized by their individual substrate specificity. They also induce regulated signalling activating caspase-driven cell death pathways (Shi *et al.*, 1992). Granzymes also regulate inflammation and interfere with viral biosynthetic pathways (Anthony *et al.*, 2010). To sum up, they induce target cell death through distinct, non-redundant pathways that work in a complementary and hierarchical manner (Sutton and Trapani, 2010). Granzyme B (GrzB) is considered the most powerful pro-apoptotic molecule from the granzyme family as it mimics caspases when cleaving proteins. It is important to note here that human and mouse GrzB have important differences, while human GrzB induces cell death in a BH3 interacting domain (BID)-dependent manner, mouse GrzB does it through activating caspases directly. Human GrzB is more toxic than the mouse one (Kaiserman *et al.*, 2006). Granzyme A (GrzA) activates cell death through different substrates to GrzB and in a slower fashion. In contrast with GrzB, mouse GrzA is more toxic than the human one (Kaiserman *et al.*, 2006). GrzA causes athetosis to the target cell, which is a type of cell death dependent on normal actin cytoskeleton physiology that provokes a change of morphology described as “twisting and turning” (Susanto *et al.*, 2013). GrzK is also upregulated by CTLs during influenza virus infection, interfering with viral replication (Jenkins *et al.*, 2008).

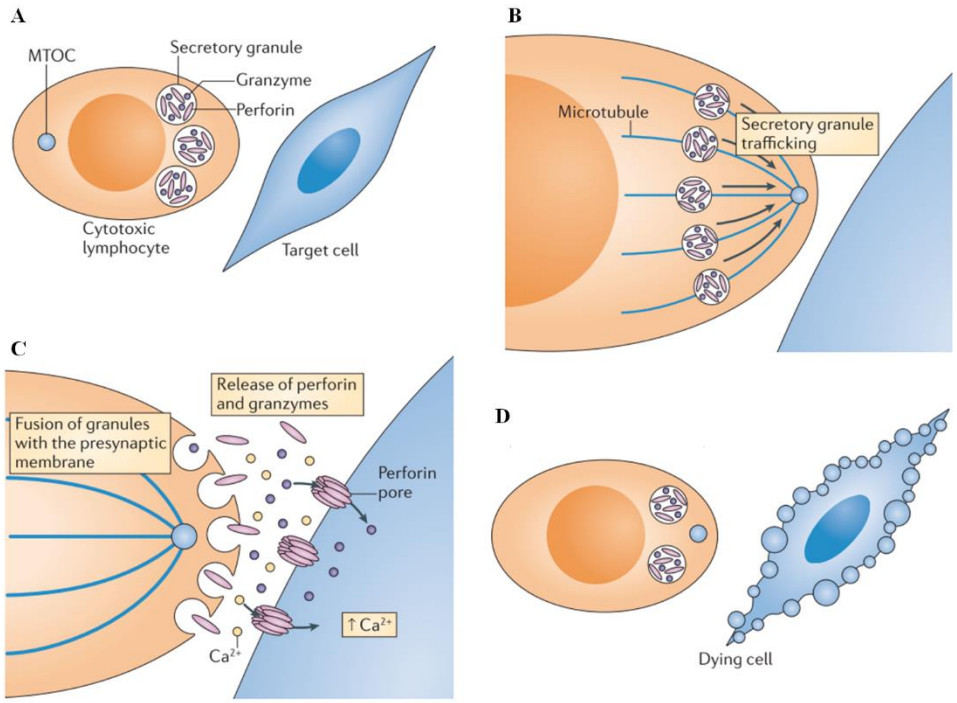

Figure 9. Cytotoxic interaction of a CD8+ T lymphocyte with a target cell. (**A**) A cytotoxic T lymphocyte recognizes its target cell and builds up an immunological synapse. (**B**) The microtubule-organizing centre (MTOC) of the cytotoxic T lymphocyte polarizes and leads to the traffic of secretory granules. (**C**) Secretory granules fusion with the presynaptic membrane and their contents are released to the immune synaptic cleft. Perforin may form pores and other structures in the postsynaptic cell membrane to allow the entrance of granzymes and other molecules. (**D**) Granzymes then initiate apoptosis of the target cell. Adapted from Voskoboinik *et al.*, 2015.

1.2.3 Immune system in the central nervous system

Initially, it was believed that CNS had a unique relationship with the immune system referred as immune privilege. This concept was risen about 100 years

ago when Shirai and collaborators (Murphy and Sturm, 1923; Medawar, 1948; Barker and Billingham, 1977; Carson *et al.*, 2006) demonstrated how tissue grafts into the brain survived long periods of time in comparison with grafting in other body areas (Carson *et al.*, 2006). Previous studies notwithstanding, immunological reactions and autoimmune responses happen inside the brain parenchyma (Forrester *et al.*, 2018). According to this, some more experiments using allografts were performed which locating the same allograft in both brain and skin created an immunization and finally a rejection of the allograft in both tissues. Thus, it seems that in the brain there is some partial tolerance for immune reactions (Medawar, 1948; Engelhardt *et al.*, 2016). This may be explained due to the presence of a semipermeable border of endothelial cells with tight junctions between the brain and the peripheral blood called BBB. Next to endothelial cells, BBB is also constituted by astrocytes end-feet ensheathing the capillary and pericytes embedded in the capillary basement (Engelhardt *et al.*, 2016). BBB permits selective passage of solutes through capillary endothelium into the CNS parenchyma (Ballabh *et al.*, 2004). It also leads the passage of cells such as T lymphocytes through receptor-mediated selective adhesion and diapedesis (Galea *et al.*, 2007; Bartholomäus *et al.*, 2009; Lyck and Engelhardt, 2012). However, they will also need to penetrate the glia limitans which surrounds the BBB. It is widely known and described how an impairment or dysfunction in the BBB complicates neuroinflammatory diseases in the brain (Ballabh *et al.*, 2004). To sum up, immune privilege in the CNS is a result of two factors: 1) BBB restricting entry of immune cells into the CNS and, 2) the absence of a typical lymphatic system in the CNS. Currently, it is widely accepted that CNS undergoes an active immune surveillance which takes place in the meningeal compartment (Louveau *et al.*, 2015*b*). This will be discussed in the next section.

Immunological reactions in the brain and elsewhere comprise two major components: an innate response and an adaptive response (Ransohoff *et al.*, 2015). Specifically for the CNS, the innate response is orchestrated by yolk sac-derived myeloid cells differentiated into brain resident microglia which upon activation can be transformed to macrophages. Nonactivated or homeostatic microglia is highly ramified and its processes are dynamically changing to obtain information about its environment. Neurons and other glia interact with microglia using different ligands to microglia receptors constituting an immune communication about the health status of the brain. MHC class-I and MHC class-II present antigens in the surface of cells when an immune response is on-going. In absence of this immune response, MHC class-I presents self-antigens of the cell to contribute to immune surveillance. Expression of both MHC class-I and MHC class-II in microglial cells has been shown to be down-regulated by normal electrical activity of neuronal cells indicating a healthy status (Neumann, 2001). Thus, in pathological conditions, an increase of cytokines expression and an abnormal neuronal activity induce the expression of MHC class-I and MHC class-II in microglial cells which will play the role of APCs exposing these antigens to T lymphocytes (Bartholomäus *et al.*, 2009; Kivisakk *et al.*, 2009; Lodygin *et al.*, 2013). Other APCs such as macrophages and dendritic cells also present antigens but in perivascular spaces and they express both MHC class-I and MHC class-II constitutively. These perivascular spaces are compartments within the walls of capillaries, arterioles and arteries and spaces around postcapillary venules (Engelhardt *et al.*, 2016). More details about microglial cells and monocyte-derived infiltrating macrophages will be exposed in the following sections.

1.2.3.1 Meninges, cerebro-spinal fluid and glymphatic system

The brain is surrounded by several layers of protection including the skull and the meningeal triad of membranes: dura, arachnoid and pia mater (Abbott *et*

al., 2018). The former is the outermost membrane just beneath the skull and it consists of both fibrous and cellular components (Alcolado *et al.*, 1988; Vandenabeele *et al.*, 1996). Arachnoid mater consists of an impermeable cellular barrier between the dura and the pia mater which envelops the CNS (Aspelund *et al.*, 2015). The region comprised between arachnoid and pia mater is known as subarachnoid space. In contrast with the arachnoid one, pia mater is permeable with solutes and immune cells (Hutchings and Weller, 1986). Cerebro-spinal fluid (CSF) is constrained in the subarachnoid space (Louveau *et al.*, 2015*a*) which has a dense stroma and it is traversed by arterial vessels which go deep into the CNS (Ransohoff and Engelhardt, 2012). These arterial vessels are lined up by arachnoid and pia mater for several millimeters once they enter the CNS. This leads the creation of perivascular spaces termed as Virchow-Robin spaces. These perivascular spaces are then enclosed and delimited by an endothelial basement membrane of the BBB (Engelhardt *et al.*, 2017).

Regarding to the lymphatic system, there are two extracellular fluids within the cranial and spinal cavities which could carry antigen or APC to regional lymph nodes (**Figure 10**). These lymph nodes are the cervical and lumbar ones as resecting them induce changes in T cell compartment in meningeal spaces (Louveau *et al.*, 2015*b*). CSF is one of the fluids and it is found in the ventricles and subarachnoid spaces. CSF is a fluid produced by the choroid plexus in the cerebral ventricular system at the rate of 350µl/min in humans. It consists of products derived from arterial blood through diffusion and active transport. CSF circulates from the ventricles through brainstem thanks to pulsations of the choroid plexus and the action of cilia on ependymal cells that line ventricles (Ransohoff and Engelhardt, 2012; Engelhardt *et al.*, 2016). Finally, it is reabsorbed into blood at arachnoid villi. Interstitial fluid (ISF) is the other fluid and it is found in the extracellular spaces of the CNS parenchyma (Engelhardt

et al., 2016). Although they drain to the same lymph nodes, CSF drains from the subarachnoid space into the lymphatic vessels in the cribriform plate of the nasal mucosa in mammals through Virchow-Robin spaces (Cserr *et al.*, 1992; Kida *et al.*, 1993; Girard *et al.*, 2012; Aspelund *et al.*, 2015; Jessen *et al.*, 2015). Existence of dura mater lymphatic vessels has been discussed since eighteenth century (Schwalbe, 1869; Andres *et al.*, 1987; Cserr and Knopf, 1992; Kida *et al.*, 1993; Bucchieri *et al.*, 2015), but increasing body of evidence supports its existence. In mice it has been recently demonstrated the presence of functional lymphatic vessels in the dura mater draining from the cribriform plate (Aspelund *et al.*, 2015, Louveau *et al.*, 2015*b*). This flow from the CSF allows carrying both antigens and lymphoid cells such as CD3+ T lymphocytes, which have been observed in high quantities around lymphatic vessel endothelial hyaluronan receptor 1 (LYVE-1)+ dura sinuses (Louveau *et al.*, 2015*b*).

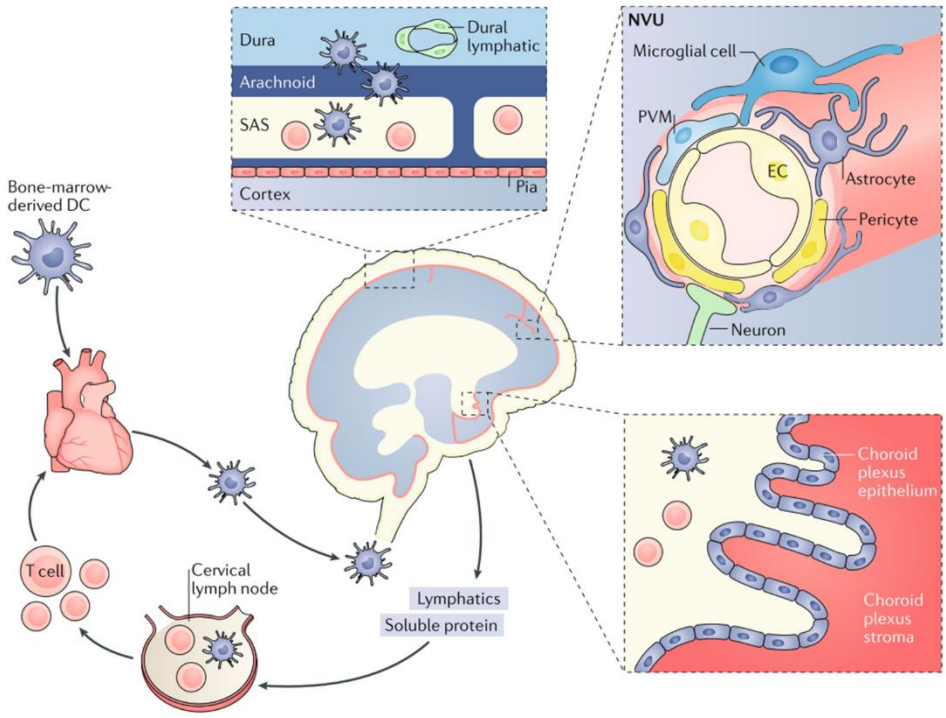

Figure 10. Immune trafficking through the central nervous system. In steady-state conditions dendritic cells act as 'sentinels' of the immune system and 'patrol' brain-covering tissues without practically not infiltrating the brain parenchyma. In homeostasis, soluble CNS antigens are drained to CNS fluids by means of glymphatic system and travel to lymph nodes. This process can also occur through the meningeal lymphatics or the cribriform plate. *EC* endothelial cell; *PVM* perivascular macrophage; *SAS* subarachnoid space. From Forrester *et al.,* 2018.

On the other hand, ISF flows in two different manners: 1) from the brain parenchyma itself to lymph nodes or 2) in exchange with CSF in Virchow-Robin spaces. This drainage goes through thin pathways that comprise 100-150nm basement membranes in the walls of blood vessels what is known as glymphatic system. ISF does not carry APC but antigens. This fact could explain somehow the immune privilege of the CNS (Engelhardt *et al.*, 2016). Whereabouts of the glymphatic system were initially described by Iliff and colleagues (Iliff *et al.*, 2012) performing two-photon fluorescence imaging of small tracers inoculated in the cistern magna. They showed the flow of CSF and ISF through all compartments mentioned above and the importance of aquaporin-4 in this process. Furthermore, the glymphatic system works as a waste clearance system to eliminate soluble proteins, metabolites but also helps on distributing non-waste compounds (Jessen *et al.*, 2015; Louveau *et al.*, 2017; Abbott *et al.*, 2018; Rasmussen *et al.*, 2018; Benveniste *et al.*, 2019).

1.2.3.2 Innate immune system: Microglia and monocyte-derived macrophages

Microglia is a cell type of glia described by Pío del Río Hortega (Ramon and Agüeras, 2016) derived from the yolk sac and it represents about 10 per cent of all glial cells in the brain (Verkhratsky and Butt, 2007). Its progenitors invade

the CNS during the development of the fetus (Alliot *et al.*, 1991; Ginhoux *et al.*, 2010; Schulz *et al.*, 2012). They form dense clusters in the *corpus callosum* called *fountains of microglia* firstly described by Pío del Río Hortega (Verkhratsky and Butt, 2007; Ransohoff and Brown, 2012). Generated microglial population is then maintained by region-dependent self-renewal under physiological conditions (Lawson *et al.*, 1992). Microglial cells reside in all parts of the brain. However, in human CNS higher densities of microglia can be found in white matter regions (Mittelbronn *et al.*, 2001). Among grey matter regions highest densities of microglia have been described in the hippocampus, olfactory telencephalon, basal ganglia and substantia nigra (Verkhratsky and Butt, 2007), some of these brain areas prominently affected in PD (Giguère *et al.*, 2018). In neurodegeneration or CNS inflammation, microglia can clonally expand to increase their numbers. However, their numbers are restored by apoptosis after damage resolution (Madore *et al.*, 2017; Tay *et al.*, 2017). It is important to note here that after BBB disruption monocyte-derived macrophages can infiltrate the CNS. Although they will not modify the final physiological number of the microglial pool, they may have important roles in neuroinflammation (Ajami *et al.*, 2011; Ginhoux and Garel, 2018).

Microglial cells are highly important in keeping the CNS in good homeostasis (Luo and Chen, 2012; Ousman and Kubes, 2012; Harry, 2013; Kipnis and Filiano, 2018; Norris and Kipnis, 2019). They participate in synapse pruning and maintenance mainly during healthy CNS development (Hong *et al.*, 2016; Sellgren *et al.*, 2019). During adulthood, they also participate in synapse remodeling, regulation of adult neurogenesis (Gemma and Bachstetter, 2013), learning and memory processes (Parkhurst *et al.*, 2013) and activity-triggered synaptic plasticity (Sipe *et al.*, 2016; Salter and Stevens, 2017). They also provide trophic support to neurons and other cell types of glia (Nakajima *et al.*, 1998; Batchelor *et al.*, 1999). Microglial cells contribute in tripartite synapse

(Volterra *et al.*, 2002; Kettenmann *et al.*, 2011) taking up neurotransmitters such as glutamate in order to avoid excitotoxicity (Shaked *et al.*, 2005). They also have a role in waste clearance as they are the primary CNS cell type involved in phagocytosis of cell debris (Li *et al.*, 2005; Popovich and Longbrake, 2008) such as NM due to dopaminergic cell loss (Carballo-Carbajal *et al.*, 2019).

However, the main role and the most interesting one for this thesis is that microglia serve as first line defenders against infectious agents and injury-related products in the brain (Verkhratsky and Butt, 2007; Ransohoff and Perry, 2009). Every microglial cell occupies a space interacting with its environment and neighboring cells (Raivich, 2005). They have minimal overlap of their branches to optimize the space they are immune-surveilling which is about 50000μm^3 each cell. During its homeostatic or non-activated state, their branches are constantly scanning its neighborhood (Nimmerjahn *et al.*, 2005; Raivich, 2005) at a mean speed of 1.2-1.5μm/min approximately. This state is also known as "resting microglia", but this gives rise to confusion due to the fact that in reality they never stop sampling their surroundings. These homeostatic microglia constitutively express MHC class-II in the healthy brain in order to perform this immune surveillance more efficiently (Hayes *et al.*, 1987). However, as it was mentioned above, its expression is immune response-dependent. Whether CNS is in a healthy status and there is normal neuronal activity, MHC class-II in microglial cells is down-regulated (although not completely silenced) (Ulvestad *et al.*, 1994). On the contrary, during an immune response, MHC class-II and other molecular markers of antigen presentation and activation are up-regulated such as CD11a, CD40, CD54, CD58, CD80 and CD86 (Akiyama and McGeer, 1990; Shrikant and Benveniste, 1996). It has been postulated that even aging could be enough to increase microglia activation (Perry and Teeling, 2013). This process is known as "microglia priming" (Wolf *et al.*, 2017). In different animal models such as rodents and non-human

primates, it has been reported an increase of cell inclusions and activation markers. In addition to this, highly ramified non-activated microglia is decreased meanwhile ameboid morphologies of activated microglia are increased (**Figure 11**) (Perry *et al.*, 1993; Ogura *et al.*, 1994; Sheffield and Berman, 1998; Sloane *et al.*, 1999; Conde and Streit, 2006; Karperien *et al.*, 2013). In aged human brain, only morphological changes and increase of MHC class-II staining has been described (Rogers *et al.*, 1988; DiPatre and Gelman, 1997; Streit and Sparks, 1997; Luo *et al.*, 2010; Harry, 2013; Zrzavy *et al.*, 2017, 2018). Altogether, these changes make primed microglia to become more responsive to proinflammatory stimuli (Wolf *et al.*, 2017). This priming is not aging specific, but it is also observed in a broad variety of neuropathological diseases. It has been proposed that microglia priming is due to a persistent neuroinflammation or chronic exposure to misfolded proteins or cell debris.

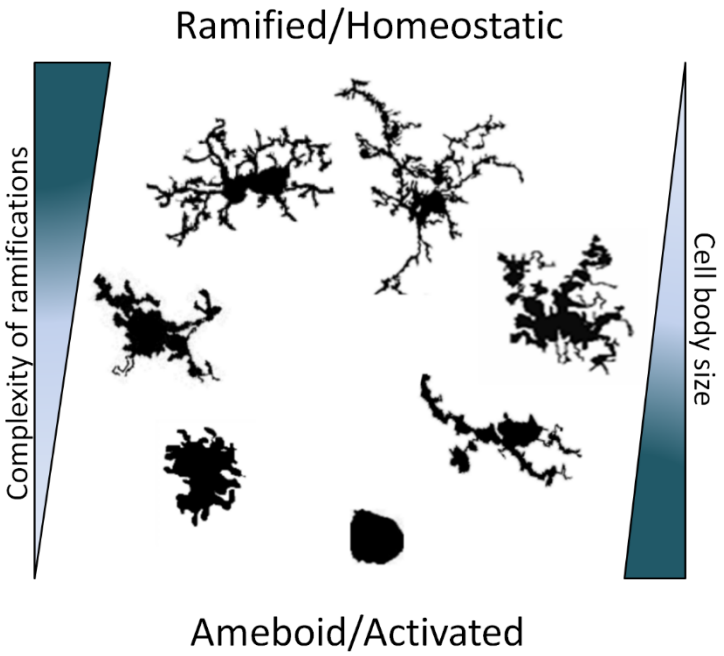

Figure 11. Microglial morphology in adult human brain. Microglia are morphologically and functionally dynamic cells able to change form from highly ramified with small cell body to non-ramified ameboid morphologies with big cell body. Intermediate morphologies can also be found. Shapes are not shown to scale. Adapted from Karperien *et al.,* 2013.

As it has been previously commented, non-activated or homeostatic microglia have a highly ramified morphology composed by a multitude of fine processes which emanate from a small cell body. Meanwhile processes have high motility in order to scan the environment, their soma has a more fixed position (Nimmerjahn *et al.*, 2005). They permanently and constitutively detect, transduce, integrate, and respond to external stimuli to maintain CNS homeostasis (Butovsky and Weiner, 2018). Signs for brain lesions or neuronal dysfunction induce a complex, multistage process of microglial "activation" (Perry *et al.*, 2010; Kettenmann *et al.*, 2011). They suffer changes in gene expression causing changes in intracellular enzymes and surface molecules (*i.e.* MHC class-II). They clonally proliferate and are attracted to the lesion by gradients of chemotactic signals. Once there, microglia are able to release a large number of substance such as cytokines which have important regulatory effects on neuroinflammation, trophic factors and chemokines which recruit other immune cell populations to the CNS (*e.g.* T lymphocytes) and present antigens to them (Perry *et al.*, 2010; Heneka *et al.*, 2014; Salter and Stevens, 2017).

Upon activation, microglial cells shorten their processes and increase their soma's size adopting an ameboid morphology. This activation is a continuous gradient and some microglia can be found in intermediate states (Boche *et al.*, 2013). However this is a simplification which is generally useful, as microglia are highly plastic cells and they can exist in distinct functional phenotypes (**Figure 12**) (Gordon and Taylor, 2005; Mosser and Edwards, 2008). These

grades of microglial activation cannot only be assessed either by morphology or cell surface antigens, hence multi-modular approaches need to be used (Perry *et al.*, 2010; Prinz and Priller, 2014). Activation of microglia has usually been associated with negative effects (Cherry *et al.*, 2014). However, this initial concept of microglia being harmful upon activation was replaced. Afterwards, microglial activation was viewed as a dichotomy depending on the pro- or anti-inflammatory cues which they sensed. M1/M2 designation was firstly described in macrophages and then used in microglia. Microglia activated via toll-like receptors (TLR) or IFNγ are known as M1 or classically activated microglia. This microglia state produces ROS and pro-inflammatory molecules such as IL-1β, IL-2, IL-6, IFNγ, c-x-c motif chemokine ligand 9 (CXCL9), CXCL10, iNOS, cyclooxygenase 2 (COX2) and/or TNFα (Varnum and Ikezu, 2012; Chhor *et al.*, 2013; Fenn *et al.*, 2014). M1 microglial cells are involved in killing intracellular pathogens and cytotoxicity, antigen presentation and induction of Th1 and Th17 lymphocytes (Cherry *et al.*, 2014; Franco and Fernández-Suárez, 2015). On the other hand, microglia with an anti-inflammatory phenotype are known as M2 or alternative activated state (Gordon, 2003). M2 microglia are involved in the resolution of inflammation, wound repair, and debris clearance. M2 microglial cells can also be classified in three distinct subtypes according to the cues they detected. M2a is characterized by the expression of anti-inflammatory molecules including arginine 1 (Arg1), mannose receptor (MR), TGFβ, among others (Chhor *et al.*, 2013; Gadani, Sachin P; Cronk, 2013). M2b microglial phenotype highly expresses IL-10, an anti-inflammatory cytokine. Altogether with MHC class-II and CD86, this microglial form helps on inducing a Th2 T cell response (Mosser and Edwards, 2008; Filardy *et al.*, 2010). Finally M2c microglial phenotype is also anti-inflammatory releasing molecules such as CXCL13 and expressing sphingosine kinase and suppressor of cytokine signaling 3 (Fenn *et al.*, 2012; Varnum and Ikezu, 2012; Chhor *et al.*, 2013). This

last form is normally involved in tissue repairing when negative/destructive inflammation has been resolved (Mantovani *et al.*, 2004).

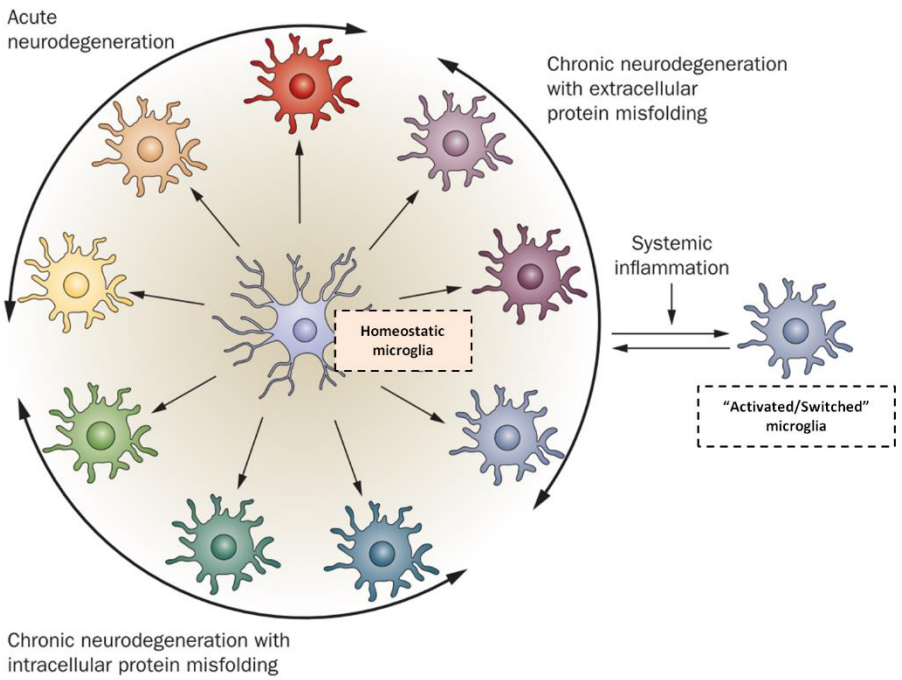

Figure 12. Microglial phenotypes. Resident homeostatic microglia can become activated/switched to adopt one of many diverse possible phenotypes depending on the environmental cues. These diverse phenotypes are represented by less ramified microglia of differing colours. Adapted from Nicoll &Perry, 2010.

To sum up, microglia activation is a complex process in which morphology and gene expression changes occur. In order to obtain a detailed picture of the scenario a multi-approach has to be performed. However, due to technical complexity and availability of post-mortem human tissue, morphological analysis may be informative for microglial activation grade (Stence *et al.*, 2001; Boche *et al.*, 2013; Anttila *et al.*, 2017; Heindl *et al.*, 2018). Correlation with

neuropathological markers of the disease may also help to elucidate its pro-inflammatory or anti-inflammatory roles.

1.2.3.3 Adaptive immune system in the CNS under physiological conditions

As it has been commented in previous sections, CSF is a fluid found in ventricles and subarachnoid spaces. CSF is produced by choroid plexus from the blood and, in low quantities, by the ISF. Some of the cell debris and molecules that normally carries may work as potential antigens. Some of the drained CSF can go to lymph nodes and, in that position, their content can be presented to APCs (**Figure 13**). In physiological conditions, it has been described that CSF is populated by mainly memory CD4+ HTLs. These CSF T cells express several markers for lymph node homing such as CCR7 (Giunti *et al.*, 2003; Kivisäkk *et al.*, 2003; Kivisakk *et al.*, 2009; De Graaf *et al.*, 2011).

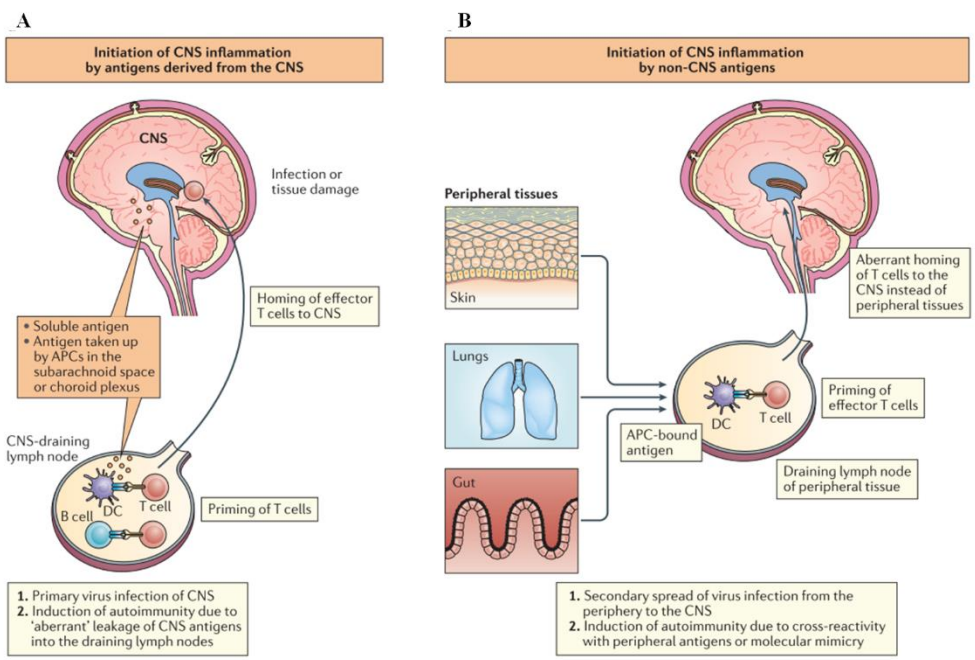

Figure 13. T cell immunity in the central nervous system. (**A**) Central nervous system inflammation resulting from adaptive immune responses against target CNS antigens which have been drained to the cervical and lumbar lymph nodes. They can be transported to the lymph nodes either in a soluble form or via APCs. Once T cells are primed by antigen-carrying APCs, they home back to the CNS in order to erase foreign antigens or to cause autoimmunity. (**B**) T cells can be primed by non-CNS antigens which mimic CNS antigens or viral-derived antigens due to systemic infection. Adapted from Korn & Kallies, 2017.

After the paradigmatic point of view change of the brain as an immunoprivileged organ, mounting evidence showed how lymphocytes could gain access to enter the brain. Several entrance routes have been noted: 1) endothelial cells of parenchymal vessels, 2) subarachnoid space, 3) circumventricular areas and 4) choroid plexus. All these routes share the fact that lymphocytes need to go through the BBB (Loeffler *et al.*, 2011; Korn and Kallies, 2017).

In 2011, there was a study which performed an extensive immunohistochemical study detecting several adaptive immune cell types in distinct brain regions (Loeffler *et al.*, 2011). These regions were selected according to differences of the BBB properties. They did not count separately both parenchymal and perivascular cells. Few CD20+ B cells were observed and they did not differ between distinct areas. Distribution of CD3+ T cells did not reach statistical significance but there were high densities in both *medulla oblongata* and area postrema in comparison with visual cortex. The bast majority of these T cells were CD8+ CTLs. Practically no CD4, CD25, FoxP3, GrzB and PRF-1 stainings were reported. They also concluded that brain areas with less complex BBB presented more CTL densities. It has been hypothesized that the presence of these CTLs in the physiological brain helps to keep CNS-tropist viruses in a latent state. Smolders and collaborators approached this hypothesis

with two elegant and informative studies. Their main goal was to deeply characterize brain T cells which were in both perivascular spaces and parenchyma. In the first study, they recollected peripheral blood (PB) and *corpus callosum* (CC) from the same cases to compare the T cell phenotype and see which type of T cells are enriched in the CC (Smolders *et al.*, 2013). They found higher number of CD8+ T cells than CD4+ ones, in line with Loeffler's study. These T cells were differentiated, and they expressed CX3CR1 and CXCR3 typical markers of homing to inflamed tissue (Fumagalli *et al.*, 2013). Brain T cells did not express PFN1, GrzA and GrzB. In the second study (Smolders *et al.*, 2018), they aimed to demonstrate the hypothesis that the majority of these brain CTLs present a tissue resident phenotype (T_{RM}). In order to do that, distinct human white matter tissues underwent flow cytometry or immunofluorescence procedures. CD8+ T cells outnumbered, again, CD4+ T cells. The vast majority of T cells were located in the perivascular space. A great percentage of brain T cells presented a T_{RM} phenotype expressing CD69 and/or CD103. T_{RM} cells also expressed several markers such as tissue-homing chemokine receptors. These T_{RM} cells expressed several granzymes, although in lower levels compared with effector CTLs. PFN1 was practically absent in both effector and tissue-resident CTLs. T_{RM} cells showed production of IFNγ and TNFα. Finally, in contrast with effector CTLs, T_{RM} cells expressed immune checkpoint markers *i.e.* CTLA-4 and PD-1.

In conclusion, the hypothesis that T lymphocytes, mainly CD8+ T cells, function as CNS immune surveillants seems quite reliable (Cabarrocas *et al.*, 2003; Korn and Kallies, 2017). One study showed how antigen-specific brain T_{RM} cells gained effector properties after viral reinfection (Steinbach *et al.*, 2016). However, differences between perivascular and parenchymal T cells are still unclear as only immunochemical procedures can approach this issue. T cells in both compartments could have distinct roles and dynamics.

1.3 Neuroinflammation in Parkinson's disease

It is becoming increasingly apparent that the immune system has a vital role in the etiopathogenesis of PD (**Figure 14**) (Kannarkat *et al.*, 2013; Wang *et al.*, 2015; Joers *et al.*, 2017; Stephenson *et al.*, 2018; Lindestam-Arlehamn *et al.*, 2019; Tansey and Romero-Ramos, 2019; Tan *et al.*, 2020). Cytokine profiling and immune cell analysis in both human and experimental animal tissues have showed immune changes generally to a pro-inflammatory environment. In this section, evidence of immune system underlying in PD etiopathogenesis will be exposed. Fluids such as CSF and blood will be addressed separately to central nervous system. Human tissue and animal models will also be addressed separately as some incoherence may be observed among these two, drawing misleading conclusions.

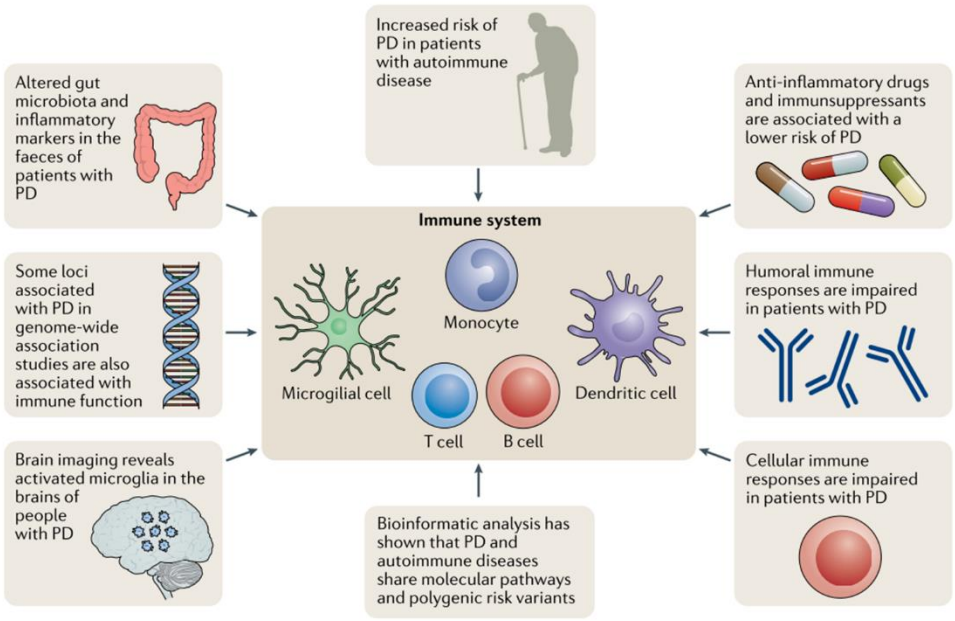

Figure 14. Evidence for the involvement of the immune system in PD. Evidence come from several sources such as clinical observations and preclinical studies. From Tan *et al.*, 2020.

1.3.1 Human tissue and fluids

Extensive work has been performed in blood immune cell characterization, while only a few have performed the same for CSF. Moreover, meanwhile many efforts have been directed to the innate immune system, only two original articles and one poster quantitatively asked the question whether there is an adaptive immune response ongoing in the human brain tissue. Nonetheless, most of these works have been the initial stand out of this thesis.

1.3.1.1 Cerebrospinal fluid and blood

Blood and CSF have been largely studied to understand immune etiopathogenesis of the disease and, at the same time, to find novel biomarkers which would improve clinical diagnosis. However, both fluids need to be studied in parallel but separately as they do not necessarily co-vary. Indeed, in a study that assessed the circadian variation of several cytokines in PD and control subjects, only found co-variation with IL-6, C-reactive protein and Neutrophil Gelatinase-Associated Lipocalin (NGAL) while other cytokines did not reach co-variation significance (Eidson *et al.*, 2017). Another study tried the same strategy but found no co-variation of IFNγ, IL-6, IL-10 and TNFα between the two fluids (Wijeyekoon *et al.*, 2020).

1.3.1.1.1 Cerebrospinal fluid

Accepting the assumption that CSF could be mirroring what is happening in the brain parenchyma, it seems that there is enough reasoning to study CSF inflammatory markers. Levels of IL-1β, IL-2, IL-4, IL-6, IL-10, IFNγ, TNFα and MCP-1/CCL2 have been reported to be increased in PD CSF compared to age-matched healthy control one (Mogi *et al.*, 1994; Blum-Degen *et al.*, 1995;

Brodacki *et al.*, 2008; Schröder *et al.*, 2018). Contrarily, IL-9 levels were found to be decreased. IL-6 levels were found to inversely correlate with severity by UPDRS score (Müller *et al.*, 1998). Regarding immune cells, no changes in the B cell component were found in PD CSF samples (Schröder *et al.*, 2018). In this same study, activated T cells, due to high expression of MHC class-II, were found increased in the disease. These were mainly CD8+ T cells. In a previous study, γδ T cells were found to be elevated in PD CSF samples compared to other neurological diseases (Fiszer *et al.*, 1994).

1.3.1.1.2 Blood

Many studies have tried to understand the role of the immune system in PD assessing cytokine levels and immune cell proportions in the blood. Nonetheless, technical and cohort heterogeneities are general issues that make comparisons between studies quite complex. In the same study which assessed cytokine circadian variation, they found lower levels of TNFα and IFNγ and higher levels of NGAL in PD serum compared to age-matched healthy control cases (Eidson *et al.*, 2017). In a study focused on studying untreated PD cases they found decreased levels of several regulatory populations such as Tregs, Tr1 and IL-10-producer CD8regs but no changes in several cytokines such as TGF-β, IL-1β, IL-6, IL-10, TNFα and IFNγ. They only found an increase of IL-13 which is associated with a Th2 phenotype (Álvarez-Luquín *et al.*, 2019). IL-4, IL-10, IL-21 and TGF-β have also been studied in a novel study without finding significant differences between PD and healthy control samples (Zhao *et al.*, 2020). One study tried to correlate inflammatory-related molecules with disease onset, severity and both autonomic and cognitive status. They analyzed more than 20 pro-inflammatory and anti-inflammatory cytokines in two separate cohorts (n =145 and n=90, respectively). In a principal component

analysis (PCA), they concluded that serum cytokine levels were not good enough to discriminate clinical subtypes of PD (Yilmaz *et al.*, 2018).

An elegant and extensive systematic review and meta-analysis on different studies published until 2016 reported that RANTES/CCL5, IL-1β, IL-2, IL-6, IL-17, TNFα and C-reactive protein blood levels were increased in PD patients compared to age-matched healthy controls (Qin *et al.*, 2016*b*; Dutta *et al.*, 2019). Nonetheless, high variability between cohorts and controversial results were reported (Rocha *et al.*, 2018). TNFα serum levels have been associated to faster motor symptoms impairment, and IL-1β and IL-2 to faster the decline of cognitive capacities (Williams-Gray *et al.*, 2018). In this same study, anti-inflammatory cytokine IL-10 was observed to be elevated in PD patients too. Another study found higher levels of several serum cytokines such as IL-2, IL-10, IL-4, IL-6, TNFα and IFNγ (Brodacki *et al.*, 2008). Regarding immune cells in the blood, several studies have consistently reported alterations in the CD4+ T cell population in PD with some exceptions (Williams-Gray *et al.*, 2018). Decrease in naïve CD4+ T cells has been reported in different independent studies (Fiszer *et al.*, 1994; Bas *et al.*, 2001, Stevens *et al.*, 2012*b*; Jiang *et al.*, 2017; Rocha *et al.*, 2018). In some of them was also found an increase of both CD4+ T cell memory populations and NK cells and a reduction of CD8+ T cells in mid-late stages of the disorder. Reduced levels of Th2, Th17 and Treg populations in PD have been stated (Kustrimovic *et al.*, 2018). The same group reported in a previous study that dopamine receptors (González *et al.*, 2015) expression in CD4+ T cells correlate with UPDRS score in PD cases (Kustrimovic *et al.*, 2016). Pro-inflammatory ratios of Th1/Th2 and Th17/Treg CD4+ T cells have been found to correlate with UPDRS severity (Chen *et al.*, 2015). Some years ago, it was described that Treg suppressive activity in PD patients is impaired (Saunders *et al.*, 2012). More recently, another study went to analyze the levels of other regulatory lymphocyte subsets and they found that not only

Tregs but Tr1 cells, IL-10-producer CD8regs and tolerogenic PD-L1+ dendritic cells were reduced in untreated PD patients (Álvarez-Luquín *et al.*, 2019). Regarding dendritic cells, reduced blood levels were also previously reported in PD patients correlating with severity (Ciaramella *et al.*, 2013). Changes in CD8+ T cell populations have only been observed in two studies in which there was an increase (Baba *et al.*, 2005) or a lack of aging-linked replicative senescence (Williams-Gray *et al.*, 2018). A slight increase of Th17 lymphocytes has also been described in PD blood samples but no differences were reported for Th1 and Th2 subsets (Sommer *et al.*, 2018). Follicular helper T lymphocytes, essential for B cell differentiation, and CD19+ B cells were reported to decrease in a recent study (Zhao *et al.*, 2020). Finally, in a very recent study, low lymphocyte counts were associated with higher risk for developing Parkinson's disease (Jensen *et al.*, 2021).

Recently, Sulzer and collaborators demonstrated how T cells from PD blood samples recognized α-synuclein-derived peptides (Sulzer *et al.*, 2017). In order to do that, α-synuclein-derived epitopes were presented to T cells to activate an immune response. These epitopes were obtained cleaving α-synuclein according to restriction sites of both MHC class-I and class-II molecules. They used ELISPOT procedure to find which cytokines were expressed and released by T cells. They reported that immune responses to α-synuclein had both MHC class-I and class-II restricted components and that Y39 and phosphorylated S129 regions of α-synuclein could elicit different type of immune responses according to HLA haplotype. T cell responses were mainly Th2 type releasing IL-5 but some Th1 were also obtained. This raised some criticism due to the fact that Th2 phenotype is not normally linked with autoimmune diseases (Mosley and Gendelman, 2017). Moreover, this study was performed in late stages of the disease when neurodegeneration is present. Thus, no causality between T cell reactivity and dopaminergic cell loss could be done. Some years later, Sulzer

and collaborators addressed this problem with a novel study taking into consideration early stages of the disease (Lindestam Arlehamn *et al.*, 2020). They found that in early stages of the disease T cell reactivity against α-synuclein was high and it decreased after PD diagnosis. In addition to this, T cell responses positively correlated with age and levodopa treatment. Recently, Sulzer's lab has also published a study in which they mapped TCR repertoire of α-syn-specific T cells from six PD patients. They compared this heterogeneity with the one observed in pertussis toxin-specific T cells as a representative foreign antigen that most individuals have been exposed to. They concluded that in both cases TCR repertoire was highly diverse (Singhania *et al.*, 2021).

Gut microbiota has also been observed to be affected in PD cases (Mulak and Bonaz, 2015). In relation to this, gut microbiota alterations have been shown to influence cytokine blood levels (Schirmer *et al.*, 2016; Bander *et al.*, 2020). One study found a correlation between microbiota alterations and plasma concentrations of IFNγ and TNFα which were seen in higher concentrations in PD samples than in age-matched healthy controls (Lin *et al.*, 2019).

According to the aforementioned results, it seems straightforward to conclude that there are peripheral inflammatory changes in PD samples compared with age-matched healthy control ones. However, there is some controversy due to high variability between cohorts and technical procedures. These results mean that these changes happen, at least, in late stages of the disease. One attempt to observe whether these inflammatory changes were observed in early stages of the disease was to assess them in idiopathic rapid eye movement disorder (iRBD) cases. High percentage of iRBD cases develop synucleinopathy related diseases when they become elder (Iranzo *et al.*, 2013). Blood levels of IL-1β, IL-2, IL-6, IL-10 and TNFα were measured in iRBD cases but only IL-1β was found to be increased. IL-10 correlated with an autonomic function score (Kim *et al.*,

2018). Thus, in contrast with PD cases, it would seem that peripheral inflammation is not as important as previously hypothesized due to the fact that only small changes may be observed. However, more studies need to be performed to obtain more robust conclusions.

1.3.1.2 Human post-mortem tissue

Several studies have reported an increase of microglial markers in several regions of PD patients. McGeer and colleagues were the first ones to report an increase of HLA-DR+ microglial cells in the SN*pc* comparing with age-matched healthy controls (McGeer *et al.*, 1988*a*, *b*). In these same studies, they also performed a CD8α immunohistochemistry in distinct neurological pathologies finding some positive cells in all of them. Deposition of complement proteins have also been detected in SN*pc* of PD cases (Yamada *et al.*, 1992). Complement-activated oligodendroglia was also seen only in PD samples but not in neurologically normal ones. Some years later, expression of pro-inflammatory mediators COX1/2 and iNOS in PD microglia were found to be increased in both SN*pc* and caudate-putamen regions (Knott *et al.*, 2000). In contrast with McGeer and colleagues' results, SN*pc* HLA-DR+ microglia was not found to differ to age-matched healthy control levels in another study (Croisier *et al.*, 2005). However, they did report an increase of the microglial phagocytic marker CD68 in PD patients which correlated with disease duration. In SN*pc*, caudate-putamen and pons CXCR4 levels were assessed. They were reported to be elevated in both SN*pc* and caudate-putamen regions of PD samples. CXCR4 has been described to induce cell death once it binds to its ligand CXCL12 (Shimoji *et al.*, 2009). In consequence, they also studied the levels of CXCL12 in the SN*pc* and, despite the dopaminergic cell death, PD cases exhibited higher expression of CXCL12 than neurological control subjects. This effect was accompanied with an increase of

ionized calcium-binding adapter molecule 1+ (Iba-1) microglia. Levels of microglial HLA-DR were again analyzed in several regions: SN*pc*, caudate-putamen, LC and midfrontal cortex (Bradaric *et al.*, 2012). Nonetheless, in this study iLBD cases were also added to understand what was happening in presumably early stages of the disease. Number of HLA-DR+ microglial cells in PD cases were found to be elevated only in the SN*pc*. iLBD cases presented higher numbers only in LC, which is a brain area normally affected before the SN*pc*. In this same study, αvβ3 integrin levels were also assessed. In practically all studied brain areas and in both iLBD and PD cases, there was an increase compared with age-matched healthy controls. This was independent of the number of vessels. Increased HLA-DR expression has also been reported in PD LC in a whole-genome RNA profiling procedure (Botta-Orfila *et al.*, 2012). Another question related with the innate immune system was about the role of phagocytes in the removal of apoptotic dopaminergic neurons. In relation to this, MFGE8, which is a soluble factor involved in phagocytic recognition, was studied in post-mortem PD human tissue and it was found to be expressed in glial cells and up-regulated in PD samples (Kinugawa *et al.*, 2013). Stereological cell counts of Iba-1+ or HLA-DR+ microglia were also elaborated in a study about the expression of proteinase-activated receptor-2, trypsin-2 and serpin protease inhibitors in distinct PD brain regions (Hurley *et al.*, 2015). In this study, PD cases were separated according to disease duration and iLBD cases were also added. In conclusion, Iba-1+ microglial cells were increased in iLBD LC samples meanwhile HLA-DR+ microglia presented high variability and some trends to be elevated in SN*pc* and LC of both iLBD and PD cases. In 2016, Walker and collaborators from the Banner Sun Health Research Institute studied inflammatory markers in both caudate-putamen and SN*pc* regions considering age-matched healthy controls, PD and iLBD cases (Walker *et al.*, 2016). In both regions, HLA-DR+ microglia was elevated although PD cases exhibited high

variability due to some of them having low positive staining. Nonetheless, glial fibrillar acidic protein (GFAP), an astrocyte marker, and Iba-1 protein levels by western blot were not different to controls. Striatal GFAP inversely correlated with TH levels. IL-5, involved in Th2 responses, was also increased in both regions only in PD samples. By immunofluorescence, SN*pc* Iba-1 and CD68 staining intensities have been reported to be elevated in PD cases compared with age-matched healthy controls (Gómez-Gálvez *et al.*, 2016). HMGB1, involved in progression of numerous chronic inflammatory and autoimmune diseases, has been found to be increased in post-mortem SN*pc* of PD cases compared with neurological controls (Santoro *et al.*, 2016). Messenger RNA expression levels of molecules associated with IFN type 1 response have been found to be elevated in post-mortem SN*pc* of PD cases (Main *et al.*, 2016). TLR signaling is a major pathway mediating inflammation and it has been linked with α-synuclein microglial response (Kim *et al.*, 2013). Neuronal TLR2 exhibited an up-regulation in PD samples comparing with healthy controls in contrast with the microglial one which was not different (Dzamko *et al.*, 2017). TLR2 staining was associated with PD disease duration and it was localized to α-synuclein positive LBs. Transcriptional signature of post-mortem PD human tissue by messenger ribonucleic acid sequencing (mRNA-Seq) has been reported to be enriched in several biological pathways which implicate neuroinflammation, apoptosis, transcriptional dysregulation and neuron-associated functions (Labadorf *et al.*, 2018). More recently, MHC class-II has also been proven to be expressed in astroglial cells (Rostami *et al.*, 2020). In this study they detected a slight increase of MHC class-II in SN*pc* PD tissue comparing with age-matched healthy controls. However, they did not find an increase of Iba-1+ or GFAP+ cells. Taking into account results from PD experimental animal models, several mechanisms have been proposed as how microglial cells can actively be damaging dopaminergic neurons (**Figure 15**).

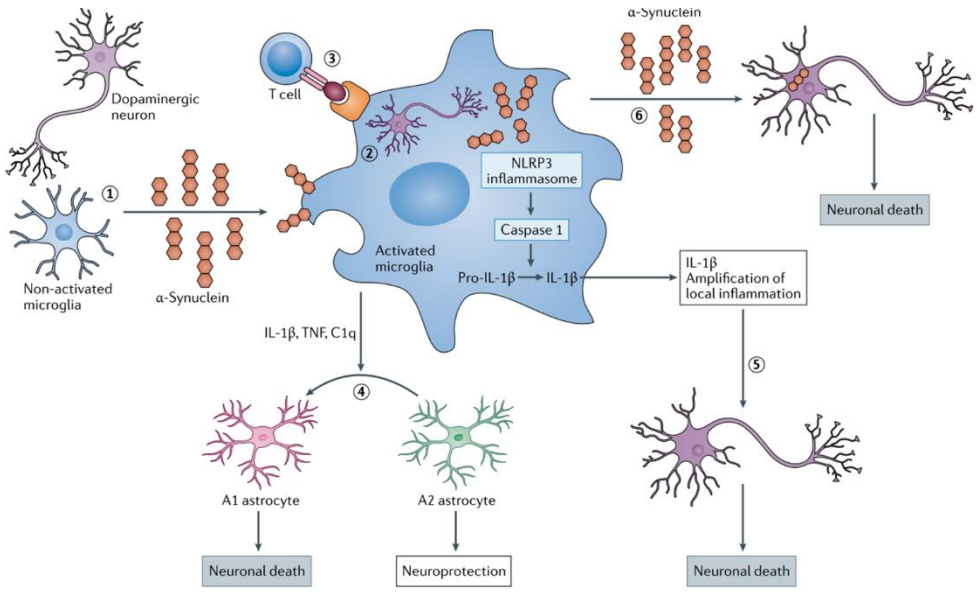

Figure 15. Mechanisms of microglial involvement in dopaminergic neuronal damage and death. (**1**) Homeostatic microglia may be activated by toxic forms of α-synuclein or pro-inflammatory molecules. (**2**) Activated microglia can directly attack neurons by phagocytosis. (**3**) Activated microglia can also act as APCs presenting dopaminergic neuronal antigens and activating T cells which can build up an adaptive immune response. (**4**) Activated microglia can release pro-inflammatory cytokines switching A1 neuroprotective astrocytes into A2 neurotoxic ones. (**5**) Release of these cytokines can also amplify local inflammation eventually causing neuronal death. (**6**) Activated microglia can help to spread toxic forms of α-synuclein from phagocytosed neurons. From Tan *et al.*, 2020.

Regarding the adaptive immune system, antibodies against IgG also detected SN*pc* LBs. Double immunohistochemistry procedure against both IgG and α-synuclein confirmed these results (Orr *et al.*, 2005). They also observed high HLA-DR positive staining in early HY stages. Even though the presence of IgG, plasma cells were not infiltrating the parenchymal tissue (Brochard *et al.*, 2009). Brochard and collaborators studied T cell SN*pc* infiltration as McGeer did in the past. However, they not only detected and quantified CD8+ T cells but

CD4+ T cells too. The former outnumbered the latter, but both were elevated in PD cases compared with age-matched healthy controls. Perivascular and parenchymal T cells were not distinctly counted. Two years later, Rohn and Catlin showed again the presence of CD3+ T cells in the SN*pc* of PD cases (Rohn and Catlin, 2011). In this original article they also showed the presence of influenza A virus in the SN*pc*. In 2012, one poster from Halliday's lab presented in the Movement Disorder Society Congress tried to reproduce Brochard's study and also to analyze caudate-putamen T cell infiltration. Notwithstanding the expected results, they only found a small non-significant increase of CD8+ T cell densities in the caudate-putamen region of PD cases (Stevens *et al.*, 2012*a*). In 2014, Cebrián and colleagues from Sulzer's lab demonstrated the expression of HLA class-I by SN*pc* dopaminergic and LC norepinephrinergic neurons (Cebrián *et al.*, 2014*b*, *a*). HLA class-I neuronal expression was regulated by several factors such as IFNγ, α-synuclein, neuromelanin, high cytosolic dopamine and oxidative stress. In addition to this, they also detected CD8+ T cells near dopaminergic neurons. In a recent study, CD3+ T cells have also been reported to be elevated in post-mortem SN*pc* PD tissue compared with age-matched healthy controls (Sommer *et al.*, 2018). In this exact study, they also performed an elegant experiment co-culturing patient-derived Th17 lymphocytes with induced pluripotent stem cells (iPSCs)-derived dopaminergic neurons. They obtained increased cell death in PD iPSC-derived neurons after co-culture with autologous T lymphocytes. Dopaminergic cell death was abolished blocking IL-17R which was expressed in iPSC-derived dopaminergic neurons. Rostami and collaborators also observed parenchymal and perivascular CD4+ T cells in SN*pc* regardless of the pathology (Rostami *et al.*, 2020).

To sum up, all these studies clearly suggest that there is an on-going immune response in the brain of PD patients. However, there is still some controversy

regarding microgliosis as not all original articles observed an increase of HLA-DR/Iba-1 expression in PD cases. Some correlation between disease duration and microgliosis has been reported. Regarding the adaptive immune system, some controversy also exists as only one study has demonstrated a significant increase of both CD4+ and CD8+ T cells in PD SN*pc*. T cell infiltration in early stages of the disease remains unknown.

1.3.2 Experimental animal models

Most of the work regarding to the role of the immune system in PD has been performed in experimental animal models. As it will be discussed in this section, the first studies to observe an immune response in experimental animal models were in the neurotoxin-based MPTP treated mice. Afterwards, with the appearance of novel animal models, microgliosis and T cell activation were also described in genetic ones.

Although in this section MPTP treated mice and overexpression of h-WT-α-synuclein will be deeply addressed, other experimental animal models also present immune responses in their etiopathogenesis. Injection of 6-OHDA strongly induced microglia activation but anti-inflammatory strategies targeting this microgliosis increased dopaminergic neuronal survival (Pabon *et al.*, 2011; Lazzarini *et al.*, 2013; Tentillier *et al.*, 2016; Machado *et al.*, 2019). Some studies showed that inducing M2-like microgliosis was neuroprotective in this model (Wright *et al.*, 2008; Choudhury *et al.*, 2011). 6-OHDA treated mice exhibited SN*pc* IgG deposition and both T and B cell infiltration (Theodore and Maragos, 2015; Olmedo-Díaz *et al.*, 2017). In 6-OHDA treated rats, no T cell infiltration was detected in the SN*pc* but there was a reduction of peripheral Tregs priming a pro-inflammatory environment (Ambrosi *et al.*, 2017). In transgenic lines such as A53T mutated α-synuclein under the prion protein

promoter (PrP) or the double mutant A30P+A53T α-synuclein under the TH promoter, microgliosis, astrogliosis and pro-inflammatory changes were observed to precede the cell death (Lee *et al.*, 2002; Miller *et al.*, 2007; Su *et al.*, 2008; Ferreira and Romero-Ramos, 2018). In other α-synuclein transgenic lines where neuronal death was absent, microgliosis was still present (Watson *et al.*, 2012). In this same study, peripheral adaptive immune response seemed activated at late timepoints.

1.3.2.1 MPTP

SN*pc* inflammation in acute MPTP treated mice was firstly described by Kurkowska-Jastrzebska and colleagues. Acute MPTP injections induced MHC-II+ microgliosis and both CD4+ and CD8+ T cell infiltration in the SN*pc* (Czlonkowska *et al.*, 1996; Kurkowska-Jastrzebska *et al.*, 1999). Diminishing glial reaction and T cell infiltration with dexamethasone also diminished neuronal damage. Since then, microglia activation has been extensively reported in both acute and subacute MPTP paradigms (Cardenas and Bolin, 2003; Kang *et al.*, 2007; Barcia *et al.*, 2011; Main *et al.*, 2016; Martin *et al.*, 2016; Liu *et al.*, 2019). Some of the studies reported the importance of several cytokines such as IFNγ, TNFα and IL-17 to induce or maintain microgliosis. In this sense, other studies showed that reducing MPTP-induced microgliosis through up-regulation of neuronal CX3CL1 attenuated nigrostriatal dysfunction (Wang *et al.*, 2015). In cell cultures with MPP+ treated cells CD200-CD200R pathway seemed to be also altered inducing microglial pro-inflammatory responses (Rabaneda-Lombarte *et al.*, 2020). Thus, the main current working hypothesis is that microglia play a negative role in PD pathogenesis (Lee *et al.*, 2019). However, some authors have opposed to this statement pointing out that

microglia shifting from M1- to M2-like phenotypes can help against neurodegeneration (Ismaiel *et al.*, 2016; Calvello *et al.*, 2017; Zhang *et al.*, 2018).

T cell infiltration in the acute paradigm was reported as soon as 2 days post-injections (Brochard et al., 2009). Actually, T cell brain infiltration peaked at 7 days post-injections. CD8+ T cells outnumbered CD4+ ones in all the studied timepoints. T cell brain infiltration has also been described in subacute MPTP treated mice but with different dynamics (Depboylu *et al.*, 2012; Zhou *et al.*, 2015). Strikingly, knocking-out CD4+ T cells bar CD8+ T cells was neuroprotective. This neuroprotection when the adaptive immune system was haltered had also been described one year earlier (Benner *et al.*, 2008). In this study, antigenicity of α-synuclein post-translational modifications was demonstrated in contrast with the native protein. Moreover, dopamine receptors D3 were significantly important to induce dopaminergic damage in acute MPTP treated mice (Elgueta *et al.*, 2017, 2019). Therapeutic immunization to induce Th2 lymphocyte phenotype has also proven to be successful for dopaminergic neuroprotection (Benner *et al.*, 2004) directly increasing IL-4 and IL-10 SN*pc* levels and indirectly elevating glial cell line-derived neurotrophic factor (GDNF). Anti-inflammatory activity of Tregs has exhibited to be neuroprotective in the MPTP model reducing Th17 T cells and microgliosis (Reynolds *et al.*, 2007, 2009*a*, 2010). Microgliosis and T cell infiltration has also been described in MPTP treated monkeys (Barcia *et al.*, 2004, 2013; Seo *et al.*, 2020). This immune response was accompanied with nigrostriatal damage. T cell SN*pc* infiltration in MPTP treated monkeys was thought to be primed due to a previous up-regulation of RANTES (regulated on activation, normal T cell expressed and secreted) and eotaxin, chemokines involved in T cell trafficking (Roy *et al.*, 2015). It seemed that microglial cells were the main producers. Blocking CCR5, which is the receptor for both eotaxin

and RANTES, attenuated nigrostriatal damage and T cell infiltration (Mondal *et al.*, 2019).

RANTES and eotaxin increase reported in MPTP treated monkeys was then described in treated mice (Chandra *et al.*, 2016). They demonstrated that blocking both chemokines with antibodies reduced T cell SN*pc* accumulation, attenuated nigral expression of pro-inflammatory molecules and gliosis. These outcomes paralleled an attenuation of nigrostriatal damage. In contrast with Brochard and Kurkowszka results for T cell infiltration in acute MPTP paradigm, Chandra and colleagues showed T cell SN*pc* infiltration peaking at 1 day post-injections and decreasing afterwards (Chandra *et al.*, 2016, 2017). To further demonstrate the role of eotaxin and RANTES on T cell SN*pc* homing, in another study they injected both chemokines to induce a chronic T cell infiltration that lasted longer than 1 day post-injection (Chandra *et al.*, 2017). T cell SN*pc* infiltration remained until 30 days due to twice-weekly administration of both chemokines. Gliosis, nigral α-synuclein induction, persistent nigrostriatal damage and continuous impairment of motor functions were observed. T cells recruited by these chemokines were mainly CD4+ Th17 lymphocytes (Dutta *et al.*, 2019).

1.3.2.2 Overexpression of α-synuclein

Overexpression of α-synuclein by means of viral vectors lead to microgliosis and, in some cases, astrogliosis. In **Table 1** there is a systematic review in PubMed database of all original articles which used this experimental animal model and worked with gliosis until 2017. This activation of the glia seemed to be independent of the rodent species and, in general terms, the overexpression of wild-type or mutated α-synuclein. Moreover, inhibiting the immune response attenuated the dopaminergic cell loss (Cao *et al.*, 2010; Harms *et al.*, 2013,

Sanchez-Guajardo *et al.*, 2013*a*; Van der Perren *et al.*, 2015). CD4+ and CD8+ T cell brain infiltration was also reported in this PD animal model (Theodore *et al.*, 2008; Sanchez-Guajardo *et al.*, 2010, 2013*a*; Harms *et al.*, 2013; Van der Perren *et al.*, 2015, Qin *et al.*, 2016*a*; Thakur *et al.*, 2017). Contrarily, only few studies described B cell infiltration or IgG deposition (Cao *et al.*, 2010, Sanchez-Guajardo *et al.*, 2013*a*). In all these studies, the role of T cells in neuroinflammation seemed to be subjugated to the microglia contrasting with the conclusions extracted from the MPTP injected mice. Ostensibly, description and importance of this PD animal model were extensively and elegantly reviewed by Volpicelli-Daley some years ago (Volpicelli-Daley *et al.*, 2016).

Table 1. Gliosis in overexpression of α-synuclein PD animal model

Reference	Species	Viral vector and titration	Nigrostriatal damage	Microgliosis and astrogliosis
Theodore *et al.*, 2008	Mouse (C57BL/6)	WT+GFP AAV2/2	NA	Microgliosis (MHC class-II and CD68)
Chung *et al.*, 2009	Rat (SD)	A53T AAV2/2	Up to 56% neuronal loss at 24w	Microgliosis in both Str and SN*pc*
Sanchez-Guajardo *et al.*, 2010	Rat (SD)	WT AAV2/5	The higher titrations and later timepoints, the higher neuronal loss	Microgliosis (mainly MHC class-II)
Cao *et al.*, 2010	Mouse (C57BL/6)	WT+GFP AAV2	Up to 27% neuronal loss at 24w	Microgliosis at 4w (gp91PHOX marker)

Lastres-Becker *et al.*, 2012	Mouse (C57BL/6)	WT AAV6	Up to 25% neuronal loss at 8w	Microgliosis (Iba-1) and astrogliosis (GFAP)
Febbraro *et al.*, 2013	Rat (SD)	WT AAV2/5	Up to 29% neuronal loss and 35% striatal fiber loss at 8w	Microgliosis mainly at 4w (CD68 and MHC class-II)
Sanchez-Guajardo *et al.*, 2013*a*	Rat (SD)	WT AAV2/5	No statistically significant degeneration	Microgliosis at 3 and 8w (CD68 and MHC class-II)
Harms *et al.*, 2013	Mouse (C57BL/6)	WT+GFP AAV2	Up to 20% neuronal loss at 24w	Microgliosis up to 24w (CD11b and MHC class-II)
Daher *et al.*, 2014	Rat (Lewis)	WT AAV2/1	Up to 25% neuronal loss at 4w	Microgliosis (CD68 and Iba-1)
Thome *et al.*, 2015	Mouse (C57BL/6)	WT+GFP AAV2	Up to 25% neuronal loss at 24w	Microgliosis at 4w (MHC class-II)
Daher *et al.*, 2015	Rat (SD)	WT AAV2/1	Up to 20% neuronal loss and 10% striatal fiber loss at 4w	Microgliosis (Iba-1, CD68 and MHC class-II)
Daniel *et al.*, 2015	Rat (SD)	WT AAV2/6	Up to 53% neuronal loss and 27.5% striatal fiber loss at 14w	Microgliosis (Iba-1) and astrogliosis (GFAP)
Van der Perren *et al.*, 2015	Rat (Wistar)	WT+GFP AAV2/7	NA	Microgliosis (CD68, CD11b and MHC class-II)
Thome *et al.*, 2016	Mouse (C57BL/6)	WT+GFP AAV2	Up to 30% neuronal loss at 24w	Microgliosis (CD68 and MHC class-II)

Qin *et al.*, 2016*a*	Rat (SD)	WT+GFP AAV2	Up to 50% neuronal loss at 12w	Microgliosis (CD11b and MHC class-II)
Lastres-Becker *et al.*, 2016	Mouse (C57BL/6)	WT AAV6	Up to 75% neuronal loss and 30% striatal fiber loss at 8w	Microgliosis (Iba-1) and astrogliosis (GFAP)
Soria *et al.*, 2017	Mouse (C57BL/6)	A53T AAV2/9	Up to 55% neuronal loss at 12w	Microgliosis (Iba-1) and astrogliosis (GFAP)
Jimenez-Ferrer *et al.*, 2017	Rat (DA)	WT AAV2/6	No neuronal loss and only 10% striatal fiber loss up to 12w	No microgliosis specific of synuclein group
Thakur *et al.*, 2017	Rat (SD)	WT AAV6	Up to 50% neuronal loss and 50% striatal fiber loss at 28w	Early and transitory microgliosis (Iba-1)

A53T alanine 53 to threonine; *AAV2* adeno-associated virus 2; *amph* amphetamine; *apo* apomorphine; *GFP* green fluorescent protein; *MHC* major histocompatibility complex; *NA* not applicated; *SD* Sprague-Dawley; *WT* wild-type

To conclude, neuroinflammation in PD is a complex system interplaying a triad of components: dopaminergic neurons, glial cells and lymphocytes. A general vision of this relationship can be observed in the **Figure 16**.

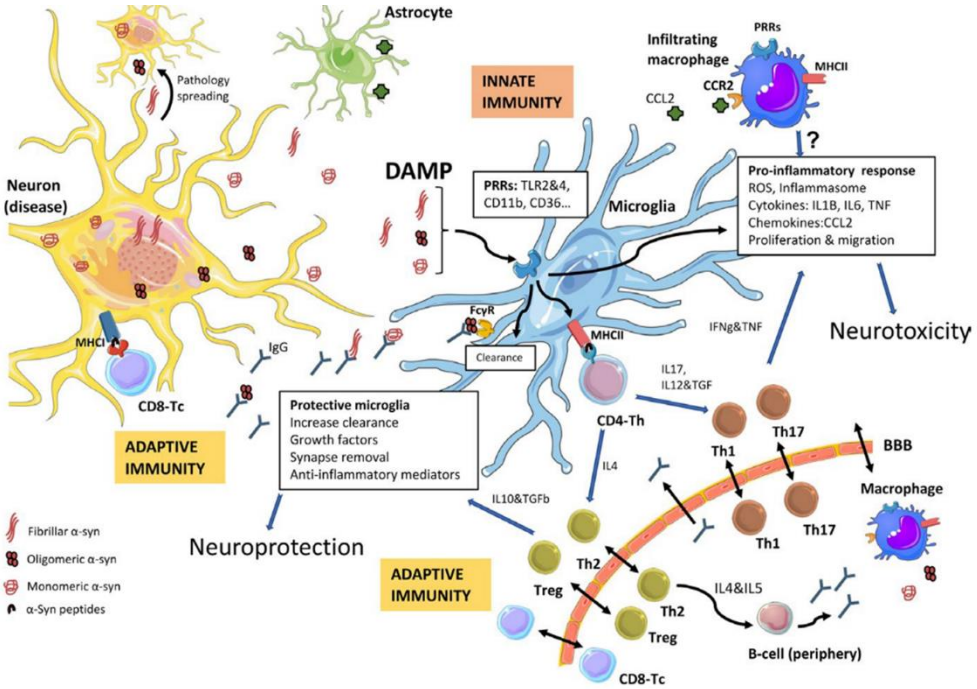

Figure 16. Immune response to α-synuclein induced neurodegeneration. General summary of all the pathways that α-synuclein can undergo inducing both innate and adaptive immune responses. A-synuclein can suffer post-translational modifications such as phosphorylation and nitration. Several monomeric α-synuclein proteins can accumulate forming first oligomers and then fibrillar forms. Neurons can release these α-synuclein forms to the extracellular media where they will be taken up and cleared by microglia and/or macrophages but also by astrocytes. A-synuclein forms can also be taken up by neighbour neurons spreading the pathology. A-synuclein can act as a damage-associate molecular pattern (DAMP) resulting in a pro-inflammatory immune response. Activated microglia and infiltrating monocytes/macrophages proliferate and migrate to the affected area. In parallel, α-synuclein peptides will be presented by neurons, through MHC class-I, and by APCs through MHC class-II. In this manner, both CD4+ and CD8+ T cells will infiltrate SN*pc*. Meanwhile CD8+ T cells can directly induce a cytotoxic attack to α-synuclein-affected dopaminergic neurons,

CD4+ T cells will release an array of cytokines and chemokines to regulate the inflammatory millieu. These molecules will vary according to the subsets of CD4+ T cells: Th1 and Th17 are normally pro-inflammatory and Th2 and Treg can resolve inflammation and lead to B-cell activation. Antibody release due to B cell-activation can help to attenuate α-synuclein spreading. From Tansey and Romero-Ramos, 2017.

HYPOTHESES AND AIMS

2. Hypotheses and aims

The main working hypothesis of this PhD thesis was that the adaptive immune system has an important role not only in Parkinson's disease pathology progression but also as an initiation factor. Studies in both post-mortem human PD tissue and animal models have pointed out both CD4+ and CD8+ T cell infiltration in the SN*pc*. CD4+ T lymphocytes could be inducing a proinflammatory environment and regulating microglia activation. CD8+ T lymphocytes could infiltrate brain parenchyma driving a cytotoxic attack to neurons. Hence, they would have a role in the onset and progression of Parkinson's disease being the adaptive immune system a good therapeutic target for the disorder. Moreover, we suggested post-translational modifications of α-synuclein as a likely source of neoantigens which could raise an adaptive immune response against dopaminergic neurons.

Thus, the main aim of this study was to determine whether T cells participate in the onset and progression of the disease. Moreover, we wanted to know whether α-synuclein behaves as a neoantigen for this adaptive immune response. In order to do that, we wanted to analyze T cell brain infiltration in both early (iLBD cases) and late stages of Parkinson's disease. iLBD cases which do not have α-synuclein aggregates in SN*pc* would help us to elucidate its possible role as neoantigen. We also coveted to analyze T cell-dopaminergic neuron interaction studying appositions and both TCR and HLA class-I expression. T cell phenotypic characterization was also necessary to understand how T cells may induce dopaminergic cell death in Parkinson's disease. Distinct CD4+ T cell subpopulations can release pro-inflammatory molecules (*i.e.* Th1, Th17) while others do the opposite releasing anti-inflammatory ones (*i.e.* Treg). CD8+ T cells may express several cell death-

inducing mechanisms and memory/residence markers. These results would allow us to discover novel therapeutic targets to halt the progression of the disease. However, to finally demonstrate their role in the pathology and to test novel therapeutic targets, appropriate animal models are necessary. We wanted to characterize the immune response in MPTP treated mice and overexpression of α-synuclein in rat SN*pc* to know which of them better resembles the human disease. The latter would also help us to understand α-synuclein role in the adaptive immune response. For this reason, we drew the following specific objectives:

1. To compare the adaptive immune response in two paradigms of MPTP intoxicated mice (acute and subacute) in order to know which one better resembles human pathology described by Brochard and collaborators.
2. To generate a PD animal model which recapitulates PD immune tolerance dysfunction, systemically depleting Treg lymphocytes.
3. To study the adaptive immune response induced by α-synuclein antigens in overexpression of h-WT-α-synuclein in rat SN*pc*.
4. To analyze both CD4+ and CD8+ T cell brain densities in SN*pc* of PD cases comparing with age-matched healthy controls. Parenchymal and perivascular T lymphocytes are counted separately as they may have distinct roles and dynamics.
5. To study both CD4+ and CD8+ T cell brain densities in SN*pc* of two different types of iLBD cases according to synucleinopathy. iLBD cases are considered early stages of the disease due to the fact that they show brain synucleinopathy, at least in the olfactory bulb, but no motor clinical symptoms. We classified iLBD cases regarding to nigral or LC synucleinopathy: iLBD SN/LC syn- would be considered an earlier stage than iLBD SN/LC syn+ although none have motor clinical symptoms.

This would allow us to better understand α-synuclein role as a neoantigen for the adaptive immune response.

6. To phenotypically characterize SN*pc* infiltrating T cells in age-matched healthy controls, iLBD and PD cases.
7. To analyze SN*pc* MHC class-II positive microgliosis to better understand antigen presentation to T cells by the innate immune system and their morphology activation status.
8. To assess SNpc synucleinopathy according to several types of α-synuclein aggregates to relate it with T cell infiltration.
9. To analyze both parenchymal and perivascular CD8+ T cell brain densities in LC of iLBD and PD cases comparing with age-matched healthy controls.

MATERIALS AND METHODS

3. Materials and Methods

3.1 Animals

8-11 weeks old wild-type inbred strain C57BL/6Ncrl mice were used for MPTP treatment. Mice were housed two to five under controlled conditions (+22ºC ± 1ºC; 12hours light/dark cycle) with food and water available *ad libitum*. 225-250g wild-type outbred Sprague-Dawley (SD) or inbred Lewis rats were kept in the same controlled conditions, but they were housed two to three in the same cage. They were used for overexpression of human-WT-α-synuclein in the SN*pc*. Acquisition, care, housing, use and disposition of laboratory experimental animals in this study have been in compliance with applicable Catalan (Decret 214/97) and Spanish (RD53/2013) laws and regulations and accordance with the European (Directive 2010/63/UE) ones. Experimental procedures were also approved by the Vall d'Hebron Research Institute (VHIR) Ethical Experimentation Committee.

3.2 MPTP intoxication

We worked with two different paradigms of MPTP intoxication in mice. Acute paradigm consisted in four intraperitoneal injections of MPTP-HCl (20mg/kg/day dosage of free base; Ref. M0896, Sigma-Aldrich) in two hour-intervals for one day. Subacute paradigm consisted in an intraperitoneal injection of MPTP-HCl (20mg/kg/day dosage of free base) administered each day during five consecutive days. Control mice received intraperitoneal saline (0.9% NaCl, Ref. B314801, Fresenius Kabi) injections instead of MPTP-HCl. For acute paradigm mice were euthanized at 2, 4 and 7 days after last injection. For

subacute paradigm mice were euthanized at 0, 1, 2, 4, 7 and 21 days after last injection.

3.3 FoxP3.LuciDTR transgenic mice and Treg depletion

FoxP3.LuciDTR transgenic mice with C57BL/6Ncrl background used in the Treg depletion experiment were received from Suffner's lab (Suffner *et al.*, 2010). Transgene construct was added at the start codon (ATG) in the third exon of the *foxp3* gene in the BAC RP23-147H5 using *Escherichia coli* EL250 (Lee *et al.*, 2001) (**Figure 17**). In brief, enhanced green fluorescent protein (eGFP), diphtheria toxin receptor (DTR) and CBGR99 luciferase (Miloud *et al.*, 2007) were added and separated by self-cleaving 2A peptide sequence from porcine teschovirus-1 for stoichiometric production of the three individual transgenic proteins (Szymczak *et al.*, 2004). All experiments were performed using mice heterozygous for the eGFP-DTR-luciferase construct as recommended by creators. Phenotyping was done by flow cytometry as it will be explained in following subchapters. Treg depletion was accomplished injecting intraperitoneally 15ng/g body weight diphtheria toxin (Ref. D0564, Sigma-Aldrich) or saline in experimental control animals.

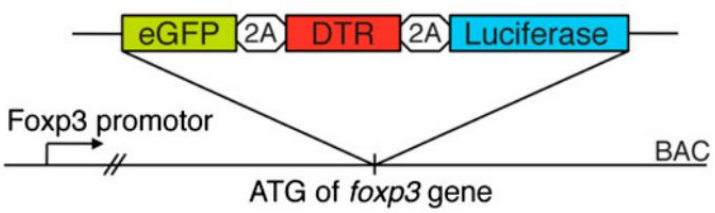

Figure 17. FoxP3.LuciDTR transgenic construct. Scheme representing all genes added in the transgenic construct and its location in the *foxp3* gene. Image adapted from Suffner *et al.*, 2010.

3.3.1 Flow cytometry

Blood was extracted from mouse facial saphenous vein and gathered in capillary Microvette® tubes with EDTA (Ref. 20.1278, SARSTEDT) to avoid coagulation. Blood was then moved to an eppendorf with phosphate buffer saline (PBS; Ref. 70011-036, Thermo Fisher Scientific) and bovine serum albumin (BSA; Ref. A4503, Sigma-Aldrich) at 1%. 0.1% sodium azide (Ref. S8032, Sigma-Aldrich) was also added to the buffer to avoid bacterial contamination. After a fast centrifugation at 10000 rotations per minute (rpm), blood cells precipitated and suspension was discarded. CD16/32 antibodies (Ref. 553141, BD Pharmingen) diluted at 1:50 in PBS+BSA were used to resuspend the cellular pellet and block Fc receptors which could bind CD4 antibodies in a non-specific way for 10 minutes in room temperature. Then anti-CD4 APC (Ref. 100412, BioLegend) was added in the cell solution in a 1:50 dilution for 30min at +4ºC. Following this, PBS+BSA was added before another fast centrifugation at 10000rpm. Supernatant was discarded and 1X PharmLyse solution was added (Ref. 555899, BD Pharmingen) for 10min at +37ºC to eliminate erythrocytes. Samples were centrifuged rapidly at 10000rpm and supernatant was again discarded. Cellular pellet was washed once and then resuspended with PBS+BSA. Afterwards, cells were analyzed on BD™ LSR II Fortessa (BD Biosciences) equipped with four laser lines (488nm, 405nm, 561nm and 640nm). Evaluation was performed using FlowJo software (BD Company, v10.7; Ashland, Oregon, USA). Gating procedure was done selecting as the gate 1 singlets (forward area vs forward height scatter), gate 2 survival cells (forward vs side scatter), gate 3 CD4 (APC signal) and gate 4 FoxP3 (eGFP signal). Percentage of CD4+ eGFP+ T cells were the final output of flow cytometry analysis.

3.3.2 Bioluminescence imaging

Mice were imaged 5min after intraperitoneally injecting 4.5mg D-luciferin (Ref. L9504, Sigma-Aldrich) using IVIS® Spectrum (Ref. 124262, Perkin Elmer) (Miloud *et al.*, 2007). Bioluminescence signal and pictures were obtained with Living Image software (Xenogen, version 2.5). Light output was quantified as luminescence units.

3.4 Adeno-associated viral vectors

AAV2/5 serotype containing the human *SNCA* cDNA under control of the chicken β-actin (CBA) promoter was produced at UNC Vector Core Facility (North Carolina, USA) (Kirik *et al.*, 2002). Enhancer elements from cytomegalovirus promoter were also added (Xu *et al.*, 2001). This adeno-associated viral vector was used for the overexpression of human-WT-α-synuclein in dopaminergic neurons of the SN*pc*. The titer of the AAV batch used in this study was $1*10^{13}$ genome copies/ml. Aside control naïve rodents, some received EV with non-coding stuffer DNA with a final titration of $5.6*10^{12}$ genome copies/ml. EV was produced by CBATEG Core Facility (Universitat Autònoma de Barcelona, Catalunya, Espanya).

AAV vectors were purified as previously described by Zolotukhin and collaborators. In brief, they were purified by optiprep iodixanol step density gradient centrifugation followed by ion exchange chromatography to reduce iodixanol concentrations (Conway *et al.*, 1997; Zolotukhin *et al.*, 1999). Titration was obtained by quantitative polymerase chain reaction (qPCR) and noted as genome copies per milliliter.

3.5 Surgical procedures for stereotaxic delivery of adeno-associated viral vectors

Rodents which underwent AAV-WT-α-synuclein stereotaxic injections were placed in stereotaxic frame under general anesthesia using isofluorane (Ref. PDG9623, Baxter) (5% for the induction phase and 2% for the maintenance phase). We injected unilaterally above right rat SN*pc* (coordinates in mm.: -5.2mm AP, -2mm ML and -7.6mm DV from Bregma) (Paxinos and Watson, 1987) with 2µl of AAV using the 10µl Neuros Hamilton syringe system (Ref. 7635-01, Hamilton 701 RN) with a glass capillary (Ref. 654560-01, Hamilton 701 RN). Flow rate was 0.4µl/min and needle was left in place for additional 4 minutes before slow withdrawal.

3.6 Euthanasia and animal brain processing for histological analyses

Rodents were deeply anesthetized with an intraperitoneal injection of 5% pentobarbital sodium (50mg/kg, Ref. 39916, Dr. Carreras) and then perfused through the left ventricle with ice-cold physiological saline (0.9% NaCl, Ref. B314801, Fresenius Kabi) at 9ml/min flow rate for 3 minutes followed by ice-cold 4% paraformaldehyde for histology (vol/vol; Ref. A3697.9010, PanReac ApplyChem) previously diluted in 0.2M phosphate buffer containing 0.15M sodium phosphate dibasic (Ref. S0876, Sigma-Aldrich) and phosphate dibasic (Ref. S9638, Sigma-Aldrich) for 4 minutes. Afterwards, brains were removed from skull and post-fixed for 24h in the same fixative at +4ºC. Crioprotection was done with 30% sucrose (vol/vol; Ref. S9378, Sigma-Aldrich) in phosphate buffer 0.1M at +4ºC for 48h. Brains were frozen using 2-methylbutane (Ref. M32631, Sigma-Aldrich) at between -30ºC and -40ºC during 30 seconds (for

mice) or 1 minute (for rats) before storage at -80ºC. In cryostat (Ref. CM3050 S, Leica) brains were cut at 20µm of thickness in mice and 30µm in rats in the coronal plane. Sections were collected in 48-well plates with phosphate buffer 0.1M + 0.01% sodium azide (Ref. S8032, Sigma-Aldrich). For long term storage sections were frozen in storing solution made of 30% glycerol (vol/vol; Ref. G5516, Sigma-Aldrich), 30% ethylene glycol (vol/vol; Ref. 141316.1211, PanReac AppliChem) and PBS made of 1.386M sodium chloride (Ref. S3014, Sigma-Aldrich) 29.51mM potassium chloride (Ref. P9541, Sigma-Aldrich), 19.8413mM monopotassium phosphate (Ref. P5379, Sigma-Aldrich) and 95.0158mM monosodium phosphate (Ref. S9638, Sigma-Aldrich).

3.7 Human post-mortem brain tissue

Formalin-fixed paraffin-embedded (FFPE) midbrain sections (thickness 6µm) from deceased PD patients (n = 15), iLBD cases (n = 9) and age-matched healthy control individuals (n = 7) were purchased from Banner Sun Health Research Institute, Sun City, Arizona, United States of America. Brain and Body Donation Program operates with the approval of Western Institutional Review Board (Puyallup, WA). We included both sexes although percentage of male over women was already higher in the bank. We chose this bank as they provided detailed neuropathological and clinical information about their cases and they collected different brain and peripheral areas which could be interesting if needed. Two cases were provided by the Neurological Tissue BioBank at IDIBAPS-Hospital Clínic (Barcelona, Catalunya, Spain). Detailed information about these 31 cases can be found in **Annex Tables 1 and 2**. The former table presents code, pathology, age and cause of decease for each subject. The latter contains the available clinical history and autopsy information with all comorbidities of subjects included in the study. Selection was based on

neuropathological diagnosis with reference to clinical information provided by the tissue bank.

3.8 Immunohistochemistry/immunofluorescence

Before commencing with immunolabelling protocol, FFPE sections which underwent an immunofluorescence procedure were photobleached using a LED light source (Ref.nHYG05-MINI-100*w-b input voltage 100-240 V AC and frequency of 50-60 Hz, TOPLANET) for 48h at +4ºC.

FFPE sections were deparaffinized at +60ºC for 30min in an oven (Ref. 03839, Memmert). Sections were rehydrated using two xylenes solutions (Ref. A2476, PanReac AppliChem) (20min total) and decreasing ethanol concentrations (Ref. 131086.1212, PanReac AppliChem) (15min 100%, 15min 95%, 5min 70%). Sections were rinsed in Tris buffered saline (TBS) between each incubation period except blocking and primary antibody. Sections underwent an antigen retrieval protocol using sodium citrate (10mM, pH6; Ref. S1804, Sigma-Aldrich) or Tris-Ethylenediamine tetraacetic acid disodium salt dihydrate (EDTA) (10mM-1mM, pH9; Trizma base Ref. T6066, EDTA Ref. E5134, Sigma-Aldrich) in a waterbath (Ref. Z615560, Merck Millipore) at 95ºC for 20min to unmask the antigen. After cooling, only FFPE and free-floating sections for immunohistochemistry were quenched in 10% methanol (vol/vol; Ref. 131091.1212, PanReac AppliChem) and 3% hydrogen peroxide (vol/vol; Ref. UN2014, PanReac AppliChem) for 5min. Species-specific serum (5% vol/vol Normal Goat serum, Ref. S-1000, Vector) and 0.1% Triton X-100 (Ref. T9254, Sigma-Aldrich) were used to block and permeabilize all sections for 1h at room temperature. Sections were incubated overnight with primary antibodies at +4ºC and wet conditions. All primary antibodies and their corresponding references can be found in **Table 2, 3 and 4**.

Following day, appropriate secondary antibodies (**Table 5**) were added for 1h incubation at room temperature. For immunohistochemistry, ABC kit (Ref. 32050 for FFPE slices and Ref. 32020 for free-floating slices, Thermo Fisher Scientific) and Vector SG (Ref. SK-4700, Vector) were used to reveal antigen-antibody reaction. Afterwards, sections were dehydrated and coverslipped with DPX (Ref. 1.00579.0500, Sigma-Aldrich). For immunofluorescence procedure, nuclei were stained with HOECHST (Ref. 33342, Thermo Fisher Scientific). Finally, sections were coverslipped too using DakoCytomation Fluorescent Mounting Medium (Ref. S3023, Dako).

3.9 Antibodies

All human (**Table 2**), mouse (**Table 3**) and rat (**Table 4**) primary antibodies were tested in positive control tissue to optimize immunohistochemistry/immunofluorescence conditions. Antibodies for human tissue T cell characterization were tested in human tonsil and/or lymph node according to human protein atlas (Uhlén *et al.*, 2015) (**Annex Figure 1**).

A complete list of secondary antibodies used can be found in **Table 5**.

Table 2. List of primary antibodies for human tissue

Antigen	Host	Source	Reference	Application and dilution
CD4	Rabbit	Sigma-Aldrich	HPA004252	IHC: 1:100
CD8α	Rabbit	Sigma-Aldrich	HPA037756	IHC: 1:200
CD8α	Rat	CNIO	NOR132	IF: Sup.
CD69	Mouse	BioLegend	310902	IF: 1:25
CD103	Rabbit	Abcam	ab129202	IF: 1:100

FasL	Rabbit	Sigma-Aldrich	HPA054959	IF: 1:500
Granzyme A	Rabbit	Thermo Fisher Scientific	PA5-30054	IF: 1:100
Granzyme B	Mouse	Merck Millipore	MAB3070	IF: 1:100
Granzyme K	Rabbit	Sigma-Aldrich	HPA063181	IF: 1:100
HLA-A/B/C	Mouse	Santa Cruz Biotechnology	Sc55582	IHC: 1:100
HLA-DR/DP/DQ	Mouse	Abcam	Ab7856	IHC: 1:200
IFNγ	Rabbit	Abcam	ab9657	IF: 1:100
PD-1	Mouse	Roche	760-4895	IF: Sup.
PD-L1	Rabbit	Cell Signaling Technology®	13684	IF: 1:200
Perforin-1	Rabbit	Abcam	ab180773	IF: 1:100
pS129 α-synuclein	Rabbit	Abcam	ab51253	IHC: 1:125
TNFα	Rabbit	Abcam	ab9635	IF: 1:500

Sup. supernatant

Table 3. List of primary antibodies for mouse tissue

Antigen	Host	Source	Reference	Application and dilution
CD3ε	Rabbit	Abcam	ab5690	IHC: 1:100
CD4	Rat	Bio-Rad	MCA2691	IF: 1:100
CD8α	Rat	Bio-Rad	MCA1768	IF: 1:100
TH	Rabbit	Calbiochem	657012	IF: 1:500

Table 4. List of primary antibodies for rat tissue

Antigen	Host	Source	Reference	Application and dilution
CD3ε	Rabbit	DAKO	A0452	IHC: 1:200
CD4	Mouse	Bio-Rad	MCA372G	IF: 1:100
CD8α	Mouse	Bio-Rad	MCA48R	IF: 1:200
α-synuclein	Mouse	Thermo Fisher Scientific	MS-1572	IF: 1:500
TH	Rabbit	Calbiochem	657012	IF: 1:500

Table 5. List of secondary antibodies

Antigen	Host	Source	Reference	Application and dilution
Anti-rabbit biotinylated	Goat	Vector	BA-1000	IHC: 1:200
Alexa Fluor 488 anti-rabbit	Goat	Thermo Fisher Scientific	A11008	IF: 1:200
Alexa Fluor 488 anti-mouse	Goat	Thermo Fisher Scientific	A11001	IF: 1:200
Alexa Fluor 488 anti-rat	Donkey	Thermo Fisher Scientific	A21208	IF: 1:200

Alexa Fluor 594 anti-rabbit	Goat	Thermo Fisher Scientific	A11012	IF: 1:200
Alexa Fluor 594 anti-rat	Goat	Thermo Fisher Scientific	A11007	IF: 1:200

3.10 Quantitative analyses

All human FFPE SN*pc* sections were obtained from the level of the third cranial nerve. Rodent SN*pc* sections were sorted in series of 12 sections separated equally.

3.10.1 Rodent tissue

3.10.1.1 Striatal optical densitometry analysis

Striatal TH fiber density was assessed by optical densitometry (OD) at four coronal levels from each animal, covering the entire striatum. Slides were scanned with a scanner (Ref. Epson Perfection V750 PRO, Epson) and intensity was analyzed with SigmaScan Pro 5.0 software (Systate Software, Inc, USA). Measured striatal intensity values (IStr) were corrected for non-specific background DAB staining by subtracting values obtained from the corpus callosum (ICC). Finally, OD was calculated with the following formula:

$$OD = -\log\left(\frac{IStr}{ICC}\right)$$

In unilateral stereotaxic AAV delivery experiments contralateral hemisphere was also used to calculate an OD ratio. Representative images were acquired using an Olympus BX61 microscope fitted with an Olympus DP72 camera.

3.10.1.2 Dopaminergic neuron counts

Assessment of the total number of TH+ neurons in the SN*pc* was made in both sides of every sixth section throughout the brain structure. A total of 12 sections per animal were used. Stereological quantification was performed employing the optical fractionator principle in the Stereo Investigator 11 software (MBF Bioscience, Version 11.06.2). SN*pc* was delineated by using a 4x objective, whereas the actual counting was performed using a 100x oil objective on a Zeiss ImagerD1 microscope. A quarter part of total counting frames was analyzed. These counting frames (50*50µm) were located in a general counting grid of 125*100µm. Representative images were acquired using an Olympus BX61 microscope fitted with an Olympus DP72 camera.

3.10.1.3 T cell counts

CD3+ T cells. Assessment of the total number of CD3+ T cells in the SN*pc* was made in both sides of every sixth section throughout the brain structure. A total of 12 sections per animal were used. Stereological quantification was performed employing the optical fractionator principle in the Stereo Investigator 11 software (MBF Bioscience, Version 11.06.2). SN*pc* was delineated by using a 4x objective, whereas the actual counting was performed using a 40x oil objective on a Zeiis ImagerD1 microscope. All counting frames (100*100µm) were analyzed. Representative images were acquired using an Olympus BX61 microscope fitted with an Olympus DP72 camera.

CD4+ and CD8+ T cells. Assessment of the total number of CD4+ and CD8+ T cells in the SN*pc* was made in both sides of every sixth section using 4 sections throughout the brain structure. Countings were performed using a 40x objective in an Olympus BX61 microscope. Results are represented as density: number of positive T cells per section. Images were acquired using standard filter sets with an Olympus FluowViewTM FV1000 confocal microscope and FV10-ASW 4.2 visualization software.

3.10.2 Human tissue

3.10.2.1 T cell density

For human analyses CD4+ and CD8+ T cell densities were quantified using three sections per case for each T cell type. Quantification was performed using a Zeiss AX10 microscope with a motorized stage and Stereo Investigator software. SN*pc* was delineated with a contour using a 4x magnification lens. All fields included in this contour were counted with a 20x magnification lens and a 450*300µm counting frame. Average fields counted per section were 140. Infiltrating and perivascular T cells were counted separately with different counting markers. To obtain the final density, numbers of CD4+ or CD8+ T cells were divided by the delineated area. Representative images were acquired using an Olympus BX61 microscope fitted with an Olympus DP72 camera.

3.10.2.2 Dopaminergic neuron density

For FFPE human brain sections, dopaminergic neurons containing neuromelanin were counted using one SN*pc* section for each case. This was

performed with a Stemi 2000-C microscope fitted with an AxioCam ERc55 camera.

3.10.2.3 MHC class-II+ microglial morphologies

For FFPE human brain sections, MHC class-II+ microglial morphologies were counted by immunohistochemistry using HLA-DR/DQ/DB antibody. Three distinct morphologies were counted: 1) homeostatic as highly ramified and with a small soma, 2) intermediate as less ramified, more intense staining and an apparent soma and 3) ameboid as practically no ramification, normally intense staining and an apparent soma. Phagocytized neuromelanin by MHC class-II+ microglia was counted as the latter morphology. Only one SN*pc* section was used for each case. A similar methodology to assess T cell density was followed. Representative images were acquired using an Olympus BX61 microscope fitted with an Olympus DP72 camera.

3.10.2.4 Phenotypic characterization of CD8+ T cells

Double staining for CD8α and various markers was performed and reported as the total number and percentage of CD8+ T cells expressing the specific marker in one section of SN*pc* for each case. Infiltrating and perivascular T cells were counted separately. Quantification was performed with an Olympus FSX100 microscope and images were acquired using standard filter sets with an Olympus FluowViewTM FV1000 confocal microscope and FV10-ASW 4.2 visualization software.

3.10.2.5 Density of synucleinopathy-related aggregates

For FFPE human brain sections, synucleinopathy-related structures were detected by immunohistochemistry using pS129 α-synuclein antibody. Neurons with diffuse synuclein staining, Lewy neurites and Lewy bodies were counted using one section of SN*pc* for each case. A similar methodology to assess T cell density was followed. Representative images were acquired using an Olympus BX61 microscope fitted with an Olympus DP72 camera.

3.11 Laser capture microdissection

Brain slices of 10μm were cut in a cryostat and transferred in polyethylene naphthalate (PEN) membrane slides (Ref. MDG3P40W, MicroDissect GmbH). These were previously treated for 1 hour under ultraviolet light radiation. Briefly, sections were firstly fixed with ethanol 75% and then stained with Arcturus® HistoGene® (Ref. 12241-05, Thermo Fisher Scientific). Sections were then dehydrated using increasing ethanol concentration solutions. For microdissection, they were located on the Leica LMD system (Ref. LMD6500, Leica) previously cleaned with RNAse Away (Ref. 700511, Molecular BioProducts). Dopaminergic neurons were blue stained, due to Arcturus® HistoGene® Frozen Section staining kit (Ref. KIT0401, Thermo Fisher Scientific), and presented dark-brown pigment neuromelanin. Dopaminergic neurons were manually drawn at 40X magnifications before cutting with the laser (**Figure 18**). Cut slices fell in a microtube (Ref. 72699, Molecular BioProducts) with RNA extraction reagent QIAzol (Ref. 79306, Qiagen).

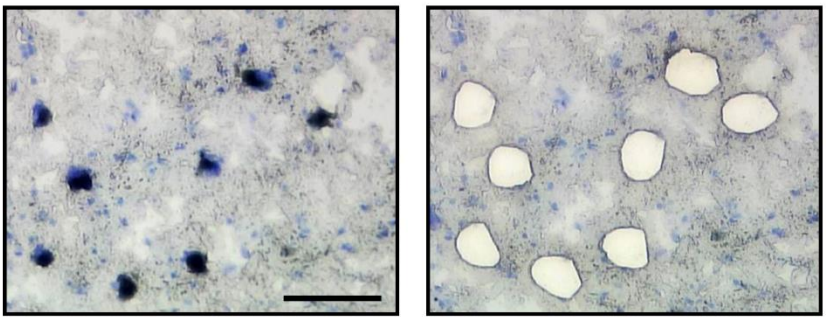

Figure 18. Laser capture microdissected SN*pc* dopaminergic neurons. Representative photomicrographs of a SN*pc* stained with Arcturus® Histogene® (blue) before and after laser capture microdissection. Neuromelanin-containing (dark-brown) dopaminergic neurons are contourned and dissected. Scale bar = 100μm.

3.12 RNA extraction and gene expression analysis by qPCR

3.12.1 RNA extraction

Total RNA from frozen midbrain human tissue was extracted using RNeasy Lipid Tissue Mini Kit (Ref. 74804, Qiagen) regarding supplier's recommendations. Briefly, QIAzol was added to samples and they were disrupted with a tissue homogenizer (Ref. OMNI-TH 220PCR, OMNI International). Chloroform was added and they were incubated for 2-3min at room temperature shaking them vigorously for 15sec. After centrifuge, QIAzol and chloroform mixture was separated into a lower red phenol-chloroform phase and a RNA-rich colorless upper aqueous phase. The latter was transferred into a new tube and 70% ethanol was added. This new mixture was then placed into a RNeasy Mini spin column in order to be centrifuged. After

some buffer washes, RNA was eluted with 30µl of RNase-free water and stored at -80ºC for its posterior analysis.

Total RNA from microdissected human dopaminergic neurons was extracted using miRNeasy Micro Kit (Ref. 217084, Qiagen). This procedure combines 18 phenol/guanidine-based lysis steps and silica-membrane-based purification of total RNA. QIAzol-added samples were vortexed for further lysis of tissue and cells. After 5min at room temperature, chloroform was added and they were incubated for 2-3min at room temperature after vigorous shaking by hand for 15s. The mixture was separated after centrifugation into a lower red phenol-chloroform phase and a RNA-rich colorless upper aqueous phase. The latter was transferred to a new tube with 100% ethanol and passed through a RNeasy MinElute spin column. Then, two buffer and one ethanol washes were performed. RNA was eluted with RNAse-free water (14µl) and stored at -80ºC for its posterior analysis.

Afterwards, midbrain RNA concentration, quality and integrity were determined using the NanoDrop 1000 assay (Ref. ND-2000, Thermo Fisher Scientific). The 260/230 and 260/280 ratios were considered for quality check. Presence of organic compounds could halter posterior reactions. For laser capture microdissected-recollected samples, an electrophoresis using an Agilent 2100 BioAnalyser instrument and an Agilent RNA 6000 Pico Kit (0,05-5ng/ul) (Ref. 5067-1513, Agilent Technologies) were performed to obtain RNA integrity number (RIN). RIN ranges from 10 (intact) to 1 (degraded). All RIN numbers obtained from the RNA samples were above 8, which ensure a good RNA quality.

3.12.2 cDNA synthesis

One microgram of RNA was used for reverse transcription with SuperScript™ III Reverse Transcriptase kit (Ref. 18080051, ThermoFisher Scientific). Firstly, RNA was diluted in RNase-free water to obtain one microgram and then, incubated for 5min at +65ºC with Oligo (dT)12-18 (0.025µg/µl) and dNTPs (0.5mM). Afterwards, First-Strand Buffer (5X), DTT (0.005M), RNaseOUT™ Recombinant Ribonuclease Inhibitor (Ref. 10777019, ThermoFisher Scientific) (2U/µl) and the Superscript III enzyme (10U/µl) were added to each sample and they were incubated for 1h at +50ºC. Retrotranscription reaction was inactivated by heating samples to +70ºC for 15min. Samples were stored at -20ºC until analyzed.

3.12.3 cDNA Preamplification

For TCR analysis, complementary deoxyribonucleic acid (cDNA) from post-mortem human SN*pc* was preamplified before qPCR procedure. TaqMan® PreAmp Master Mix (Ref. 4391128, Applied Biosystems) was used. In brief, all TaqMan® Assays which were going to be analyzed were mixed in a pool at 0.2X. cDNA from each sample was diluted with nuclease-free water to obtain 250ng and added to TaqMan® Assays for a final reaction concentration of 5ng/µl. Finally, TaqMan® PreAmp Master Mix was added at 1X. A total of 14 cycles were performed in the manufacturer recommended conditions.

3.12.4 qPCR analyses

QPCR analysis was performed to determine gene expression levels. 10ng of cDNA samples per well were mixed with Taqman Gene Expression Master Mix (Ref. 4440038, Applied Biosystems) and FAM-labelled Taqman gene expression

assays (**Table 6**, Applied Biosystems) were used on MicroAmp Optical 384-Well Reaction Plate (Ref. 4326270, Applied Biosystems) and an ABI PRISM 7900HT (Ref., 4317596, Applied Biosystems). Standard PCR cycling program was performed (+50ºC 2min, 95ºC 10min, 95ºC 15sec * 40 cycles, 60ºC 1min * 40 cycles). Threshold cycles (C_t) for each target gene were normalized to the endogenous control hypoxhanthine phosphoribosyltransferase 1 gene (*HPRT1*). Difference between target genes and endogenous control C_t were expressed as ΔC_t.

Table 6. List of human Taqman gene expression assays

Gene	Taqman Ref.
B-2-Microglobulin	Hs00187842_m1
CD1A	Hs00381754_g1
CD1B	Hs00957537_m1
CD1C	Hs00233509_m1
CD1D	Hs00939886_g1
CD1E	Hs05057834_s1
CD8A	Hs00233520_m1
HLA-A	Hs01058806_g1
HLA-B	Hs00818803_g1
HLA-C	Hs00740298_g1
HLA-E	Hs03045171_m1
HPRT1	Hs02800695_m1
KLRB1	Hs00174469_m1

TRAC	Hs05285118_g1
TRAV20	Hs00413676_g1
TRBC1	Hs01588269_g1
TRDV3	Hs01669899_m1
TH	Hs00165941_m1

3.13 Statistical analyses

All values are expressed as the mean ± standard error of the mean (SEM). Statistical analyses were performed using GraphPad Prism 6 software (version 6, GraphPad Software, USA). Comparisons between two groups were performed by Student's *t*-test or Mann-Whitney U-test for groups with unequal variances. Comparisons between more than two groups of only one variable were done by one-way ANOVA. The Tukey's test for *post-hoc* multiple comparisons was used as recommended by the software itself. Correlations between two numerical variables were performed using Pearson correlation test or sigmoidal tests. Results were considered to be significant for values $P < 0.05$.

RESULTS

4. Results

4.1 T cell infiltration in Parkinson's disease animal models

Our first four subobjectives were mainly focused to analyze T cell brain infiltration in several PD animal models. Among all available PD experimental animal models, we chose MPTP treated mice and overexpression of h-WT-α-synuclein. On the one hand, we started with MPTP treated mice because T cell brain infiltration in PD animal models was firstly described in this one and, strikingly, they had a prominent role in dopaminergic cell loss (Brochard *et al.*, 2009). Other studies have used this model to demonstrate that several anti-inflammatory strategies, such as priming Treg-induced immune tolerance (Reynolds *et al.*, 2007; Olson and Gendelman, 2016; Gendelman *et al.*, 2017), are neuroprotective. Moreover, we wanted to mimic the decrease of blood Treg numbers and their effector T cell-suppression capabilities observed in PD cases (Niwa *et al.*, 2012; Saunders *et al.*, 2012; Kustrimovic *et al.*, 2018; Álvarez-Luquín *et al.*, 2019). To do this, we used FoxP3.LuciDTR transgenic mice which allowed us to systemically deplete Tregs injecting diphtheria toxin. Altogether, we wanted to obtain a PD animal model with consistent T cell SN*pc* infiltration, Treg deficiency and dopaminergic cell loss. On the other hand, recent studies have proposed α-synuclein as the potential antigen for the adaptive immune response in PD (Reynolds *et al.*, 2009*a*; Sanchez-Guajardo *et al.*, 2010). To study this possibility, we wanted to overexpress h-WT-α-synuclein in rat SN*pc* and analyze T cell infiltration dynamics and their relationship with nigrostriatal degeneration.

4.1.1 Not consistent SN*pc* T cell infiltration in acute MPTP treated C57BL/6Ncrl mice

Our first main objective was to study the role of adaptive immune system in MPTP treated mice. To do that, we first tried to reproduce T cell brain infiltration in acute MPTP treated mice with a pilot experiment of 3 animals per group. As it has been previously mentioned in both Introduction and Hypotheses chapters, T cell brain infiltration in PD animal models was initially described in acute MPTP treated C57BL/6JRj mice (Kurkowska-Jastrzebska *et al.*, 1999; Brochard *et al.*, 2009). They found that both CD4+ and CD8+ T cells infiltrated SN*pc*. This infiltration started at 2 days post-injection (d2) but it was not statistically significant until d4. At d7 it reached its maximum peak. CD8+ T cell densities outnumbered CD4+ T cell ones. In addition to this, using several knock-out mice, they demonstrated that CD4+ T cells were necessary for dopaminergic cell loss in acute MPTP treated mice.

As this project was at its beginnings, this also served to set up experimental protocols for T cell counts. We started injecting C57BL6/Ncrl inbred mice intraperitoneally with 4 MPTP (20mg/kg) injections in 2h-intervals for one day (**Figure 19A**). Control mice received saline injections. Due to previous studies in our lab, nigrostriatal degeneration dynamics are very well established in this mice strain. Afterwards, we ensured the efficacy of MPTP. We analyzed at d7 after last injection both depletion of TH+ striatal optical density in the striatum and the dopaminergic cell loss in the SN*pc*. Acute MPTP treated mice had 65% reduction of TH+ axon terminals in the striatum compared with saline treated ones (0.0251 A.U. saline vs 0.0097 A.U. acute MPTP; **Figure 19B**). They also had a 46% reduction of dopaminergic neurons in the SN*pc* (6795 TH+ neurons saline vs 3660 TH+ neurons acute MPTP; **Figure 19C**).

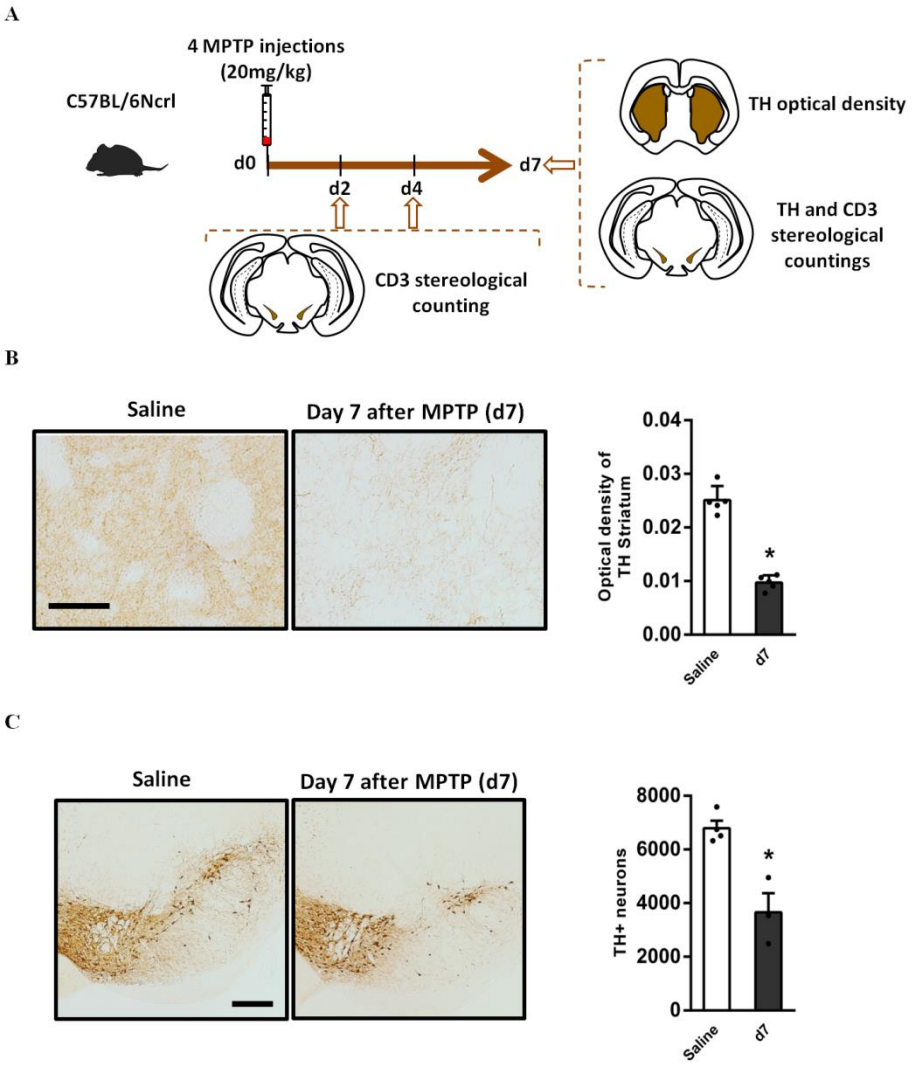

Figure 19. TH+ axon terminal and dopaminergic cell losses in acute MPTP treated C57BL/6Ncrl mice. (**A**) Diagram showing the timecourse and associated experiments in the acute MPTP treated mice. (**B**) Left: Representative striatal TH immunostaining in both saline and MPTP treated mice at day 7 after last injection (scale bar = 30µm). Right: Striatal TH optical density of both saline (n = 5) and MPTP (n = 5) treated mice. Un-paired *t*-test: **P*-value < 0.05 compared to saline, $t = 11.53$, $df = 8$. (**C**) Left: Representative photomicrographs of SN*pc* TH immunostaining in both saline and MPTP treated mice at day 7 after last injection (scale bar = 100µm). Right: Stereological TH+ cell counting of both saline (n = 4) and MPTP (n = 3)

treated mice. Un-paired *t*-test: **P*-value < 0.05 compared to saline, $t = 4.601$, $df = 5$. Bars represent mean value ± SEM in all graphs.

We counted stereologically CD3+ T cells in both parenchyma and perivascular spaces (**Figure 20**). In contrast with the state-of-the-art, we could not find any differences in both compartments. We only found a small increase at d2 after last injection in perivascular spaces (326 CD3+ cells saline vs 447 CD3+ cells d2; **Figure 20, Right Bottom**) and at d4 in the brain parenchyma (72 CD3+ cells saline vs 103 CD3+ cells d4; **Figure 20, Right Top**). Thus, we were not able to reproduce the T cell brain infiltration in the acute MPTP PD animal model. Moreover, we also checked T cell brain infiltration in acute MPTP treated CD57BL/6JRj mice. T cell brain infiltration was initially described in this substrain of mice (Kurkowska-Jastrzebska *et al.*, 1999; Brochard *et al.*, 2009). Although it was a qualitative analysis, we did not find evident CD3+ T cell brain infiltration at d7. Due to these negative results, we contacted the authors of the paper and they reported that 8 years after publishing they were unable to obtain the same results with the same substrain that they had used. Altogether, we decided to change MPTP paradigm to the subacute one as neither us nor the first group reporting MPTP T cell brain infiltration could not reproduce this adaptive immune response. In the subacute MPTP paradigm, T cell brain infiltration had also been demonstrated (Depboylu *et al.*, 2012).

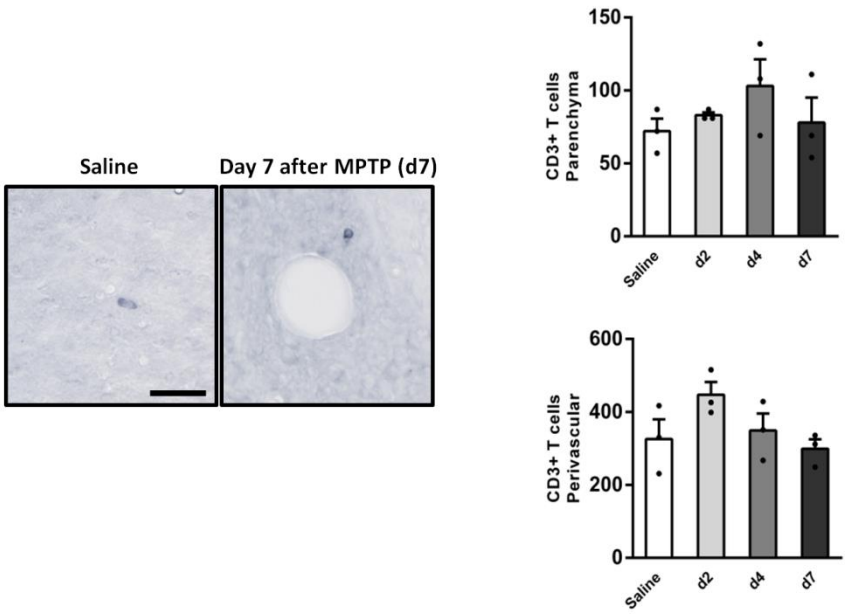

Figure 20. CD3+ T cell infiltration in the SN*pc* of MPTP treated C57BL/6Ncrl mice. Left: Representative photomicrographs of CD3 immunostaining in the SN*pc* of both saline and acute MPTP treated mice at day 7. Right: Stereological CD3+ cell counts in both saline (n = 3) and acute MPTP (n = 3 animals/timepoint) treated mice. T cells in the brain parenchyma and perivascular spaces were counted separately. Scale bar = 15µm. One-way ANOVA, *post-hoc* Tukey's test. *P*-value < 0.05. Bars represent mean value ± SEM in all graphs.

4.1.2 T cells transiently infiltrate SN*pc* of subacute MPTP treated C57BL/6Ncrl mice

In contrast with acute MPTP regimen, the subacute MPTP one consists of one MPTP (30mg/kg) intraperitoneal injection daily for 5 consecutive days. These low dose insults provoke less nigrostriatal impairment compared with acute MPTP. A longer timecourse and less toxic insults are two factors that could help to raise an adaptive immune response. Several days are needed to raise an adaptive immune response in mice (Robinson *et al.*, 2015). In contrast with

acute MPTP, subacute regimen leads to a lower dopaminergic cell death but, at the same time, it also creates mitochondria-mediated oxidative stress and lisosomal dysfunction. These two processes and dysfunctional and dystrophic dopaminergic neurons (Torra *et al.*, 2018) could help to present more neoantigens to the immune system. Moreover, one previous study had reported T cell brain infiltration in the SN*pc* of subacute MPTP treated mice (Depboylu *et al.*, 2012). This infiltration was detected at day 1 post-injection and it had returned to basal levels before 10 days post-injection. They did not perform a detailed timecourse study to show T cell nigral infiltration dynamics in the subacute MPTP paradigm. CD8+ T cells outnumbered CD4+ ones just like in the acute MPTP.

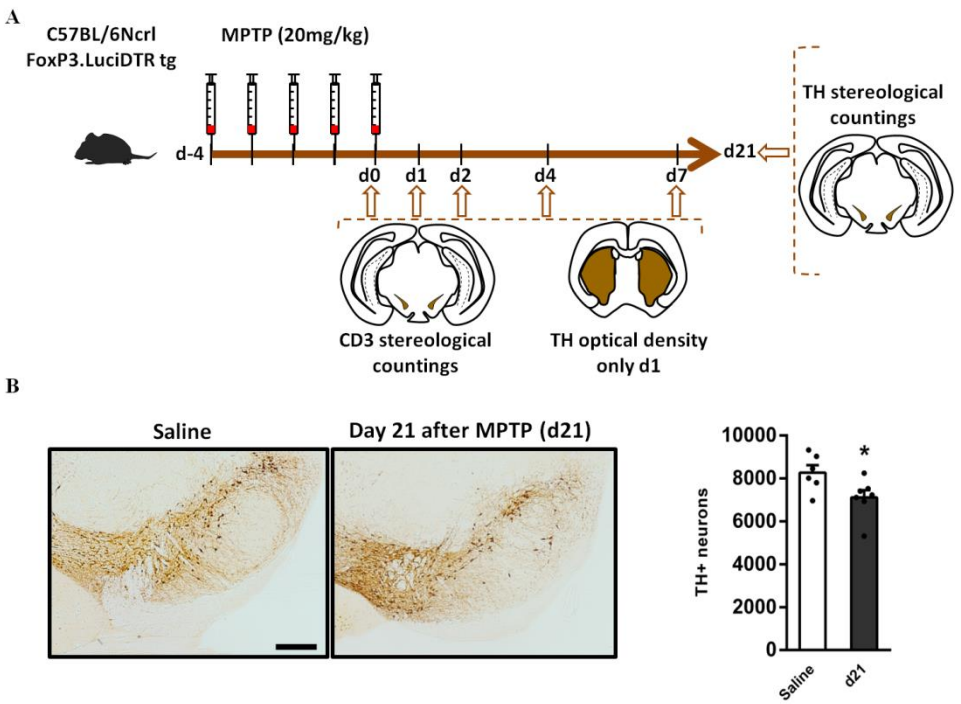

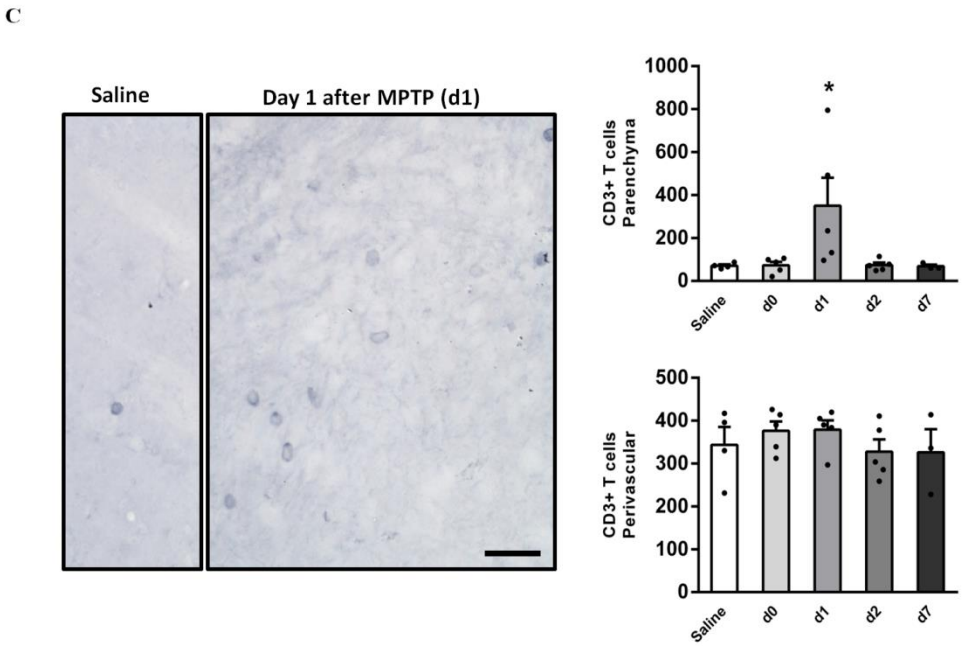

Figure 21. Dopaminergic cell loss and CD3+ T cell brain infiltration in the subacute MPTP treated C57BL/6Ncrl FoxP3.LuciDTR transgenic mice. (**A**) Diagram representing timecourse and associated experiments in the subacute MPTP treated mice. (**B**) Left: Representative photomicrographs of SN*pc* TH immunostaining in both saline and MPTP treated mice at day 21 after last injection. Scale bar = 100µm. Right: Stereological TH+ cell counts in both saline (n = 6) and MPTP (n = 7) treated mice. Un-paired *t*-test: **P*-value < 0.05 compared to saline, $t = 2.349$, $df = 11$. (**C**) Left: Representative photomicrographs of SN*pc* CD3 immunostaining in saline and MPTP treated mice at several days after last injection. Right: Stereological CD3+ cell counts in both saline (n = 4) and MPTP treated mice at several timepoints: d0 (n = 5), d1 (n = 5), d2 (n = 5), d7 (n= 3). Both parenchyma and perivascular spaces were counted separately. Scale bar = 15µm. Parenchyma one-way ANOVA, *post-hoc* Tukey's test: **P*-value < 0.05 compared to d0. Bars represent mean values ± SEM in all graphs.

We intraperitoneally injected C57BL/6Ncrl mice with 30mg/kg MPTP doses. However, unlike acute MPTP experiment, we were using transgenic mice:

FoxP3.LuciDTR. This transgenic mouse had been genetically modified to add DTR under FoxP3 promoter. This receptor allowed as to completely deplete regulatory T cells (Treg), which are anti-inflammatory, by means of intraperitoneally injecting diphtheria toxin. Green fluorescent protein (GFP) and luciferase were also added. GFP helped us to separate Tregs by flow cytometry and luciferase was useful for *in vivo* bioluminescence imaging. In this genetic background, 30mg/kg dose induced high mortality because of peripheral side effects of MPTP. When high mortality is found with a particular strain, the dose can be reduced to 20mg/kg which produces less dopaminergic cell death than higher dosages (**Figure 21A**). Dopaminergic cell loss was statistically significant at 21 days post-injection (8265 TH+ cells saline vs 7110 TH+ cells d21; **Figure 21B**). Perivascular CD3+ T cells did not increase in any timepoint analyzed (**Figure 21C, Right Bottom**). Nonetheless, there was a CD3+ T cell brain infiltration at day 1 post-injection (70.5 CD3+ T cells saline vs 349.8 CD3+ T cells d1; **Figure 21C, Right Top**). This T cell infiltration was transient as one day after it returned to basal levels. CD3+ T cell infiltration at day 1 post-injection positively correlated with striatal TH loss in a sigmoidal function (r = 0.9990; **Figure 22A**). These results indicated that T cell brain infiltration is related with dopaminergic dysfunction. Although this correlation does not indicate causality, it suggests that T cell infiltration is impairing dopaminergic neurons that will eventually die. Both CD4+ (20 cells/section) and CD8+ (13.4 cells/section) T cells infiltrated SN*pc* of subacute MPTP treated mice (**Figure 22B**). Striatal TH optical density negatively correlated in a sigmodial function with both CD4+ T cell (r = 0.9992; **Figure 22C**) infiltration and CD8+ (r = 0.6753; **Figure 22D**) T cell infiltration. It is very likely that dopaminergic cell loss would be more extensive in the case that T cell infiltration was sustained after day 1.

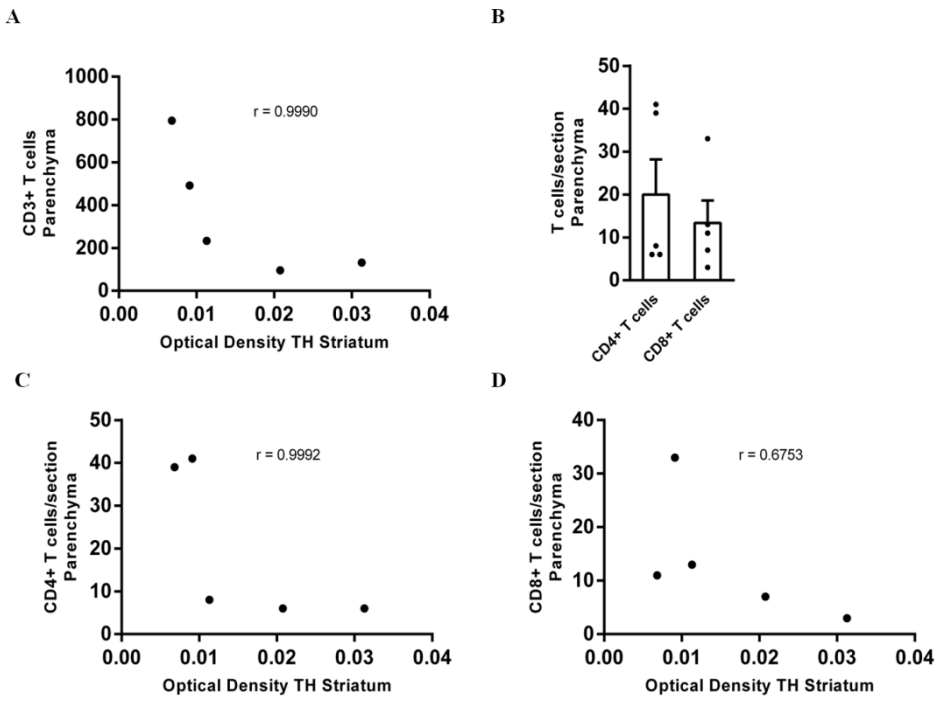

Figure 22. Number of SN*pc* T lymphocytes correlates with TH+ immunostaining in the striatum at d1. (**A**) Scatter diagram of CD3+ T cells in the SN*pc* parenchyma and TH+ immunostaining in the striatum at day 1 after last injection of MPTP (n = 5). Sigmoidal correlation *r* = 0.9990. (**B**) Parenchymal CD4+ and CD8+ T cells in the SN*pc* of subacute MPTP at day 1. (**C**) Scatter diagram of CD4+ T cells in the SN*pc* parenchyma and TH+ immunostaining in the striatum at day 1 after last injection of MPTP (n = 5). Sigmoidal correlation *r* = 0.9992. (**D**) Scatter diagram of CD8+ T cells in the SN*pc* parenchyma and TH+ immunostaining in the striatum at day 1 after last injection of MPTP (n = 5). Sigmoidal correlation *r* = 0.6753.

4.1.3 Systemic Treg depletion in C57BL6/Ncrl mice does not exacerbate nigrostriatal degeneration in the subacute MPTP model

To finally complete our two first subobjectives, we wanted to mimic the decrease of the Treg suppressive capacity that characterizes PD patients by depleting them systemically in a mouse model. We expected that this break in

immune tolerance could boost nigrostriatal degeneration in MPTP treated mice and, thus, generate a more accurate model of the disease regarding the adaptive immune response.

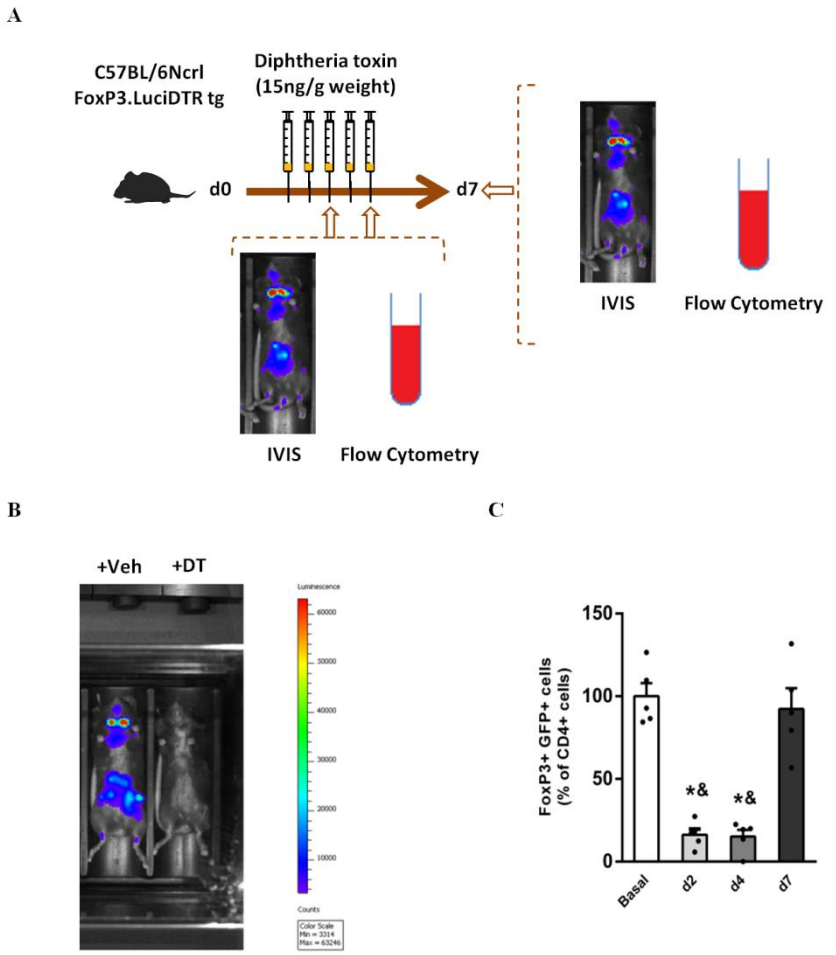

Figure 23. **Systemic Treg depletion injecting diphtheria toxin in C57BL/6Ncrl FoxP3.LuciDTR transgenic mice.** (**A**) Diagram representing timecourse and associated experiments in systemic Treg depletion with diphtheria toxin. (**B**) Representative bioluminescence IVIS pictures of Treg depleted mice. Left: one animal with two vehicle

injections. Right: one animal with two diphtheria toxin injections. (**C**) Percentage of FoxP3+ GFP+ cells among CD4+ T cells at distinct timepoints: baseline (n = 5), d2 (n = 5), d4 (n = 5) and d7 (n = 7). One-way ANOVA repeated measures, *post-hoc* Tukey's test: **P*-value < 0.05 compared to baseline; &*P*-value < 0.05 compared to d7; $F = 27.99$, $df = 19$. Bars represent mean ± SEM.

In order to do that, we used the C57BL/6Ncrl FoxP3.LuciDTR transgenic mice that allow depleting Treg lymphocytes by injecting systemically diphtheria toxin. First of all, before depleting Tregs in MPTP treated mice, we set up diphtheria injections protocol in our transgenic mice. We started injecting intraperitoneally diphtheria toxin in a dosage of 15 ng/g body weight according to previous studies (Suffner *et al.*, 2010). We injected once each day during 4 days (**Figure 23A**). Due to luciferase expression in Tregs, we could follow Treg depletion by bioluminescence in *in vivo* imaging system (IVIS) (**Figure 23B**). Bioluminiscence was totally decreased with only one injection. Flow cytometry was used to detect CD4+ FoxP3+ GFP+ Tregs in the peripheral blood. Two injections were enough to decrease a total of 83.6% of peripheral CD4+ FoxP3+ GFP+ Tregs (**Figure 23C**). This decrease was maintained until three days after last diphtheria toxin injection increasing until practically basal levels (92.34% of peripheral CD4+ FoxP3+ GFP+ Tregs).

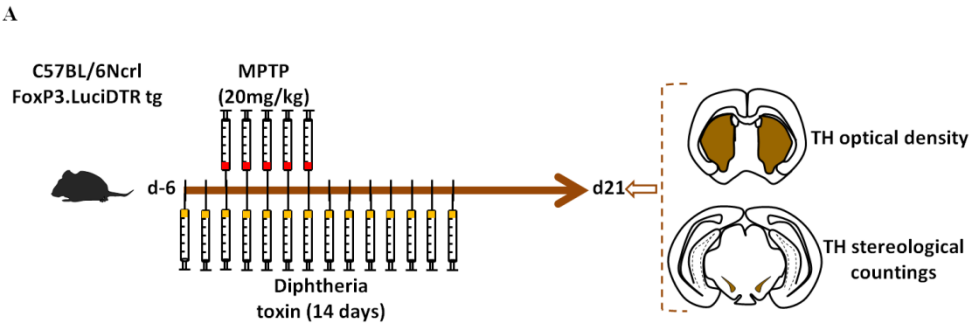

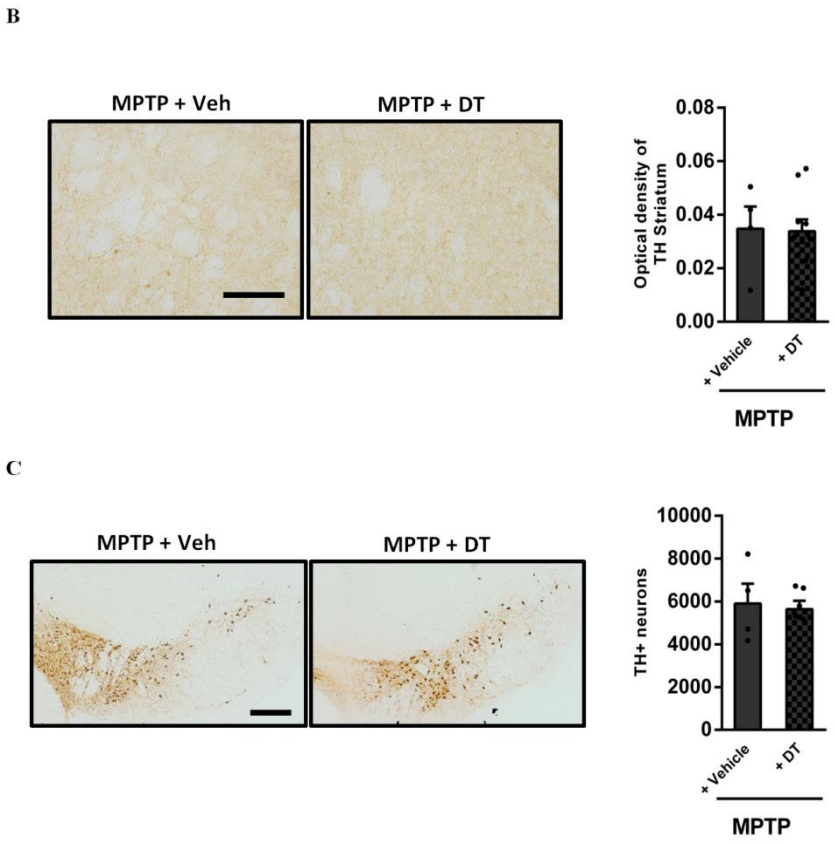

Figure 24. Loss of TH+ striatal axon terminal and dopaminergic cell losses in subacute MPTP treated C57BL/6Ncrl FoxP3.LuciDTR transgenic mice after Treg depletion. (**A**) Diagram representing timecourse and associated experiments in the subacute MPTP treated mice with Treg depletion. (**B**) Left: Representative striatal TH immunostaining in both MPTP+Vehicle and MPTP+Diphtheria Toxin treated mice. Right: Striatal TH Optic density of both MPTP+Vehicle (n = 4) and MPTP+Diphtheria Toxin (n = 10) treated mice. Un-paired *t*-test: *P*-value < 0.05. (**C**) Left: Representative photomicrographs of SN*pc* TH immunostaining in both MPTP+Vehicle and MPTP+DT. Right: Stereological TH cell counts in both MPTP+Vehicle (n = 4) and MPTP+Diphtheria Toxin (n = 6). Scale bar = 100µm. Un-paired *t*-test: *P*-value < 0.05. Bars represent mean ± SEM in all graphs.

Regarding the above results, we started injecting diphtheria toxin two days before starting with the subacute MPTP treatment (**Figure 24A**). Diphtheria toxin vehicle was injected as a control. Daily diphtheria toxin injections were kept until seven days after the last injection of MPTP. This frequency allowed us to have Treg depletion during neuronal MPTP insults, T cell brain infiltration and the beginning of dopaminergic dysfunction. TH+ striatal optic density at d21 was not increased due to Treg ablation (0.0348 A.U. vehicle vs 0.0339 diphtheria toxin; **Figure 24B**). Dopaminergic cell loss was neither increased in Treg depleted animals (5902 TH+ cells vehicle vs 5645 TH+ cells diphtheria toxin; **Figure 24C**). Due to the fact that we did not observe an increase of dopaminergic cell loss, T cell infiltration was not explored.

4.1.4 Overexpression of human wild-type α-synuclein in Sprague-Dawley rats SN*pc* induces behavioural motor changes and striatal tyrosine hydroxylase depletion but no dopaminergic cell loss. Non-conclusive results on T cell infiltration due to distinct status of purification between EV and α-synuclein vector.

Our second main objective was to understand the relationship between α-synuclein and the adaptive immune system. Some authors have proposed α-synuclein as an antigen candidate with which an immune response is risen around (Benner *et al.*, 2008; Theodore *et al.*, 2008, Reynolds *et al.*, 2009*b*; Cao *et al.*, 2010; Harms *et al.*, 2013, 2017, Sanchez-Guajardo *et al.*, 2013*b*, *a*; Reish and Standaert, 2015; Thome *et al.*, 2016, Qin *et al.*, 2016*a*). In order to study this relationship and hypothesis we chose a PD animal model which express α-synuclein in great quantities. Recombinant adeno-associated virus (AAV)-based overexpression of α-synuclein in animal models has been used as an

alternative to toxin-based animal models. They present α-synuclein accumulations better resembling one of the hallmarks of the disorder. Previous studies showed T cell brain infiltration in this PD animal model. However, many of them used genetic constructions overexpressing both α-synuclein and GFP. Other studies also used GFP viral vectors as experimental controls. In our hands, but not displayed in this thesis, GFP overexpression in rat SN*pc* may provoke high levels of T cell brain infiltration and dopaminergic cell death.

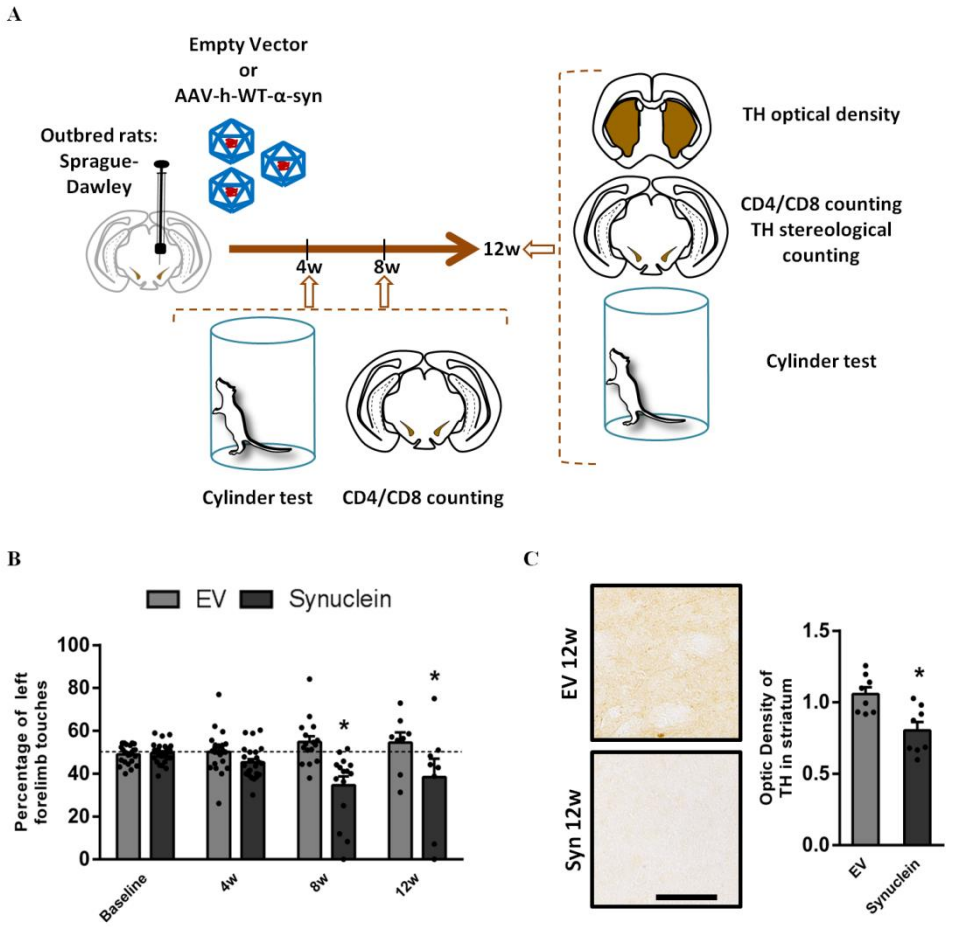

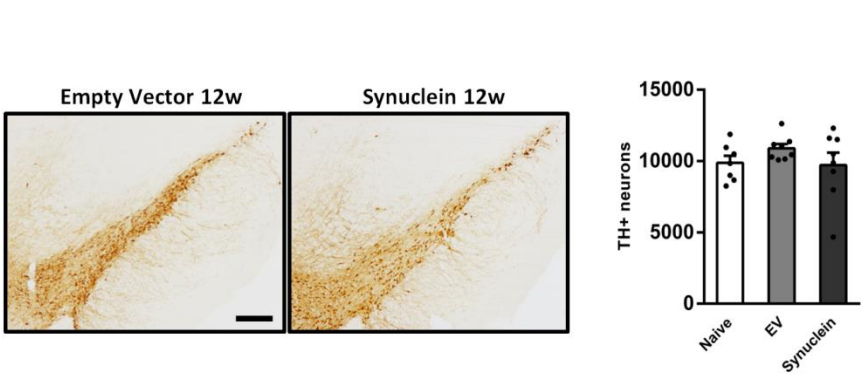

Figure 25. Overexpression of h-WT-α-synuclein in Sprague-Dawley strain rat SN*pc* induces motor asymmetry and loss of striatal TH+ axon terminals without SN*pc* dopaminergic cell loss. (**A**) Diagram representing timecourse and associated experiments in the rat SN*pc* overexpression of h-WT-α-synuclein. (**B**) Percentage of forelimb usage in the cylinder test in both EV (n = 24) and Synuclein (n = 26) groups during 4 weeks-interval until 12 weeks after viral vector injection. Two-way ANOVA, *post-hoc* Tukey's test: **P*-value < 0.05 compared to baseline. Interaction *F* (3, 136) = 7.467; Row Factor *F* (3, 136) = 1.283; Column *F* (1,136) = 27.88. (**C**) Left: Representative photomicrographs of striatal TH immunostaining for both EV and Synuclein groups. Right: Striatal TH optic density in both EV (n = 6) and Syn (n = 6) groups at 12w after viral vector injection. Scale bar = 30µm. Un-paired *t*-test: **P*-value < 0.05 compared to EV group, *t* = 3.402, *df* = 14. (**D**) Left: Representative photomicrographs of SN*pc* TH immunostaining of naïve, EV and Syn groups at 12w after viral vector injection. Right: Stereological counting of TH+ cells in the SN*pc* of naïve (n = 7), EV (n = 8) and Syn (n = 8) groups at 12w. Scale bar = 100µm. One-way ANOVA, *post-hoc* Tukey's test: *P*-value < 0.05. Bars represent mean ± SEM in all graphs.

We injected rAAV2/5 h-WT-α-synuclein (Syn) in the right SN*pc* of Sprague-Dawley rats. Our experimental control was an empty vector (EV) which did not cause any protein overexpression (**Figure 25A**). Both vectors had a difference in the purification protocol due to the fact that they were produced by two distinct laboratories: the Syn vector had been purified by iodixanol gradient and

chromatography and the EV only by the latter. We followed the animals until 12 weeks (12w) performing cylinder tests each 4 weeks to evaluate locomotor asymmetry. EV injected animals had some variability, but they did not show any asymmetry (54.62% left forelimb usage at 12w; **Figure 25B**). Nonetheless, Syn animals showed statistically significant impairment in the left forelimb usage since 8w (34.63% and 38.42% left forelimb usage at 8w and 12w, respectively). This behavioural change may be explained by the statistically decrease of TH+ striatal axon terminals at 12w (1.0581 A.U. EV vs 0.8037 A.U. Syn; **Figure 25C**). Overexpression of h-WT-α-synuclein was examined as a quality check (data not shown). Dopaminergic cell loss was not observed at 12w (9870 TH+ cells naïve, 10987.5 TH+ cells EV, 9716.25 TH+ cells Syn; **Figure 25D**). Finally, we analyzed T cell brain infiltration for both CD4+ and CD8+ T lymphocytes. Even though any of the results were statistically significant, a few CD4+ T cells were observed in all time points in the EV group (1 cell/section 4w, 0.125 cells/section 8w, 0.25 cells/section 12w; **Figure 26A**) meanwhile only at 12w in the Syn group (0.125 cells/section 12w). CD8+ T cells infiltrated in higher densities than CD4+ T cells did. EV injected animals presented high variability of CD8+ T cell densities between timepoints (1.25 cells/section at 4w, 0.0833 cells/section 8w, 0.7813 cells/section 12w; **Figure 26B**). Syn injected animals had practically no infiltration until 12 weeks (0.0833 cells/section 4w, 0 cells/section 8w, 1.531 cells/section 12w). EV immunogenicity makes difficult to interpret whether h-WT-α-synuclein overexpression also induces by itself a T cell brain infiltration. With this we demonstrated that with no iodixanol purification gradient, EV can induce T cell infiltration. For the following experiment, we purified EV with iodixanol gradient protocol expecting to lessen T cell SN*pc* infiltration in our experimental control.

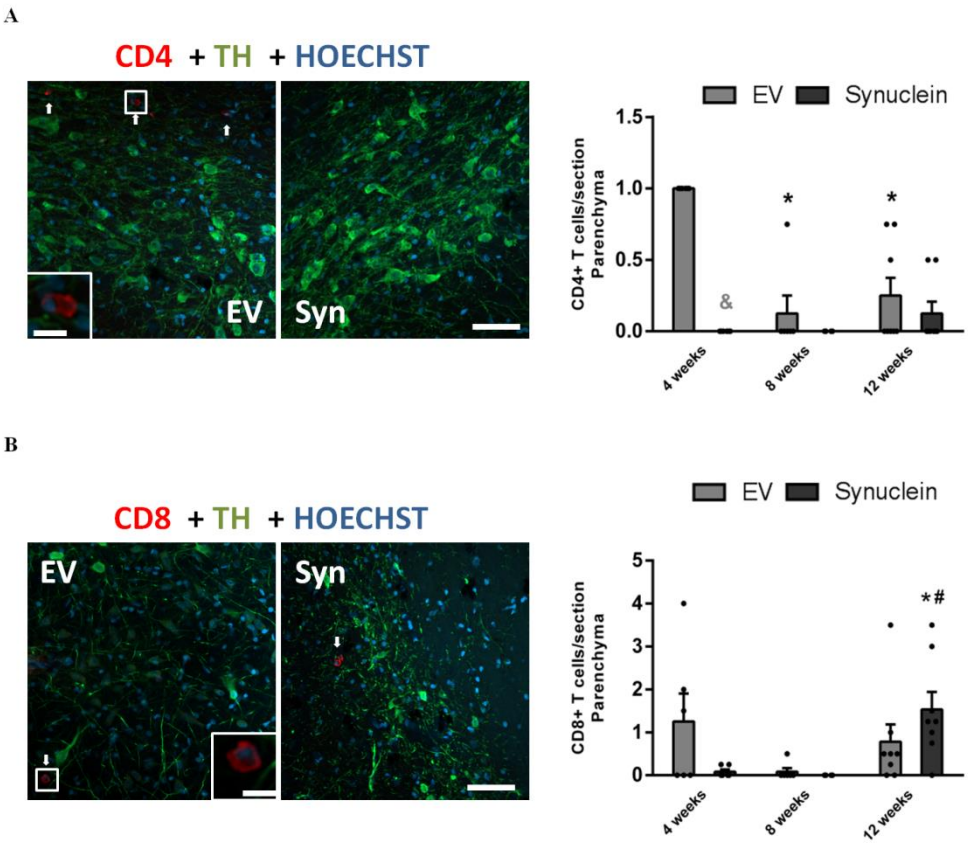

Figure 26. Empty vector and overexpression of h-WT-α-synuclein in Sprague-Dawley strain rat SN*pc* trigger both CD4+ and CD8+ T cell infiltration. (**A**) Left: Representative photomicrographs of CD4 (red) and TH (green) immunofluorescence in rat SN*pc* overexpressing h-WT-α-synuclein. Nuclei are stained with HOECHST (blue). White arrows point to CD4+ T cells. Scale bar = 50µm. Inset scale bar = 10µm. Right: CD4+ T cell densities in EV (n = 6-8 animals/timepoint) and Synuclein (n = 6-8 animals/timepoint) groups in both hemispheres. Two-way ANOVA, *post-hoc* Tukey's test: **P*-value < 0.05 compared to same group 4w, &*P*-value < 0.05 compared to EV same timepoint. Interaction $F(2,32) = 14.56$; Row Factor $F(2,32) = 10.70$; Column $F(1,32) = 29.09$. (**B**) Left: Representative photomicrographs of CD8 (red) and TH (green) immunofluorescence in rat SN*pc* overexpressing h-WT-α-synuclein. White arrows point to CD8+ T cells. Nuclei are stained with HOECHST (blue). White arrows point to CD8+ T cells. Scale bar = 50µm. Inset scale bar = 10µm. Right: CD8+ T cell densities in EV (n = 6-8 animals/timepoint) and Synuclein (n = 6-8 animals/timepoint)

groups in both hemispheres. Two-way ANOVA, *post-hoc* Tukey's test: **P*-value < 0.05 compared to same group 4w; #*P*-value < 0.05 compared to same group 8w. Interaction $F(2,32) = 3.171$; Row Factor $F(2,32) = 3.774$; Column $F(2,32) = 0.2518$. Bars represent mean ± SEM in all graphs.

4.1.5 Overexpression of α-synuclein in Lewis rats SN*pc* induce T cell brain infiltration which is not accompanied with motor impairment and nigrostriatal damage

In the next experiment we changed two aspects compared with the previous one. First of all, as it was commented in the last section, EV was better purified by the provider reducing iodixanol levels. Secondly, we changed rat strain from outbred Sprague-Dawley to inbred Lewis. We were interested in an inbred rat strain in order to eventually use bioinformatic methods to predict peptide-MHC binding modes using "immune epitope database and analysis resource" (www.iedb.org).

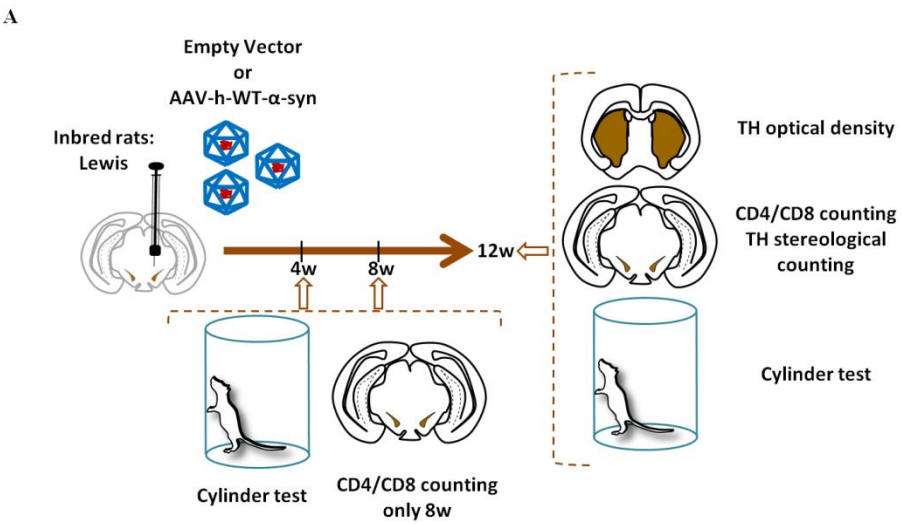

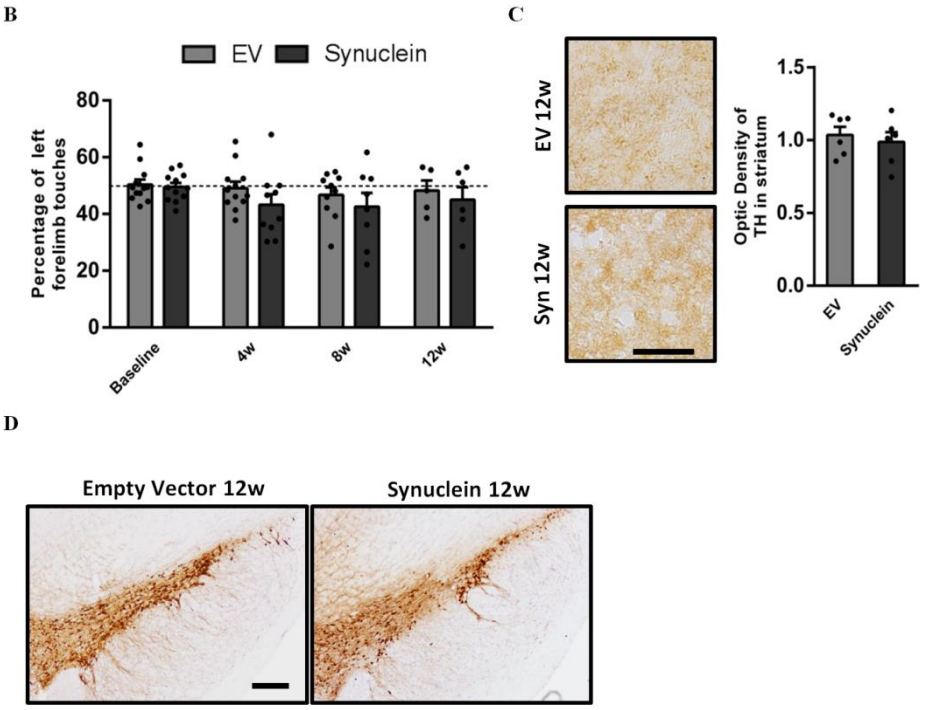

Figure 27. Overexpression of h-WT-α-synuclein in Lewis strain rat SN*pc* does not induce motor asymmetry, striatal TH loss and SN*pc* dopaminergic cell death. (**A**) Diagram representing timecourse and associated experiments in the rat SN*pc* overexpression of h-WT-α-synuclein. (**B**) Percentage of forelimb usage in the cylinder test in both EV (n = 12) and Synuclein (n = 12) groups during 4 weeks-interval until 12 weeks after viral vector injection. Two-way ANOVA, *post-hoc* Tukey's test: *P*-value < 0.05 compared to baseline. (**C**) Left: Representative photomicrographs of striatal TH immunostaining for both EV and Synuclein groups. Right: Striatal TH optic density in both EV (n = 6) and Syn (n = 6) groups at 12w after viral vector injection. Scale bar = 30µm. Un-paired *t*-test: *P*-value < 0.05 compared to EV group. (**D**) Left: Representative photomicrographs of SN*pc* TH immunostaining in EV and Synuclein groups at 12w after viral vector injection. Right: Stereological counting of TH+ cells in the SN*pc* of EV (n = 8) and Syn (n = 8) groups at 12w after viral vector injection. Scale bar = 100µm. One-way ANOVA, *post-hoc* Tukey's test: *P*-value < 0.05. Bars represent mean ± SEM in all graphs.

We stereotaxically injected Lewis rats SN*pc* with either Syn viral vector or EV. Behavioural test analyses were performed in 4-weeks interval until 12 weeks which was the last timepoint. T cell brain infiltration was studied at both 8w and 12w. TH immunostaining in the striatum and dopaminergic cell numbers in the SN*pc* were only analyzed at 12 weeks (**Figure 27A**). Overexpression of h-WT-α-synuclein was examined as a quality check (data not shown). Forelimb usage asymmetry was not detected in any of the timepoints in both groups (48.26% forelimb usage 12w EV; **Figure 27B**), even though some decrease in left forelimb usage was detected in the Syn group (43.30%, 42.60%, 45.05% forelimb usage Syn at 4w, 8w and 12w, respectively). In the same sense, there was no decrease in TH+ axon terminals in the striatum (1.0347 A.U. EV vs 0.9880 A.U. Syn; **Figure 27C**). Dopaminergic cell loss seemed to be qualitatively absent although quantitative counts need to be performed (**Figure 27D**). CD4+ T cells already infiltrated SN*pc* at 8w in the Syn group (8.667 cells/section Syn 8w ipsi vs 1.833 cells/section EV 8w ipsi; **Figure 28A**). However, this infiltration did not increase with time (11.33 cells/section Syn 12w ipsi vs 8.667 cells/section Syn 8w ipsi) but it remained higher than EV group (11.33 cells/section Syn 12w ipsi vs 0.1667 cells/section EV 12w ipsi). CD8+ T cell brain infiltration was already statistically significant at 8w in the Syn group (8 cells/section Syn 8w ipsi vs 2 cells/section EV 8w ipsi; **Figure 28B**) and it remained in this manner until at least 12w (13.17 cells/section Syn 12w ipsi vs 0.8333 cells/section EV 12w ipsi) but it did not increase with time (13.17 cells/section Syn 12w ipsi vs 8 cells/section Syn 8w ipsi).

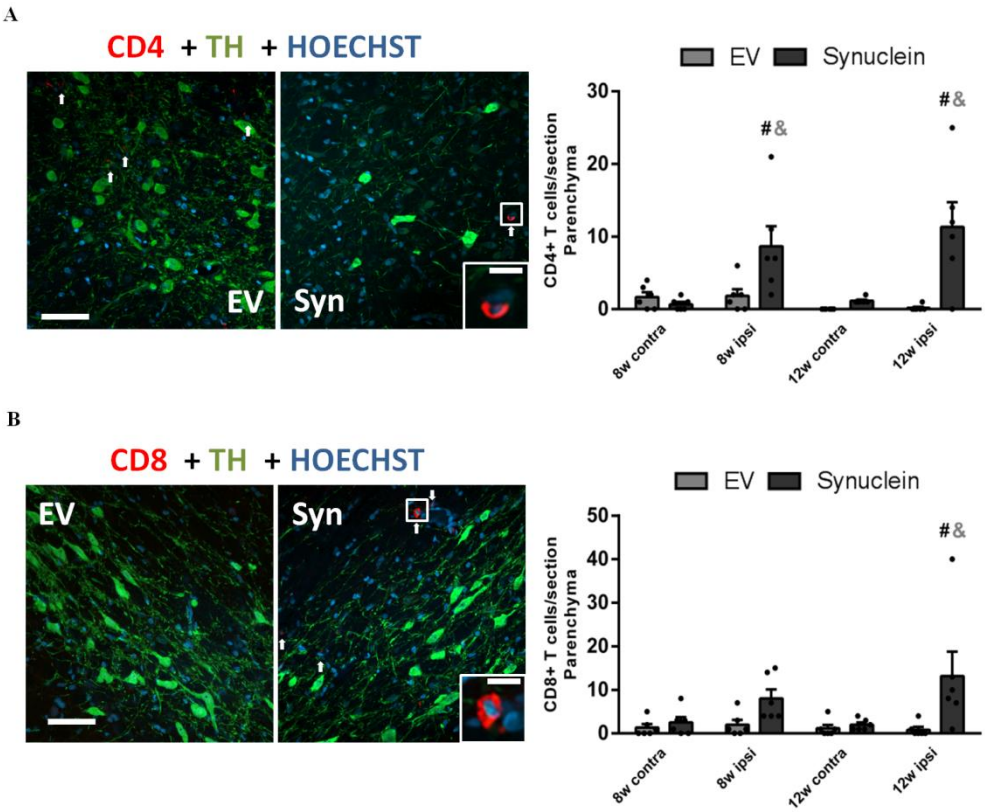

Figure 28. Overexpression of h-WT-α-synuclein in Lewis strain rat SN*pc* does increase both CD4+ and CD8+ T cell brain infiltration. (**A**) Left: Representative photomicrographs of CD4 (red) and TH (green) immunofluorescence in rat SN*pc* overexpressing h-WT-α-synuclein. Nuclei are stained with HOECHST (blue). White arrows point to CD4+ T cells. Scale bar = 50µm. Inset scale bar = 10µm. Right: CD4+ T cell densities in EV (n = 6 animals/timepoint) and Synuclein (n = 6 animals/timepoint) groups in both hemispheres. Two-way ANOVA, *post-hoc* Tukey's test: #*P*-value < 0.05 compared to contralateral same timepoint, grey-&*P*-value < 0.05 compared to EV same timepoint. Interaction $F(3,30) = 5.979$; Row Factor $F(3,30) = 5.684$; Column $F(1,10) = 15.66$; Subjects matching $F(10,30) = 1.036$. (**B**) Left: Representative photomicrographs of CD8 (red) and TH (green) immunofluorescence of rat SN*pc* overexpressing h-WT-α-synuclein. White arrows point to CD8+ T cells. Nuclei are stained with HOECHST (blue). White arrows point to CD8+ T cells. Scale bar = 50µm. Inset scale bar = 10µm. Right: CD8+ T cell densities in EV (n = 6 animals/timepoint) and Synuclein (n = 6 animals/timepoint) groups in both hemispheres. Two-way ANOVA, *post-hoc* Tukey's

test: #*P*-value < 0.05 compared to contralateral same timepoint, grey-&*P*-value < 0.05 compared to EV same timepoint. Interaction F (3,30) = 2.864; Row Factor F (3,30) = 2.655; Column F (1,10) = 10.06; Subjects matching F (10,30) = 1.017. Bars represent mean ± SEM in all graphs.

During T cell infiltration analysis in the overexpression of h-WT-α-synuclein in SN*pc* Lewis rat, we were also doing the study in the human post-mortem tissue presented in the following sections. We had initially hypothesized that T cell infiltration was a consequence, *ergo*, later in time to α-synuclein deposition in the SN*pc*. However, we found the other way around. Due to non-concordant results with the human post-mortem tissue, we decided to cease PD animal model experiments.

4.2 T cell infiltration in human post-mortem tissue

As it has been previously commented in the Introduction, even though many published studies have tried to elucidate the importance of the adaptive immune system in PD, only two had analyzed and reported T cell SN*pc* infiltration in post-mortem human tissue (Brochard *et al.*, 2009; Sommer *et al.*, 2018). Contrarily, one congress poster has reported no significant results in T cell SN*pc* infiltration, which contradicted previous works (Stevens *et al.*, 2012*a*). In these studies, phenotypic characterization of these CD4+ and CD8+ T cells was absent. Moreover, T cell SN*pc* infiltration had not been assessed in iLBD cases which are assumed to be a pre-motor stage of the disease. Thus, reproducing T cell SN*pc* infiltration and performing a phenotypic characterization was needed to better elucidate their role in the disease.

4.2.1 Density of CD8+ T cells but not CD4+ T cells is increased in SNpc of Parkinson's disease cases

We counted CD4+ and CD8+ T cells in age-matched healthy controls and PD SN*pc* to determine the density of lymphocytes remaining in the perivascular space (**Figure 29A, Bottom**) and the ones that have infiltrated into the brain parenchyma (**Figure 29A, Top**). We counted them separately as one could hypothesize that both perivascular and parenchymal T cells could have different roles and dynamics. CD4+ T cells are not as abundant as CD8+ T cells in both compartments: parenchyma (0.267 cells/mm^2; **Figure 29B, Top**) and perivascular space (0.25 cells/mm^2; **Figure 29B, Bottom**) of control SN*pc* tissue. This T cell population was not increased in SN*pc* of PD cases (0.295 cells/mm^2; **Figure 29B, Top**). However, in perivascular spaces there was a trend to increase in PD although it did not reach statistical significance (0.741 cells/mm^2; **Figure 29B, Bottom**). While some cases had high perivascular CD4+ T cell densities, others were at control levels.

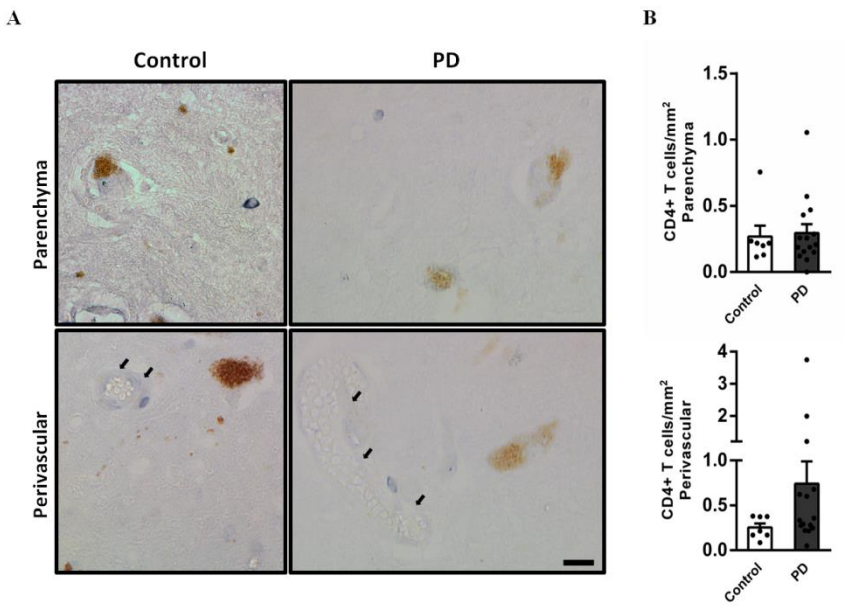

Figure 29. CD4+ T cell densities in control and Parkinson's disease SN*pc*. (**A**) Representative photomicrographs of parenchymal and perivascular CD4+ T cells (blue). Black arrows point to blood vessels (**B**) Density of CD4+ T cells in the parenchyma and in perivascular spaces in both control (n = 7) and PD (n = 15) groups. Scale bar = 15µm. Un-paired *t*-test: **P*-value < 0.05 compared to control. Bars represent mean ± SEM.

For CD8+ T cells, results were different compared with the ones observed from CD4+ T cells. Firstly, their densities in age-matched healthy controls were higher than the ones from CD4+ T cells for both parenchyma (0.86 cells/mm^2; **Figure 30A, Top**) and perivascular spaces (4.518 cells/mm^2; **Figure 30A, Bottom**). Secondly, we observed 2.5 fold increase of CD8+ T cell density in the brain parenchyma of PD cases (2.093 cells/mm^2; **Figure 30B, Top**). Nevertheless, there was a high variability in perivascular CD8+ T cells reporting a statistically non-significant increase in PD cases (7.281 cells/mm^2; **Figure 30B, Bottom**).

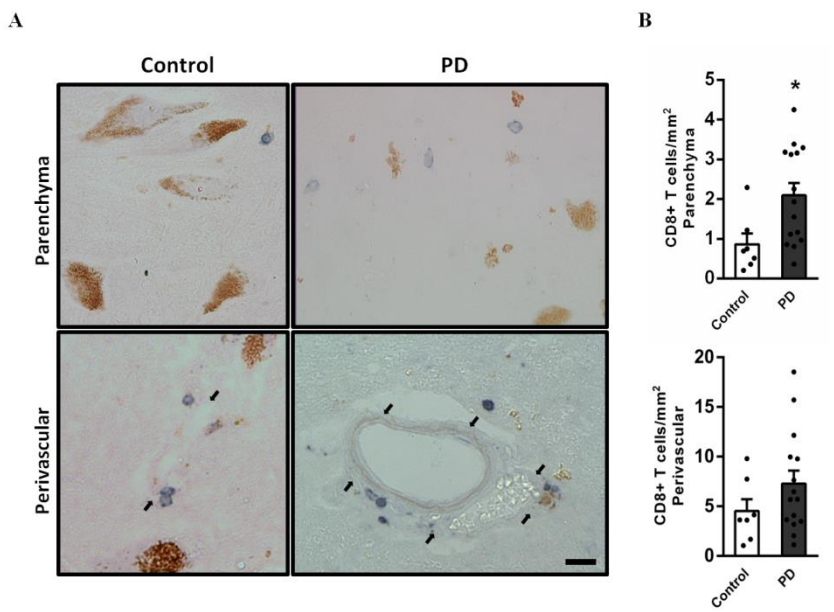

Figure 30. CD8+ T cell densities in control and Parkinson's disease SN*pc*. (**A**) Representative photomicrographs of parenchymal and perivascular CD8+ T cells (blue). Black arrows point to blood vessels. (**B**) Density of CD8+ T cells in the parenchyma and in perivascular spaces in both control (n = 7) and PD (n = 15) groups. Scale bar = 15µm. Unpaired *t*-test: **P*-value < 0.05 compared to control. Bars represent mean ± SEM.

4.2.2 Infiltrating CD8+ T cells contact with dopaminergic neurons and their densities correlate with dopaminergic neuronal death in Parkinson's disease SN*pc*

Due to the increase of parenchymal CD8+ T cells in PD cases and their cytotoxic capacity, we focused on exploring the possible role of these T lymphocytes in the dopaminergic cell death. In order to provoke the death of a cell target, a CTL needs to migrate to the brain parenchyma, interact with its TCR and the cognate peptide-MHC class-I complex presented by the target cell and use mixed cytokines, FasL- and/or granzyme/perforin-dependent mechanisms once the immunological synapse has been established (Kabanova *et al.*, 2018).

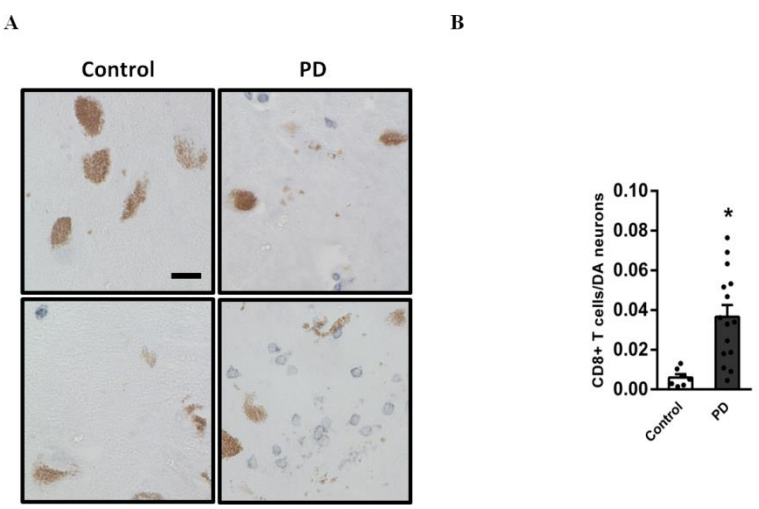

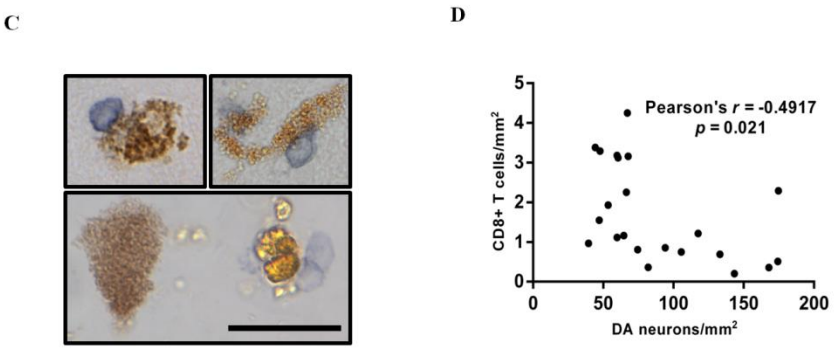

Figure 31. CD8+ T cells make contact/appositions with dopaminergic neurons and their density correlate with dopaminergic cell loss. (**A**) Photomicrographs of CD8+ T cells in the SN*pc* of two controls and two PD cases. Left: Top control photomicrograph shows no parenchymal CD8+ T cell meanwhile bottom image only one CD8+ T cell can be observed. Right: PD cases show much more variability, from just a few CD8+ T cells (top) to many (bottom), particularly in regions with extracellular neuromelanin. Scale bar = 15µm. (**B**) Ratio between both CD8+ T cell and dopaminergic cell densities in control (n = 7) and PD (n = 15) cases. Mann-Whitney test: **P*-value < 0.05 compared to control. Bars represent mean ± SEM. (**C**) Photomicrographs showing CD8+ T cells in close contact/apposition with dopaminergic neurons. The neuron contacted by multiple CTLs (bottom) is likely dying if not already dead. Scale bar = 15µm. (**D**) Scatter diagram of dopaminergic cell density versus CD8+ T cell density in control (n = 7) and PD (n = 15). Pearson correlation *r* = -0.4917; *P*-value < 0.05.

We analyzed the disposition of CTLs in the SN*pc* and their relationship with dopaminergic neurons. In PD cases, CTLs were surrounding (**Figure 31A**) or contacting dopaminergic neurons (**Figure 31C**) and they could be found in regions where extracellular neuromelanin was also present (**Figure31C, Bottom**) as an indicator of dopaminergic neuronal death. A bunch of CTLs cooperate contacting with a dopaminergic neuron at the same time (**Figure 31C**), as it has been demonstrated *in vivo* where the progressive accumulation of sub-lethal pro-death signals delivered by several CTLs lead to faster

apoptosis of the target cell (Halle *et al.*, 2016, 2017). In this sense, we found CTLs surrounding degenerating neurons (**Figure 31C**). Thus, the idea of a ratio between CTLs and target cells, in this case dopaminergic neurons, is interesting and a critical parameter for CTL-mediated cytotoxic attack. We found a striking increase of this ratio in PD patients compared with age-matched healthy controls (**Figure 31B**). These results mean that CTLs have a higher probability of contacting with a target cell. To further examine the concept of CTLs directing a cytotoxic attack to a dopaminergic neuron, we performed a correlation between infiltrating CD8+ T cells and dopaminergic neurons only in age-matched healthy controls and PD cases (**Figure 31D**). There was a linear positive correlation between CD8+ T cells and neuronal death (r = -0.4917, p = 0.021). These results point out that infiltrating CD8+ T cells could have a role in dopaminergic cell death of PD SN*pc*.

4.2.3 CD8+ T cell infiltration is an early event of the disease occurring in absence of neuronal death and synucleinopathy in SN*pc* of incidental Lewy body disease cases

To assess whether CD8+ T cell infiltration may have a relevant role in early stages of Parkinson's disease and to determine its relationship with synucleinopathy, we included two iLBD groups in the study. iLBD cases consisted of autopsied healthy control individuals who had Lewy bodies and/or Lewy neurites without motor clinical findings of Parkinson's disease and are generally considered premotor stages of the disease (Dickson *et al.*, 2008; Iacono *et al.*, 2015). iLBD SN syn- group showed α-synuclein aggregates in the olfactory bulb, but not in the SN*pc*, while iLBD SN syn+ group also presented α-synuclein aggregates in the SN*pc*. Accepting the proposition about Lewy body

staging, iLBD SN syn- group would be considered as an earlier stage than iLBD SN syn+ (Beach *et al.*, 2009*a*, *b*).

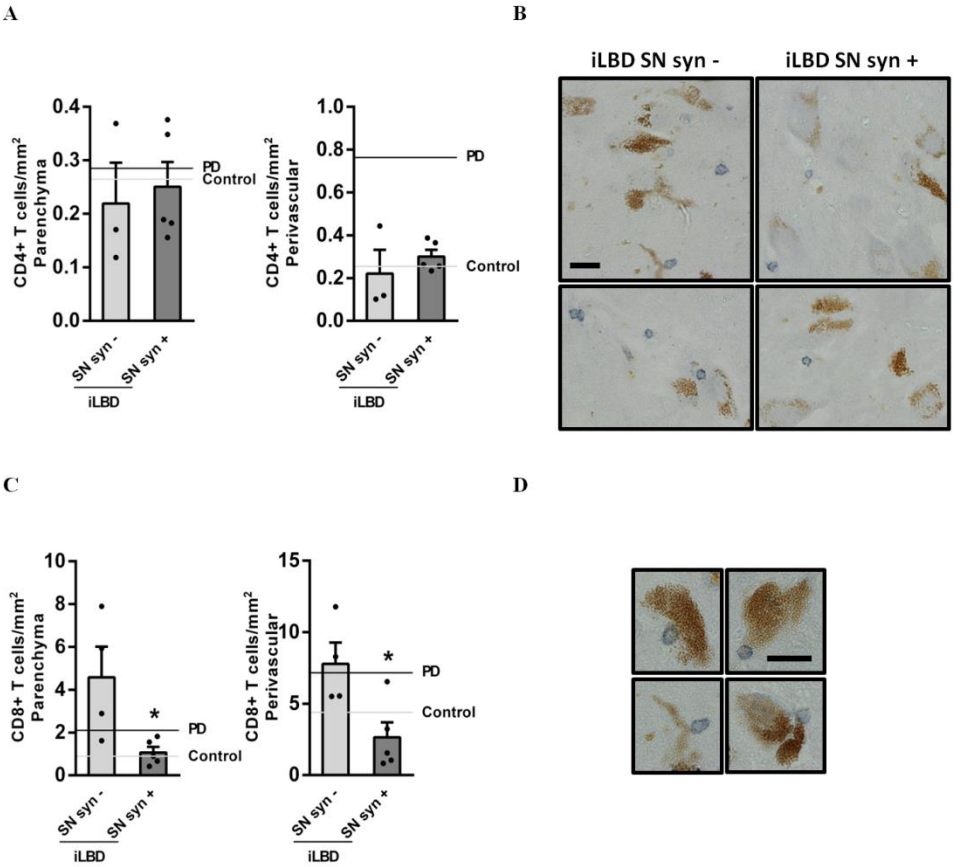

Figure 32. CD4+ and CD8+ T cell densities in iLBD cases with or without nigral synucleinopathy. (**A**) CD4+ T cell (blue) SN*pc* density in the parenchyma (left) and perivascular spaces (right) of iLBD SN syn- (n = 3) and iLBD SN syn+ (n = 5) cases. Grey and black lines show mean densities of control and PD cases, respectively. Mann-Whitney for parenchyma and Un-paired *t*-test for perivascular spaces: *P*-value < 0.05 compared to iLBD SN syn-. (**B**) Representative SN*pc* CD8+ T cell (blue) photomicrographs of two iLBD SN syn- and two iLBD SN syn+ cases. Scale bar = 15µm. (**C**) CD8+ T cell SN*pc* density in the parenchyma (left) and perivascular spaces (right) of iLBD SN syn- (n = 4) and iLBD SN syn+ (n = 5) cases. Grey and black lines show mean densities of control and PD cases, respectively.

Mann-Whitney test for parenchyma and un-paired *t*-test for perivascular spaces: **P*-value < 0.05 compared to iLBD SN syn-. (**D**) Photomicrographs showing CD8+ T cells (blue) contacting neuromelanin-containing dopaminergic neurons. Scale bar = 15μm. Bars represent mean ± SEM in all graphs.

First of all, we analyzed CD4+ T cell densities in iLBD cases. Low densities were observed in both parenchyma (0.2193 cells/mm^2 iLBD SN syn- vs 0.2505 cells/mm^2 iLBD SN syn+; **Figure 32A, Left**) and perivascular spaces (0.2211 cells/mm^2 iLBD SN syn- vs 0.3007 cells/mm^2 iLBD SN syn+; **Figure 32A, Right**). No significant differences were observed between two iLBD groups (**Figure 32A**). Afterwards, we analyzed CD8+ T cell densities in both iLBD groups (**Figure 32B&C**). iLBD SN syn- cases had higher densities of CD8+ T cells than iLBD SN syn+ cases in both parenchyma (4.58 vs 1.07 cells/mm^2; **Figure 32C, Left**) and perivascular spaces (7.381 vs 2.634 cells/mm^2; **Figure 32C, Right**). Moreover, one of the iLBD SN syn- cases examined was the case with highest infiltrating CD8+ T cell density (7.9 cells/mm^2) of the entire cohort. Some of the CD8+ T cells were found in contact with dopaminergic neurons (**Figure 32D**).

4.2.4 SN*pc* dopaminergic cell loss appears simultaneously with nigral synucleinopathy

First of all, we determined the density of dopaminergic neurons in all groups (**Figure 33A**). Age-matched healthy controls had 145.173 cells/mm^2, same levels than iLBD SN syn- cases 147.902 cells/mm^2. iLBD SN syn+ cases, which would be a later stage than iLBD SN syn-, had 109.532 cells/mm^2 representing a 24.5% neuronal loss. PD cases of this cohort had 68.178 cells/mm^2, representing a 53% of neuronal loss. Nigral dopaminergic cell density

correlated with UPDRS off motor score for both iLBD SN syn+ and PD cases (Pearson's correlation *r* = -0.61; **Figure 33B**), indicating the goodness of dopaminergic cell density analysis and the relationship between clinical motor symptoms and SN*pc* degeneration. These results indicate that in early stages of the disease no nigral dopaminergic cell death may be observed but it is made evident when synucleinopathy appears. Dopaminergic cell loss is then increased in chronic late stages of the disease.

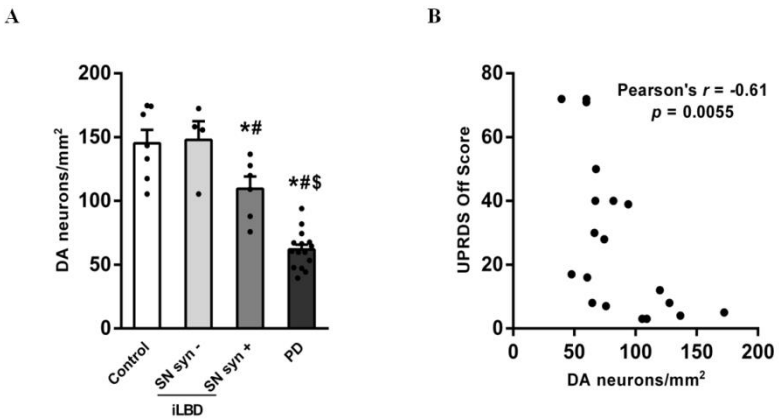

Figure 33. Dopaminergic cell densities in control, iLBD SN syn-/+ and PD cases and its correlation with UPDRS Off motor score. (**A**) Dopaminergic neuron density in control (n = 7), iLBD SN syn- (n = 4), iLBD SN syn+ (n = 5) and PD (n = 15) cases. One-way ANOVA; *post-hoc* Tukey's test: **P*-value < 0.05 compared to control; #*P*-value < 0.05 compared to iLBD SN syn-; $*P*-value < 0.05 compared to iLBD SN syn+. (**B**) Scatter diagram of dopaminergic cell density versus UPDRS Off score in iLBD SN syn+ (n = 5) and PD (n = 15) cases. Pearson correlation *r* = -0.61; *P*-value < 0.05.

4.2.5 Total MHC class-II+ microglial cells are decreased in early stages of the disease and low densities of ameboid microglia correlate with higher neuronal loss

In previous results we found a transient but acute increase of parenchymal CD8+ T cells in early stages of the disease preceding both nigral synucleinopathy and dopaminergic cell loss. We then checked for MHC class-II expression as a marker of antigen presentation and microgliosis in order to elucidate the role of different activated morphologies throughout the different stages of the disease. First of all, we analyzed the general expression of MHC class-II as percentage of SN*pc* area occupied by the positive staining (**Figure 34**). High variability was found between individuals of the same group as it can be observed in **Figure 34A**. Although there were no statistical changes, a reduction in both iLBD groups was noted (**Figure 34B**). This reduction was more severe in iLBD SN syn- cases and it was practically recovered in PD.

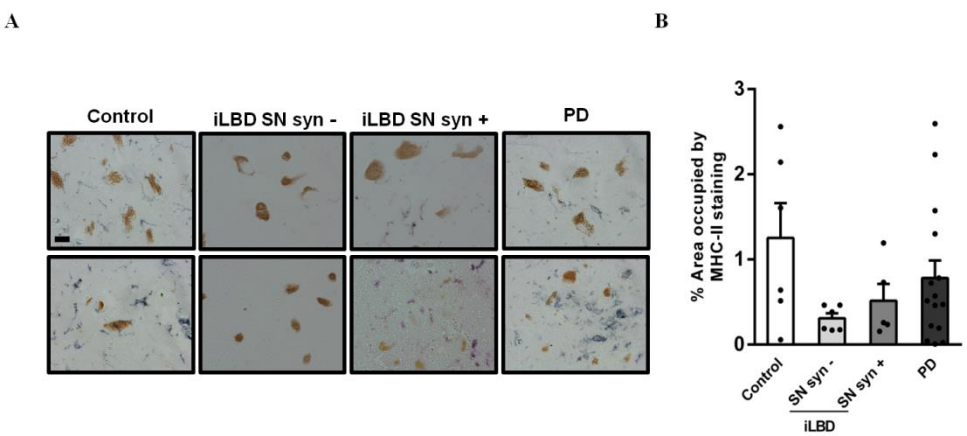

Figure 34. Low magnification analysis of MHC class-II+ staining in SN*pc*. (**A**) Representative SN*pc* MHC class-II+ glia (blue) photomicrographs of control, iLBD SN syn-/+ and PD cases. Scale bar = 15μm. (**B**) Percentage of SN*pc* area occupied by MHC-II immunopositive staining of control (n = 6), iLBD SN syn- (n = 6), iLBD SN syn+ (n = 5) and PD

(n = 15) cases. One-way ANOVA, *post-hoc* Tukey's test: *P*-value < 0.05. Bars represent means ± SEM in graphs.

However, this analysis was generally rough, and differences could be better understood studying the different activation morphologies. We differentiated between three morphologies of MHC class-II+ microglia: highly ramified with a small body called homeostatic (**Figure 35A, Top**), rod or bushy which have less ramifications and they present more intense staining with a visible body called intermediate microglia (**Figure 35B, Top**) and circular body with practically no ramifications and intense staining called ameboid microglia (**Figure 35C, Top**). Neuromelanin pigment from dead dopaminergic neurons could be found in some cells of the latter morphology (**Figure 35C, Top**). For homeostatic MHC class-II+ microglia we obtained a non-significant small decrease in iLBD SN syn- cases (14.4 cells/mm^2; **Figure 35A, Bottom**). iLBD SN syn+ (60.956 cells/mm^2) and PD (51.284 cells/mm^2) were unchanged compared with age-matched healthy controls (69.252 cells/mm^2). For intermediate activated MHC class-II+ microglia we found similar trends, with a tendency to decrease in iLBD SN syn- group (2.196 cells/mm^2; **Figure 35B, Bottom**) meanwhile the levels in iLBD SN syn+ (5.098 cells/mm^2) and age-matched healthy controls (7.288 cells/mm^2) were comparable. For this intermediate morphology, PD cases had a small non-significant increase (12.238 cells/mm^2). Finally, ameboid MHC class-II+ microglia was increased in iLBD SN syn+ (3.732 cells/mm^2; **Figure 35C, Bottom**) and PD cases (2.051 cells/mm^2) in comparison with iLBD SN syn- (1.31 cells/mm^2) and age-matched healthy controls (0.743 cells/mm^2).

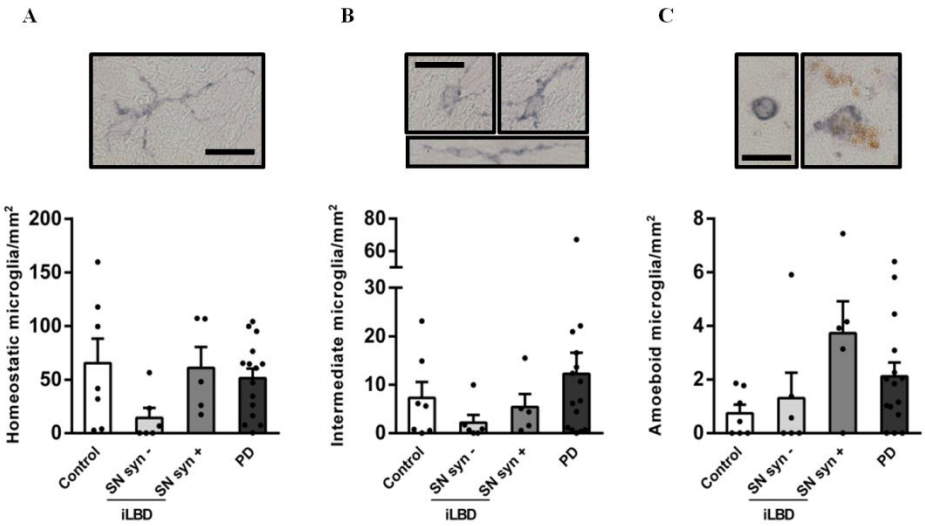

Figure 35. Density of SN*pc* MHC class-II+ glia morphologies. (**A**) Top: Representative SN*pc* MHC class-II+ homeostatic glia (blue) photomicrograph. Scale bar = 15µm. Bottom: SN*pc* MHC class-II+ homeostatic glia density of control (n = 7), iLBD SN syn- (n = 6), iLBD SN syn+ (n = 5) and PD (n = 15) cases. One-way ANOVA, *post-hoc* Tukey's test: *P*-value < 0.05. (**B**) Top: Representative SN*pc* MHC class-II+ intermediate glia (blue) photomicrographs. Scale bar = 15µm. Bottom: SN*pc* MHC-II+ intermediate glia density of control (n = 7), iLBD SN syn- (n = 6), iLBD SN syn+ (n = 5) and PD (n = 15) cases. One-way ANOVA, *post-hoc* Tukey's test: *P*-value < 0.05. (**C**) Top: Representative SN*pc* MHC class-II+ ameboid glia (blue) photomicrographs. Ameboid glia can phagocyte neuromelanin as it is shown in the right image. Scale bar = 15 µm. Bottom: SN*pc* MHC class-II+ ameboid glia density of control (n = 7), iLBD SN syn- (n = 6), iLBD SN syn+ (n = 5) and PD (n = 15) cases. One-way ANOVA, *post-hoc* Tukey's test: *P*-value < 0.05. Bars represent mean ± SEM in all graphs.

In relation with the ameboid MHC class-II+ morphology, we found the presence of neuromelanin phagocytosis independent of the group although it seemed more common in PD cases (**Figure 36B**). The role of this ameboid MHC class-II+ microglia is still unclear and controversial as, after a chronic inflammation,

it could be damaging dopaminergic neurons, *ergo* provoking their death or it could be just getting rid of their cell corpses or debris such as neuromelanin. In order to shed light on this, we correlated the density of ameboid MHC class-II+ microglia with the density of dopaminergic neurons (**Figure 36A**). PD cases with no nigral MHC class-II expression were discarded for this analysis as they gave rise to confusion. We found a positive correlation between neuronal survival and ameboid MHC class-II+ morphology ($r = 0.5962$; $p = 0.0315$). Thus, these results suggest a possible positive role of MHC class-II+ ameboid microglia in the disease phagocyting neuromelanin debris which could be highly antigenic (**Figure 36B**). PD cases in which MHC class-II+ ameboid microglia is totally or practically absent, dopaminergic cell death is higher than cases with evident MHC class-II+ ameboid microglia. One explanation could be that neuronal death had stopped and microglia did not need to phagocyte more extracellular NM. However, these cases still had dopaminergic cell death on-going as extracellular NM can be observed (**Figure 36C**).

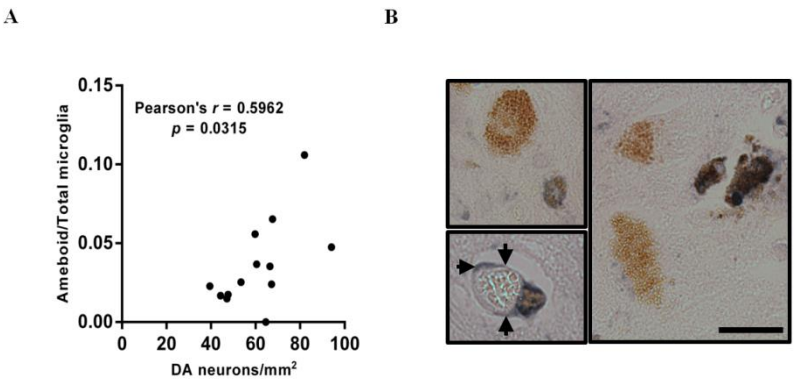

C

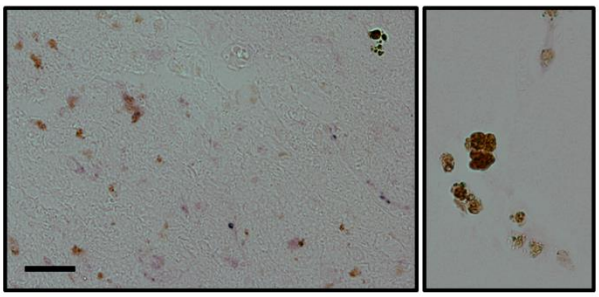

Figure 36. Correlation between MHC class-II+ ameboid glia and dopaminergic neuronal density. (**A**) Scatter diagram of MHC-II+ ameboid/total glia ratio versus dopaminergic neuronal density in PD (n = 13) cases which had some SN*pc* MHC class-II expression. Pearson correlation *r* = 0.5962; *P*-value < 0.05. (**B**) Photomicrographs of MHC class-II+ ameboid glia (blue) phagocyting NM in both parenchyma (top left and right pictures) and perivascular spaces (bottom left picture). Black arrows point to blood vessel. Scale bar = 15μm. (**C**) Photomicrographs of extracellular NM in two PD cases without MHC class-II+ ameboid glia. Scale bar = 15μm.

4.2.6 A high proportion of SNpc CD8+ T cells express CD103 tissue-resident memory T cell marker

With the above results we have demonstrated that there is CTL infiltration in the SN*pc* of PD cases and this process also happens in absence of synucleinopathy and dopaminergic cell loss. Moreover, we have also demonstrated the presence of high densities of CTLs in the SN*pc* perivascular spaces which are not disease-dependent. Thus, T cell brain phenotypic characterization under both physiological and pathological conditions may be interesting to better understand how this CNS immune surveillance works. Moreover, as we have previously done in T cell counts, we have differentiated between infiltrating and perivascular T cells.

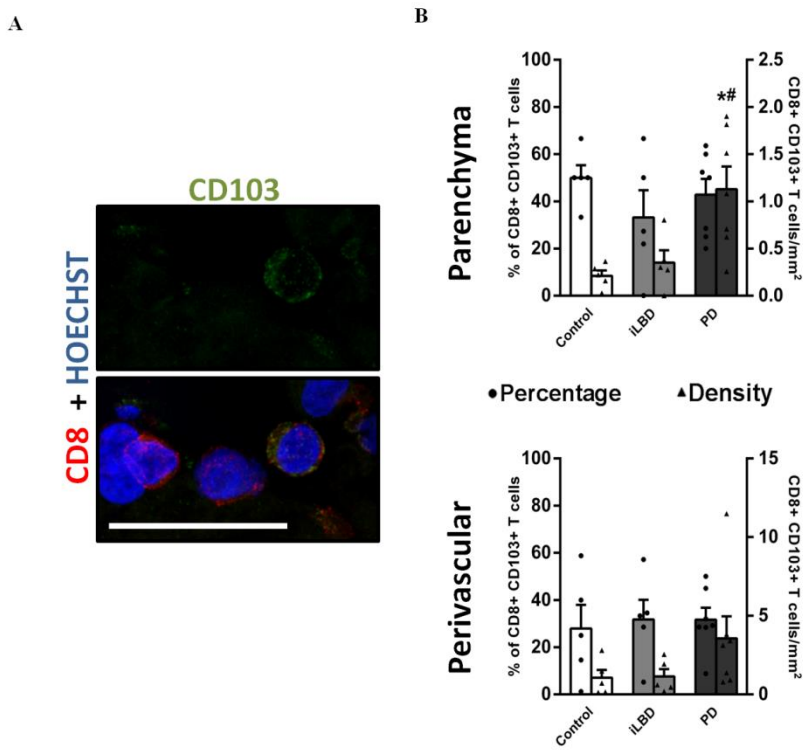

Figure 37. CD8+ CD103+ T cells in SN*pc* of control, iLBD and PD cases. (**A**) Immunofluorescence image showing once CD103+ (green) and two CD103- CD8+ (red) T cells. CD103 can be seen in the membrane. Nuclei were stained with HOECHST (blue). Scale bar = 15µm. (**B**) Percentages (dots) and densities (triangles) of CD8+ CD103+ T cells in the parenchyma (top graph) and perivascular spaces (bottom graph) in control (n = 5), iLBD (n = 5) and PD (n = 7) cases. One-way ANOVA, *post-hoc* Tukey's test: **P*-value < 0.05 compared to controls; #*P*-value < 0.05 compared to iLBD. For parenchyma analysis $F = 7.463$, total $df = 16$. Bars represent means ± SEM in all graphs.

One of our hypotheses according to the obtained results was that CTLs in the brain parenchyma are performing an active immune surveillance against any possible pathogen. We thought that some of these CTLs that stay in the brain in physiological conditions could be tissue-resident memory T cells (T_{RM}) which

express different markers such as CD103 and CD69 among others, being the former more restrictive than the latter (CD69 can also be a marker for T cell activation). Moreover, in rodent brains (Wakim *et al.*, 2010) and human *CC* (Smolders *et al.*, 2018) the expression of CD103 by T_{RM} cells has been demonstrated. We analyzed the expression of CD103 by CD8+ T cells in SN*pc* double immunofluorescences of age-matched healthy controls, iLBD and PD cases in general. Due to the fact that we did not see general differences between both iLBD groups, we added them up to a general iLBD group as the presence of neuronal loss and synucleinopathy are not having an effect in the phenotypic characterization of CTLs. A high percentage of CD8+ T cells coexpressed the plasma membrane marker CD103 (**Figure 37A**). In the brain parenchyma, we found around 35-50% of CD8+ CD103+ T cells although we did not see differences between groups (50% Control, 33.1879% iLBD, 42.7984% PD; **Figure 37B, Top**). For total number of double positive T cells we found a significant increase in PD cases (1.1284 cells/mm^2). iLBD ones were not increased (0.3520 cells/mm^2) due to a slight decrease in percentages compared with age-matched healthy controls (0.2116 cells/mm^2). In perivascular spaces (**Figure 37B, Bottom**), percentage of CD8+ CD103+ T cells were lower than in the parenchyma and were similar among all groups (27.9253% Control, 31.7532% iLBD, 31.7062% PD). Total numbers of CD8+ CD103+ T cells in perivascular spaces were not statistically different although there was a slight increase in PD cases (1.0574 cells/mm^2 Control, 1.1457 cells/mm^2 iLBD, 3.5684 cells/mm^2 PD). To further demonstrate the presence of T_{RM} cells in the SN*pc*, we qualitatively checked the presence of CD8+ CD69+ T cells (**Annex Figure 2**). Independently of the pathology, CD8+ T cells expressing CD69 were found in both compartments. Some studies have found the expression of PD-1 in T_{RM} cells. We studied the expression for programmed death 1 (PD-1) and programmed death ligand 1 (PD-L1) complex in both T cells and neurons,

respectively. This immune checkpoint complex was analyzed to understand the reduction of parenchymal CD8+ T cells in iLBD SN syn+ cases. Nonetheless, we did not find expression of both proteins. These results show how T_{RM} cells are present in the SN*pc* in a pathology independent manner. Moreover, these tissue-resident memory T cells do not show PD-1 staining by immunofluorescence.

4.2.7 SN*pc* CTLs display IFNγ and several granzymes to potentially induce dopaminergic cell death

4.2.7.1 Half of CD8+ T cells in human SN*pc* express IFNγ but not TNFα

So far, we have showed how CTLs infiltrate and make contact with dopaminergic neurons. Contact probability becomes higher in PD cases compared with age-matched healthy controls due to infiltration increase and dopaminergic neuronal density decrease. Furthermore, this increase of CTL infiltration correlates with the loss of dopaminergic neurons suggesting a potential role in their death. In this sense, we next moved to analyze several mechanisms which CTLs could use to kill their cell target.

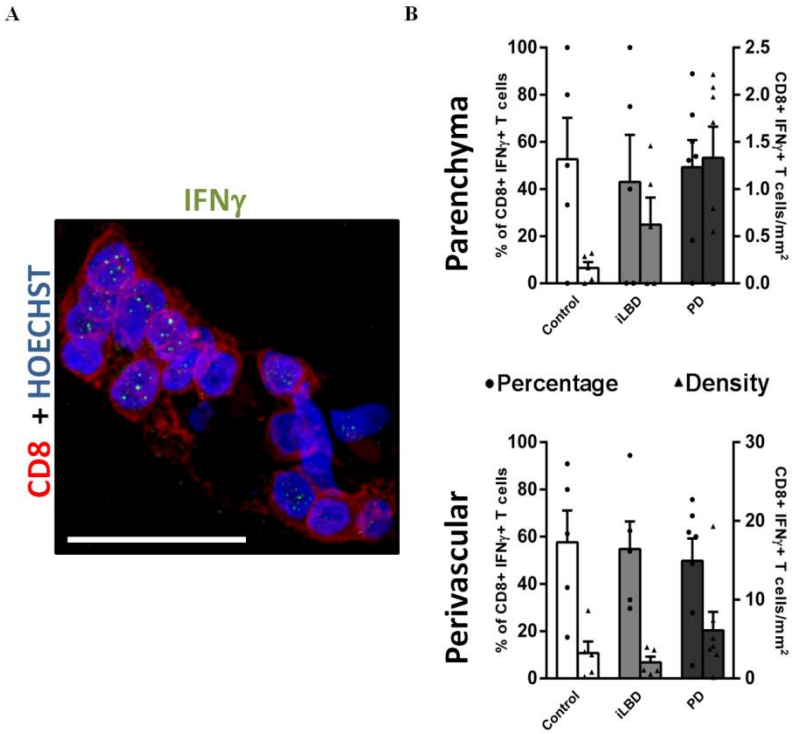

Figure 38. CD8+ IFNγ+ T cells in SN*pc* of control, iLBD and PD cases. (**A**) Immunofluorescence of IFNγ+ (green) and IFNγ- CD8+ (red) T cells. Nuclei were stained with HOECHST (blue). Scale bar = 15μm. (**B**) Percentages (dots) and densities (triangles) of CD8+ IFNγ+ T cells in the parenchyma (top graph) and perivascular spaces (bottom graph) in control (n = 5), iLBD (n = 5) and PD (n = 7) cases. One-way ANOVA, *post-hoc* Tukey's test: *P*-value < 0.05. Bars represent mean ± SEM in all graphs.

Firstly, we analyzed by double immunofluorescence the presence of CD8+ IFNγ+ and CD8+ TNFα+ T cells as these two cytokines can be expressed by CTLs and be used to provoke cell death. We did not find CD8+ TNFα+ T cells in both compartments in any of the studied groups. However, we did find CD8+ IFNγ+ T cells in all groups and in high percentages (**Figure 38A**). In the parenchyma, percentage of CD8+ IFNγ+ T cells was around 50-60% and there

were no differences between the three groups (52.6667 Control, 43% iLBD, 49.217% PD; **Figure 38B, Top**). For total number of CD8+ IFNγ+ T cells there was a tendency to increase with pathology, but this trend was not statistically significant (0.1629 cells/mm^2 Control, 0.6222 cells/mm^2 iLBD, 1.3317 cells/mm^2 PD). In perivascular spaces, results were in the same way as the parenchyma (**Figure 38B, Bottom**). Percentages were also around 50-60% (57.6105% Control, 54.7507% iLBD, 49.7517% PD) and total numbers were also increased with pathology (6.1135 cells/mm^2 PD) although iLBD cases (2.0415 cells/mm^2) had the same numbers as age-matched healthy controls (3.2141 cells/mm^2).

4.2.7.2 Granzymes but no FasL are present in SN*pc*-infiltrating CTLs

After analyzing the expression of two cytokines in CTLs we moved to study the expression of two other mechanisms which CTLs could use to cause cell death in their target. First of all, we explored FasL expression in CD8+ T cells by double immunofluorescence. No CD8+ FasL+ T cells were found in both parenchyma and perivascular spaces in all the groups.

Granzymes induce targeted cell death through non-redundant diverse pathways that complement each other (Voskoboinik *et al.*, 2015). Among these serine proteases expressed in CTLs, granzyme A (GrzA) and granzyme B (GrzB) are the most abundant ones while granzyme K (GrzK) expression is more restricted. These different granzymes have been shown to be present in T_{RM} cells of the human *CC* (Smolders *et al.*, 2018). Furthermore, we assessed by double immunofluorescence the presence of granzyme positive granules inside CD8+ T cells in both brain compartments.

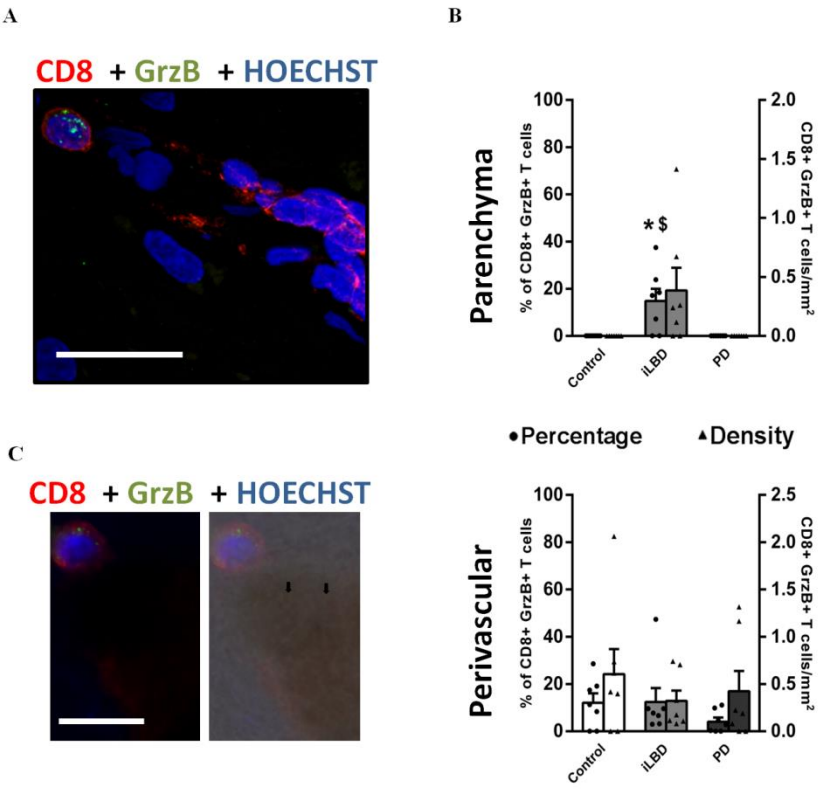

Figure 39. CD8+ Granzyme B+ T cells in SN*pc* of control, iLBD and PD cases. (**A**) Immunofluorescence image showing a CD8+ (red) T cell with many granzyme B (green) granules among several CD8+ granzyme B- T cells and some with one or two granules. Scale bar = 15µm. (**B**) Percentages (dots) and densities (triangles) of CD8+ GrzB+ T cells in the parenchyma (top graph) and perivascular spaces (bottom graph) in control (n = 7), iLBD (n = 7) and PD (n = 7) cases. One-way ANOVA, *post-hoc* Tukey's test: **P*-value < 0.05 compared to controls; $*P*-value < 0.05 compared to PD. For parenchyma analysis $F = 8.342$, total $df = 20$. (**C**) Photomicrograph showing a CD8+ T cell containing several granzyme B granules and contacting a dopaminergic neuron of an iLBD case. Black arrows point to a NM-containing neuron. Scale bar = 15µm. Bars represent mean ± SEM in all graphs.

GrzB positive granules were found in low quantities inside CD8+ T cells, although in some cases these granules were more abundant (**Figure 39A**).

Strikingly, we found that CD8+ T cells containing GrzB+ granules were infiltrating only in five of seven iLBD cases regardless of synucleinopathy (**Figure 39B, Top**). Their percentage in the parenchyma was low compared with the double positive CD8+ T cells for the aforementioned cytokines (14.86%). While one iLBD case had almost 40% of CD8+ T cells positive for GrzB, none of the control or PD cases had a single infiltrating CD8+ T cell with GrzB+ granules. For the total number of CD8+ GrzB+ T cells results were the same but with no statistical differences (0.386 cells/mm^2 iLBD). In iLBD cases CD8+ GrzB+ T cells could be found in contact with dopaminergic neurons (**Figure 39C**). In perivascular spaces, CD8+ GrzB+ T cells were found in all groups but in low percentages (**Figure 39B, Bottom**). Surprisingly, PD cases had no statistically different lower percentages of CD8+ GrzB+ T cells (4.08%) than age-matched healthy controls (11.13%) and iLBD cases (12.434% iLBD). Total number of CD8+ GrzB+ T cells in perivascular spaces had similar trends than percentages (2.069 cells/mm^2 Control, 1.874 cells/mm^2 iLBD, 2.262 cells/mm^2 PD). Overall, infiltrating CTLs containing GrzB+ granules are present in early stages of the disease but not in late stages although they are always present in perivascular spaces.

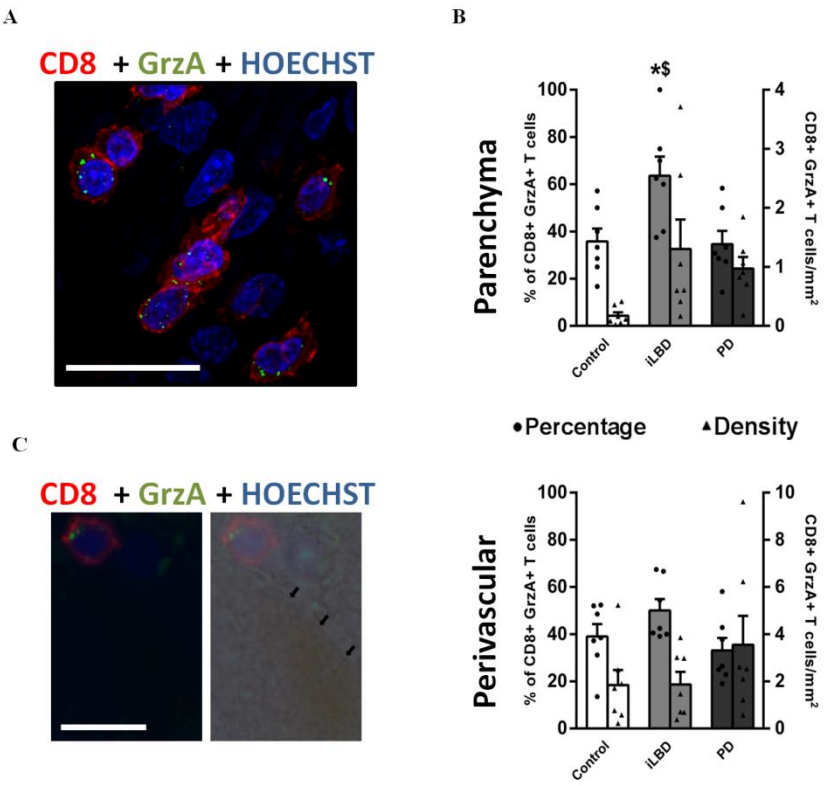

Figure 40. CD8+ Granzyme A+ T cells in SN*pc* of control, iLBD and PD cases. (**A**) Immunofluorescence image of CD8+ (red) T cells positively and negatively stained for granzyme A (green). Nuclei were stained with HOECHST (blue). Scale bar = 15µm. (**B**) Percentages (dots) and densities (triangles) of CD8+ GrzA+ T cells in the parenchyma (top graph) and perivascular spaces (bottom graph) of control (n = 7), iLBD (n = 7) and PD (n = 7) cases. One-way ANOVA, *post-hoc* Tukey's test: **P*-value < 0.05 compared to controls; $*P*-value < 0.05 compared to PD. For parenchyma analysis $F = 6.391$, total $df = 16$. (**D**) Photomicrograph of a CD8+ T cell with GrzA+ granules contacting a NM-containing dopaminergic neuron (black arrows). Bars represent mean ± SEM in all graphs.

In contrast with GrzB+ granules, GrzA+ ones were more abundant per CTL (**Figure 40A**). In the brain parenchyma, there was an increase in percentages of CD8+ GrzA+ T cells in iLBD cases (63.571%; **Figure 40B, Top**) compared

with age-matched healthy controls (35.861%) and PD cases (34.652%). For total numbers, similar tendencies were obtained although PD cases (0.972 cells/mm^2) were much higher than age-matched healthy controls (0.173 cells/mm^2) and similar to iLBD cases (1.301 cells/mm^2). In perivascular spaces no changes were observed in percentages although iLBD cases were again the highest ones (39.0151% Control, 50.052% iLBD, 33.13% PD; **Figure 40B, Bottom**). Total number of CD8+ GrzA+ T cells in perivascular spaces was practically the same in all groups (1.838 cells/mm^2 Control, 1.871 cells/mm^2 iLBD, 3.554 cells/mm^2 PD). In the same sense as CD8+ GrzB+ T cells, some CD8+ GrzA+ T cells could be found in contact with dopaminergic neurons (**Figure 40C**).

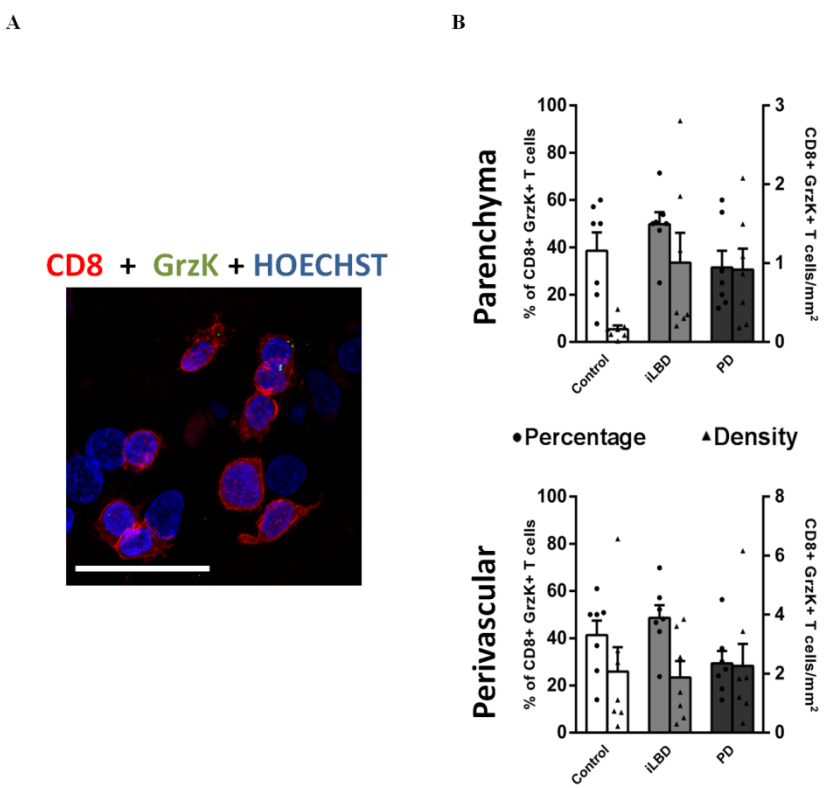

Figure 41. CD8+ Granzyme K+ T cells in SN*pc* of control, iLBD and PD cases. (**A**) Immunofluorescence image showing CD8+ (red) T cells in the SN*pc* which are positively and negatively stained for granzyme K (green). Nuclei were stained with HOECHST (blue). Scale bar = 15µm. (**B**) Percentages (dots) and densities (triangles) of CD8+ GrzK+ T cells in the parenchyma (top graph) and perivascular spaces (bottom graph) of control (n = 7), iLBD (n = 7) and PD (n = 7) cases. One-way ANOVA, *post-hoc* Tukey's test: *P*-value < 0.05. Bars represent mean ± SEM in all graphs.

Finally, we also assessed GrzK expression in granules contained in CD8+ T cells. Beside CD8+ GrzA+ T cells, CD8+ GrzK+ T cells were present in both compartments in all groups (**Figure 41A**). In brain parenchyma, percentage of CD8+ GrzK+ T cells was higher in iLBD cases (49.738%; **Figure 41B, Top**) than age-matched healthy controls (35.813%) and PD cases (34.418%) although this increase was not statistically significant. Total numbers were higher in iLBD (1.01 cells/mm^2) and PD (0.919 cells/mm^2) cases compared with age-matched healthy controls (0.162 cells/mm^2) but again with no significant differences. In perivascular spaces, percentages of CD8+ GrzK+ T cells were similar between age-matched healthy controls (40.278%; **Figure 41B, Bottom**) and iLBD cases (48.661%) even though PD cases were a bit lower (30.255%). Total numbers were practically the same in all groups (2.069 cells/mm^2 Control, 1.874 cells/mm^2 iLBD, 2.262 cells/mm^2 PD).

PRF-1 is also important for CTLs to induce pores in the membrane of the cell target. These pores serve as entries for cytolytic molecules such as granzymes. By double immunofluorescence, we did not find CD8+ PRF-1+ T cells in both parenchyma and perivascular spaces and in all groups.

To sum up, from these results we can conclude that CD8+ T cells in charge of immune surveillance in perivascular spaces express GrzA, GrzB and GrzK in their granules. Moreover, they also express IFNγ but not PRF-1 or FasL

mechanism. In early stages of the disease, even before cell death and synucleinopathy occur, CD8+ GrzB+ T cells infiltrate SN*pc* along with other CD8+ T cells expressing GrzA, GrzK and/or IFNγ. In this early stage, percentages of CD8+ GrzA+ T cells are higher than age-matched healthy control cases.

4.2.8 SN*pc* CTLs express distinct T cell receptors indicating the presence of heterogeneous subpopulations of CD8+ T cells

After analyzing the expression of cytotoxic machinery expressed in SN*pc* CTLs, we wanted to characterize which TCR they expressed. These experiments would help demonstrating the presence of CD8+ T cells in SN*pc* and the nature of antigens which they could recognize. We extracted RNA from frozen post-mortem SN*pc* of four cases which were one age-matched healthy control, one iLBD SN syn-, one iLBD SN syn+ and one PD as, initially, we were not looking for differences between groups. We included blood samples as positive controls for TCR analyses. This RNA was retrotranscribed to cDNA before performing the qPCR. We used *HPRT1* as a housekeeping gene due to the fact it has been used in other studies. We analyzed *TH* expression as a positive marker for quality check. We detected expression of *TH* in all groups although C_t were higher in the PD case as a *TH* downregulation could be expected (**Figure 42A**). We also studied *CD8α* as a typical and general marker for CD8+ T cells and we found low expression in all four cases reinforcing the idea of CD8+ T cells being present but in low densities in SN*pc* (**Figure 42A**). Due to the fact that these T cells are found in low quantities and many of the probes with which we were interested in were not detectable, we performed a preamplification of our cDNA samples using the target probes by 14 cycles. With these pre-amplified samples we ran another qPCR. We again detected *CD8α* and the housekeeping gene *HPRT1*. This preamplification process decreased C_t of these two probes. Negative controls

for qPCR *per se* and for preamplification process were passed indicating that positive signals came from amplification between probe and cDNA sample.

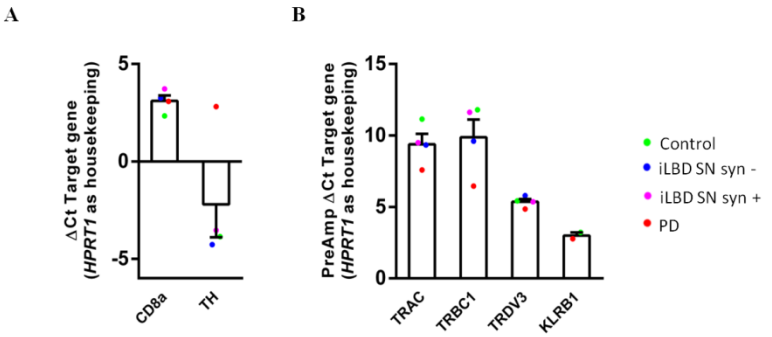

Figure 42. Expression of TCR genes in fresh frozen post-mortem SN*pc* of control, iLBD SN syn-/+ and PD cases. (**A**) ΔC_t of both *CD8α* and *TH* genes with *HPRT1* as housekeeping gene. (**B**) ΔC_t of *TRAC*, *TRBC1*, *TRDV3* and *KLRB1* genes with *HPRT1* as housekeeping gene. For both graphs, each dot represents one case of each group: control (green), iLBD SN syn- (blue), iLBD SN syn+ (violet) and PD (red). Bars represent mean ± SEM for all graphs.

First of all, we analyzed T cell receptor alpha chain constant gene (*TRAC*) expression. In the first qPCR there was not detection of this probe in all samples. After cDNA preamplification we detected ΔC_t around 9.39 ± 0.7287 (**Figure 42B**). T cell receptor beta chain constant 1 gene (*TRBC1*) expression was also present after preamplification (ΔC_t = 9.872 ± 1.242). Both together suggest the presence of αβTCR CD8+ T cells in the SN*pc*. T cell receptor delta variable 3 gene (*TRDV3*) expression was detected in one case out of four before preamplification. Afterwards, it was detected in all cases (ΔC_t = 5.362 ± 0.1929). These results meant that γδTCR CD8+ T cells were detected in SN*pc* independently of pathology. Moreover, we also detected kill cell lectin like receptor B1 gene (*KLRB1*) expression after preamplification in two out of four cases (ΔC_t = 2.993 ± 0.2190). This glycoprotein can be expressed on both natural killer T cells and γδTCR CD8+ T cells.

4.2.9 SN*pc* dopaminergic neurons express HLA class-I but not CD1 molecules

So far, we have demonstrated that CTLs infiltrate SN*pc* in early and late stages of PD. CTLs make contacts/appositions with dopaminergic neurons and they express cytolytic machinery to likely induce dopaminergic cell death. In order to do this, a CD8+ T cell needs to bind its TCR with its cognate HLA class-I molecule in the target cell. As we have recently seen, SN*pc* CD8+ T cells express a variety of TCRs. However, we still do not know which HLA class-I molecules are expressed by dopaminergic neurons. Cebrián and collaborators showed how dopaminergic neurons express HLA class-I molecules (Cebrián *et al.*, 2014*b*). Nonetheless, no other study has reassessed this. HLA class-I molecules present peptide antigens to be recognized by TCRs. Glycolipids are presented to TCRs by CD1 molecules. Thus, we also analyzed CD1 molecules expression in dopaminergic neurons.

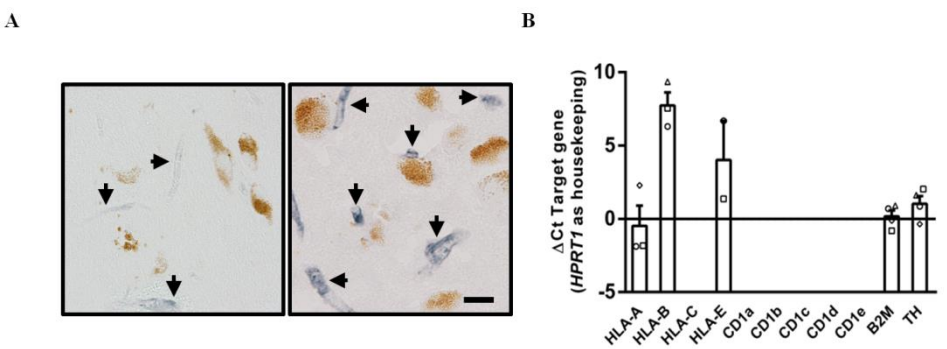

Figure 43. HLA class-I and CD1 genes expression in SN*pc* microdissected dopaminergic neurons of four control cases. (**A**) Representative SN*pc* HLA-A/B/C immunostaining (blue) photomicrographs of two control cases. Black arrows point to blood vessels which serve as positive controls. Scale bar = 15μm. (**B**) ΔC_t of *HLA-A*, *HLA-B*, *HLA-C*, *HLA-C*, *CD1a*, *CD1b, CD1c*, *CD1d*, *CD1e*, *B2M* and *TH* genes with *HPRT1* as housekeeping gene. Each geometrical form means a distinct control case. Bars represent mean ± SEM.

HLA class-I complexes are made of an α-polipeptide chain and β-2 microglobulin. Immunohistochemistry for HLA-A/B/C showed an extensive positive staining although it was more intense in blood vessels (**Figure 43A**). Nevertheless, it was not clear whether dopaminergic neurons had a positive staining. To further demonstrate this, we extracted RNA from microdissected dopaminergic neurons from frozen midbrain blocks of four different healthy controls and retrotranscribed this RNA to cDNA. Afterwards, we analyzed the RNA expression of different HLA class-I and CD1 molecules, β-2 microglobulin and tyrosine hydroxylase. Regarding to *TH* expression, we obtained a dopaminergic enriched RNA from cell-microdissection (ΔC_t = 1.037 ± 0.5245; **Figure 43B**). HLA class-I light chain, β-2 microglobulin gene, was found to be expressed in all four cases (ΔC_t = 0.1685 ± 0.3958). For HLA class-I molecules we observed no expression of *HLA-C* in any of the four cases but yes for *HLA-A* (ΔC_t = -0.4727 ± 1.382), *B* (ΔC_t = 7.736 ± 0.8865) and *E* (ΔC_t = 4.025 ± 2.657). However, the presence and total expression of the distinct genes was variable among cases. We did not find any expression in all four cases for CD1 molecules (a, b, c and d).

4.2.10 SN*pc* CTLs increase their densities in parallel with synucleinopathy and dopaminergic cell loss

Regarding to the state-of-the-art, one of the possible antigens could be α-synuclein. Mounting evidence and our results have showed how an adaptive immune response can be raised around human-WT-α-synuclein. But in PD animal models both CD4+ and CD8+ T cells infiltrate SN*pc* parenchyma. These results contrast with our adaptive immune response characterization of post-mortem PD human tissue as we only see CD8+ T cells infiltrating SN*pc* parenchyma. Moreover, we observe this CD8+ T cell brain infiltration before

nigral synucleinopathy becomes evident. Nevertheless, α-synuclein continues to be a plausible antigen, at least, for late stages of the disease. Thus, we studied in more detail the relationship between CD8+ T cell infiltration and synucleinopathy in our cases. We reanalyzed CD8+ T cell densities and neuronal loss according to the unified staging system for Lewy body disorders (stages I to IV) (Beach *et al.*, 2009*a*). iLBD SN syn- and iLBD SN syn+ belonged to stages I and II, respectively. Stage III affects the brainstem and limbic structures, while in stage IV α-synuclein aggregates are also found in the cerebral cortex. We performed and analyzed an immunohistochemistry for phospho-serine129-α-synuclein aggregates in the SN*pc* to understand the temporal dynamics of their formation and to understand whether synucleinopathy progressively increases in the SN*pc* throughout stages. We checked for the percentage of dopaminergic neurons with diffuse staining of α-synuclein in the cytoplasm (**Figure 44, Left**), density of Lewy neurites (**Figure 44, Middle**) and density of Lewy bodies regardless of whether they were intra- or extracellular (**Figure 44, Right**). Overall, all three α-synuclein aggregates progressively increased in each stage (**Figure 44**). It would seem that LN appear before than LB because some iLBD SN syn+ cases (stage II) had no LB bar LN in the SN*pc*. Moreover, although there was neuronal cell death in late stages of the USSLBD, LB tended to get accumulated.

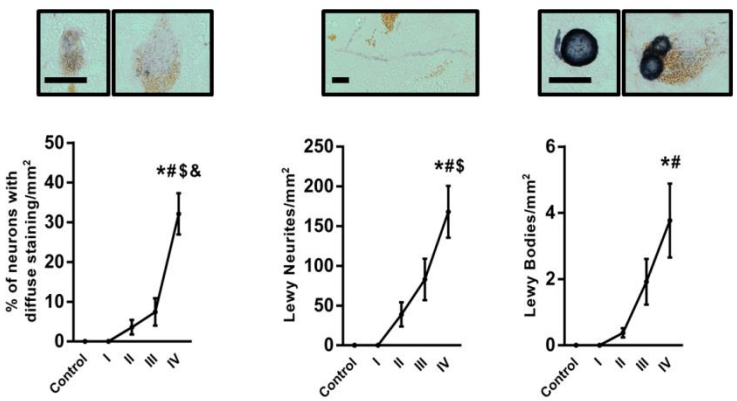

Figure 44. Density of distinct phospho-serine129-α-synuclein aggregates at distinct stages of the unified scale for Lewy body disorders. (**A**) From left to right: Percentage of neurons with diffuse aggregates (*P*-value < 0.05; *F* = 12.83; *df* = 30), density of LN (*P*-value < 0.05; *F* = 6.957; *df* = 30) and density of intracellular and extracellular LB (*P*-value < 0.05; *F* = 4.786; *df* = 30) from stages I to IV of the Lewy body disorders scale. Representative images are presented above each graph (scale bar = 15μm). A total of 7 control, 4 stage I, 4 stage II, 11 stage III and 5 stage IV cases were used. All analyses are One-way ANOVA; *post-hoc* Tukey's test: **P*-value compared to control; #*P*-value compared to stage I; $*P*-value compared to stage II; &*P*-value compared to stage III. Values are represented as mean ± SEM in all graphs.

To sum up, **Figure 45** is a general view of CTLs-DA neurons-Synucleinopathy relationship. In control and stage I cases, in which there is no α-synuclein accumulation in the SN*pc*, neuronal death has not already started (144.9 cells/mm^2) but there is the highest peak of infiltrating CD8+ T cells (3.59 cells/mm^2). When synucleinopathy begins in the SN*pc* (stage II) CD8+ T cell density is dramatically decreased (similar levels to healthy controls, 0.983 cells/mm^2) and dopaminergic cell death gets started (110.567 cells/mm^2). At later stages (III and IV) of the unified Lewy body staging, synucleinopathy increased rapidly while dopaminergic cell death (69.1 cells/mm^2 and 55.5 cells/mm^2) and CD8+ T cell infiltration increased in a slower fashion (2.092 cells/mm^2 and 2.397 cells/mm^2).

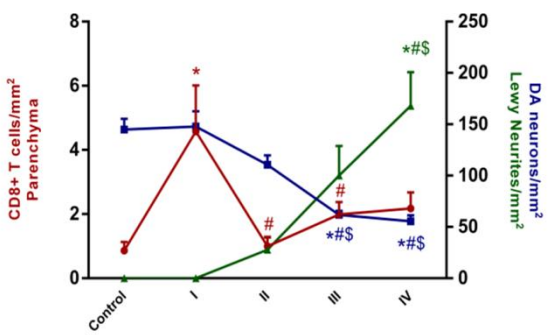

Figure 45. Relationship between CD8+ T cells, dopaminergic neurons and synucleinopathy. Density of dopaminergic neurons (blue), Lewy neurites (green) and parenchymal CD8+ T cells (red) for the different stages. One-way ANOVA, *post-hoc* Tukey's test: **P*-value < 0.05 compared to controls; #*P*-value < 0.05 compared to stage I; $*P*-value < 0.05 compared to stage II. Values are represented as mean ± SEM.

4.2.11 CTLs also infiltrate locus coeruleus in early and late stages of Parkinson's disease

Until now we have seen how CTLs infiltrate SN*pc* of Parkinson's disease in a biphasic way: an acute but transient peak in early stages of the disease when no synucleinopathy is observed and a chronic peak in late stages correlating with dopaminergic neuronal loss. However, we do not know if this T cell brain infiltration is happening in other brain areas which are also affected in the disorder. To approach this question, we chose LC which is an area normally affected in the disease. Norepinephrinergic neurons, which are affected in PD, also present accumulation of NM such as dopaminergic neurons in SN*pc*.

First of all, we analyzed our LC cases to classify them according to synucleinopathy. We sorted them out regarding the USSLBD score of the bank (Beach *et al.*, 2009*a*). Afterwards, we focused on the adaptive immune response. CD4+ T cells were found in very low densities in both parenchyma and perivascular spaces. In many of the cases, CD4+ T cells were totally absent. Due to low number of cases per group and the few CD4+ T cell numbers, no statistical differences were retrieved (data not shown).

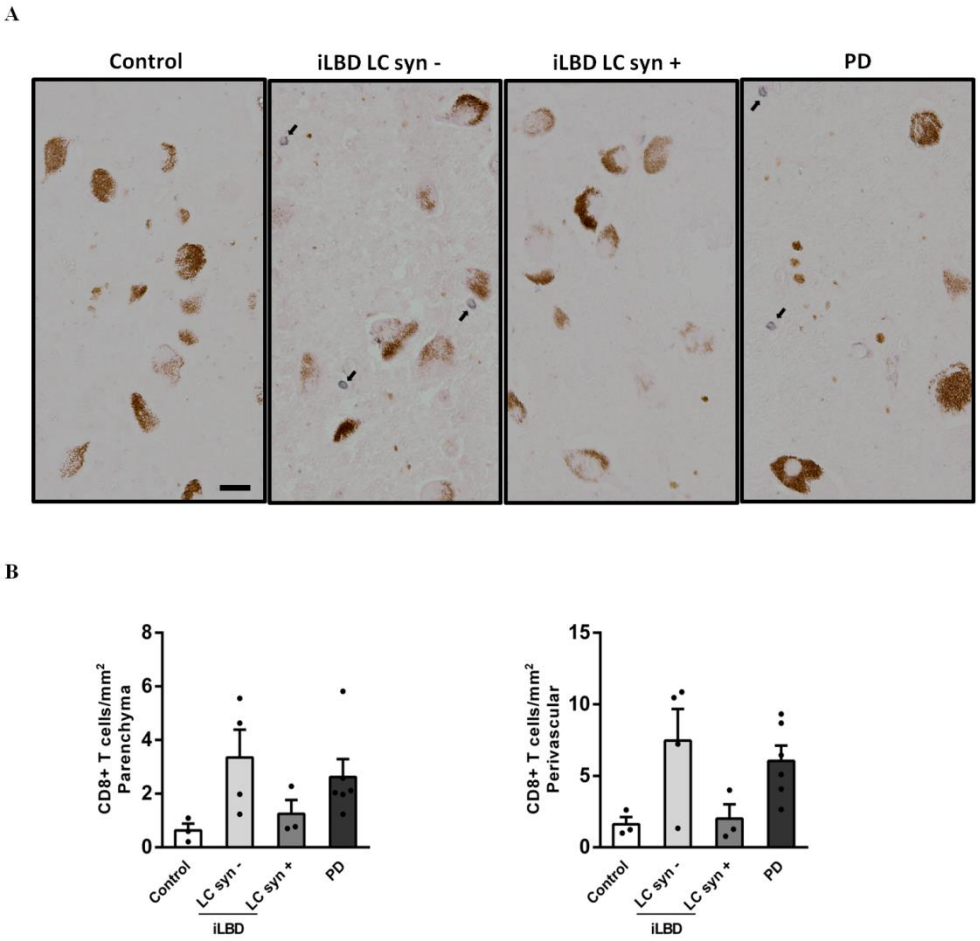

Figure 46. Locus coeruleus CD8+ T cell infiltration in control, iLBD LC syn-/+ and PD cases. (**A**) Representative CD8+ T cell immunostaining (blue) photomicrographs of LC from control, iLBD LC syn-, iLBD LC syn+ and PD cases. Black arrows point to CD8+ T cells. Scale bar = 15µm. (**B**) LC CD8+ T cell densities in both parenchyma (left graph) and perivascular spaces (right graph) of control (n = 3), iLBD LC syn- (n = 4), iLBD LC syn+ (n = 3) and PD (n = 6) cases. One-way ANOVA, *post-hoc* Tukey's test: *P*-value < 0.05. Bars represent mean ± SEM in all graphs.

In contrast with CD4+ T cell densities, CD8+ T cells were present in higher numbers (**Figure 46A**). As a mirror of what was observed in the SN*pc*, there

was an acute and transient peak of CD8+ T cell infiltration before synucleinopathy occured (3.3488 cells/mm^2 iLBD LC syn-; **Figure 46B, Left**) compared with age-matched healthy controls (0.6319 cells/mm^2). This infiltration was resolved when α-synuclein aggregation happened (1.2481 cells/mm^2 iLBDsyn+) but increases again in PD (2.6254 cells/mm^2). Again, due to low number of cases and interindividual variability only statistical trends were found. In perivascular spaces, CD8+ T cells presented similar group trends that parenchymal ones. iLBD LC syn- (7.4667 cells/mm^2; **Figure 46B, Right**) and PD (6.0410 cells/mm^2) cases were the highest ones. Age-matched healthy controls (1.6167 cells/mm^2) and iLBD LC syn+ (2.0043 cells/mm^2) were at same levels of immune surveillance and much lower than the other two groups.

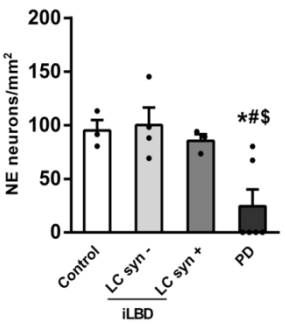

Figure 47. Norepinephrinergic neuronal loss in LC of control, iLBD LC syn-/+ and PD cases. Norepinephrinergic cell densities in LC of control (n = 3), iLBD LC syn- (n = 4), iLBD LC syn+ (n =3) and PD (n = 6) cases. One-way ANOVA, *post-hoc* Tukey's test: **P*-value < 0.05 compared to control; #*P*-value < 0.05 compared to iLBD LC syn-; $*P*-value < 0.05 compared to iLBD LC syn+. Bars represent mean ± SEM.

Unlike SN*pc*, evident norepinephrinergic neuronal loss started in PD cases (24.5705 cells/mm^2; **Figure 47**). Even though there was a small decrease in iLBD LC syn+ cases (85.4965 cells/mm^2) compared with age-matched healthy controls (95.035 cells/mm^2) and iLBD LC syn- (100.198 cells/mm^2) cases, it

was small and non-statistically significant. Thus, in contrast with SN*pc*, it would seem that neuronal loss does not start altogether with synucleinopathy appearance. In order to further demonstrate this conclusion more cases would need to be analyzed.

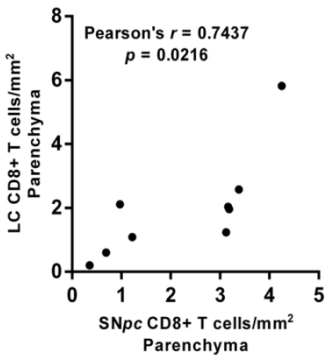

Figure 48. Correlation between infiltrating CD8+ T cells in both LC and SN*pc* of control and PD cases. Scatter diagram of parenchymal LC CD8+ T cells versus parenchymal SN*pc* CD8+ T cells in control (n = 3) and PD (n = 6) cases. Pearson correlation $r = 0.7437$; *P*-value < 0.05.

Usage of the same cases to study the two brain areas (SN*pc* and LC) allowed us to analyze what is happening in the two brain areas in the same end point. It is normally believed that LC is affected earlier in time than SN*pc*, although it is a generalization, and it does not happen in all cases as some iLBD cases have α-synuclein depositions in SN*pc* but no in LC. We performed a correlation between parenchymal CD8+ T cell densities of both areas in age-matched healthy controls and PD cases (**Figure 48**). We chose these two groups as all of their cases have these two areas with or without pathology (in contrast with iLBD cases). This correlation is statistically significant and positive as the more CD8+ T cells we observe in the SN*pc*, the more CD8+ T cells we also observe in LC ($p = 0.0216$; $r = 0.7437$).

DISCUSSION

5. Discussion

So far, it was unknown and remained elusive which were the factors and how they initiate the pathogenic cascade leading to neuronal death and, *propter hoc*, Parkinson's disease onset. During the last 20 years, extensive work has shed light on the role of the immune system in the disease (Mosley *et al.*, 2012; Mosley and Gendelman, 2017; Tan *et al.*, 2020). Most of the works have addressed the question in PD experimental animal models, obtaining striking results. However, scarce studies have assessed the role of the immune system in human tissue. These studies have served to detect peripheral blood changes in leukocyte populations and to correlate them with disease duration and severity. Solely two works analyzed and detected T cell infiltration in PD post-mortem human tissue. Even though they observed an increase of infiltrating T cell densities, a better phenotypic characterization was necessary to better elucidate their role, as T lymphocytes can perform both pro-inflammatory and anti-inflammatory tasks. In addition to this, these results only exhibited a final snapshot, what is happening in late stages of PD. Thus, these studies did not resolve the question of what is taking place in the brain when neuronal death and synucleinopathy initiates.

5.1 Parkinson's disease experimental animal models

This thesis has focused on studying the role of the adaptive immune system in PD etiopathogenesis. We first approached the question in PD experimental animal models. As it can be observed in **Table 6**, T cell brain infiltration had been described in some of them such as MPTP treated mice and overexpression of α-synuclein in rodents.

Table 7. Adaptive immunity in MPTP and OE of h-WT-α-synuclein models

Animal model	Reference	T and B cell infiltration
Acute MPTP injected mice	Kurkowska-Jastrzebska *et al.*, 1999	CD4+ and CD8+ T cell infiltration at d7
	Brochard *et al.*, 2009	CD4+ and CD8+ T cell infiltration at d2, d4 and d7 (tni d0.5, d1)
	Reynolds *et al.*, 2010	CD4+ T cell infiltration at d7
	Chandra *et al.*, 2016	CD4+ and CD8+ T cell infiltration at d7
	Chandra *et al.*, 2017	CD4+ T cell infiltration at d1 and less at d7
	Dutta *et al.*, 2019	CD4+ T cell infiltration at d7
Subacute MPTP injected mice	Depboylu *et al.*, 2012	CD4+ and CD8+ T cell infiltration at d1 (tni d10)
	Zhou *et al.*, 2015	CD3+ T cell infiltration at d15
MPTP injected non-human primates	Roy *et al.*, 2015	CD4+ and CD8+ T cell infiltration at d30
	Mondal *et al.*, 2019	CD4+ and CD8+ T cell infiltration at d30
	Seo *et al.*, 2020	CD4+ and CD8+ T cell infiltration at 48w

OE h-WT-α-synuclein in mice	Theodore *et al.*, 2008	CD3+ T and B cell infiltration at 2w, 4w and 12w
	Qin *et al.*, 2016*a*	CD4+ T cell infiltration at 4w No CD8+ T cell infiltration
OE h-WT-α-synuclein in rats	Sanchez-Guajardo *et al.*, 2010	CD4+ and CD8+ T cell infiltration at 8w (tni 4w and 15w)
	Sanchez-Guajardo *et al.*, 2013*a*	CD4+ and CD8+ T cell infiltration at 3w and 8w
	Van der Perren *et al.*, 2015	CD4+ and CD8+ T cell infiltration at 2w and 4w (tni 0.5w)

d days; *h* human; *OE* overexpression; *tni* timepoints no infiltration; *w* weeks; *WT* wild-type
The absence of CD4+ or CD8+ T cells means they were not addressed in the study.

We chose MPTP treated mice as our starter PD animal model as vast literature had reported the importance of the immune system in dopaminergic neuronal death in this model (Czlonkowska *et al.*, 1996; Kurkowska-Jastrzebska *et al.*, 1999; Barcia *et al.*, 2004, 2011). Previous studies had shown T cell SN*pc* infiltration and their temporal dynamics (Kurkowska-Jastrzebska *et al.*, 1999; Benner *et al.*, 2008; Brochard *et al.*, 2009; Depboylu *et al.*, 2012; Chandra *et al.*, 2016). Elegantly, Brochard and colleagues were the first ones to show the importance of T cells in this model as knocking-out CD4+ T cells was sufficient

to obtain a practically full neuroprotection against MPTP neurotoxin. Incoming studies tried to phenotypically characterize these infiltrating CD4+ T cells reporting a Th17 polarization and the importance of IL-17 for neuronal death (Liu *et al.*, 2016; Sommer *et al.*, 2018; Dutta *et al.*, 2019). Despite the fact that there are distinct MPTP paradigms *i.e.* acute (20 mg/kg, 4 injections in 2h-intervals) and subaucte ones (30mg/kg, one daily injections in 5 consecutive days), we chose the former to begin with as it was the one which both Brochard and Kurkowska-Jastrzebska's studies had used. We initially quality checked the experimental model performing TH immunohistochemistry in both striatum and SN*pc* detecting both fiber and dopaminergic neuronal loss at the end of the timecourse. Nonetheless, we were unable to reproduce T cell SN*pc* infiltration by means of CD3 immunohistochemistry. We thought that mice substrain could be a possible explanation due to small genetic differences. Thus, we repeated the experiment with C57BL/6JRj animals of the same vendor as Brochard's study and we checked for T cell SN*pc* infiltration at 7 days post-injections, when Brochard detected the highest peak. Again, we observed no statistically significant infiltration. We contacted with the authors of Brochard's study, and they commented to us that they were also finding significantly less T cell SN*pc* infiltration than before. Several possible explanations for these negative results could be drawn but, probably, C57BL/6 substrain was not the same as before due to genetic drift. Currently, MPTP treatment does not induce the same infiltration dynamics as before. We cannot discard that a transient infiltration could happen in non-studied timepoints.

We decided to move to the subacute paradigm as T cell brain infiltration had also been described at 1 day post-injections (Depboylu *et al.*, 2012). Theoretically and in our opinion, subacute paradigm was a better recall than the acute one to induce an adaptive immune response due to a longer timecourse (5 injection-days and 21 timecourse-days versus 1 injection-day

and 7 timecourse-days) and small MPTP insults could cause some initial neuronal dysfunction. This could lead to the exposition of neo-antigens while large MPTP insults could directly provoke immune independent neuronal death. We performed subacute MPTP treatment in C57BL/6Ncrl mice because, in foreseeable future experiments, we were going to use transgenic mice for systemic Treg depletion, and this mouse colony was designed in this genetic background. After quality checking via TH immunohistochemistry the loss of dopaminergic neurons at the end of the timecourse, we analyzed T cell SN*pc* infiltration in several timepoints. We obtained similar results as Depboylu's study, finding a statistically significant increase of CD3+ T cell densities at 1 day post-injections. This infiltration was acute and transient as the following day it completely subsided. However, we could not compare this T cell temporal dynamics with Depboylu's study as they only examined day 1 and day 10. Infiltrating T cells were both CD4+ and CD8+ in similar numbers. SN*pc* infiltrating T cells at day 1 correlated with striatal TH loss suggesting interplay between T cells and dopaminergic neurons. Due to the fact that this was a correlation we cannot conclude the causality of these events. Having said this, it is very likely that T cells first impairs neuronal function before killing dopaminergic neurons. We believe that this is the case in the actual disease, where CD8+ T cells do not induce an acute and fast neuronal death.

In order to better mimic the human disease, we decided to try to maintain T cell infiltration for longer periods than just 1 day, likely inducing higher levels of dopaminergic loss. Our strategy was to induce a systemic pro-inflammatory environment depleting anti-inflammatory Treg lymphocytes. It has been extensively reported that Treg numbers and their immune suppressive functions are haltered in peripheral blood of PD patients (Niwa *et al.*, 2012; Saunders *et al.*, 2012; Kustrimovic *et al.*, 2018; Álvarez-Luquín *et al.*, 2019). Treg depletion was transient and we decided to provoke it during the temporal

moment when dopaminergic neuronal death mechanisms initiates (Torra *et al.*, 2018). In contraposition of what we had hypothesized, Treg depletion did not increase nigrostriatal damage. However, we do not know whether systemic Treg depletion could boost the pro-inflammatory environment in the SN*pc* maintaining the CNS homing of T lymphocytes. Further experiments would need to be performed to better understand whether T cell infiltration was maintained regardless of dopaminergic loss.

Comparing the obtained results from subacute MPTP treated mice and T cell infiltration previously reported by Brochard's work, it seems that these T cells can infiltrate the SN*pc*, but their densities cannot be maintained at high levels for longer periods. A strategy similar to Treg depletion was the one performed by Chandra and collaborators who demonstrated the importance of chemokines eotaxin and RANTES/CCL5 to induce T cell trafficking to the CNS (Roy *et al.*, 2015; Chandra *et al.*, 2016, 2017). Thus, one possible explanation for transient T cell SN*pc* infiltration could be the lack of these chemokines. Although we could explore this likely possibility, we moved to genetic animal models because we also wanted to study the relationship between T cells and α-synuclein because it has been proposed as antigen candidate for the human disease (Benner *et al.*, 2008; Sulzer *et al.*, 2017; Garretti *et al.*, 2019; Lindestam Arlehamn *et al.*, 2020).

T cell infiltration in rodent SN*pc* overexpressing α-synuclein had been previously shown (Theodore *et al.*, 2008; Sanchez-Guajardo *et al.*, 2010, 2013*b*). We chose rats over mice due to the fact that, in our hands, mice overexpressing h-WT-α-synuclein do not present consistent dopaminergic loss. In a previous study of our lab, we did observe dopaminergic cell and striatal fiber losses altogether with motor asymmetry in the cylinder test in rats. Furthermore, we chose the rat model to begin with. In our hands, overexpressing h-WT-α-

synuclein in Sprague-Dawley rats we found statistically significant motor asymmetry at 12w and some trends already at 8w. These results could be explained by the loss of striatal TH+ fibers at 12w because they are the dopamine producers necessary for motor regulation. However, we did not observe substantial dopaminergic cell loss at 12w. Some studies with the same model had reported moderate dopaminergic cell loss at 12w or even before. We went directly to analyze T cell SN*pc* infiltration performing double immunofluorescences against TH and CD4 or CD8 to detect both T lymphocyte populations separately. We detected a few numbers of parenchymal CD4+ T cells and bit higher of CD8+ ones. However, we detected similar numbers in the empty viral vector experimental control. Thus, we cannot conclude that this T cell infiltration was provoked due to the viral vector itself and not the α-synuclein. At that moment, we realized that this empty viral vector was not as purified as the h-WT-α-synuclein one because they were produced by different providers.

For the following experiment, beyond better purifying empty viral vector, we changed the rat strain to the inbred Lewis one. We made this decision because we were highly interested on dissecting which α-synuclein epitopes were the ones which were inducing an adaptive immune response. Using inbred rat strains, we could use bioinformatic tools to obtain MHC restriction positions for α-synuclein. In contrast with Sprague-Dawlay rats, overexpression of h-WT-α-synuclein in Lewis rats did not cause both motor behavioural dysfunction and striatal TH+ fiber loss. Nonetheless, we did obtain both CD4+ and CD8+ T cells SN*pc* infiltration which began at 8w and it was maintained up to 12w. Empty viral vector did not produce any apparent adaptive immune response. However, at that point, we discovered that CD8+ T cell brain infiltration preceded α-synuclein accumulation and aggregation in PD. Therefore, we

discarded this model to study the adaptive immune response linked to PD neurodegeneration.

Altogether, T cell brain infiltration in both MPTP injected mice and rats overexpressing of h-WT-α-synuclein did not mimic the actual PD adaptive immune response that we have also reported. In both PD experimental animal models, CD4+ and CD8+ T cells infiltrate SN*pc*. Nonetheless, we have not found a statistically significant increase of CD4+ T cells in the human tissue. CD4+ T cells seemed to have a relevant role in dopaminergic cell death in the MPTP animal model (Brochard *et al.*, 2009). This difference between the human disease and the animal model has also been reported in multiple sclerosis (MS) and experimental autoimmune encephalomyelitis (EAE). Brain tissue from MS patients presents higher CD8+ T cell densities than CD4+ ones. EAE brain pathology is mainly driven by CD4+ T cells (Machado-Santos *et al.*, 2018). Our results indicate that T cell brain infiltration in rats overexpressing h-WT-α-synuclein was elicited by α-synuclein as EV control did not show any increase of infiltrating T cell densities. Contrarily, T cell SN*pc* infiltration in the human disease precedes α-synuclein aggregation suggesting that, at least in early stages, α-synuclein is not the antigen which activated the adaptive immune response. Furthermore, rats overexpressing h-WT-α-synuclein are good models to understand intrinsic cell-autonomous mechanisms in which α-synuclein is related and how it spreads to other neurons, but it is not a useful model to recapitulate PD adaptive immune response. In both models we have observed strain and likely genetic drift effects. These two variables need to be taken into account for futurible experiments due to the fact that they make reproducibility difficult.

5.2 Parkinson's disease post-mortem human tissue

Presence of CD4+ and CD8+ T cells in PD post-mortem human SN*pc* tissue had been previously reported (McGeer *et al.*, 1988*a*; Brochard *et al.*, 2009; Rohn and Catlin, 2011, Stevens *et al.*, 2012*b*; Sommer *et al.*, 2018). However, the two studies which assessed the question in a quantitative way raised some controversy as they draw distinct conclusions. Brochard and colleagues demonstrated an increase of both CD4+ and CD8+ T cells being the latter the highest in cell densities. Stevens and collaborators presented a poster in Movement Disease Society Congress in which no differences were found but only some trends for CD8+ T cells. Moreover, as we commented before, no phenotypic characterization had been performed and no studies had taken into account early stages of the disease. Thus, before building up a PD experimental animal model which recapitulates PD neuroinflammation, these aforementioned questions needed to be answered.

Our first main goal was to study T cell SN*pc* infiltration in PD cases comparing with age-matched healthy controls. Contrarily with Brochard's study, we did not find an increase of parenchymal CD4+ T cells but only a trend for the perivascular ones. As Brochard's study did not count T cells according to the compartment, it is logical to think that these differences with our results could be explained by that. In addition to this, we observed an evident increase in the CD4+ T cell perivascular compartment. We separated both compartment counts as parenchymal and perivascular T cells can have distinct roles and dynamics. Age-matched healthy controls presented high cell density levels of perivascular T cells in comparison with parenchymal ones indicating a possible immune surveillance role for perivascular T cells as it had been previously suggested (Loeffler *et al.*, 2011; Ousman and Kubes, 2012; Ransohoff and Engelhardt, 2012; Smolders *et al.*, 2013, 2018). CD8+ T cells were statistically significant increased in the parenchymal compartment and a trend was found

in perivascular spaces. Moreover, CD8+ T cells outnumbered CD4+ ones in the same way as Brochard's study. The presence of T cells in the brain had also been documented in previous studies regarding healthy and pathological brains. Smolders and colleagues showed the presence of T cell populations in both perivascular and parenchymal spaces. CD8+ T cells exhibited higher densities than CD4+ ones. In MS, a primary autoimmune neurological disease, CD8+ T cells were present in higher densities than CD4+ T cells which contrasted with CSF where the trends were totally the opposite (van Nierop *et al.*, 2017; Machado-Santos *et al.*, 2018). Thus, it seemed that CSF compartment is different from the CNS. However, they did not differentiate between parenchyma and perivascular spaces because of the non-spatial resolution of the flow cytometry technique. In other neurological disorders such as Alzheimer's disease, T cell CNS infiltration has also been reported in post-mortem human tissue (Togo *et al.*, 2002; Merlini *et al.*, 2018; Gate *et al.*, 2020) and experimental animal models (Ferretti *et al.*, 2016; Unger *et al.*, 2020). In the human tissue, T lymphocytes mainly expressed CD8 indicating, again, the outnumbering of CTL over helper ones. One hypothesis was that both tau and amyloid β (Aβ) plaques could be the antigens against which T cells were being activated. In Merlini's study, T cell infiltration correlated with tau pathology in all studied brain regions, but it did not with Aβ pathology. Nevertheless, this was only a correlation, and no final demonstration was provided. Clonally expanded TEMRA CD8+ T cells have been found in AD CSF samples with antigen specificity against EBV-derived antigens (Gate *et al.*, 2020). These results raised the question whether the adaptive immune response in AD was against a virus itself or due to immune cross-recognition of neuronal peptides. T cell responses against neuronal auto-antigens, *i.e*. APP, Aβ, tau, α-synuclein and TDP-43, in AD seemed to be not different to the ones in age-matched healthy controls (Dhanwani *et al.*, 2020). In this same study they did find an increase of peripheral CD4+ TEMRA cells but

no immune reactivity against EBV-derived antigens. These negative results could be explained by the fact that CSF- and blood-derived T cells may behave differently and present distinct clonal expansions. Further experiments would need to be performed analyzing PD CSF-derived T cells against the same neuronal-derived auto-antigens.

One measure for detecting *in vivo* cytotoxicity is the ratio between CD8+ T cells and the target cell. This is due to the fact that the greater the ratio, the higher the probability of CD8+ T cells making contact with the target cell (Halle *et al.*, 2016). As it was expected, PD cases presented a higher ratio than age-matched healthy controls. This led to us to check whether there was any correlation between CD8+ T cell densities and dopaminergic cell loss and we found a statistically significant inverse one. The more infiltrating CD8+ T cells, the less surviving dopaminergic neurons. Even though these results suggested a likely negative role of CD8+ T cells in the pathology, a statistical correlation do not show any final causality.

So far, we have demonstrated an increase of parenchymal CD8+ T cells in PD samples comparing with age-matched healthy controls and that they correlate with dopaminergic cell loss. Nonetheless, PD cases represent a late-stage of the disorder. In order to answer the question whether the adaptive immune response had a role in the initiation and progression of the pathology we analyzed T cell SN*pc* infiltration in iLBD cases. These samples come from healthy donors in which, after a neuropathological analysis, brain synucleinopathy was found. This synucleinopathy can be highly variable and sparse between brain regions. Although some constructive discussion has been raised around iLBD cases representing early pre-motor stages of the disease, mounting evidence has been pointing to that conclusion (DelleDonne *et al.*, 2008; Dickson *et al.*, 2008, Beach *et al.*, 2009*b*; Iacono *et al.*, 2015; Walker *et al.*,

2016). Practically all of our post-mortem human tissue samples came from Banner Sun Health Bank which beyond proportioning accurate and detail clinical information of each case, they also had classified each of them with USSLBD scale (Beach *et al.*, 2009*a*). Thus, we were able to select iLBD cases with distinct brain areas affected by α-synuclein pathology. Some of them had synucleinopathy restricted to the Ob but no in the SN*pc*. For sake of simplicity, these cases were named iLBD SN syn- individuals. iLBD cases with apparent synucleinopathy in the SN*pc* were called iLBD SN syn+. Analyzing SN*pc* dopaminergic neuronal densities, we found a decrease from iLBD SN syn+ to PD cases. iLBD SN syn- samples presented no loss of dopaminergic neurons meaning that cell loss appeared with nigral synucleinopathy deposition. These results reinforced the hypothesis which classified iLBD individuals as early pre-motor stages of PD. Both parenchymal and perivascular CD4+ T cells were presented in low densities. Strikingly, CD8+ T cells were elevated in iLBD SN syn- samples in both parenchyma and perivascular compartments. Moreover, iLBD SN syn- CD8+ T cell densities were higher than the ones from PD indivdiuals. Immune appositions between CD8+ T cells and dopaminergic neurons were reported. These results suggested that nigral CD8+ T cells preceded synucleinopathy deposition and that there are two adaptive immune response phases in the disease: i) acute and transient CD8+ T cell SN*pc* infiltration before synucleinopathy and dopaminergic cell loss, and ii) chronic and subacute CD8+ T cell SN*pc* infiltration once synucleinopathy and dopaminergic cell death have begun.

Because CD8+ T cell SN*pc* infiltration preceded α-synuclein aggregation, we speculate that the cytotoxic attack can be triggering this aggregation. In this line, we assessed the formation of different phospho-α-synuclein aggregates in the SN*pc* and related them with CTL SN*pc* infiltration and dopaminergic neuronal loss. We analyzed the density of LNs, LBs and the percentage of

dopaminergic neurons with punctuated phospho-α-synuclein throughout USSLBD staging. All three parameters progressively increased in each stage. LNs seemed to form before LBs because several stage II cases harboured LNs but no LBs. In consequence, we can conclude that during late stages of the disease both CTL infiltration and Lewy body pathology parallelly increase meanwhile dopaminergic neuronal densities decrease.

Antigen presentation by means of MHC class-II in the SN*pc* exhibited a decrease in iLBD SN syn- cases, *ergo*, preceding nigral synucleinopathy. In later stages, MHC class-II expression reached control levels and it was accompanied by a slight increase of ameboid/activated morphologies. Our results contrast with some part of the literature which did observe a general increase of MHC class-II expression or intensity (McGeer *et al.*, 1988*a*; Bradaric *et al.*, 2012; Rostami *et al.*, 2020), although another part did not observe that increase (Croisier *et al.*, 2005; Hurley *et al.*, 2015). One possible explanation for this disagreement is the fact that in PD cases compared to the other groups there was high variability. Some cases presented practically no staining meanwhile others totally presented the opposite way. This could explain the fact that these results could be also cohort dependent. Orr and Walker studies also observed this heterogeneity (Orr *et al.*, 2005; Walker *et al.*, 2016). Due to the fact that microglial cells act as macrophages and they can phagocytise NM (Carballo-Carbajal *et al.*, 2019) we checked the interplay between MHC class-II and NM-containing dopaminergic neurons. We reported MHC class-II cells with NM inside independently of the group. However, taking only into account PD cases with MHC class-II staining, we found a positive correlation: the more MHC class-II staining, the more surviving dopaminergic neurons. Again, even though this is a correlation, and it does not mean causality, it suggests a possible positive role for MHC class-II microglia. NM phagocytising by MHC class-II+ cells was found in all groups, likely indicating a role in aging. The decrease of MHC class-

II+ microglia in iLBD SN syn- cases was noteworthy as we expected the opposite way around. It is important to highlight the fact that substantia nigra is a brain region with prominent microglia densities. The fact that microglial cells may have brain region-specific phenotypes is a plausible explanation (Abellanas *et al.*, 2019). In this last study, it was suggested that under an inflammatory response, SN*pc* microglia downregulates MHC class-II and upregulates some anti-inflammatory cytokines such as IL-10 and TGF-β. These results reinforce the idea that microglial cells may have a beneficial role in the disease. Furthermore, a better characterization of SN*pc* microglial cells throughout PD stages is necessary to fully understand the brain immune response.

This thesis has been the first one to report the idea that T cells precede both synucleinopathy and dopaminergic cell death. These results boost the importance of the adaptive immune system in PD etiopathogenesis. Despite the fact that replication and increasing the number of samples need to be performed, presumably reducing CD8+ T cell densities during the beginning of the disease could have some effects in the posterior pathogenic cascade of events. At least for the initial CD8+ T cell SN*pc* infiltration wave (iLBD SN syn- cases), it would seem logical to assume that α-synuclein would not be the antigen. However, we cannot discard this during the second and chronic wave (PD individuals). These results made us to discard the overexpression of h-WT-α-synuclein animal model as synucleinopathy preceded T cell SN*pc* infiltration. To a certain extent, overexpression of h-WT-α-synuclein animal model could serve to understand the relation between dopaminergic neurons and α-synuclein and to work on the possibility of α-synuclein as the antigen for the second chronic CD8+T cell wave.

The fact that CD8+ T cells preceded α-synuclein deposition led us to construct one hypothesis: CD8+ T cells directly attack dopaminergic neurons, and this

stress could help to up-regulate α-synuclein deposition. The former hypothesis comes from the fact that in inflammatory diseases have been detected an up-regulation of α-synuclein (Follmer, 2020). In MS human post-mortem tissue has been detected an increase of α-synuclein reactivity in brain regions with inflammatory activity (Lu *et al.*, 2009). LPS and pro-inflammatory cytokines have been described to stimulate α-synuclein aggregation in enteric neurons (Kelly *et al.*, 2014). This process could be replicated with a specific gut bacterium treatment (Choi *et al.*, 2018). This immune system and α-synuclein relationship have shown increasing interest and novel works have suggested that α-synuclein facilitates the immune responses to infection. Viral infection by West Nile virus is able to induce α-synuclein up-regulation in primary neurons (Beatman *et al.*, 2015). This up-regulation is beneficial as knocking-out α-synuclein increases infection and animal mortality. The main hypothesis beyond this is that α-synuclein could help to restrict viral RNA replication (Follmer, 2020; Wahmane *et al.*, 2020). It is worth mentioning that one recent study in which mice stereotaxically injected with α-synuclein preformed fibrils presented T cell CNS infiltration, but same treated immunocompetent mice presented higher phosphorylated α-synuclein levels (George *et al.*, 2020). This study reinforced the idea that immune system and α-synuclein are closely related.

Afterwards, we moved to phenotypically characterize the cytotoxic machinery which was expressed by nigral CD8+ T cells. We checked for several typical CD8+ T cell markers that had also been reported by previous studies (Smolders *et al.*, 2013, 2018; van Nierop *et al.*, 2017). We observed that a great percentage of both parenchymal and perivascular CD8+ T cells were IFNγ+ too. This pro-inflammatory cytokine had already been associated with PD pathology (Mount *et al.*, 2007; Barcia *et al.*, 2011; Walker *et al.*, 2016). In these same studies, TNFα was also found to be associated with the disease. Strikingly, we did not observe

any TNFα+ CD8+ T cell in our individuals. This two-phase model of CD8+ T cell SN*pc* infiltration that we reported between iLBD SN syn- and PD cases, was also supported by the fact that iLBD SN*pc* infiltrating CD8+ T cells presented GrzB+ granules in contrast with the other groups. This reinforced the idea of an initial acute inflammatory response during early stages of the disease. Inflammatory dynamics between the brain parenchyma and the perivascular space were more apparent when we found perivascular GrzB+ CD8+ T cells in all groups including age-matched healthy controls. CD8+ T cells expressing other granzymes such as GrzA and GrzK, which are less cytotoxic than GrzB, were found in all groups although an increase in parenchymal T cells was found in the iLBD group again. Surprisingly, PRF-1+ CD8+ T cells were completely absent in all the groups. Although PRF-1 may help inducing target cell death, granzymes can do so independently (Haile *et al.*, 2011). This result is in agreement with previous studies (Loeffler *et al.*, 2011; Smolders *et al.*, 2018) and it would explain the lower cytotoxic capacities of these CD8+ T cells. Fas/FasL pathway was neither found expressed. We also finally checked PD-1/PD-L1 checkpoint pathway in order to study whether some immune inhibitory pathways are relevant for brain infiltrating CTL. However, we did not detect expression of both PD-1 and PD-L1. Further studies need to address which immune tolerance mechanisms can be abused to stop the adaptive immune response.

Mounting evidence have demonstrated the presence of T_{RM} T cells in the brain parenchyma (Steinbach *et al.*, 2016; Smolders *et al.*, 2018). In our study we observed the presence of CD8+ T_{RM} T cells in both compartments expressing CD103 and CD69. Steinbach and colleagues demonstrated in mice that after viral reinfection and presentation of cognate antigen by means of MHC class-I, T_{RM} T cells rapidly acquire a cytotoxic effector function preventing fatal brain infection. This occurred even in absence of circulating CD8+ T cells. Smolders'

study demonstrated that human brain T_{RM} T cells are equipped with the cytotoxic machinery that we have also described. Furthermore, our results indicate that this CD8+ T_{RM} T cells we have found in both parenchyma and perivascular spaces may be activated under an inflammatory condition and present cytotoxic effector capabilities.

One criticism that has recently been made to our published results is the fact that synucleinopathy is not restricted to PD pathology (Halliday, 2020). Halliday commented that in other pathologies which presents synucleinopathy *i.e*. AD (Toledo *et al.*, 2016) and MSA, T cell CNS infiltration has also been reported (Togo *et al.*, 2002; Merlini *et al.*, 2018; Unger *et al.*, 2020; Williams *et al.*, 2020). Tauopathy is also not restricted to AD as it has been found to colocalize with α-synuclein in LBs (Pan *et al.*, 2021). In all groups, individuals with Aβ plaques and tau tangles are present with no significant changes, showing no specificity for synucleinopathy. CD8+ T cell SN*pc* infiltration did correlate with general brain tau pathology but no with Aβ. In another study, PD-derived peripheral CD4+ T cells reacted more against tau than α-synuclein (Arlehamn *et al.*, 2019). Nonetheless, our results need to be reproduced with a greater number of cases and SN*pc* tau pathology would need to be analyzed as we cannot discard that adaptive immune response against α-synuclein and tau may be linked. It is necessary to highlight at this point that the main risk factor for both diseases is aging. It is still unknown how brain adaptive immune surveillance behaves with aging. Moreover, we observed infiltrating SN*pc* GrzB+ CD8+ T cells in iLBD cases which contrasted with the results of Merlini's study in which no GrzB+ CD8+ T cells were observed in all cases, among them individuals with mild-cognitive impairment as an early stage of AD (Merlini *et al.*, 2018).

After knowing which cytotoxic machinery express SN*pc* CTL, we analyzed which type of TCRs they presented and which MHC class-I proteins were expressed by dopaminergic neurons. For the first question we used whole SN*pc* tissue to extract RNA. We detected high variability of TCR which could be concluded in the presence of both TCRαβ and TCRγδ. For the second question, we isolated dopaminergic neurons by means of laser capture microdissection. Dopaminergic neurons from age-matched healthy controls expressed HLA-A, -B and -E but we did not report HLA-C expression. This contrasts with the literature (Cebrián *et al.*, 2014*b*) in which HLA-C was also found. In order to verify this, a greater number of samples would need to be analyzed. We explored whether glycolipids could be presented as antigens via CD1. Nonetheless, we did not find expression of any CD1 isoform in dopaminergic neurons. As a result, dopaminergic neurons can only present protein antigens through MHC class-I.

Finally, we wanted to know whether this T cell brain infiltration was SN*pc* specific. We examined T cell infiltration in the LC as another brain area affected in PD pathology (Giguère *et al.*, 2018). LC is normally affected before SN*pc* in USSLBD and Braak staging (Braak *et al.*, 2003*a*, Beach *et al.*, 2009*a*). This analysis was also interesting as we could study same individuals and correlate T cell infiltration for both brain areas. In the same way as SN*pc*, we differentiated iLBD cases according to LC synucleinopathy. Strikingly, we obtained remarkably similar results to SN*pc*. CD8+ T cells, again, outnumbered CD4+ T cells which were practically absent. For both brain parenchyma and perivascular spaces, we observed a slight increase of CD8+ T cell densities for both iLBD LC syn- and PD individuals. However, our results did not reach statistically significance due to a low number of cases. Norepinephrinergic cell death was clearly detected in PD cases. Interestingly, CD8+ T cell infiltration in both areas, taking into account PD and age-matched healthy controls,

significantly correlated. These results suggest that dynamics of the adaptive immune response in the PD brain are related among two affected brain areas *i.e.* LC and SN*pc*. Nevertheless, both areas share the fact that the immunogenic dark brown pigment NM is present. As a result, more studies would need to approach the question whether this PD T cell brain infiltration also occurs in other areas without NM-containing neurons.

Overall, the study has several limitations which would need to be addressed in further studies to make our conclusions more robust. One of the aspects that challenged the interpretation of any study performed with aged population is the existence of comorbidities. In **Annex Tables 1 & 2** we show age, synuclein pathology, sex variable, comorbidities, and clinical history of all our human cases. The vast majority of the cases, regardless of the experimental groups, exhibited several diseases during their lives. As a result, we cannot completely rule out that that their health status and medication had influenced our results. We have analyzed whether some common pathologies had some effects on our reported results. For instance, administration of chemotherapeutics or the co-existence of infection or inflammatory diseases did not affect CD8+ T cell infiltration. White blood cell counts are known to transiently decline in most cancer patients due to chemotherapy. Most of the cases that died of cancer did not receive chemotherapy or received it several months or years before death. Chemotherapeutics affect T cells but it depends on T cell population (Zhang *et al.*, 2008) and the therapeutic itself. For instance, normal white blood counts were reached 28 days after the last administration of the chemotherapeutic gemcitabine (Plate *et al.*, 2005). In reference to inflammatory diseases, no individuals suffered sepsis during the last disease. Chronic inflammatory diseases were present in our cases but regardless of the group. The second limitation of our study is the fact that ratio between males and females is not

the same among the different groups and we cannot tell whether there is a sex effect.

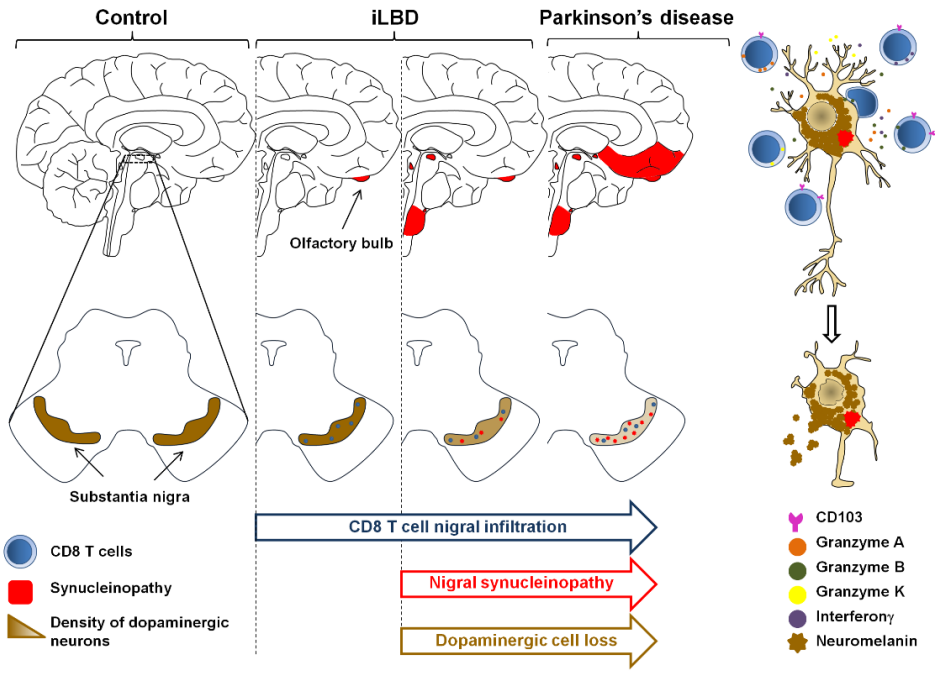

Figure 49. CD8+ T cell SN*pc* infiltration precedes both synucleinopathy and dopaminergic cell loss and express markers of cytotoxic machinery and tissue resident memory T cells. SN*pc* is partly preserved in age-matched healthy controls and no synucleinopathy is observed. Nonetheless, when synucleinopathy starts in the olfactory bulb, CD8+ T cells infiltrate SN*pc* in great quantities. Afterwards, synucleinopathy spreads throughout several brain areas among them SN*pc* where CD8+ T cell infiltration decreases. At that point, neuromelanin-containing dopaminergic neurons loss begins to be apparent. In PD cases, both SN*pc* synucleinopathy and dopaminergic cell loss have skyrocket meanwhile CD8+ T cells increases again parallelly with synucleinopathy. These CD8+ T cells express several markers for cytotoxicity such as Grz A, B and K, IFNγ and they also express CD103 which is a marker for tissue resident memory T cells.

All things considered, our results indicate that CD8+ T cells have an important role in the etiopathogenesis of the disease as SN*pc* infiltration precedes two main hallmarks of the disease such as α-synuclein deposition and dopaminergic cell loss (**Figure 49**). This study, which was performed using post-mortem human tissue, is a descriptive one. The etiopathogenic relevance of CD8+ T cells should need to be confirmed with an appropriate PD experimental animal model. However, we were unable to find one which recapitulates the adaptive immune response we have reported in the human disorder. This PD experimental animal model would need to reproduce CD8+ T cell temporal dynamics and the accumulation of CD8+ T_{RM} T cells (**Figure 50**). In addition to this, α-synuclein deposition and dopaminergic cell death would need to occur after a first acute and transient CD8+ T cell SN*pc* infiltration. One possible experiment would be to provoke a SN*pc* inflammation with viruses, LPS or small MPTP insults, to transiently increase CD8+ T cells and to provoke the raise of CD8+ T_{RM} T cells. Once this is resolved there could be two options: i) synucleinopathy would be induced due to the inflammatory response as it has been previously published (Lu *et al.*, 2009; Kelly *et al.*, 2014; Beatman *et al.*, 2015), or ii) synucleinopathy would be induced by a conditional transgenic construct. Regarding the post-mortem human tissue, studying other affected brain areas in PD pathology can bring up some important clues about these temporal dynamics. In this thesis we have mainly focused on SN*pc* and slightly in LC. However, we cannot discard that CD8+ T cell brain infiltration is dependent of the immunogenic dark-brown pigment NM because both analyzed areas present NM-containing neurons. Studying other affected PD brain areas without NM-containing neurons of the same individuals could bring us a more general snapshot of what is happening in the whole brain. Analyzing adaptive immune brain surveillance changes with aging is also worth to taking a look in foreseeable studies as aging is the main risk factor for AD and PD.

Finally, and potentially most importantly, more effort needs to be put in order to identify the antigen/s presented by cells targeted for degeneration at different disease stages. Although many authors have proposed α-synuclein as a possible antigen, our study suggests that in early stages of the disease α-synuclein is not the antigen recognized by SN*pc* infiltrating CD8+ T cells. In late stages has been observed in peripheral blood-derived T cells that α-synuclein elicits a Th2 response which is not a classical pro-inflammatory one such as Th1 and Th17 (Mosley and Gendelman, 2017; Sulzer *et al.*, 2017). These results need to be confirmed using brain and/or CSF-extracted T cells. Another possibility would be the absence of a specific antigen, as Togo showed in AD samples the presence of activated T cells but without fully differentiation meaning no antigen specificity overall (Togo *et al.*, 2002).

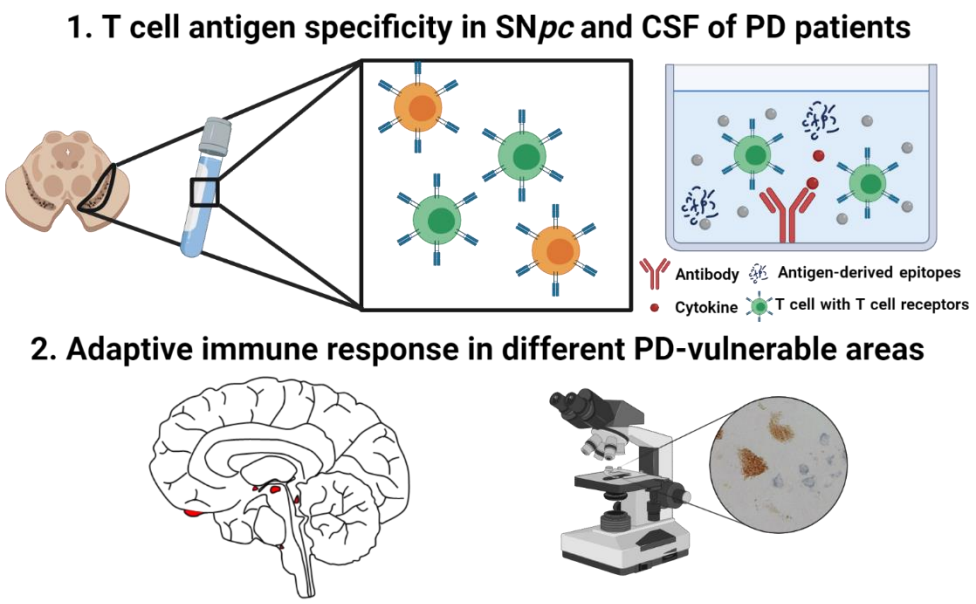

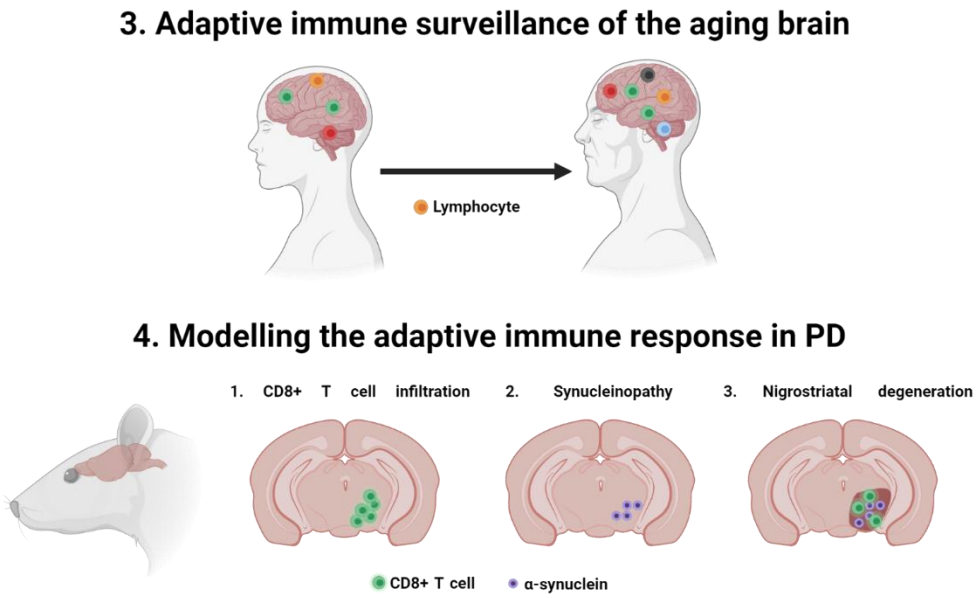

Figure 50. **Foreseeable open questions about adaptive immunity in PD.** After finding striking CD8+ T cell infiltration in both early and late stages of PD, it is necessary to address the question which is the main antigen/s that induce an adaptive immune response in the disorder. In order to do that, T cells extracted from post-mortem human SN*pc* and CSF can be cultured with several likely antigens which may be obtained through TCR sequencing. In the case there is antigen recognition and these T cells become activated, antibody-coated surfaces would recognize which cytokines are released. It is also important to study other PD-vulnerable areas which present synucleinopathy in distinct stages to better understand the dynamics of this adaptive immune response which we have described. Strikingly, recent evidence has brought importance to the active adaptive immune brain surveillance. However, we still do not know how this T cell 'patrolling' changes during aging which is considered the most important risk factor for several neurodegenerative diseases such as PD and AD. Finally, once we better understand the human pathology, trying to create a new experimental animal model which resembles the adaptive immunity of the human disorder is necessary to test novel therapeutic targets. Created with BioRender.com

CONCLUSIONS

6. Conclusions

1. Acute MPTP treatment to C57BL/6Ncrl (and C57BL/6JRj) mice does not elicit the T cell SN*pc* infiltration previously described in the literature.
2. Subacute MPTP treatment to C57BL/6Ncrl FoxP3.LuciDTR transgenic mice induces CD4+ and CD8+ T cell SN*pc* infiltration only at 1 day after last injection. This infiltration correlates with TH+ striatal fiber loss.
3. Treg depletion in the subacute MPTP treated mice does not boost nigrostriatal damage.
4. Overexpression of h-WT-α-synuclein in Sprague-Dawley rat SN*pc* dopaminergic neurons induces behavioural changes and TH+ striatal fiber loss but not dopaminergic cell loss up to 12 weeks post-injection.
5. Not totally purified empty vectors may induce CD4+ T cell SN*pc* infiltration in Sprague-Dawley rats.
6. Overexpression of h-WT-α-synuclein in Lewis rat SN*pc* dopaminergic neurons induces both CD4+ and CD8+ T cell SN*pc* infiltration from 8 weeks to 12 weeks post-injection. However, this T cell infiltration is not accompanied with nigrostriatal dysfunction.
7. Aged human healthy controls present both perivascular and infiltrating T cells in SN*pc* and LC. CD8+ T cells outnumber CD4+ ones in both compartments.
8. Perivascular but not parenchymal CD4+ T cells in SN*pc* of PD cases present a case-dependent increase comparing with age-matched healthy controls. In LC no differences were detected.
9. SN*pc* infiltrating CD8+ T cells increase in PD individuals compared with age-matched healthy controls. In LC this increase is also noted but it does not reach significant values due to low number of cases.

10. CD8+ T cell SN*pc* infiltration correlates with dopaminergic cell loss in PD. Moreover, there are cytotoxic appositions between CD8+ T cells and dopaminergic neurons.
11. Increase of CD8+ T cells in both parenchyma and perivascular spaces in both SN*pc* and LC happens in early stages of the disease (iLBD SN/LC syn- cases) preceding both synucleinopathy and dopaminergic cell loss. Cytotoxic appositions between CD8+ T cells and dopaminergic neurons can also be observed in iLBD SN syn+ cases.
12. When synucleinopathy appears in SN*pc* (iLBD SN syn+ cases) CD8+ T cell infiltration is reduced to age-matched healthy control levels. This reduction altogether with the increase in PD cases suggests a biphasic dynamic of T cell SN*pc* infiltration.
13. SN*pc* synucleinopathy increases along with unified staging system for Lewy body disorders score.
14. In both physiological and pathological conditions and in the same individuals, the more CD8+ T cells infiltrate SN*pc*, the more CD8+ T cells also infiltrate LC. Hence, CD8+ T cell infiltration dynamics in both SN*pc* and LC coevolve.
15. Dopaminergic cell loss begins in early stages of the disease (iLBD SN syn+ cases) when synucleinopathy is apparent. The loss progresses altogether with α-synuclein aggregate burden and correlates with clinical motor scores.
16. SN*pc* MHC class-II+ staining has a trend to decrease in iLBD SN syn- cases. Recovery of MHC class-II+ microglia is pathology-dependent but do not surpass age-matched healthy control levels. Activated SN*pc* MHC class-II+ microglial morphologies present a tendency to increase when nigral synucleinopathy is patent.

17. Ameboid/phagocytic SN*pc* MHC class-II+ morphologies are non-significantly increased in practically all iLBD SN syn+ cases and then maintained in PD individuals.
18. SN*pc* dopaminergic cell loss inversely correlates with ameboid/homeostatic ratio of MHC class-II+ microglia in PD cases.
19. High percentage of CD8+ T cells in the SN*pc* express CD103 marker of tissue resident memory T cells (T_{RM}), increasing significantly in PD cases.
20. CD8+ T cells in the SN*pc* express IFNγ but neither TNFα nor PD-1. Nevertheless, they express several granzymes such as granzyme A, B and K.
21. Infiltrating CD8+ T cells with granzyme B+ granules can only be found in early stages of the disease (iLBD cases). CD8+ T cells containing granzyme A are increased as total number in iLBD cases. Both conclusions reinforce the idea of a more cytotoxic acute adaptive immune response in early stages of the disease.
22. There is the presence of αβ and γδ T cells in post-mortem human SN*pc*.
23. CD1 genes, as indicators of glycolipidic antigen presentation, and HLA-C are not expressed in dopaminergic neurons. Conversely, HLA-E along with HLA-A and -B, both previously described, are expressed in dopaminergic neurons.
24. Lewy neurites are the earliest phospho-serine129-α-synuclein+ aggregates to form and precede formation of diffuse aggregates and Lewy bodies in iLBD cases.

REFERENCES

7. References

Abbott NJ, Pizzo ME, Preston JE, Janigro D, Thorne RG. The role of brain barriers in fluid movement in the CNS: is there a 'glymphatic' system? Acta Neuropathol 2018; 135: 387–407.

Abellanas MA, Zamarbide M, Basurco L, Luquin E, Garcia-Granero M, Clavero P, et al. Midbrain microglia mediate a specific immunosuppressive response under inflammatory conditions. J Neuroinflammation 2019; 16: 1–15.

Adler CH, Beach TG, Zhang N, Shill HA, Driver-Dunckley E, Caviness JN, et al. Unified staging system for Lewy body disorders: Clinicopathologic correlations and comparison to Braak staging. J Neuropathol Exp Neurol 2019; 78: 891–9.

Ajami B, Bennett JL, Krieger C, McNagny KM, Rossi FM V. Infiltrating monocytes trigger EAE progression, but do not contribute to the resident microglia pool. Nat Neurosci 2011; 14: 1142–50.

Akiyama H, McGeer PL. Brain microglia constitutively express β-2 integrins. J Neuroimmunol 1990; 30: 81–93.

Albert K, Voutilainen M, Domanskyi A, Airavaara M. AAV Vector-Mediated Gene Delivery to Substantia Nigra Dopamine Neurons: Implications for Gene Therapy and Disease Models. Genes (Basel) 2017; 8: 63.

Alberts B, Johnson A, Lewis J, Raff M, Roberts K, Walter P. Moleculer Biology of the Cell. 4th editio. New York: Garland Science; Taylor and Francis; 2002

Alcolado R, Weller RO, Parrish EP, Garrod D. The Cranial Arachnoid and Pia Mater in Man: Anatomical and Ultrastructural Observations. Neuropathol Appl Neurobiol 1988; 14: 1–17.

Alliot F, Lecain E, Grima B, Pessac B. Microglial progenitors with a high proliferative potential in the embryonic and adult mouse brain. Proc Natl Acad Sci U S A 1991; 88: 1541–5.

Álvarez-Luquín DD, Arce-Sillas A, Leyva-Hernández J, Sevilla-Reyes E, Boll MC, Montes-Moratilla E, et al. Regulatory impairment in untreated Parkinson's disease is not restricted to Tregs: Other regulatory populations are also involved. J Neuroinflammation 2019; 16: 1–11.

Amancha PK, Ackerley CG, Duphare C, Lee M, Hu YJ, Amara RR, et al. Distribution of Functional CD4 and CD8 T cell Subsets in Blood and Rectal Mucosal Tissues. Sci Rep 2020; 10: 1–9.

Ambrosi G, Kustrimovic N, Siani F, Rasini E, Cerri S, Ghezzi C, et al. Complex Changes in the Innate and Adaptive Immunity Accompany Progressive Degeneration of the Nigrostriatal Pathway Induced by Intrastriatal Injection of 6-Hydroxydopamine in the Rat. Neurotox Res 2017; 32: 71–81.

Andres KH, von Düring M, Muszynski K, Schmidt RF. Nerve fibres and their terminals of the dura mater encephali of the rat. Anat Embryol (Berl) 1987; 175: 289–301.

Anfossi N, André P, Guia S, Falk CS, Roetynck S, Stewart CA, et al. Human NK Cell Education by Inhibitory Receptors for MHC Class I. Immunity 2006; 25: 331–42.

Angelova PR, Choi ML, Berezhnov A V., Horrocks MH, Hughes CD, De S, et al. Alpha synuclein aggregation drives ferroptosis: an interplay of iron, calcium and lipid peroxidation. Cell Death Differ 2020; 27: 2781–96.

Ansari AM, Ahmed AK, Matsangos AE, Lay F, Born LJ, Marti G, et al. Cellular GFP Toxicity and Immunogenicity: Potential Confounders in in Vivo Cell Tracking Experiments. Stem Cell Rev Reports 2016; 12: 553–9.

Anthony DA, Andrews DM, Chow M, Watt S V., House C, Akira S, et al. A Role for Granzyme M in TLR4-Driven Inflammation and Endotoxicosis. J Immunol 2010; 185: 1794–803.

Anttila JE, Whitaker KW, Wires ES, Harvey BK, Airavaara M. Role of microglia in ischemic focal stroke and recovery: focus on Toll-like receptors. Prog Neuro-Psychopharmacology Biol Psychiatry 2017; 79: 3–14.

Antzoulatos E, Jakowec MW, Petzinger GM, Wood RI. Sex differences in motor behavior in the MPTP mouse model of Parkinson's disease. Pharmacol Biochem Behav 2010; 95: 466–72.

Arlehamn CSL, Pham J, Alcalay RN, Frazier A, Shorr E, Carpenter C, et al. Widespread tau-specific CD4 T cell reactivity in the general population. J Immunol 2019; 203: 84–92.

Asanuma M, Miyazaki I. Nonsteroidal Anti-Inflammatory Drugs in Experimental Parkinsonian Models and Parkinsons Disease. Curr Pharm Des 2008; 14: 1428–34.

Ascherio A, Schwarzschild MA. The epidemiology of Parkinson's disease: risk factors and prevention. Lancet Neurol 2016; 15: 1257–72.

Ascherio A, Tanner CM. Use of antihypertensives and the risk of parkinson disease. Neurology 2009; 72: 578–9.

Ascherio A, Zhang SM, Hernán MA, Kawachi I, Colditz GA, Speizer FE, et al. Prospective study of caffeine consumption and risk of Parkinson's disease in men and women. Ann Neurol 2001; 50: 56–63.

Aspelund A, Antila S, Proulx ST, Karlsen TV, Karaman S, Detmar M, et al. A dural lymphatic vascular system that drains brain interstitial fluid and macromolecules. J Exp Med 2015; 212: 991–9.

Athauda D, Foltynie T. The ongoing pursuit of neuroprotective therapies in Parkinson disease. Nat Rev Neurol 2014; 11: 25–40.

Baba Y, Kuroiwa A, Uitti RJ, Wszolek ZK, Yamada T. Alterations of T-lymphocyte populations in Parkinson disease. Park Relat Disord 2005; 11: 493–8.

Bakshi R, Zhang H, Logan R, Joshi I, Xu Y, Chen X, et al. Neuroprotective effects of urate are mediated by augmenting astrocytic glutathione synthesis and release. Neurobiol Dis 2015; 82: 574–9.

Balato A, Unutmaz D, Gaspari AA. Natural killer T cells: An unconventional T-cell subset with diverse effector and regulatory functions. J Invest Dermatol 2009; 129: 1628–42.

Ballabh P, Braun A, Nedergaard M. The blood-brain barrier: An overview: Structure, regulation, and clinical implications. Neurobiol Dis 2004; 16: 1–13.

Banchereau J, Briere F, Caux C, Davoust J, Lebecque S, Liu YJ, et al. Immunobiology of dendritic cells. Annu Rev Immunol 2000; 18: 767–811.

Bander Z Al, Nitert MD, Mousa A, Naderpoor N. The gut microbiota and inflammation: An overview. Int J Environ Res Public Health 2020; 17: 1–22.

Barcia C, Ros CM, Annese V, Gómez A, Ros-Bernal F, Aguado-Yera D, et al. IFN-γ signaling, with the synergistic contribution of TNF-α, mediates cell specific microglial and astroglial activation in experimental models of Parkinson's disease. Cell Death Dis 2011; 2: e142.

Barcia C, Ros CM, Ros-Bernal F, Gómez A, Annese V, Carrillo-de Sauvage MA, et al. Persistent phagocytic characteristics of microglia in the substantia nigra of long-term parkinsonian macaques. J Neuroimmunol 2013; 261: 60–6.

Barcia C, Sánchez Bahillo A, Fernández-Villalba E, Bautista V, Poza Y Poza M, Fernández-Barreiro A, et al. Evidence of active microglia in substantia nigra pars compacta of parkinsonian monkeys 1 year after MPTP exposure. Glia 2004; 46: 402–9.

Barker CF, Billingham RE. Immunologically privileged sites. Adv Immunol 1977; 25: 1–54.

Barron AB, Søvik E, Cornish JL. The roles of dopamine and related compounds in reward-seeking behavior across animal phyla. Front Behav Neurosci 2010; 4: 1–9.

Bartholomäus I, Kawakami N, Odoardi F, Schläger C, Miljkovic D, Ellwart JW, et al. Effector T cell interactions with meningeal vascular structures in nascent autoimmune CNS lesions. Nature 2009; 462: 94–8.

Bas J, Calopa M, Mestre M, Molleví DG, Cutillas B, Ambrosio S, et al. Lymphocyte populations in Parkinson's disease and in rat models of parkinsonism. J Neuroimmunol 2001; 113: 146–52.

Batchelor PE, Liberatore GT, Wong JYF, Porritt MJ, Frerichs F, Donnan GA, et al. Activated macrophages and microglia induce dopaminergic sprouting in the injured striatum and express brain-derived neurotrophic factor and glial cell line-derived neurotrophic factor. J Neurosci 1999; 19: 1708–16.

Beach TG, Adler CH, Dugger BN, Hidalgo J, Henry-watson J, Shill H a, et al. Submandibular Gland Biopsy for the Diagnosis of Parkinson Disease. 2013; 72: 130–6.

Beach TG, Adler CH, Lue L, Sue LI, Bachalakuri J, Sasse J, et al. Unified Staging System for Lewy Body Disorders: Correlation with Nigrostriatal Degeneration, Cognitive Impairment and Motor Dysfunction. Acta Neuropathol 2009; 117: 613–34.

Beach TG, White III CL, Hladik CL, Sabbagh MN, Connor DJ, Shill HA, et al. Olfactory bulb α-synucleinopathy has high specificity and sensitivity for Lewy body disorders. Acta Neuropathol

2009; 117: 167–74.

Beatman EL, Massey A, Shives KD, Burrack KS, Chamanian M, Morrison TE, et al. Alpha-synuclein expression restricts RNA viral infections in the brain. J Virol 2015; 90: 2767–82.

Becker C, Jick SS, Meier CR. NSAID use and risk of Parkinson disease: A population-based case-control study. Eur J Neurol 2011; 18: 1336–42.

Benner EJ, Banerjee R, Reynolds AD, Sherman S, Pisarev VM, Tsiperson V, et al. Nitrated a-synuclein immunity accelerates degeneration of nigral dopaminergic neurons. PLoS One 2008; 3

Benner EJ, Mosley RL, Destache CJ, Lewis TB, Jackson-lewis V, Gorantla S, et al. Therapeutic immunization protects dopaminergic neurons in a mouse model of Parkinson ' s disease. 2004; 101

Benveniste H, Liu X, Koundal S, Sanggaard S, Lee H, Wardlaw J. The glymphatic system and waste clearance with brain aging. Gerontology 2019; 65: 106–19.

Bezard E, Przedborski S. A tale on animal models of Parkinson's Disease. Mov Disord 2011; 26: 993–1002.

Billingsley KJ, Bandres-Ciga S, Saez-Atienzar S, Singleton AB. Genetic risk factors in Parkinson's disease. Cell Tissue Res 2018; 373: 9–20.

Björklund A, Dunnett SB. Fifty years of dopamine research. Trends Neurosci 2007; 30: 185–7.

Bjorkman PJ. MHC restriction in three dimensions: A view of T cell receptor/ligand interactions. Cell 1997; 89: 167–70.

Blandini F, Armentero MT. Animal models of Parkinson's disease. FEBS J 2012; 279: 1156–66.

Blauwendraat C, Heilbron K, Vallerga CL, Bandres-Ciga S, von Coelln R, Pihlstrøm L, et al. Parkinson disease age at onset GWAS: defining heritability, genetic loci and α-synuclein mechanisms. Mov Disord 2019; 34: 866–75.

Blauwendraat C, Nalls MA, Singleton AB. The genetic architecture of Parkinson's disease. Lancet Neurol 2020; 19: 170–8.

Blum-Degen D, Müller T, Kuhn W, Gerlach M, Przuntek H, Riederer P. Interleukin-1beta and interleukin-6 are elevated in the cerebrospinal fluid of Alzheimer's and de novo Parkinson's disease patients. Neurosci Lett 1995; 202: 17–20.

Boche D, Perry VH, Nicoll JAR. Review: Activation patterns of microglia and their identification in the human brain. Neuropathol Appl Neurobiol 2013; 39: 3–18.

Boehm T. Design principles of adaptive immune systems. Nat Rev Immunol 2011; 11: 307–17.

Bonci A, Grillner P, Mercuri NB, Bernardi G. L-type calcium channels mediate a slow excitatory synaptic transmission in rat midbrain dopaminergic neurons. J Neurosci 1998; 18: 6693–703.

Bonilla FA, Oettgen HC. Adaptive immunity. J Allergy Clin Immunol 2010; 125: S33–40.

Borghammer P, Van Den Berge N. Brain-First versus Gut-First Parkinson's Disease: A Hypothesis. J Parkinsons Dis 2019; 9: S281–95.

Botta-Orfila T, Sànchez-Pla A, Fernández M, Carmona F, Ezquerra M, Tolosa E. Brain transcriptomic profiling in idiopathic and LRRK2-associated Parkinson's disease. Brain Res 2012; 1466: 152–7.

Bourdenx M, Dovero S, Engeln M, Bido S, Bastide MF, Dutheil N, et al. Lack of additive role of ageing in nigrostriatal neurodegeneration triggered by α-synuclein overexpression. Acta Neuropathol Commun 2015; 3: 46.

Bousso P, Robey E. Dynamics of CD8 + T cell priming by dendritic cells in intact lymph nodes. 2003; 4: 579–85.

Bové J, Perier C. Neurotoxin-based models of Parkinson's disease. Neuroscience 2012; 211: 51–76.

Bové J, Prou D, Perier C, Przedborski S. Toxin-induced models of Parkinson's disease. NeuroRx 2005; 2: 484–94.

Boyd JD, Jang H, Shepherd KR, Faherty C, Slack S, Jiao Y, et al. Response to 1-methyl-4-phenyl-1,2,3,6-tetrahydropyridine (MPTP) differs in mouse strains and reveals a divergence in JNK signaling and COX-2 induction prior to loss of neurons in the substantia nigra pars compacta. Brain Res 2007; 1175: 107–16.

Braak H, Del K, Rüb U, Vos RAI De, Jansen ENH, Braak E. Staging of brain pathology related to sporadic Parkinson's disease. Neurobiol Aging 2003; 24: 197–211.

Braak H, Rüb U, Gai WP, Del Tredici K. Idiopathic Parkinson's disease: Possible routes by which vulnerable neuronal types may be subject to neuroinvasion by an unknown pathogen. J Neural Transm 2003; 110: 517–36.

Braak H, Del Tredici K. Neuropathological Staging of Brain Pathology in Sporadic Parkinson's disease: Separating the Wheat from the Chaff. J Parkinsons Dis 2017; 7: S73–87.

Bradaric BD, Patel A, Schenider JA, Carvey PM, Hendey B. Evidence for Angiogenesis in Parkinson's disease, Incidental Lewy Body disease, and Progressive Supranuclear Palsy. J Neural Transm 2012; 119: 59–71.

Brigl M, Brenner MB. CD1: Antigen presentation and T cell function. Annu Rev Immunol 2004; 22: 817–90.

Brinkmann V, Reichard U, Goosmann C, Fauler B, Uhlemann Y, Weiss DS, et al. Neutrophil Extracellular Traps Kill Bacteria. Science (80-) 2004; 303: 1532–5.

Brochard V, Combadière B, Prigent A, Laouar Y, Perrin A, Beray-berthat V, et al. Infiltration of CD4+ lymphocytes into the brain contributes to neurodegeneration in a mouse model of Parkinson disease. J Clin Invest 2009; 119: 182–92.

Brodacki B, Staszewski J, Toczyłowska B, Kozłowska E, Drela N, Chalimoniuk M, et al. Serum interleukin (IL-2, IL-10, IL-6, IL-4), TNFα, and INFγ concentrations are elevated in patients with atypical and idiopathic parkinsonism. Neurosci Lett 2008; 441: 158–62.

Bucchieri F, Farina F, Zummo G, Cappello F. Lymphatic vessels of the dura mater: A new discovery? J Anat 2015; 227: 702–3.

Buchwalow I, Samoilova V, Boecker W, Tiemann M. Non-specific binding of antibodies in immunohistochemistry: fallacies and facts. Sci Rep 2011; 1: 1–6.

Burke RE, Dauer WT, Vonsattel JPG. Critical evaluation of the braak staging scheme for Parkinson's disease. Ann Neurol 2008; 64: 485–91.

Butkovich LM, Houser MC, Tansey MG. α-synuclein and noradrenergic modulation of immune cells in Parkinson's disease pathogenesis. Front Neurosci 2018; 12: 1–13.

Butovsky O, Weiner HL. Microglial signatures and their role in health and disease. Nat Rev Neurosci 2018; 19: 622–35.

Cabarrocas J, Bauer J, Piaggio E, Liblau R, Lassmann H. Effective and selective immune surveillance of the brain by MHC class I-restricted cytotoxic T lymphocytes. Eur J Immunol 2003; 33: 1174–82.

Caggiu E, Arru G, Hosseini S, Niegowska M, Sechi G Pietro, Zarbo IR, et al. Inflammation, infectious triggers, and Parkinson's disease. Front Neurol 2019; 10: 122.

Caggiu E, Paulus K, Arru G, Piredda R, Sechi G Pietro, Sechi LA. Humoral cross reactivity between α-synuclein and herpes simplex-1 epitope in Parkinson's disease, a triggering role in the disease? J Neuroimmunol 2016; 291: 110–4.

Callaghan RC, Cunningham JK, Sajeev G, Kish SJ. Incidence of Parkinson's disease among hospital patients with methamphetamine-use disorders. Mov Disord 2010; 25: 2333–9.

Calvello R, Cianciulli A, Nicolardi G, De Nuccio F, Giannotti L, Salvatore R, et al. Vitamin D Treatment Attenuates Neuroinflammation and Dopaminergic Neurodegeneration in an Animal Model of Parkinson's Disease, Shifting M1 to M2 Microglia Responses. J Neuroimmune Pharmacol 2017; 12: 327–39.

Cao S, Theodore S, Standaert DG. Fcγ receptors are required for NF-κB signaling, microglial activation and dopaminergic neurodegeneration in an AAV-synuclein mouse model of Parkinson's disease. Mol Neurodegener 2010; 5: 42.

Carballo-Carbajal I, Laguna A, Romero-Giménez J, Cuadros T, Bové J, Martinez-Vicente M, et al. Brain tyrosinase overexpression implicates age-dependent neuromelanin production in Parkinson's disease pathogenesis. Nat Commun 2019; 10: 973.

Cardenas H, Bolin LM. Compromised reactive microgliosis in MPTP-lesioned IL-6 KO mice. Brain Res 2003; 985: 89–97.

Carlsson A, Lindqvist M, Magnusson T. 3,4-dihydroxyphenylalanine and 5- hydroxytryptophan as

reserpine antagonists. Nature 1957; 180: 1200.

Carlsson A, Lindqvist M, Magnusson T, Waldeck B. On the presence of 3-hydroxytyramine in brain. Science (80-) 1958; 127: 471.

Carson MJ, Doose JM, Melchior B, Schmid CD, Ploix CC. CNS immune privilege: Hiding in plain sight. Immunol Rev 2006; 213: 48–65.

Cartelli D, Aliverti A, Barbiroli A, Santambrogio C, Ragg EM, Casagrande FVM, et al. α-Synuclein is a Novel Microtubule Dynamase. Sci Rep 2016; 6: 1–13.

Castello PR, Drechsel DA, Patel M. Mitochondria Are a Major Source of Paraquat-induced Reactive Oxygen Species Production in the Brain. J Biol Chem 2007; 282: 14186–93.

Caudal D, Alvarsson A, Björklund A, Svenningsson P. Depressive-like phenotype induced by AAV-mediated overexpression of human alpha-synuclein in midbrain dopaminergic neurons. Exp Neurol 2015; 273: 243–52.

Cebrián C, Loike JD, Sulzer D. Neuronal MHC-I expression and its implications in synaptic function, axonal regeneration and Parkinson's and other brain diseases. Front Neuroanat 2014; 8: 114.

Cebrián C, Zucca F a, Mauri P, Steinbeck J a, Studer L, Scherzer CR, et al. MHC-I expression renders catecholaminergic neurons susceptible to T-cell-mediated degeneration. Nat Commun 2014; 5: 3633.

Chandra G, Rangasamy SB, Roy A, Kordower JH, Pahan K. Neutralization of RANTES and eotaxin prevents the loss of dopaminergic neurons in a mouse model of Parkinson disease. J Biol Chem 2016; 291: 15267–81.

Chandra G, Roy A, Rangasamy SB, Pahan K. Induction of Adaptive Immunity Leads to Nigrostriatal Disease Progression in MPTP Mouse Model of Parkinson's Disease. J Immunol 2017; 198: 4312–26.

Chang D, Nalls MA, Hallgrímsdóttir IB, Hunkapiller J, van der Brug M, Cai F, et al. A meta-analysis of genome-wide association studies identifies 17 new Parkinson's disease risk loci Diana. Nat Genet 2017; 49: 1511–6.

Chaplin DD. Overview of the immune response. J Allergy Clin Immunol 2010; 125: S3-23.

Chatila TA, Angeles L. Role of regulatory T cells in human diseases. 2005

Chen H, Huang X, Guo X, Mailman RB, Park Y, Kamel F, et al. Smoking duration, intensity, and risk of Parkinson disease. Neurology 2010; 74: 878–84.

Chen H, Jacobs E, Schwarzschild MA, McCullough ML, Calle EE, Thun MJ, et al. Nonsteroidal antiinflammatory drug use and the risk for Parkinson's disease. Ann Neurol 2005; 58: 963–7.

Chen H, Ritz B. The search for environmental causes of Parkinson's disease: Moving forward. J Parkinsons Dis 2018; 8: S9–17.

Chen H, Zhang SM, Hernán MA, Schwarzschild MA, Willett WC, Colditz GA, et al. Nonsteroidal anti-inflammatory drugs and the risk of Parkinson disease. Neuroepidemiology 2007; 28: 193–6.

Chen L, Mo M, Li G, Cen L, Wei L, Xiao Y, et al. The biomarkers of immune dysregulation and inflammation response in Parkinson disease. Transl Neurodegener 2016; 5: 16.

Chen X, Burdett TC, Desjardins CA, Logan R, Cipriani S, Xu Y, et al. Disrupted and transgenic urate oxidase alter urate and dopaminergic neurodegeneration. Proc Natl Acad Sci U S A 2013; 110: 300–5.

Chen Y, Qi B, Xu W, Ma B, Li L, Chen Q, et al. Clinical correlation of peripheral CD4+-cell sub-sets, their imbalance and Parkinson's disease. Mol Med Rep 2015; 12: 6105–11.

Cheng H-C, Ulane CM, Burke RE. Clinical Progression in Parkinson's Disease and the Neurobiology of Axons. Ann Neurol 2010; 67: 715–25.

Cherry JD, Olschowka JA, O'Banion MK. Are 'resting' microglia more 'M2'? Front Immunol 2014; 5: 1–5.

Chhor V, Le Charpentier T, Lebon S, Oré MV, Celador IL, Josserand J, et al. Characterization of phenotype markers and neuronotoxic potential of polarised primary microglia In vitro. Brain Behav Immun 2013; 32: 70–85.

Chien YH, Meyer C, Bonneville M. γδ T cells: First line of defense and beyond. Annu Rev Immunol 2014; 32: 121–55.

Choi HK, Atkinson K, Karlson EW, Willett W, Curhan G. Purine-Rich Foods, Daily and Protein Intake, and the Risk of Gout in Men. N Engl J Med 2004; 350: 1093–103.

Choi JG, Kim N, Ju IG, Eo H, Lim S, Jang S. Oral administration of Proteus mirabilis damages dopaminergic neurons and motor functions in mice. Sci Rep 2018: 1–13.

Choudhury ME, Sugimoto K, Kubo M, Nagai M, Nomoto M, Takahashi H, et al. A cytokine mixture of GM-CSF and IL-3 that induces a neuroprotective phenotype of microglia leading to amelioration of (6-OHDA)-induced Parkinsonism of rats. Brain Behav 2011; 1: 26–43.

Chovatiya R, Medzhitov R. Stress, inflammation, and defense of homeostasis. Mol Cell 2014; 54: 281–8.

Chung CY, Koprich JB, Siddiqi H, Isacson O. Dynamic Changes in Presynaptic and Axonal Transport Proteins Combined with Striatal Neuroinflammation Precede Dopaminergic Neuronal Loss in a Rat Model of AAV -Synucleinopathy. J Neurosci 2009; 29: 3365–73.

Church WH, Ward VL. Uric acid is reduced in the substantia nigra in parkinson's disease: Effect on dopamine oxidation. Brain Res Bull 1994; 33: 419–25.

Ciaramella A, Salani F, Bizzoni F, Pontieri FE, Stefani A, Pierantozzi M, et al. Blood Dendritic Cell Frequency Declines in Idiopathic Parkinson's Disease and Is Associated with Motor Symptom Severity. PLoS One 2013; 8

Cohen AD, Tillerson JL, Smith AD, Schallert T, Zigmond MJ. Neuroprotective effects of prior limb use in 6-hydroxydopamine-treated rats: Possible role of GDNF. J Neurochem 2003; 85: 299–305.

Conde JR, Streit WJ. Microglia in the aging brain. J Neuropathol Exp Neurol 2006; 65: 199–203.

Constantinescu R, Elm J, Auinger P, Sharma S, Augustine EF, Khadim L, et al. Malignant melanoma in early-treated Parkinson's disease: The NET-PD trial. Mov Disord 2014; 29: 263–5.

Constantinescu R, Romer M, Kieburtz K. Malignant melanoma in early Parkinson's disease: The DATATOP trial. Mov Disord 2007; 22: 720–2.

Conway JE, Zolotukhin S, Muzyczka N, Hayward GS, Byrne BJ. Recombinant adeno-associated virus type 2 replication and packaging is entirely supported by a herpes simplex virus type 1 amplicon expressing Rep and Cap. J Virol 1997; 71: 8780–9.

Cooper AA, Gitler AD, Cashikar A, Haynes CM, Kathryn J, Bhullar B, et al. α-synuclein blocks ER-Golgi traffic and Rab1 rescues neuron loss in Parkinson's models. Science (80-) 2006; 313: 324–8.

Cooper MD, Alder MN. The evolution of adaptive immune systems. Cell 2006; 124: 815–22.

Corti O, Lesage S, Brice A. What genetics tells us about the causes and mechanisms of Parkinson's disease. Physiol Rev 2011; 91: 1161–218.

Cotzias GC, Van Woert MH, Schiffer LM. Aromatic amino acids and modification of parkinsonism. N Engl J Med 1967; 276: 374–9.

Croisier E, Moran LB, Dexter DT, Pearce RKB, Graeber MB. Microglial inflammation in the parkinsonian substantia nigra: Relationship to alpha-synuclein deposition. J Neuroinflammation 2005; 2: 1–8.

Crome SQ, Wang AY, Levings MK. Translational Mini-Review Series on Th 17 Cells : Function and regulation of human T helper 17 cells in health and disease. Clin Exp Immunol 2009; 159: 109–19.

Crosby CM, Kronenberg M. Tissue-specific functions of invariant natural killer T cells. Nat Rev Immunol 2018; 18: 559–74.

Cserr HF, Harling-Berg CJ, Knopf PM. Drainage of Brain Extracellular Fluid into Blood and Deep Cervical Lymph and its Immunological Significance. Brain Pathol 1992; 2: 269–76.

Cserr HF, Knopf PM. Cervical lymphatics, the blood-brain barrier and the immunoreactivity of the brain: a new view. Immunol Today 1992; 13: 507–12.

Czlonkowska A, Kohutnicka M, Kurkowska-Jastrzebska I, Czlonkowski A. Microglial Reaction in MPTP (1-methyl-4-phenyl- Disease Mice Model. Neurodegeneration 1996; 5: 137–43.

Daher JPL, Abdelmotilib HA, Hu X, Volpicelli-Daley LA, Moehle MS, Fraser KB, et al. Leucine-rich repeat kinase 2 (LRRK2) pharmacological inhibition abates α-synuclein gene-induced neurodegeneration. J Biol Chem 2015; 290: 19433–44.

Daher JPL, Volpicelli-Daley LA, Blackburn JP, Moehle MS, West AB. Abrogation of alpha-synuclein-mediated dopaminergic neurodegeneration in LRRK2-deficient rats. Proc Natl Acad Sci 2014; 111: 9289–94.

Daniel G, Musso A, Tsika E, Fiser A, Glauser L, Pletnikova O, et al. Alpha-Synuclein-induced dopaminergic neurodegeneration in a rat model of Parkinson's disease occurs independent of ATP13A2 (PARK9). Neurobiol Dis 2015; 73: 229–43.

Dauer W, Przedborski S. Parkinson's disease: mechanisms and models. Neuron 2003; 39: 889–909.

Davey GP, Tipton KF, Murphy MP. Uptake and accumulation of 1-methyl-4-phenylpyridinium by rat liver mitochondria measured using an ion-selective electrode. Biochem J 1992; 288: 439–43.

Davies SE, Hallett PJ, Moens T, Smith G, Mangano E, Kim HT, et al. Enhanced ubiquitin-dependent degradation by Nedd4 protects against α-synuclein accumulation and toxicity in animal models of Parkinson's disease. Neurobiol Dis 2014; 64: 79–87.

Davis JW, Grandinetti A, Waslien CI, Ross GW, White LR, Morens DM. Observations on serum uric acid levels and the risk of idiopathic Parkinson's disease. Am J Epidemiol 1996; 144: 480–4.

Dawson TM, Ko HS, Dawson VL. Genetic Animal Models of Parkinson's Disease. Neuron 2010; 66: 646–61.

Decressac M, Kadkhodaei B, Mattsson B, Laguna A, Perlmann T, Bjorklund A. Alpha-Synuclein-Induced Down-Regulation of Nurr1 Disrupts GDNF Signaling in Nigral Dopamine Neurons. Sci Transl Med 2012; 4: 163ra156-163ra156.

Decressac M, Mattsson B, Björklund A. Comparison of the behavioural and histological characteristics of the 6-OHDA and α-synuclein rat models of Parkinson's disease. Exp Neurol 2012; 235: 306–15.

Decressac M, Mattsson B, Weikop P, Lundblad M, Jakobsson J, Bjorklund A. TFEB-mediated autophagy rescues midbrain dopamine neurons from -synuclein toxicity. Proc Natl Acad Sci 2013; 110: E1817–26.

Decressac M, Ulusoy A, Mattsson B, Georgievska B, Romero-Ramos M, Kirik D, et al. GDNF fails to exert neuroprotection in a rat α-synuclein model of Parkinson's disease. Brain 2011; 134: 2302–11.

Degl'Innocenti F, Maurello MT, Marini P. A parkinsonian kindred. Ital J Neurol Sci 1989; 10: 307–10.

DelleDonne A, Klos KJ, Fujishiro H, Ahmed Z, Parisi JE, Josephs KA, et al. Parkinson disease and incidental Lewy body disease. Arch Neurol 2008; 65: 1074–80.

Denson MA, Wszolek ZK, Pfeiffer RF, Wszolek EK, Paschall TM, McComb RD. Familial Parkinsonism, Dementia, and Lewy body disease: Study of family G. Ann Neurol 1997; 42: 638–43.

Depboylu C, Stricker S, Ghobril JP, Oertel WH, Priller J, Höglinger GU. Brain-resident microglia predominate over infiltrating myeloid cells in activation, phagocytosis and interaction with T-lymphocytes in the MPTP mouse model of Parkinson disease. Exp Neurol 2012; 238: 183–91.

Devine MJ, Gwinn K, Singleton A, Hardy J. Parkinson's Disease and α-synuclein Expression. Mov Disord 2011; 26: 2160–8.

Dhanwani R, Pham J, Premlal ALR, Frazier A, Kumar A, Pero ME, et al. T Cell Responses to Neural Autoantigens Are Similar in Alzheimer's Disease Patients and Age-Matched Healthy Controls. Front Neurosci 2020; 14: 1–13.

Dick FD, De Palma G, Ahmadi A, Scott NW, Prescott GJ, Bennett J, et al. Environmental risk factors for Parkinson's disease and parkinsonism: The Geoparkinson study. Occup Environ Med 2007; 64: 666–72.

Dickson DW, Fujishiro H, DelleDonne A, Menke J, Ahmed Z, Klos KJ, et al. Evidence that incidental Lewy body disease is pre-symptomatic Parkinson's disease. Acta Neuropathol 2008; 115: 437–44.

Dijkstra AA, Voorn P, Berendse HW, Groenewegen HJ, Rozemuller AJM, van de Berg WDJ. Stage-dependent nigral neuronal loss in incidental Lewy body and parkinson's disease. Mov Disord 2014; 29: 1244–51.

Dinis-Oliveira RJ, Remião F, Carmo H, Duarte JA, Navarro AS, Bastos ML, et al. Paraquat exposure as an etiological factor of Parkinson's disease. Neurotoxicology 2006; 27: 1110–22.

DiPatre PL, Gelman BB. Microglial Cell Activation in Aging and Alzheimer Disease: Partial Linkage with Neurofibrillary Tangle Burden in the Hippocampus. J Neuropathol Exp Neurol 1997; 56: 143–9.

Doppler K, Jentschke HM, Schulmeyer L, Vadasz D, Janzen A, Luster M, et al. Dermal phospho-alpha-synuclein deposits confirm REM sleep behaviour disorder as prodromal Parkinson's disease. Acta Neuropathol 2017; 133: 535–45.

Dorn HF. Tobacco consumption and mortality from cancer and other diseases. Pub 1959; 74: 581–94.

Dun VM, Thao DTP. Repeat Expansion Disease Models. Drosoph Model Hum Dis 2018: 41–61.

Dustin ML, Long EO. Cytotoxic immunological synapses. Immunol Rev 2010; 235: 24–34.

Dutta D, Kundu M, Mondal S, Roy A, Ruehl S, Hall DA, et al. RANTES-induced invasion of Th17 cells into substantia nigra potentiates dopaminergic cell loss in MPTP mouse model of Parkinson's disease. Neurobiol Dis 2019; 132: 104575.

Dzamko N, Gysbers A, Perera G, Bahar A, Shankar A, Gao J, et al. Toll-like receptor 2 is increased in neurons in Parkinson's disease brain and may contribute to alpha-synuclein pathology. Acta Neuropathol 2017; 133: 303–19.

Ehringer H, Hornykiewicz O. Verteilung Von Noradrenalin Und Dopamin (3-Hydroxytyramin) Im

Gehirn Des Menschen Und Ihr Verhalten Bei Erkrankungen Des Extrapyramidalen Systems. Klin Wochenschr 1960; 38: 1236–9.

Eidson LN, Kannarkat GT, Barnum CJ, Chang J, Chung J, Caspell-Garcia C, et al. Candidate inflammatory biomarkers display unique relationships with alpha-synuclein and correlate with measures of disease severity in subjects with Parkinson's disease. J Neuroinflammation 2017; 14: 1–16.

Elgueta D, Aymerich MS, Contreras F, Montoya A, Celorrio M, Rojo-Bustamante E, et al. Pharmacologic antagonism of dopamine receptor D3 attenuates neurodegeneration and motor impairment in a mouse model of Parkinson's disease. Neuropharmacology 2017; 113: 110–23.

Elgueta D, Contreras F, Prado C, Montoya A, Ugalde V, Chovar O, et al. Dopamine receptor D3 expression is altered in CD4+ T-cells from Parkinson's disease patients and its pharmacologic inhibition attenuates the motor impairment in a mouse model. Front Immunol 2019; 10: 1–17.

Engelhardt B, Carare RO, Bechmann I, Flügel A, Laman JD, Weller RO. Vascular, glial, and lymphatic immune gateways of the central nervous system. Acta Neuropathol 2016; 132: 317–38.

Engelhardt B, Vajkoczy P, Weller RO. The movers and shapers in immune privilege of the CNS. Nat Immunol 2017; 18: 123–31.

Fahn S, Elton R, Members of the UPDRS Development Committee *. Unified Parkinson's Disease Rating Scale. Florham Park, NJ: Macmillan Health Care Information; 1987

Falkenburger BH, Saridaki T, Dinter E. Cellular models for Parkinson's disease. J Neurochem 2016: 121–30.

Fall PA, Fredrikson M, Axelson O, Granérus AK. Nutritional and occupational factors influencing the risk of Parkinson's disease: A case-control study in southeastern Sweden. Mov Disord 1999; 14: 28–37.

Fazzini E, Fleming J, Fahn S. Cerebrospinal fluid antibodies to coronavirus in patients with Parkinson's disease. Mov Disord 1992; 7: 153–8.

Fearnley JM, Lees AJ. Ageing and parkinson's disease: Substantia nigra regional selectivity. Brain 1991; 114: 2283–301.

Febbraro F, Andersen KJ, Sanchez-Guajardo V, Tentillier N, Romero-Ramos M. Chronic intranasal deferoxamine ameliorates motor defects and pathology in the α-synuclein rAAV Parkinson's model. Exp Neurol 2013; 247: 45–58.

Fenn AM, Hall JCE, Gensel JC, Popovich PG, Godbout JP. IL-4 signaling drives a unique arginase+/IL-1β+ microglia phenotype and recruits macrophages to the inflammatory CNS: Consequences of age-related deficits in IL-4Rα after traumatic spinal cord injury. J Neurosci 2014; 34: 8904–17.

Fenn AM, Henry CJ, Huang Y, Dugan A, Godbout JP. Lipopolysaccharide-induced interleukin (IL)-4 receptor-α expression and corresponding sensitivity to the M2 promoting effects of IL-4 are

impaired in microglia of aged mice. Brain Behav Immun 2012; 26: 766–77.

Fernagut PO, Chesselet MF. Alpha-synuclein and transgenic mouse models. Neurobiol Dis 2004; 17: 123–30.

Ferreira SA, Romero-Ramos M. Microglia response during Parkinson's disease: Alpha-synuclein intervention. Front Cell Neurosci 2018; 12: 1–17.

Ferretti MT, Merlini M, Späni C, Gericke C, Schweizer N, Enzmann G, et al. T-cell brain infiltration and immature antigen-presenting cells in transgenic models of Alzheimer's disease-like cerebral amyloidosis. Brain Behav Immun 2016; 54: 211–25.

Figerio R, Fujishiro H, Ahn T-B, Josephs KA, Maraganore DM, DelleDonne A, et al. Incidental Lewy Body Disease: Do some cases represent a preclinical stage of Dementia with Lewy Bodies? Neuriobiol Aging 2011; 32: 857–63.

Filardy AA, Pires DR, Nunes MP, Takiya CM, Freire-de-Lima CG, Ribeiro-Gomes FL, et al. Proinflammatory Clearance of Apoptotic Neutrophils Induces an IL-12 low IL-10 high Regulatory Phenotype in Macrophages . J Immunol 2010; 185: 2044–50.

Filograna R, Beltramini M, Bubacco L, Bisaglia M. Anti-Oxidants in Parkinson's Disease Therapy: A Critical Point of View. Curr Neuropharmacol 2016; 14: 260–71.

Fiszer U, Mix E, Fredrikson S, Kostulas V, Link H. Parkinson's disease and immunological abnormalities: increase of HLA-DR expression on monocytes in cerebrospinal fluid and of CD45RO+ T cells in peripheral blood. Acta Neurol Scand 1994; 90: 160–6.

Fløtnes IH, Fernandez-Vizarra E, Lykouri M, Brakedal B, Skeie GO, Miletic H, et al. Neuronal complex I deficiency occurs throughout the Parkinson's disease brain, but is not associated with neurodegeneration or mitochondrial DNA damage. Acta Neuropathol 2018; 135: 409–25.

Follmer C. Viral Infection-Induced Gut Dysbiosis, Neuroinflammation, and α-Synuclein Aggregation: Updates and Perspectives on COVID-19 and Neurodegenerative Disorders. ACS Chem Neurosci 2020

Forrester J V., McMenamin PG, Dando SJ. CNS infection and immune privilege. Nat Rev Neurosci 2018; 19: 655–71.

Franco R, Fernández-Suárez D. Alternatively activated microglia and macrophages in the central nervous system. Prog Neurobiol 2015; 131: 65–86.

Fujimi K, Sasaki K, Noda K, Wakisaka Y, Tanizaki Y, Matsui Y, et al. Clinicopathological outline of dementia with Lewy bodies applying the revised criteria: The Hisayama study. Brain Pathol 2008; 18: 317–25.

Fumagalli S, Perego C, Ortolano F, De Simoni MG. CX3CR1 deficiency induces an early protective inflammatory environment in ischemic mice. Glia 2013; 61: 827–42.

Gadani, Sachin P; Cronk J. Interleukin-4: A Cytokine to Remember. J Immunol 2013; 189: 4213–9.

Gagliano SA, Pouget JG, Hardy J, Knight J, Barnes MR, Ryten M, et al. Genomics implicates adaptive and innate immunity in Alzheimer's and Parkinson's diseases. Ann Clin Transl Neurol 2016; 3: 924–33.

Galea I, Bernardes-Silva M, Forse PA, van Rooijen N, Liblau RS, Perry VH. An antigen-specific pathway for CD8 T cells across the blood-brain barrier. J Exp Med 2007; 204: 2023–30.

Gao X, Chen H, Schwarzschild MA, Ascherio A. Use of ibuprofen and risk of Parkinson disease. Neurology 2011; 76: 863–9.

Gao X, O'Reilly EJ, Schwarzschild MA, Ascherio A. Prospective study of plasma urate and risk of Parkinson disease in men and women. Neurology 2016; 86: 520–6.

Garretti F, Agalliu D, Arlehamn CSL, Sette A, Sulzer D. Autoimmmunity in parkinson's disease: The role of α:-synuclein-specific T cells. Front Immunol 2019; 10: 1–12.

Gasteiger G, D'osualdo A, Schubert DA, Weber A, Bruscia EM, Hartl D. Cellular Innate Immunity: An Old Game with New Players. J Innate Immun 2017; 9: 111–25.

Gate D, Saligrama N, Yang A, Middeldorp J, Levanthal O, Chen K, et al. Clonally Expanded CD8 T Cells Patrol Alzheimer'S Cerebrospinal Fluid. Nature 2020; 577: 399–404.

Gaugler MN, Genc O, Bobela W, Mohanna S, Ardah MT, El-Agnaf OM, et al. Nigrostriatal overabundance of α-synuclein leads to decreased vesicle density and deficits in dopamine release that correlate with reduced motor activity. Acta Neuropathol 2012; 123: 653–69.

Gemma C, Bachstetter AD. The role of microglia in adult hippocampal neurogenesis. Front Cell Neurosci 2013; 7: 1–5.

Gendelman HE, Zhang Y, Santamaria P, Olson KE, Schutt CR, Bhatti D, et al. Evaluation of the safety and immunomodulatory effects of sargramostim in a randomized , double-blind phase 1 clinical Parkinson ' s disease trial. npj Park Dis 2017; 2017: 1–11.

George S, Tyson T, Rey NL, Sheridan R, Peelaerts W, Becker K, et al. T cells limit accumulation of aggregate pathology following intrastriatal injection of α -synuclein fibrils. bioRxic 2020

Gibberd FB, Page NGR, Spencer KM, Kinnear E, Hawksworth JB. Controlled trial of physiotherapy and occupational therapy for Parkinson's disease. Br Med J 1981; 282: 1196.

Giguère N, Nanni SB, Trudeau LE. On cell loss and selective vulnerability of neuronal populations in Parkinson's disease. Front Neurol 2018; 9

Ginhoux F, Garel S. The mysterious origins of microglia. Nat Neurosci 2018; 21: 897–9.

Ginhoux F, Greter M, Leboeuf M, Nandi S, See P, Gokhan S, et al. Fate mapping analysis reveals that adult microglia derive from primitive macrophages. Science (80-) 2010; 330: 841–5.

Giovanni A, Sieber B-A, Heikkiila RE, Sossalla PK. Studies on species sensitivity to the dopaminergic neurotoxin. Part 1: Systemic. J Pharmacol Exp Ther 1994; 270: 1000–7.

Girard JP, Moussion C, Förster R. HEVs, lymphatics and homeostatic immune cell trafficking in lymph nodes. Nat Rev Immunol 2012; 12: 762–73.

Gitler AD, Bevis BJ, Shorter J, Strathearn KE, Hamamichi S, Su LJ, et al. The Parkinson's disease protein α-synuclein disrupts cellular Rab homeostasis. Proc Natl Acad Sci U S A 2008; 105: 145–50.

Giunti D, Borsellino G, Benelli R, Marchese M, Capello E, Valle MT, et al. Phenotypic and functional analysis of T cells homing into the CSF of subjects with inflammatory diseases of the CNS. J Leukoc Biol 2003

Godfrey DI, MacDonald HR, Kronenberg M, Smyth MJ, Van Kaer L. NKT cells: What's in a name? Nat Rev Immunol 2004; 4: 231–7.

Godfrey DI, Uldrich AP, Mccluskey J, Rossjohn J, Moody DB. The burgeoning family of unconventional T cells. Nat Immunol 2015; 16: 1114–23.

Goedert M. Alpha-synuclein and neurodegenerative diseases. Nat Rev Neurosci 2001; 2: 492–501.

Goetz CG. The history of Parkinson's disease: Early clinical descriptions and neurological therapies. Cold Spring Harb Perspect Med 2011; 1

Golbe LI, Di Iorio G, Bonavita V, Miller DC, Duvoisin RC. A large kindred with autosomal dominant Parkinson's disease. Ann Neurol 1990; 27: 276–82.

Gombash SE, Manfredsson FP, Kemp CJ, Kuhn NC, Fleming SM, Egan AE, et al. Morphological and behavioral impact of AAV2/5-mediated overexpression of human wildtype alpha-synuclein in the rat nigrostriatal system. PLoS One 2013; 8: 1–16.

Gómez-Gálvez Y, Palomo-Garo C, Fernández-Ruiz J, García C. Potential of the cannabinoid CB2 receptor as a pharmacological target against inflammation in Parkinson's disease. Prog Neuro-Psychopharmacology Biol Psychiatry 2016; 64: 200–8.

Gong L, Zhang QL, Zhang N, Hua WY, Huang YX, Di PW, et al. Neuroprotection by urate on 6-OHDA-lesioned rat model of Parkinson's disease: Linking to Akt/GSK3β signaling pathway. J Neurochem 2012; 123: 876–85.

Gonzalez-Sepulveda M, Laguna A, Carballo-Carbajal I, Galiano-Landeira J, Romero-Gimenez J, Cuadros T, et al. Validation of a reversed phase UPLC-MS/MS method to determine dopamine metabolites and oxidation intermediates in neuronal differentiated SH-SY5Y cells and brain tissue. ACS Chem Neurosci 2020

González H, Contreras F, Pacheco R. Regulation of the Neurodegenerative Process Associated to Parkinson's Disease by CD4+ T-cells. J Neuroimmune Pharmacol 2015; 10: 561–75.

González H, Pacheco R. T-cell-mediated regulation of neuroinflammation involved in neurodegenerative diseases. J Neuroinflammation 2014; 11: 201.

Gorbatyuk OS, Li S, Sullivan LF, Chen W, Kondrikova G, Manfredsson FP, et al. The phosphorylation state of Ser-129 in human alpha-synuclein determines neurodegeneration in a

rat model of Parkinson disease. Proc Natl Acad Sci U S A 2008; 105: 763–8.

Gordon S. Alternative activation of macrophages. Nat Rev Immunol 2003; 3: 23–35.

Gordon S, Taylor PR. Monocyte and macrophage heterogeneity. Nat Rev Immunol 2005; 5: 953–64.

Goropevšek A, Holcar M, Avčin T. The Role of STAT Signaling Pathways in the Pathogenesis of Systemic Lupus Erythematosus. Clin Rev Allergy Immunol 2017; 52: 164–81.

De Graaf MT, Sillevis Smitt PAE, Luitwieler RL, Van Velzen C, Van Den Broek PDM, Kraan J, et al. Central memory CD4+ T cells dominate the normal cerebrospinal fluid. Cytom Part B - Clin Cytom 2011; 80 B: 43–50.

Groom JR, Luster AD. CXCR3 ligands: Redundant, collaborative and antagonistic functions. Immunol Cell Biol 2011; 89: 207–15.

Groux H, O'Garra A, Bigler M, Rouleau M, Antonenko S, De Vries JE, et al. A CD4+ T-cell subset inhibits antigen-specific T-cell responses and prevents colitis. Nature 1997; 389: 737–42.

Gubellini P, Kachidian P. Animal models of Parkinson's disease: An updated overview. Rev Neurol (Paris) 2015; 171: 750–61.

Guerreiro S, Ponceau A, Toulorge D, Martin E, Alvarez-Fischer D, Hirsch EC, et al. Protection of midbrain dopaminergic neurons by the end-product of purine metabolism uric acid: Potentiation by low-level depolarization. J Neurochem 2009; 109: 1118–28.

Guilarte TR, Nihei MK, McGlothan JL, Howard AS. Methamphetamine-induced deficits of brain monoaminergic neuronal markers: Distal axotomy or neuronal plasticity. Neuroscience 2003; 122: 499–513.

Guisier F. Janus or Hydra: The Many Faces of T Helper Cells in the Human Tumour Microenvironment. 2020

Haaxma CA, Bloem BR, Borm GF, Oyen WJG, Leenders KL, Eshuis S, et al. Gender differences in Parkinson's disease. J Neurol Neurosurg Psychiatry 2007; 78: 819–24.

Häger M, Cowland JB, Borregaard N. Neutrophil granules in health and disease. J Intern Med 2010; 268: 25–34.

Haile Y, Simmen KC, Pasichnyk D, Touret N, Simmen T, Lu J-Q, et al. Granule-Derived Granzyme B Mediates the Vulnerability of Human Neurons to T Cell-Induced Neurotoxicity. J Immunol 2011; 187: 4861–72.

Hall BM. T cells: Soldiers and spies—the surveillance and control of effector T cells by regulatory T cells. Clin J Am Soc Nephrol 2015; 10: 2050–64.

Halle S, Halle O, Förster R. Mechanisms and Dynamics of T Cell-Mediated Cytotoxicity In Vivo. Trends Immunol 2017; 38: 432–43.

Halle S, Keyser KA, Stahl FR, Busche A, Marquardt A, Zheng X, et al. In Vivo Killing Capacity of Cytotoxic T Cells Is Limited and Involves Dynamic Interactions and T Cell Cooperativity. Immunity 2016; 44: 233–45.

Halliday G. Neglected cytotoxic T cell invasion of the brain: how specific for Parkinson's disease? Brain 2020; 143: 3518–20.

Hamadjida A, Frouni I, Kwan C, Huot P. Classic animal models of Parkinson's disease: A historical perspective. Behav Pharmacol 2019; 30: 291–310.

Hamre K, Tharp R, Poon K, Xiong X, Smeyne RJ. Differential strain susceptibility following 1-methyl-4-phenyl-1,2,3,6- tetrahydropyridine (MPTP) administration acts in an autosomal dominant fashion: Quantitative analysis in seven strains of Mus musculus. Brain Res 1999; 828: 91–103.

Hamza TH, Zabetian CP, Tenesa A, Laederach A, Montimurro J, Yearout D, et al. Common genetic variation in the HLA region is associated with late-onset sporadic Parkinson's disease. Nat Genet 2010; 42: 781–5.

Hardy J. Genetic analysis of pathways to Parkinson disease. Neuron 2010; 68: 201–6.

Hardy J, Cookson M, Singleton A. Genes and parkinsonism. J Neurol Neurosurg Psychiatry 2003; 62: 305–9.

Harms AS, Cao S, Rowse AL, Thome AD, Li X, Mangieri LR, et al. MHCII Is Required for -Synuclein-Induced Activation of Microglia, CD4 T Cell Proliferation, and Dopaminergic Neurodegeneration. J Neurosci 2013; 33: 9592–600.

Harms AS, Delic V, Thome AD, Bryant N, Liu Z, Chandra S, et al. α-Synuclein fibrils recruit peripheral immune cells in the rat brain prior to neurodegeneration. Acta Neuropathol Commun 2017; 5: 85.

Harry GJ. Microglia During Development and Aging. Pharmacol Ther 2013; 139: 313–26.

Hashimoto M, Masliah E. Alpha-synuclein in Lewy body disease and Alzheimer's disease. Brain Pathol 1999; 9: 707–20.

Hatami A, Chesselet M-F. Transgenic Rodent Models to Study Alpha-Synuclein Pathogenesis, with a Focus on Cognitive Deficits. Curr Top Behav Neurosci 2015; 22: 303–30.

Hawkes CH, Del Tredici K, Braak H. Parkinson's disease: A dual-hit hypothesis. Neuropathol Appl Neurobiol 2007; 33: 599–614.

Hayes GM, Woodroofe MN, Cuzner ML. Microglia are the major cell type expressing MHC class II in human white matter. J Neurol Sci 1987; 80: 25–37.

Heikkila RE, Hess A, Duvoisin RC. Dopaminergic neurotoxicity of1-methyl-4-phenyl-1,2,5,6-tetrahydropyridine (MPTP) in the mouse: Relationships between monoamine oxidase, MPTP metabolism and neurotoxicity. Life Sci 1985; 36: 231–6.

Heindl S, Gesierich B, Benakis C, Llovera G, Duering M, Liesz A. Automated morphological analysis of microglia after stroke. Front Cell Neurosci 2018; 12: 1–11.

Hellenbrand W, Seidler A, Robra BP, Vieregge P, Oertel WH, Joerg J, et al. Smoking and Parkinson's disease: A case-control study in Germany. Int J Epidemiol 1997; 26: 328–39.

Heneka MT, Kummer MP, Latz E. Innate immune activation in neurodegenerative disease. Nat Rev Immunol 2014; 14: 463–77.

Hernán MA, Logroscino G, García Rodríguez LA. inflammatory drugs and the incidence of Parkinson disease. Neurology 2006; 34: 1097–9.

Hernán MA, Zhang SM, Rueda-DeCastro AM, Colditz GA, Speizer FE, Ascherio A. Cigarette smoking and the incidence of Parkinson's disease in two prospective studies. Ann Neurol 2001; 50: 780–6.

Hewitt VL, Whitworth AJ. Mechanisms of Parkinson's Disease: Lessons from Drosophila. In: Current Topics in Developmental Biology. Elsevier Inc.; 2017. p. 173–200

Hill-Burns EM, Factor SA, Zabetian CP, Thomson G, Payami H. Evidence for more than one parkinson's Disease-Associated variant within the HLA region. PLoS One 2011; 6: 0–7.

Hirsch EC, Hunot S. Neuroinflammation in Parkinson's disease: a target for neuroprotection? Lancet Neurol 2009; 8: 382–97.

Hoehn MM, Yahr MD. Parkinsonism : onset , progression , and mortality. 1967; 17

Holmans P, Moskvina V, Jones L, Sharma M, Vedernikov A, Buchel F, et al. A pathway-based analysis provides additional support for an immune-related genetic susceptibility to Parkinson's disease. Hum Mol Genet 2013; 22: 1039–49.

Holmqvist S, Chutna O, Bousset L, Aldrin-Kirk P, Li W, Björklund T, et al. Direct evidence of Parkinson pathology spread from the gastrointestinal tract to the brain in rats. Acta Neuropathol 2014; 128: 805–20.

Hong S, Dissing-Olesen L, Stevens B. New insights on the role of microglia in synaptic pruning in health and disease. Curr Opin Neurobiol 2016; 36: 128–34.

Hoppel CL, Greenblatt D, Kwok H chi, Arora PK, Singh MP, Sayre LM. Inhibition of mitochondrial respiration by analogs of 4-phenylpyridine and 1-methyl-4-phenylpyridinium cation (MPP+), the neurotoxic metabolite of MPTP. Biochem Biophys Res Commun 1987; 148: 684–93.

Hori S, Nomura T, Sakaguchi S. Control of regulatory T cell development by the transcription factor Foxp3. J Immunol 2017; 198: 981–5.

Hu G, Bidel S, Jousilahti P, Antikainen R, Tuomilehto J. Coffee and tea consumption and the risk of Parkinson's disease. Mov Disord 2007; 22: 2242–8.

Hurley MJ, Durrenberger PF, Gentleman SM, Walls AF, Dexter DT. Altered Expression of Brain Proteinase-Activated Receptor-2, Trypsin-2 and Serpin Proteinase Inhibitors in Parkinson's

Disease. J Mol Neurosci 2015; 57: 48–62.

Hutchings M, Weller RO. Anatomical relationships of the pia mater to cerebral blood vessels in man. J Neurosurg 1986; 65: 316–25.

Iacono D, Geraci-erck M, Rabin ML, Adler CH, Beach TG. Parkinson disease and incidental Lewy body disease. 2015: 1–11.

Iliff JJ, Wang M, Liao Y, Plogg BA, Peng W, Gundersen GA, et al. A paravascular pathway facilitates CSF flow through the brain parenchyma and the clearance of interstitial solutes, including amyloid β. Sci Transl Med 2012; 4

Iranzo A, Tolosa E, Gelpi E, Molinuevo JL, Valldeoriola F, Serradell M, et al. Neurodegenerative disease status and post-mortem pathology in idiopathic rapid-eye-movement sleep behaviour disorder : an observational cohort study. Lancet Neurol 2013; 4422: 1–11.

Ismaiel AAK, Espinosa-Oliva AM, Santiago M, García-Quintanilla A, Oliva-Martín MJ, Herrera AJ, et al. Metformin, besides exhibiting strong in vivo anti-inflammatory properties, increases mptp-induced damage to the nigrostriatal dopaminergic system. Toxicol Appl Pharmacol 2016; 298: 19–30.

Iwasaki A, Medzhitov R. Toll-like receptor control of the adaptive immune responses. Nat Immunol 2004; 5: 987–95.

Jackson-Lewis V, Blesa J, Przedborski S. Animal models of Parkinson's disease. Park Relat Disord 2012; 18: S183–5.

Jackson-Lewis V, Jakowec M, Burke RE, Przedborski S. Time course and morphology of dopaminergic neuronal death caused by the neurotoxin 1-methyl-4-phenyl-1,2,3,6-tetrahydropyridine. Neurodegeneration 1995; 4: 257–69.

Jackson-Lewis V, Przedborski S. Protocol for the MPTP mouse model of Parkinson's disease. Nat Protoc 2007; 2: 141–51.

Jain S, Ton TG, Boudreau RM, Yang M, Thacker EL, Studenski S, et al. The risk of parkinson disease associated with urate in a community-based cohort of older adults. Neuroepidemiology 2011; 36: 223–9.

Javitch JA, D'Amato RJ, Strittmatter SM, Snyder SH. Parkinsonism-inducing neurotoxin, N-methyl-4-phenyl-1,2,3,6-tetrahydropyridine: Uptake of the metabolite N-methyl-4-phenylpyridine by dopamine neurons explains selective toxicity. Proc Natl Acad Sci U S A 1985; 82: 2173–7.

Jellinger KA. A critical evaluation of current staging of α-synuclein pathology in Lewy body disorders. Biochim Biophys Acta - Mol Basis Dis 2009; 1792: 730–40.

Jenkins MR, Trapani JA, Doherty PC, Turner SJ. Granzyme K expressing cytotoxic T lymphocytes protects against influenza virus in granzyme AB-/- mice. Viral Immunol 2008; 21: 341–6.

Jensen MP, Jacos BM, Dobson R, Bandres-Ciga S, Blauwendraat C, Schrag A, et al. Lower lymphocyte count is associated with increased risk of Parkinson's disease Running. 2021

Jessen NA, Munk ASF, Lundgaard I, Nedergaard M. The Glymphatic System - A Beginner's Guide. Neurochem Res 2015; 40: 2583–99.

Jiang S, Gao H, Luo Q, Wang P, Yang X. The correlation of lymphocyte subsets, natural killer cell, and Parkinson's disease: a meta-analysis. Neurol Sci 2017; 38: 1373–80.

Jimenez-Ferrer I, Jewett M, Tontanahal A, Romero-Ramos M, Swanberg M. Allelic difference in Mhc2ta confers altered microglial activation and susceptibility to α-synuclein-induced dopaminergic neurodegeneration. Neurobiol Dis 2017; 106: 279–90.

Joers V, Tansey MG, Mulas G, Carta AR. Microglial phenotypes in Parkinson's disease and animal models of the disease. Prog Neurobiol 2017; 155: 57–75.

Kabanova A, Zurli V, Baldari CT. Signals controlling lytic granule polarization at the cytotoxic immune synapse. Front Immunol 2018; 9: 307.

Kaiserman D, Bird CH, Sun J, Matthews A, Ung K, Whisstock JC, et al. The major human and mouse granzymes are structurally and functionally divergent. J Cell Biol 2006; 175: 619–30.

Kalaitzakis ME, Graeber MB, Gentleman SM, Pearce RKB. The dorsal motor nucleus of the vagus is not an obligatory trigger site of Parkinson's disease: A critical analysis of α-synuclein staging. Neuropathol Appl Neurobiol 2008; 34: 284–95.

Kalia L V., Lang AE. Parkinson's disease. Lancet 2015; 386: 896–912.

Kang JM, Park HJ, Choi YG, Choe IH, Park JH, Kim YS, et al. Acupuncture inhibits microglial activation and inflammatory events in the MPTP-induced mouse model. Brain Res 2007; 1131: 211–9.

Kannarkat GT, Boss JM, Tansey MG. The role of innate and adaptive immunity in parkinson's disease. J Parkinsons Dis 2013; 3: 493–514.

Kannarkat GT, Cook DA, Lee JK, Chang J, Chung J, Sandy E, et al. Common genetic variant association with altered HLA expression, synergy with pyrethroid exposure, and risk for Parkinson's disease: An observational and case-control study. Parkinsons Dis 2015; 1

Karperien A, Ahammer H, Jelinek HF. Quantitating the subtleties of microglial morphology with fractal analysis. Front Cell Neurosci 2013: 1–34.

Kelly LP, Carvey PM, Keshavarzian A, Shannon KM, Shaikh M, Bakay RAE, et al. Progression of Intestinal Permeability Changes and Alpha-Synuclein Expression in a Mouse Model of Parkinson ' s Disease. Mov Disord 2014; 29: 999–1009.

Kettenmann H, Hanisch UK, Noda M, Verkhratsky A. Physiology of microglia. Physiol Rev 2011; 91: 461–553.

Kida S, Pantazis A, Weller RO. CSF drains directly from the subarachnoid space into nasal lymphatics in the rat. Anatomy, histology and immunological significance. Neuropathol Appl Neurobiol 1993; 19: 480–8.

Kim C, Ho DH, Suk JE, You S, Michael S, Kang J, et al. Neuron-released oligomeric α-synuclein is an endogenous agonist of TLR2 for paracrine activation of microglia. Nat Commun 2013; 4: 1–24.

Kim R, Kim H, Kim A, Jang M, Kim A, Kim Y, et al. Peripheral blood inflammatory markers in early Parkinson ' s disease. J Clin Neurosci 2018; 58: 30–3.

Kim SK, Schluns KS, Lefrançois L. Induction and visualization of mucosal memory CD8 T cells following systemic virus infection. J Immunol 1999; 163: 4125–32.

Kin K, Yasuhara T, Kameda M, Date I. Animal models for Parkinson's disease research: Trends in the 2000s. Int J Mol Sci 2019; 20

Kinugawa K, Monnet Y, Lu L, Bekaert AJ, Théry C, Mallat Z, et al. MFGE8 does not orchestrate clearance of apoptotic neurons in a mouse model of Parkinson's disease. Neurobiol Dis 2013; 51: 192–201.

Kipnis J, Filiano AJ. The central nervous system: Privileged by immune connections. Nat Rev Immunol 2018; 18: 83–4.

Kirik D, Rosenblad C, Burger C, Lundberg C, Johansen TE, Muzyczka N, et al. Parkinson-like neurodegeneration induced by targeted overexpression of α-synuclein in the nigrostriatal system. J Neurosci 2002; 22: 2780–91.

Kitada T, Tong Y, Gautier CA, Shen J. Absence of nigral degeneration in aged parkin/DJ-1/PINK1 triple knockout mice. J Neurochem 2009; 111: 696–702.

Kivisakk P, Imitola J, Rasmussen S, Elyaman W, Zhu B, Ransohoff RM, et al. Localizing central nervous system immune surveillance: Meningeal antigen-presenting cells activate T cells during experimental autoimmune encephalomyelitis. Ann Neurol 2009; 65: 457–69.

Kivisäkk P, Mahad DJ, Callahan MK, Trebst C, Tucky B, Wei T, et al. Human cerebrospinal fluid central memory CD4+ T cells: Evidence for trafficking through choroid plexus and meninges via P-selectin. Proc Natl Acad Sci U S A 2003; 100: 8389–94.

Klein RL, King MA, Hamby ME, Meyer EM. Dopaminergic Cell Loss Induced by Human A30P α -Synuclein Gene Transfer to the Rat Substantia Nigra. Hum Gene Ther 2002; 13: 605–12.

Klion AD, Ackerman SJ, Bochner BS. Contributions of Eosinophils to Human Health and Disease. Annu Rev Pathol Mech Dis 2020; 15: 179–209.

Knott C, Stern G, Wilkin GP. Inflammatory regulators in Parkinson's disease: iNOS, lipocortin-1, and cyclooxygenases-1 and -2. Mol Cell Neurosci 2000; 16: 724–39.

Kopin IJ, Markey SP. MPTP toxicity: Implications for research in Parkinson's disease. Annu Rev Neurosci 1988; 11: 81–96.

Koprich JB, Johnston TH, Huot P, Reyes MG, Espinosa M, Brotchie JM. Progressive neurodegeneration or endogenous compensation in an animal model of Parkinson's disease produced by decreasing doses of alpha-synuclein. PLoS One 2011; 6: 1–10.

Koprich JB, Johnston TH, Reyes MG, Sun X, Brotchie JM. Expression of human A53T alpha-synuclein in the rat substantia nigra using a novel AAV1/2 vector produces a rapidly evolving pathology with protein aggregation, dystrophic neurite architecture and nigrostriatal degeneration with potential to model the pat. Mol Neurodegener 2010; 5: 43.

Koprich JB, Kalia L V., Brotchie JM. Animal models of α-synucleinopathy for Parkinson disease drug development. Nat Rev Neurosci 2017; 18: 515–29.

Korn T, Kallies A. T cell responses in the central nervous system. Nat Rev Immunol 2017; 17: 179–94.

Kotas ME, Medzhitov R. Homeostasis, Inflammation, and Disease Susceptibility. Cell 2015; 160: 816–27.

Kronenberg M. Toward an understanding of NKT cell biology: Progress and paradoxes. Annu Rev Immunol 2005; 23: 877–900.

Krystel-Whittemore M, Dileepan KN, Wood JG. Mast cell: A multi-functional master cell. Front Immunol 2016; 6: 1–12.

Kurkowska-Jastrzebska I, Wronska A, Kohutnicka M, Czlonkowski A, Czlonkowska A. The Inflammatory Reaction Following 1-Methyl-4-phenyl-1,2,3,6-tetrahydropyridine Intoxication in Mouse. Exp Neurol 1999; 156: 50–61.

Kustrimovic N, Comi C, Magistrelli L, Rasini E, Legnaro M, Bombelli R, et al. Parkinson's disease patients have a complex phenotypic and functional Th1 bias: Cross-sectional studies of CD4+ Th1/Th2/T17 and Treg in drug-naïve and drug-treated patients. J Neuroinflammation 2018; 15

Kustrimovic N, Rasini E, Legnaro M, Bombelli R, Aleksic I, Blandini F, et al. Dopaminergic Receptors on CD4+ T Naive and Memory Lymphocytes Correlate with Motor Impairment in Patients with Parkinson's Disease. Sci Rep 2016; 6: 33738.

Labadorf A, Choi SH, Myers RH. Evidence for a Pan-Neurodegenerative Disease Response in Huntington's and Parkinson's Disease Expression Profiles. Front Mol Neurosci 2018; 10: 1–12.

Lam HA, Wu N, Cely I, Kelly RL, Hean S, Richter F, et al. Elevated tonic extracellular dopamine concentration and altered dopamine modulation of synaptic activity precede dopamine loss in the striatum of mice overexpressing human α-synuclein. J Neurosci Res 2011; 89: 1091–102.

Langston JW. The MPTP story. J Parkinsons Dis 2017; 7: S11–9.

Langston JW, Ballard P, Tetrud JW, Irwin I. Chronic parkinsonism in humans due to a product of meperidine-analog synthesis. Science (80-) 1983; 219: 979–80.

Langston JW, Forno LS, Tetrud J, Reeves AG, Kaplan JA, Karluk D. Evidence of active nerve cell degeneration in the substantia nigra of humans years after 1-methyl-4-phenyl-1,2,3,6-tetrahydropyridine exposure. Ann Neurol 1999; 46: 598–605.

Langston JW, Irwin I, Langston EB, Forno LS. Pargyline Prevents MPTP-Induced Parkinsonism in Primates. Science (80-) 1984; 225: 1480–2.

Lashuel HA, Overk CR, Oueslati A, Masliah E. The many faces of α-synuclein: from structure and toxicity to therapeutic target. Nat Rev Neurosci 2013; 14: 38–48.

Lastres-Becker I, García-Yagüe AJ, Scannevin RH, Casarejos MJ, Kügler S, Rábano A, et al. Repurposing the NRF2 Activator Dimethyl Fumarate as Therapy Against Synucleinopathy in Parkinson's Disease. Antioxid Redox Signal 2016; 25: 61–77.

Lastres-Becker I, Ulusoy A, Innamorato NG, Sahin G, Rábano A, Kirik D, et al. α-synuclein expression and Nrf2 deficiency cooperate to aggravate protein aggregation, neuronal death and inflammation in early-stage Parkinson's disease. Hum Mol Genet 2012; 21: 3173–92.

de Lau LML, Breteler MMB. The epidemiology of Parkinson's disease. Lancet Neurol 2006; 5: 525–35.

de Lau LML, Koudstaal PJ, Hofman A, Breteler MMB. Serum uric acid levels and the risk of Parkinson disease. Ann Neurol 2005; 58: 797–800.

Lavedan C. The synuclein family. Genome Res 1998; 8: 871–80.

Lawson LJ, Perry VH, Gordon S. Turnover of resident microglia in the normal adult mouse brain. Neuroscience 1992; 48: 405–15.

Lazzarini M, Martin S, Mitkovski M, Vozari RR, Stühmer W, Bel E Del. Doxycycline restrains glia and confers neuroprotection in a 6-OHDA Parkinson model. Glia 2013; 61: 1084–100.

Le W, Sayana P, Jankovic J. Animal Models of Parkinson's Disease: A Gateway to Therapeutics? Neurotherapeutics 2014; 11: 92–110.

Leclair-Visonneau L, Neunlist M, Derkinderen P, Lebouvier T. The gut in Parkinson's disease: Bottom-up, top-down, or neither? Neurogastroenterol Motil 2020; 32: 1–6.

Lee E, Hwang I, Park S, Hong S, Hwang B, Cho Y, et al. MPTP-driven NLRP3 inflammasome activation in microglia plays a central role in dopaminergic neurodegeneration. Cell Death Differ 2019; 26: 213–28.

Lee EC, Yu D, Martínez de Velasco J, Tessarollo L, Swing DA, Court DL, et al. A highly efficient Escherichia coli-based chromosome engineering system adapted for recombinogenic targeting and subcloning of BAC. Genomics 2001; 73: 56–65.

Lee MK, Stirling W, Xu Y, Xu E, Qui D, Mandir AS, et al. Human α-synuclein-harboring familial Parkinson's disease-linked Ala-53 → Thr mutation causes neurodegenerative disease with α-synuclein aggregation in transgenic mice. Proc Natl Acad Sci U S A 2002; 99: 8968–73.

Lee YC, Lin CH, Wu RM, Lin JW, Chang CH, Lai MS. Antihypertensive agents and risk of Parkinson's disease: A nationwide cohort study. PLoS One 2014; 9: 17–21.

Leverenz JB, Hamilton R, Tsuang DW, Schantz A, Vavrek D, Larson EB, et al. Empiric refinement of the pathologic assessment of Lewy-related pathology in the dementia patient. Brain Pathol 2008; 18: 220–4.

Levings MK, Sangregorio R, Galbiati F, Squadrone S, de Waal Malefyt R, Roncarolo M-G. IFN-α and IL-10 Induce the Differentiation of Human Type 1 T Regulatory Cells. J Immunol 2001; 166: 5530–9.

Lewis CE, Pollard JW. Distinct role of macrophages in different tumor microenvironments. Cancer Res 2006; 66: 605–12.

Lewy F. Paralysis agitans. Handb der Neurol hsg von Max Lewandowsky, Dritter Band, Spez Neurol II Für Später Vor 1912; 3: 920–58.

Li WW, Setzu A, Zhao C, Franklin RJM. Minocycline-mediated inhibition of microglia activation impairs oligodendrocyte progenitor cell responses and remyelination in a non-immune model of demyelination. J Neuroimmunol 2005; 158: 58–66.

Liberatore GT, Jackson-Lewis V, Vukosavic S, Mandir AS, Vila M, Mcauliffe WG, et al. Inducible nitric oxide synthase stimulates dopaminergic neurodegeneration in the MPTP model of Parkinson disease. Nat Med 1999; 5: 1403–9.

Lin CH, Chen CC, Chiang HL, Liou JM, Chang CM, Lu TP, et al. Altered gut microbiota and inflammatory cytokine responses in patients with Parkinson's disease. J Neuroinflammation 2019; 16: 1–9.

Linazasoro G. Classical Parkinson disease versus Parkinson complex - Reflections against staging and in favour of heterogeneity. Eur J Neurol 2007; 14: 721–8.

Lindestam-Arlehamn CS, Garretti F, Sulzer D, Sette A. Roles for the adaptive immune system in Parkinson's and Alzheimer's diseases. Curr Opin Immunol 2019; 59: 115–20.

Lindestam Arlehamn CS, Dhanwani R, Pham J, Kuan R, Frazier A, Rezende Dutra J, et al. α-Synuclein-specific T cell reactivity is associated with preclinical and early Parkinson's disease. Nat Commun 2020; 11

Liu R, Gao X, Lu Y, Chen H. Meta-analysis of the relationship between Parkinson disease and melanoma. Neurology 2011; 76: 2002–9.

Liu R, Guo X, Park Y, Huang X, Sinha R, Freedman ND, et al. Caffeine intake, smoking, and risk of parkinson disease in men and women. Am J Epidemiol 2012; 175: 1200–7.

Liu Y, Roghani A, Edwards RH. Gene transfer of a reserpine-sensitive mechanism of resistance to N-methyl-4-phenylpyridinium. Proc Natl Acad Sci U S A 1992; 89: 9074–8.

Liu Z, Huang Y, Cao B-B, Qiu Y-H, Peng Y-P. Th17 Cells Induce Dopaminergic Neuronal Death via LFA-1/ICAM-1 Interaction in a Mouse Model of Parkinson's Disease [Internet]. Mol Neurobiol 2016Available from: http://link.springer.com/10.1007/s12035-016-0249-9

Liu Z, Qiu AW, Huang Y, Yang Y, Chen JN, Gu TT, et al. IL-17A exacerbates neuroinflammation and neurodegeneration by activating microglia in rodent models of Parkinson's disease. Brain Behav Immun 2019; 81: 630–45.

Lodygin D, Odoardi F, Schläger C, Körner H, Kitz A, Nosov M, et al. A combination of fluorescent

NFAT and H2B sensors uncovers dynamics of T cell activation in real time during CNS autoimmunity. Nat Med 2013; 19: 784–90.

Loeffler C, Dietz K, Schleich A, Schlaszus H, Stoll M, Meyermann R, et al. Immune surveillance of the normal human CNS takes place in dependence of the locoregional blood-brain barrier configuration and is mainly performed by CD3+/CD8+ lymphocytes. Neuropathology 2011; 31: 230–8.

Lopez JA, Susanto O, Jenkins MR, Lukoyanova N, Sutton VR, Law RHP, et al. Perforin forms transient pores on the target cell plasma membrane to facilitate rapid access of granzymes during killer cell attack. Blood 2013; 121: 2659–68.

Louveau A, Harris TH, Kipnis J. Revisiting the Mechanisms of CNS Immune Privilege. Trends Immunol 2015; 36: 569–77.

Louveau A, Plog BA, Antila S, Alitalo K, Nedergaard M, Kipnis J. Understanding the functions and relationships of the glymphatic system and meningeal lymphatics. J Clin Invest 2017; 127: 3210–9.

Louveau A, Smirnov I, Keyes TJ, Eccles JD, Rouhani SJ, Peske JD, et al. Structural and functional features of central nervous system lymphatic vessels. Nature 2015; 523: 337–41.

Lu J-Q, Fan Y, Mitha AP, Bell R, Metz L, Moore GRW, et al. Association of α-Synuclein Immunoreactivity With Inflammatory Activity in Multiple Sclerosis Lesions. J Neuropathol Exp Neurol 2009; 68: 179–89.

Luk KC, Kehm V, Carroll J, Zhang B, O'Brien P, Trojanowski JQ, et al. Pathological α-synuclein transmission initiates Parkinson-like neurodegeneration in nontransgenic mice. Science (80-) 2012; 338: 949–53.

Luk KC, Kehm VM, Zhang B, O'Brien P, Trojanowski JQ, Lee VMY. Intracerebral inoculation of pathological α-synuclein initiates a rapidly progressive neurodegenerative α-synucleinopathy in mice. J Exp Med 2012; 209: 975–88.

Luo X, Chen S. The changing phenotype of microglia from homeostasis to disease. 2012: 1–13.

Luo XG, Ding JQ, Chen S Di. Microglia in the aging brain: Relevance to neurodegeneration. Mol Neurodegener 2010; 5: 1–9.

Lyck R, Engelhardt B. Going against the tide - How encephalitogenic T cells breach the blood-brain barrier. J Vasc Res 2012; 49: 497–509.

Ma SY, Röyttä M, Rinne JO, Collan Y, Rinne UK. Correlation between neuromorphometry in the substantia nigra and clinical features in Parkinson's disease using disector counts. J Neurol Sci 1997; 151: 83–7.

Machado-Santos J, Saji E, Tröscher AR, Paunovic M, Liblau R, Gabriely G, et al. The compartmentalized inflammatory response in the multiple sclerosis brain is composed of tissue-resident CD8+ T lymphocytes and B cells. Brain 2018; 141: 2066–82.

Machado MMF, Bassani TB, Cóppola-Segovia V, Moura ELR, Zanata SM, Andreatini R, et al. PPAR-γ agonist pioglitazone reduces microglial proliferation and NF-κB activation in the substantia nigra in the 6-hydroxydopamine model of Parkinson's disease. Pharmacol Reports 2019; 71: 556–64.

Madore C, Baufeld C, Butovsky O. Microglial confetti party. Nat Neurosci 2017; 20: 762–3.

Madras BK, Fahey MA, Goulet M, Lin Z, Bendor J, Goodrich C, et al. Dopamine transporter (DAT) inhibitors alleviate specific parkinsonian deficits in monkeys: Association with DAT occupancy in vivo. J Pharmacol Exp Ther 2006; 319: 570–85.

Main BS, Zhang M, Brody KM, Ayton S, Frugier T, Steer D, et al. Type-1 interferons contribute to the neuroinflammatory response and disease progression of the MPTP mouse model of Parkinson's disease. Glia 2016; 64: 1590–604.

Malyshkina A, Littwitz-Salomon E, Sutter K, Zelinskyy G, Windmann S, Schimmer S, et al. Fas Ligand-mediated cytotoxicity of CD4+ T cells during chronic retrovirus infection. Sci Rep 2017; 7: 1–10.

Mantovani A, Sica A, Sozzani S, Allavena P, Vecchi A, Locati M. The chemokine system in diverse forms of macrophage activation and polarization. Trends Immunol 2004; 25: 677–86.

Marras C, Hincapié CA, Kristman VL, Cancelliere C, Soklaridis S, Li A, et al. Systematic review of the risk of parkinson's disease after mild traumatic brain injury: Results of the international collaboration on mild traumatic brain injury prognosis. Arch Phys Med Rehabil 2014; 95: 238–44.

Marshall JS, Warrington R, Watson W, Kim HL. An introduction to immunology and immunopathology. Allergy, Asthma Clin Immunol 2018; 14: 1–10.

Martin HL, Santoro M, Mustafa S, Riedel G, Forrester J V., Teismann P. Evidence for a role of adaptive immune response in the disease pathogenesis of the MPTP mouse model of Parkinson's disease. Glia 2016; 64: 386–95.

Marttila RJ. Herpesviruses and Parkinsonism. Arch Neurol 1981; 38: 19–21.

Marttila RJ, Rinne UK, Tiilikainen A. Virus antibodies in Parkinson's disease. Herpes simplex and measles virus antibodies in serum and CSF and their relation to HLA types. J Neurol Sci 1982; 54: 227–38.

Masilamoni GJ, Smith Y. Chronic MPTP Administration Regimen in Monkeys: A Model of Dopaminergic and Non-dopaminergic Cell Loss in Parkinson's Disease. J Neural Transm 2018; 125: 337–63.

Masopust D, Vezys V, Marzo AL, Lefrançois L. Preferential Localization of Effector Memory Cells in Nonlymphoid Tissue. Science (80-) 2001; 291: 2413–7.

McFarland NR, Fan Z, Xu K, Schwarzschild MA, Feany MB, Hyman BT, et al. alpha-Synuclein S129 Phosphorylation Mutants Do Not Alter Nigrostriatal Toxicity in a Rat Model of Parkinson Disease. J Neuropathol Exp Neurol 2009; 68: 515–24.

McFarland NR, Lee JS, Hyman BT, McLean PJ. Comparison of transduction efficiency of recombinant AAV serotypes 1, 2, 5, and 8 in the rat nigrostriatal system. J Neurochem 2009; 109: 838–45.

McGeer PL, Itagaki S, Boyes BE, McGeer EG. Reactive microglia are positive for HLA-DR in the substantia nigra of Parkinson's and Alzheimer's disease brains. Neurology 1988; 38: 1285–91.

McGeer PL, Itagaki S, McGeer EG. Expression of the histocompatibility glycoprotein HLA-DR in neurological disease. Acta Neuropathol 1988; 76: 550–7.

McHugh RS, Whitters MJ, Piccirillo CA, Young DA, Shevach EM, Collins M, et al. CD4+CD25+ Immunoregulatory T Cells: Gene expression analysis reveals a functional role for the glucocorticoid-induced TNF receptor. Immunity 2002; 16: 311–23.

McKeith IG, Dickson DW, Lowe J, Emre M, O'Brien JT, Feldman H, et al. Diagnosis and management of dementia with Lewy bodies: Third report of the DLB consortium. Neurology 2005; 65: 1863–72.

McKeith IG, Galasko D, Kosaka K, Perry EK, Dickson DW, Hansen LA, et al. Consensus guidelines for the clinical and pathologic diagnosis of dementia with Lewy bodies (DLB): Report of the consortium on DLB international workshop. Neurology 1996; 47: 1113–24.

Medawar PB. Immunity to homologous grafted skin. III. The fate of skin homografts transplanted to the brain, to subcutaneous tissue, and to the anterior chamber of the eye. Br J Exp Pathol 1948; 29: 58–69.

Mellman I, Steinman RM. Dendritic cells: Specialized and regulated antigen processing machines. Cell 2001; 106: 255–8.

Mempel TR, Henrickson SE, Andrian UH Von. T-cell priming by dendritic cells in lymph nodes occurs in three distinct phases. 2004; 427: 2–7.

Meoni S, Macerollo A, Moro E. Sex differences in movement disorders. Nat Rev Neurol 2020; 16: 84–96.

Merlini M, Kirabali T, Kulic L, Nitsch RM, Ferretti MT. Extravascular CD3+ T Cells in Brains of Alzheimer Disease Patients Correlate with Tau but Not with Amyloid Pathology: An Immunohistochemical Study. Neurodegener Dis 2018; 18: 49–56.

Mescher MF, Curtsinger JM, Casey KA, Hammerbeck CD. Signals required for programming effector and memory development by CD8 + T cells. 2006; 211: 81–92.

Miller LR, Das SK. Review article: Cigarette Smoking and Parkinson's Disease. EXCLI J 2007; 6: 93–9.

Miller MJ, Wei SH, Cahalan MD, Parker I. Autonomous T cell trafficking examined in vivo with intravital two-photon microscopy. 2003; 100

Miller RM, Kiser GL, Kaysser-Kranich T, Casaceli C, Colla E, Lee MK, et al. Wild-type and mutant α-synuclein induce a multi-component gene expression profile consistent with shared

pathophysiology in different transgenic mouse models of PD. Exp Neurol 2007; 204: 421–32.

Miloud T, Henrich C, Hämmerling GJ. Quantitative comparison of click beetle and firefly luciferases for in vivo bioluminescence imaging. J Biomed Opt 2007; 12: 054018.

Miraglia F, Ricci A, Rota L, Colla E. Subcellular localization of alpha-synuclein aggregates and their interaction with membranes. Neural Regen Res 2018; 13: 1136–44.

Mittelbronn M, Dietz K, Schluesener HJ, Meyermann R. Local distribution of microglia in the normal adult human central nervous system differs by up to one order of magnitude. Acta Neuropathol 2001; 101: 249–55.

Mizuno Y, Ohta S, Tanaka M, Takamiya S, Suzuki K, Sato T, et al. Deficiencies in Complex I subunits of the respiratory chain in Parkinson's disease. Biochem Biophys Res Commun 1989; 163: 1450–5.

Mogi M, Harada M, Kondo T, Riederer P, Inagaki H, Minami M, et al. Interleukin-1β, interleukin-6, epidermal growth factor and transforming growth factor-α are elevated in the brain from parkinsonian patients. Neurosci Lett 1994; 180

Molinoff PB, Axelrod J. Biochemistry of catecholamines. Annu Rev Biochem 1971; 40: 465–500.

Mondal S, Rangasamy SB, Roy A, Dasarathy S, Kordower JH, Pahan K. Low-Dose Maraviroc, an Antiretroviral Drug, Attenuates the Infiltration of T Cells into the Central Nervous System and Protects the Nigrostriatum in Hemiparkinsonian Monkeys. J Immunol 2019; 202: 3412–22.

Montagu KA. Catechol Compounds in Rat Tissues and in Brains of Different Animals. Nature 1957; 180: 244–5.

Moody DB, Zajonc DM, Wilson IA. Anatomy of CD1-lipid antigen complexes. Nat Rev Immunol 2005; 5: 387–99.

Morens DM, Grandinetti A, Reed D, White LR, Ross GW. Cigarette smoking and protection from parkinson's disease: False association or etiologic clue? Neurology 1995; 45: 1041–51.

Mosley RL, Gendelman HE. T cells and Parkinson's disease. Lancet Neurol 2017; 16: 769–71.

Mosley RL, Hutter-Saunders J a., Stone DK, Gendelman HE. Inflammation and adaptive immunity in Parkinson's disease. Cold Spring Harb Perspect Med 2012; 2: 1–17.

Mosmann TR, Cherwinski H, Bond MW, Giedlin MA, Coffman RL. Two types of murine helper T cell clone. I. Definition according to profiles of lymphokine activities and secreted proteins. J Immunol 1986; 136: 2348–57.

Mosser DM, Edwards JP. Exploring the full spectrum of macrophage activation. Nat Rev Immunol 2008; 8: 958–69.

Mougenot AL, Nicot S, Bencsik A, Morignat E, Verchère J, Lakhdar L, et al. Prion-like acceleration of a synucleinopathy in a transgenic mouse model. Neurobiol Aging 2012; 33: 2225–8.

Mount MP, Lira A, Grimes D, Smith PD, Faucher S, Slack R, et al. Involvement of Interferon-gamma in Microglial-Mediated Loss of Dopaminergic Neurons. Neurobiol Dis 2007; 27: 3328–37.

Movement Disorder Society Task Force on Rating Scales for Parkinson's Disease *. The Unified Parkinson's Disease Rating Scale (UPDRS): Status and Recommendations. Mov Disord 2003; 18: 738–50.

Mueller SN, Gebhardt T, Carbone FR, Heath WR. Memory T cell subsets, migration patterns, and tissue residence. Annu Rev Immunol 2013; 31: 137–61.

Mulak A, Bonaz B. Brain-gut-microbiota axis in Parkinson's disease. World J Gastroenterol 2015; 21: 10609–20.

Müller T, Blum-Degen D, Przuntek H, Kuhn W. Interleukin-6 levels in cerebrospinal fluid inversely correlate to severity of Parkinson' s disease. Acta Neurol Scand 1998; 98: 142–4.

Murphy DD, Rueter SM, Trojanowski JQ, Lee VMY. Synucleins Are Developmentally Expressed, and alpha -Synuclein Regulates the Size of the Presynaptic Vesicular Pool in Primary Hippocampal Neurons. J Neurosci 2000; 20: 3214–20.

Murphy JB, Sturm E. Conditions determining the transplantability of tissues in the brain. J Exp Med 1923; 38: 183–97.

Murphy K. Janeway's Immunobiology. 8th editio. New York: Garland Science, Taylor and Francis; 2011

Musgrove RE, Helwig M, Bae EJ, Aboutalebi H, Lee SJ, Ulusoy A, et al. Oxidative stress in vagal neurons promotes parkinsonian pathology and intercellular α-synuclein transfer. J Clin Invest 2019; 129: 3738–53.

Muthane U, Ramsay KA, Jiang H, Jackson-Lewis V, Donaldson D, Fernando S, et al. Differences in Nigral Neuron Number and Sensitivity to 1-Methyl-4-phenyl-1,2,3,6-tetrahydropyridine in C57/bl and CD-1 Mice. Exp Neurol 1994; 126: 195–204.

Nagatsu T, Sawada M. l-dopa therapy for Parkinson's disease: Past, present, and future. Park Relat Disord 2009; 15: 3–8.

Nakajima K, Kikuchi Y, Ikoma E, Honda S, Ishikawa M, Liu Y, et al. Neurotrophins regulate the function of cultured microglia. Glia 1998; 24: 272–89.

Nalls MA, Blauwendraat C, Vallerga CL, Heilbron K, Bandres-Ciga S, Chang D, et al. Identification of novel risk loci, causal insights, and heritable risk for Parkinson's disease: a meta-analysis of genome-wide association studies. Lancet Neurol 2019; 18: 1091–102.

Neumann H. Control of glial immune function by neurons. Glia 2001; 36: 191–9.

Nicholson LB. The immune system. Essays Biochem 2016; 60: 275–301.

van Nierop GP, van Luijn MM, Michels SS, Melief M-J, Janssen M, Langerak AW, et al. Phenotypic and functional characterization of T cells in white matter lesions of multiple sclerosis patients.

Acta Neuropathol 2017; 134: 383–401.

Nimmerjahn A, Kirchhoff F, Helmchen F. Resting microglial cells are highly dynamic surveillants of brain parenchyma in vivo. Neuroforum 2005; 11: 95–6.

Niwa F, Kuriyama N, Nakagawa M, Imanishi J. Effects of peripheral lymphocyte subpopulations and the clinical correlation with Parkinson's disease. Geriatr Gerontol Int 2012; 12: 102–7.

Nonnekes J, Post B, Tetrud JW, Langston JW, Bloem BR. MPTP-induced parkinsonism: an historical case series. Lancet Neurol 2018; 17: 300–1.

Norris GT, Kipnis J. Immune cells and CNS physiology: Microglia and beyond. J Exp Med 2019; 216: 60–70.

Noyce AJ, Bestwick JP, Silveira-Moriyama L, Hawkes CH, Giovannoni G, Lees AJ, et al. Meta-analysis of early nonmotor features and risk factors for Parkinson disease. Ann Neurol 2012; 72: 893–901.

O'Garra A, Vieira PL, Vieira P, Goldfeld AE. IL-10–producing and naturally occurring CD4+ Tregs: limiting collateral damage. J Clin Invest 2004; 114: 1372–8.

O'Reilly ÉJ, Gao X, Weisskopf MG, Chen H, Schwarzschild MA, Spiegelman D, et al. Plasma urate and Parkinson's disease in women. Am J Epidemiol 2010; 172: 666–70.

Obeso JA, Stamelou M, Goetz CG, Poewe W, Lang AE, Weintraub D, et al. Past, present, and future of Parkinson's disease: A special essay on the 200th Anniversary of the Shaking Palsy. Mov Disord 2017; 32: 1264–310.

Ogura K, Ogawa M, Yoshida M. Effects of ageing on microglia in the normal rat brain: immunohistochemical observations. Neuroreport 1994; 5: 1224–6.

Okabe Y, Medzhitov R. Tissue biology perspective on macrophages. Nat Immunol 2016; 17: 9–17.

Olmedo-Díaz S, Estévez-Silva H, Orädd G, af Bjerkén S, Marcellino D, Virel A. An altered blood–brain barrier contributes to brain iron accumulation and neuroinflammation in the 6-OHDA rat model of Parkinson's disease. Neuroscience 2017; 362: 141–51.

Olsen LK, Dowd E, McKernan DP. A role for viral infections in Parkinson's etiology? Neuronal Signal 2018; 2

Olson KE, Gendelman HE. Immunomodulation as a neuroprotective and therapeutic strategy for Parkinson's disease. Curr Opin Pharmacol 2016; 26: 87–95.

Orr CF, Rowe DB, Mizuno Y, Mori H, Halliday GM. A possible role for humoral immunity in the pathogenesis of Parkinson's disease. Brain 2005; 128: 2665–74.

Ousman SS, Kubes P. Immune surveillance in the central nervous system. Nat Neurosci 2012; 15: 1096–101.

Pabon MM, Bachstetter AD, Hudson CE, Gemma C, Bickford PC. CX3CL1 reduces neurotoxicity and

microglial activation in a rat model of Parkinson's disease. J Neuroinflammation 2011; 8: 9.

Palmer EM, Holbrook BC, Arimilli S, Parks GD, Martha A. IFNγ-producing, virus-specific CD8+ effector cells acquire the ability to produce IL-10 as a result of entry into the infected lung environment. Virology 2010; 404: 225–30.

Palmer SS, Mortimer JA, Webster DD, Bistevins R, Dickinson GL. Exercise Therapy for Parkinson's Disease. Arch Phys Med Rehabil 1986; 67: 741–5.

Pan L, Meng L, He M, Zhang Z. Tau in the Pathophysiology of Parkinson's Disease [Internet]. J Mol Neurosci 2021Available from: https://doi.org/10.1007/s12031-020-01776-5

Parish CL, Castelo-branco G, Rawal N, Tonnesen J, Toft A, Salto C, et al. Nurul Afiqah Mohamed Hisham , Ling King Hwa and Norshariza Nordin Genetics and Regenerative Medicine Research Centre , Faculty of Medicine and Health Sciences , Universiti Putra Malaysia RESULTS. 2013; 110: 32273.

Parkhurst CN, Yang G, Ninan I, Savas JN, Iii JRY, Lafaille JJ, et al. Microglia promote learning-dependent synapse formation through BDNF. Cell 2013; 155: 1596–609.

Parkinson J. An Essay on the Shaking Palsy. Whittingham Rowl Sherwood, Neely Jones 1817

Parkkinen L, Kauppinen T, Pirttilä T, Autere JM, Alafuzoff I. Alpha-Synuclein Pathology Does Not Predict Extrapyramidal Symptoms or Dementia. Ann Neurol 2005; 57: 82–91.

Parkkinen L, Pirttilä T, Alafuzoff I. Applicability of current staging/categorization of α-synuclein pathology and their clinical relevance. Acta Neuropathol 2008; 115: 399–407.

St. Paul M, Ohashi PS. The Roles of CD8+ T Cell Subsets in Antitumor Immunity. Trends Cell Biol 2020; 30: 695–704.

Paxinos G, Watson C. The rat brain in stereotaxic coordinates. Compact Th. Academic Press; 1987

Perier C, Bové J, Wu DC, Dehay B, Choi DK, Jackson-Lewis V, et al. Two molecular pathways initiate mitochondria-dependent dopaminergic neurodegeneration in experimental Parkinson's disease. Proc Natl Acad Sci U S A 2007; 104: 8161–6.

Van der Perren A, Macchi F, Toelen J, Carlon MS, Maris M, de Loor H, et al. FK506 reduces neuroinflammation and dopaminergic neurodegeneration in an α-synuclein-based rat model for Parkinson's disease. Neurobiol Aging 2015; 36: 1559–68.

Perry VH, Matyszak MK, Fearn S. Altered antigen expression of microglia in the aged rodent CNS. Glia 1993; 7: 60–7.

Perry VH, Nicoll JAR, Holmes C. Microglia in neurodegenerative disease. Nat Rev Neurol 2010; 6: 193–201.

Perry VH, Teeling J. Microglia and macrophages of the central nervous system: The contribution of microglia priming and systemic inflammation to chronic neurodegeneration. Semin Immunopathol 2013; 35: 601–12.

Pfeiffer RF. Parkinson disease: Calcium channel blockers and Parkinson disease. Nat Rev Neurol 2010; 6: 188–9.

Ping HX, Shepard PD. Apamin-sensitive Ca2+-activated K+ channels regulate pacemaker activity in nigral dopamine neurons. Neuroreport 1996; 7: 809–14.

Plate JMD, Plate AE, Shott S, Bograd S, Harris JE. Effect of gemcitabine on immune cells in subjects with adenocarcinoma of the pancreas. Cancer Immunol Immunother 2005; 54: 915–25.

Poewe W, Seppi K, Tanner CM, Halliday GM, Brundin P, Volkmann J, et al. Parkinson disease. Nat Rev Dis Prim 2017; 3: 1–21.

Polymeropoulos MH, Higgins JJ, Golbe LI, Johnson WG, Ide SE, Di Iorio G, et al. Mapping of a gene for Parkinson's disease to chromosome 4q21-q23. Science (80-) 1996; 274: 1197–9.

Polymeropoulos MH, Lavedan C, Leroy E, Ide SE, Dehejia A, Dutra A, et al. Mutation in the α-synuclein gene identified in families with Parkinson's disease. Science (80-) 1997; 276: 2045–7.

Popovich PG, Longbrake EE. Can the immune system be harnessed to repair the CNS? Nat Rev Neurosci 2008; 9: 481–93.

Porras G, Li Q, Bezard E. Modeling Parkinson's Disease in Primates: The MPTP Model. Cold Spring Harb Perspect Med 2012; 2: 1–10.

Prinz M, Priller J. Microglia and brain macrophages in the molecular age: From origin to neuropsychiatric disease. Nat Rev Neurosci 2014; 15: 300–12.

Przedborski S, Vila M. The 1-methyl-4-phenyl-1,2,3,6-tetrahydropyridine mouse model: A tool to explore the pathogenesis of Parkinson's disease. Ann N Y Acad Sci 2003; 991: 189–98.

Puopolo M, Raviola E, Bean BP. Roles of subthreshold calcium current and sodium current in spontaneous firing of mouse midbrain dopamine neurons. J Neurosci 2007; 27: 645–56.

Qin H, Buckley JA, Li X, Liu Y, Fox TH 3rd, Meares GP, et al. Inhibition of the JAK/STAT Pathway Protects Against alpha-Synuclein-Induced Neuroinflammation and Dopaminergic Neurodegeneration. J Neurosci 2016; 36: 5144–59.

Qin XY, Zhang SP, Cao C, Loh YP, Cheng Y. Aberrations in peripheral inflammatory cytokine levels in Parkinson disease: A systematic review and meta-analysis. JAMA Neurol 2016; 73: 1316–24.

Rabaneda-Lombarte N, Blasco-Agell L, Serratosa J, Ferigle L, Saura J, Solà C. Parkinsonian neurotoxicants impair the anti-inflammatory response induced by IL4 in glial cells: involvement of the CD200-CD200R1 ligand-receptor pair. Sci Rep 2020; 10: 1–19.

Raivich G. Like cops on the beat: The active role of resting microglia. Trends Neurosci 2005; 28: 571–3.

Ramirez GA, Yacoub MR, Ripa M, Mannina D, Cariddi A, Saporiti N, et al. Eosinophils from Physiology to Disease: A Comprehensive Review. Biomed Res Int 2018; 2018

Ramon S, Agüeras C. Pío del río ortega: A pioneer in the pathology of central nervous system tumors. Front Neuroanat 2016; 10: 1–8.

Ransohoff RM, Brown MA. Innate immunity in the central nervous system Find the latest version : Review series Innate immunity in the central nervous system. J Clin Invest 2012; 122: 1164–71.

Ransohoff RM, Engelhardt B. The anatomical and cellular basis of immune surveillance in the central nervous system. Nat Rev Immunol 2012; 12: 623–35.

Ransohoff RM, Perry VH. Microglial physiology: Unique stimuli, specialized responses. Annu Rev Immunol 2009; 27: 119–45.

Ransohoff RM, Schafer D, Vincent A, Blachère NE, Bar-Or A. Neuroinflammation: Ways in Which the Immune System Affects the Brain. Neurotherapeutics 2015; 12: 896–909.

Rasmussen MK, Mestre H, Nedergaard M. The glymphatic pathway in neurological disorders. Lancet Neurol 2018; 17: 1016–24.

Ray Dorsey E, Elbaz A, Nichols E, Abd-Allah F, Abdelalim A, Adsuar JC, et al. Global, regional, and national burden of Parkinson's disease, 1990–2016: a systematic analysis for the Global Burden of Disease Study 2016. Lancet Neurol 2018; 17: 939–53.

Read S, Malmström V, Powrie F. Cytotoxic T lymphocyte-associated antigen 4 plays an essential role in the function of CD25+CD4+ regulatory cells that control intestinal inflammation. J Exp Med 2000; 192: 295–302.

Recasens A, Ulusoy A, Kahle PJ, Di Monte DA, Dehay B. In vivo models of alpha-synuclein transmission and propagation. Cell Tissue Res 2017; 373: 183–93.

Reichmann H, Bilsing A, Ehret R, Greulich W, Schulz JB, Schwartz A, et al. Ergoline and non-ergoline derivatives in the treatment of Parkinson's disease. J Neurol 2006; 253: 36–8.

Reish HEA, Standaert DG. Role of α-synuclein in inducing innate and adaptive immunity in Parkinson disease. J Parkinsons Dis 2015; 5: 1–19.

Ren L, Yi J, Yang J, Li P, Cheng X, Mao P. Nonsteroidal anti-inflammatory drugs use and risk of Parkinson disease. Medicine (Baltimore) 2018; 97: e12172.

Rescigno M, Borrow P. The host-pathogen interaction: New themes from dendritic cell biology. Cell 2001; 106: 267–70.

Reynolds AD, Banerjee R, Liu J, Gendelman HE, Mosley RL. Neuroprotective activities of CD4+CD25+ regulatory T cells in an animal model of Parkinson's disease. J Leukoc Biol 2007; 82: 1083–94.

Reynolds AD, Stone DK, Hutter JAL, Benner EJ, Lee R, Gendelman HE. Regulatory T cells attenuate Th17 cell-mediated nigrostriatal dopaminergic neurodegeneration in a model of Parkinson's disease. J Immunol 2010; 184: 2261–71.

Reynolds AD, Stone DK, Mosley RL, Gendelman HE. Nitrated Alpha Synuclein Induced Alterations

in Microglial Immunity is Regulated by CD4+ T cell Subsets. J Immunol 2009; 182: 4137–49.

Reynolds AD, Stone DK, Mosley RL, Gendelman HE. Proteomic Studies of Nitrated Alpha-Synuclein Microglia Regulation by CD4+CD25+ T Cells. J Proteome Res 2009; 8: 3497–511.

Rinkevich B. Invertebrates versus vertebrates innate immunity: In the light of evolution. Scand J Immunol 1999; 50: 456–60.

Ritz B, Rhodes SL, Qian L, Schernhammer E, Olsen JH, Friis S. L-type calcium channel blockers and parkinson disease in Denmark. Ann Neurol 2010; 67: 600–6.

Robinson RT, Orme IM, Cooper AM. The onset of adaptive immunity in the mouse model of tuberculosis and the factors that compromise its expression. Immunol Rev 2015; 264: 46–59.

Rocha NP, Assis F, Scalzo PL, Vieira ÉLM, Barbosa IG, de Souza MS, et al. Reduced Activated T Lymphocytes (CD4+CD25+) and Plasma Levels of Cytokines in Parkinson's Disease. Mol Neurobiol 2018; 55: 1488–97.

Rodríguez-Moreno A, Banerjee A, Paulsen O. Presynaptic NMDA Receptors and Spike Timing-Dependent Depression at Cortical Synapses. Front Synaptic Neurosci 2010; 2: 18.

Rogers J, Luber-Narod J, Styren SD, Civin WH. Expression of immune system-associated antigens by cells of the human central nervous system: Relationship to the pathology of Alzheimer's disease. Neurobiol Aging 1988; 9: 339–49.

Rohn TT, Catlin LW. Immunolocalization of influenza a virus and markers of inflammation in the human Parkinson's disease brain. PLoS One 2011; 6

Rosenberg HF, Dyer KD, Foster PS. Eosinophils: Changing perspectives in health and disease. Nat Rev Immunol 2013; 13: 9–22.

Ross GW, Abbott RD, Petrovitch H, Morens DM, Grandinetti A, Tung KH, et al. Association of coffee and caffeine intake with the risk of Parkinson disease. J Am Med Assoc 2000; 283: 2674–9.

Rostami J, Fotaki G, Sirois J, Mzezewa R, Bergström J, Essand M, et al. Astrocytes have the capacity to act as antigen-presenting cells in the Parkinson's disease brain. J Neuroinflammation 2020; 17: 1–19.

Roy A, Mondal S, Kordower JH, Pahan K. Attenuation of microglial RANTES by NEMO-binding domain peptide inhibits the infiltration of CD8+ T cells in the nigra of hemiparkinsonian monkey. Neuroscience 2015; 302: 36–46.

Rüb U, Del Tredici K, Schultz C, Ghebremedhin E, De Vos RAI, Jansen Steur E, et al. Parkinson's disease: The thalamic components of the limbic loop are severely impaired by α-synuclein immunopositive inclusion body pathology. Neurobiol Aging 2002; 23: 245–54.

Sääksjärvi K, Knekt P, Rissanen H, Laaksonen MA, Reunanen A, Männistö S. Prospective study of coffee consumption and risk of Parkinson's disease. Eur J Clin Nutr 2008; 62: 908–15.

Sakaguchi S, Sakaguchi N, Masanao A, Misako I, Masaaki T. Immunologic Self-Tolerance

Maintained by Activated T Cells Expressing 11-2 Receptor a-Chains (CD25). J Immunol 1995; 155: 1151–64.

Salat D, Tolosa E. Levodopa in the treatment of Parkinson's disease: Current status and new developments. J Parkinsons Dis 2013; 3: 255–69.

Salter MW, Stevens B. Microglia emerge as central players in brain disease. Nat Med 2017; 23: 1018–27.

Samji T, Khanna KM. Understanding Memory CD8+ T cells. Immunol Lett 2017; 185: 32–9.

Sanchez-Guajardo V, Annibali A, Jensen PH, Romero-Ramos M. α-Synuclein Vaccination Prevents the Accumulation of Parkinson Disease-Like Pathologic Inclusions in Striatum in Association With Regulatory T Cell Recruitment in a Rat Model. J Neuropathol Exp Neurol 2013; 72: 624–45.

Sanchez-Guajardo V, Barnum CJ, Tansey MG, Romero-Ramos M. Neuroimmunological processes in Parkinson's disease and their relation to α-synuclein: Microglia as the referee between neuronal processes and peripheral immunity. ASN Neuro 2013; 5: 113–39.

Sanchez-Guajardo V, Febbraro F, Kirik D, Romero-Ramos M. Microglia acquire distinct activation profiles depending on the degree of alpha-synuclein neuropathology in a rAAV based model of Parkinson's disease. PLoS One 2010; 5

Santoro M, Maetzler W, Stathakos P, Martin HL, Hobert MA, Rattay TW, et al. In-vivo evidence that high mobility group box 1 exerts deleterious effects in the 1-methyl-4-phenyl-1,2,3,6-tetrahydropyridine model and Parkinson's disease which can be attenuated by glycyrrhizin. Neurobiol Dis 2016; 91: 59–68.

Sasco AJ, Paffenbarger RS, Gendre I, Wing AL. The Role of Physical Exercise in the Occurrence of Parkinson's Disease. Arch Neurol 1992; 49: 360–5.

Sato K, Fujita S. Dendritic cells-nature and classification. Allergol Int 2007; 56: 183–91.

Saunders JAH, Estes KA, Kosloski LM, Allen HE, Dempsey KM, Torres-Russotto DR, et al. CD4+ regulatory and effector/memory T cell subsets profile motor dysfunction in Parkinson's disease. J Neuroimmune Pharmacol 2012; 7: 927–38.

Schapira AHV, Cooper JM, Dexter D, Clark JB, Jenner P, Marsden CD. Mitochondrial Complex I Deficiency in Parkinson's Disease. J Neurochem 1990; 54: 823–7.

Schirmer M, Smeekens SP, Vlamakis H, Jaeger M, Oosting M, Franzosa EA, et al. Linking the Human Gut Microbiome to Inflammatory Cytokine Production Capacity. Cell 2016; 167: 1125–36.

Schröder JB, Pawlowski M, Meyer zu Hörste G, Gross CC, Wiendl H, Meuth SG, et al. Immune Cell Activation in the Cerebrospinal Fluid of Patients With Parkinson's Disease. Front Neurol 2018; 9: 1–7.

Schulz C, Perdiguero EG, Chorro L, Szabo-Rogers H, Cagnard N, Kierdorf K, et al. A lineage of myeloid cells independent of myb and hematopoietic stem cells. Science (80-) 2012; 336: 86–90.

Schwalbe G. Der Arachnoidalraum, ein Lymphraum und sein Zusammenhang mit dem Perichoroidalraum. Zentralblatt für medizinische Wiss 1869; 7: 465–7.

Scudamore O, Ciossek T. Increased oxidative stress exacerbates α-synuclein aggregation in vivo. J Neuropathol Exp Neurol 2018; 77: 443–53.

Sedelis M, Hofele K, Auburger GW, Morgan S, Huston JP, Schwarting RKW. MPTP susceptibility in the mouse: Behavioral, neurochemical, and histological analysis of gender and strain differences. Behav Genet 2000; 30: 171–82.

Sellgren CM, Gracias J, Watmuff B, Biag JD, Thanos JM, Whittredge PB, et al. Increased synapse elimination by microglia in schizophrenia patient-derived models of synaptic pruning. Nat Neurosci 2019; 22: 374–85.

Seo J, Park J, Kim K, Won J, Yeo HG, Jin YB, et al. Chronic Infiltration of T Lymphocytes into the Brain in a Non-human Primate Model of Parkinson's Disease. Neuroscience 2020; 431: 73–85.

Shaked I, Tchoresh D, Gersner R, Meiri G, Mordechai S, Xiao X, et al. Protective autoimmunity: Interferon-γ enables microglia to remove glutamate without evoking inflammatory mediators. J Neurochem 2005; 92: 997–1009.

Shameli A, Xiao W, Zheng Y, Shyu S, Sumodi J, Meyerson HJ, et al. A critical role for alpha-synuclein in development and function of T lymphocytes. Immunobiology 2015; 221: 333–40.

Sharon R, Goldberg MS, Bar-Josef I, Betensky RA, Shen J, Selkoe DJ. A-Synuclein Occurs in Lipid-Rich High Molecular Weight Complexes, Binds Fatty Acids, and Shows Homology To the Fatty Acid-Binding Proteins. Proc Natl Acad Sci U S A 2001; 98: 9110–5.

Sheffield LG, Berman NEJ. Microglial expression of MHC class II increases in normal aging of nonhuman primates. Neurobiol Aging 1998; 19: 47–55.

Shi L, Kam CM, Powers JC, Aebersold R, Greenberg AH. Purification of three cytotoxic lymphocyte granule serine proteases that induce apoptosis through distinct substrate and target cell interactions. J Exp Med 1992; 176: 1521–9.

Shichiri M. The role of lipid peroxidation in neurological disorders. J Clin Biochem Nutr 2014; 54: 151–60.

Shimohama S, Sawada H, Kitamura Y, Taniguchi T. Disease model: Parkinson's disease. Trends Mol Med 2003; 9: 360–5.

Shimoji M, Pagan F, Healton EB, Mocchetti I. CXCR4 and CXCL12 expression is increased in the nigro-striatal system of Parkinson's disease. Neurotox Res 2009; 16: 318–28.

Shortman K, Liu YJ. Mouse and human dendritic cell subtypes. Nat Rev Immunol 2002; 2: 151–61.

Shrikant P, Benveniste EN. The central nervous system as an immunocompetent organ: role of glial cells in antigen presentation. J Immunol 1996; 157: 1819–22.

Shulman LM. Gender differences in Parkinson's disease. Gend Med 2007; 4: 8–18.

Sidransky E, Lopez G. The link between the GBA gene and parkinsonism. Lancet Neurol 2012; 11: 986–98.

da Silva EZM, Jamur MC, Oliver C. Mast Cell Function: A New Vision of an Old Cell. 2014

da Silveira SA, Schneider BL, Cifuentes-Diaz C, Sage D, Abbas-Terki T, Iwatsubo T, et al. Phosphorylation does not prompt, nor prevent, the formation of α-synuclein toxic species in a rat model of Parkinson's disease. Hum Mol Genet 2009; 18: 872–87.

Simola N, Morelli M, Carta AR. The 6-hydroxydopamine model of Parkinson's disease. Neurotox Res 2007; 11: 151–67.

Simon KC, Gao X, Chen H, Schwarzschild MA, Ascherio A. Calcium channel blocker use and risk of Parkinson's disease. Mov Disord 2010; 25: 1818–22.

Singh A, Kukreti R, Saso L, Kukreti S. Oxidative stress: A key modulator in neurodegenerative diseases. Molecules 2019; 24: 1–20.

Singhania A, Pham J, Dhanwani R, Frazier A, Rezende Dutra J, Marder KS, et al. The TCR repertoire of α-synuclein-specific T cells in Parkinson's disease is surprisingly diverse. Sci Rep 2021; 11: 1–11.

Sipe GO, Lowery RL, Tremblay M, Kelly EA, Lamantia CE, Majewska AK. Microglial P2Y12 is necessary for synaptic plasticity in mouse visual cortex. Nat Commun 2016; 7

Skorvanek M, Martinez-Martin P, Kovacs N, Rodriguez-Violante M, Corvol JC, Taba P, et al. Differences in MDS-UPDRS Scores Based on Hoehn and Yahr Stage and Disease Duration. Mov Disord Clin Pract 2017; 4: 536–44.

Sloane JA, Hollander W, Moss MB, Rosene DL, Abraham CR. Increased microglial activation and protein nitration in white matter of the aging monkey. Neurobiol Aging 1999; 20: 395–405.

Smeyne M, Goloubeva O, Smeyne RJ. Strain-dependent susceptibility to MPTP and MPP+-induced parkinsonism is determined by glia. Glia 2001; 34: 73–80.

Smolders J, Heutinck KM, Fransen NL, Remmerswaal EBM, Hombrink P, ten Berge IJM, et al. Tissue-resident memory T cells populate the human brain. Nat Commun 2018; 9: 1–14.

Smolders J, Remmerswaal EBM, Schuurman KG, Melief J, Van Eden CG, Van Lier RAW, et al. Characteristics of differentiated CD8+ and CD4+ T cells present in the human brain. Acta Neuropathol 2013; 126: 525–35.

Solleiro-Villavicencio H, Rivas-Arancibia S. Effect of chronic oxidative stress on neuroinflammatory response mediated by CD4+T cells in neurodegenerative diseases. Front Cell Neurosci 2018; 12: 1–13.

Sommer A, Maxreiter F, Krach F, Fadler T, Grosch J, Maroni M, et al. Th17 Lymphocytes Induce Neuronal Cell Death in a Human iPSC-Based Model of Parkinson's Disease. Cell Stem Cell 2018;

23: 123-131.e6.

Soria FN, Engeln M, Martinez-Vicente M, Glangetas C, López-González MJ, Dovero S, et al. Glucocerebrosidase deficiency in dopaminergic neurons induces microglial activation without neurodegeneration. Hum Mol Genet 2017; 26: 2603–15.

Spillantini MG, Schmidt ML, Lee VM-Y, Trojanowski JQ. a -Synuclein in Lewy bodies. Nature 1997; 388: 839–40.

Staffen W, Mair A, Unterrainer J, Trinka E, Ladurner G. Measuring the progression of idiopathic Parkinson's disease with [123I] β-CIT SPECT. J Neural Transm 2000; 107: 543–52.

Steinbach K, Vincenti I, Kreutzfeldt M, Page N, Muschaweckh A, Wagner I, et al. Brain-resident memory T cells represent an autonomous cytotoxic barrier to viral infection. J Exp Med 2016; 213: 1571–87.

Stence N, Waite M, Dailey ME. Dynamics of microglial activation: A confocal time-lapse analysis in hippocampal slices. Glia 2001; 33: 256–66.

Stephenson J, Nutma E, van der Valk P, Amor S. Inflammation in CNS neurodegenerative diseases. Immunology 2018; 154: 204–19.

Stevens CH, Lewis S, Halliday GM. CD4 and CD8 T lymphocytes in Parkinson's disease and multiple system atrophy. Mov Disord 2012; 27: S29–30.

Stevens CH, Rowe D, Morel-Kopp MC, Orr C, Russell T, Ranola M, et al. Reduced T helper and B lymphocytes in Parkinson's disease. J Neuroimmunol 2012; 252: 95–9.

Streit WJ, Sparks DL. Activation of microglia in the brains of humans with heart disease and hypercholesterolemic rabbits. J Mol Med 1997; 75: 130–8.

Su X, Maguire-zeiss KA, Giuliano R, Prifti L, Venkatesh K, Federoff HJ. Synuclein activates microglia in a model of Parkinson's Disease Xiaomin. Neurobiol Aging 2008; 29: 1690–701.

Suffner J, Hochweller K, Kühnle M-C, Li X, Kroczek R a, Garbi N, et al. Dendritic cells support homeostatic expansion of Foxp3+ regulatory T cells in Foxp3.LuciDTR mice. J Immunol 2010; 184: 1810–20.

Sulzer D, Alcalay RN, Garretti F, Cote L, Kanter E, Agin-Liebes J, et al. T cells from patients with Parkinson's disease recognize α-synuclein peptides. Nature 2017; 546: 656–61.

Sulzer D, Antonini A, Leta V, Nordvig A, Smeyne RJ, Goldman JE, et al. COVID-19 and possible links with Parkinson's disease and parkinsonism: from bench to bedside [Internet]. npj Park Dis 2020; 6Available from: http://dx.doi.org/10.1038/s41531-020-00123-0

Sulzer D, Surmeier DJ. Neuronal vulnerability, pathogenesis, and Parkinson's disease. Mov Disord 2013; 28: 41–50.

Sun J, Madan R, Karp CL, Braciale TJ. Effector T cells control lung inflammation during acute influenza virus infection by producing IL-10. Nat Med 2009; 15: 277–84.

Surmeier DJ. Calcium, ageing, and neuronal vulnerability in Parkinson's disease. Lancet Neurol 2007; 6: 933–8.

Susanto O, Stewart SE, Voskoboinik I, Brasacchio D, Hagn M, Ellis S, et al. Mouse granzyme A induces a novel death with writhing morphology that is mechanistically distinct from granzyme B-induced apoptosis. Cell Death Differ 2013; 20: 1183–93.

Sutton VR, Trapani JA. Proteases in lymphocyte killer function: Redundancy, polymorphism and questions remaining. Biol Chem 2010; 391: 873–9.

Szymczak AL, Workman CJ, Wang Y, Vignali KM, Dilioglou S, Vanin EF, et al. Correction of multi-gene deficiency in vivo using a single 'self-cleaving' 2A peptide-based retroviral vector. Nat Biotechnol 2004; 22: 589–94.

Takahashi BT, Tagami T, Yamazaki S, Uede T, Shimizu J, Sakaguchi N, et al. Immunologic Self-Tolerance Maintained by CD25. J Exp Med 2000; 192

Tan EK, Chao YX, West A, Chan LL, Poewe W, Jankovic J. Parkinson disease and the immune system — associations, mechanisms and therapeutics. Nat Rev Neurol 2020; 16: 303–18.

Tansey MG, Romero-Ramos M. Immune system responses in Parkinson's disease: Early and dynamic. Eur J Neurosci 2019; 49: 364–83.

Tarlinton D. B cells still front and centre in immunology. Nat Rev Immunol 2019; 19: 85–6.

Taschenberger G, Garrido M, Tereshchenko Y, Bähr M, Zweckstetter M, Kügler S. Aggregation of alpha-synuclein promotes progressive in vivo neurotoxicity in adult rat dopaminergic neurons. Acta Neuropathol 2012; 123: 671–83.

Tatton NA, Kish SJ. In situ detection of apoptotic nuclei in the substantia nigra compacta of 1-methyl-4-phenyl-1,2,3,6-tetrahydropyridine-treated mice using terminal deoxynucleotidyl transferase labelling and acridine orange staining. Neuroscience 1997; 77: 1037–48.

Tay TL, Mai D, Dautzenberg J, Fernández-Klett F, Lin G, Sagar S, et al. A new fate mapping system reveals context-dependent random or clonal expansion of microglia. Nat Neurosci 2017; 20: 793–803.

Tentillier N, Etzerodt A, Olesen MN, Rizalar FS, Jacobsen J, Bender D, et al. Anti-inflammatory modulation of microglia via CD163-targeted glucocorticoids protects dopaminergic neurons in the 6-OHDA Parkinson's disease model. J Neurosci 2016; 36: 9375–90.

Thacker EL, O'Reilly EJ, Weisskopf MG, Chen H, Schwarzschild MA, McCullough ML, et al. Temporal relationship between cigarette smoking and risk of Parkinson disease. Neurology 2007; 68: 764–8.

Thakur P, Breger LS, Lundblad M, Wan OW, Mattsson B, Luk KC, et al. Modeling Parkinson's disease pathology by combination of fibril seeds and α-synuclein overexpression in the rat brain. Proc Natl Acad Sci 2017: 201710442.

Thayanidhi N, Helm JR, Nycz DC, Bentley M, Liang Y, Hay JC. Alpha-Synuclein Delays Endoplasmic

Reticulum (ER)-to-Golgi Transport in Mammalian Cells by Antagonizing ER/Golgi SNAREs. Mol Biol Cell 2010; 21: 1850–63.

Theodore S, Cao S, McLean PJ, Standaert DG. Targeted Overexpression of Human Alpha-Synuclein Triggers Microglial Activation and an Adaptive Immune Response in a Mouse Model of Parkinson Disease. J Neuropathol Exp Neurol 2008; 67: 1149–58.

Theodore S, Maragos W. 6-Hydroxydopamine as a tool to understand adaptive immune system-induced dopamine neurodegeneration in Parkinson's disease. Immunopharmacol Immunotoxicol 2015; 37: 393–9.

Thomas B, Flint Beal M. Parkinson's disease. Hum Mol Genet 2007; 16: 183–94.

Thome AD, Harms AS, Volpicelli-Daley LA, Standaert DG. microRNA-155 Regulates Alpha-Synuclein-Induced Inflammatory Responses in Models of Parkinson Disease. J Neurosci 2016; 36: 2383–90.

Thome AD, Standaert DG, Harms AS. Fractalkine signaling regulates the inflammatory response in an α-synuclein model of Parkinson disease. PLoS One 2015; 10: 1–13.

Togo T, Akiyama H, Iseki E, Kondo H, Ikeda K, Kato M, et al. Occurrence of T cells in the brain of Alzheimer's disease and other neurological diseases. J Neuroimmunol 2002; 124: 83–92.

Toledo JB, Gopal P, Raible K, Irwin DJ, Sedor S, Watts K, et al. Pathological α-synuclein Distribution in Subjects with Coincident Alzheimer's and Lewy Body Pathology. Acta Neuropathol 2016; 131: 393–409.

Ton TG, Heckbert SR, Longstreth WT, Rossing MA, Kukull WA, Franklin GM, et al. Nonsteroidal anti-inflammatory drugs and risk of Parkinson's disease. Mov Disord 2006; 21: 964–9.

Ton TGN, Heckbert SR, Longstreth WT, Rossing MA, Kukull WA, Franklin GM, et al. Calcium channel blockers and β-blockers in relation to Parkinson's disease. Park Relat Disord 2007; 13: 165–9.

Torra A, Parent A, Cuadros T, Rodríguez-Galván B, Ruiz-Bronchal E, Ballabio A, et al. Overexpression of TFEB Drives a Pleiotropic Neurotrophic Effect and Prevents Parkinson's Disease-Related Neurodegeneration. Mol Ther 2018; 26: 1552–67.

Tran HT, Chung CHY, Iba M, Zhang B, Trojanowski JQ, Luk KC, et al. α-Synuclein Immunotherapy Blocks Uptake and Templated Propagation of Misfolded α-Synuclein and Neurodegeneration. Cell Rep 2014; 7: 2054–65.

Trandem K, Zhao J, Fleming E, Perlman S. Highly Activated Cytotoxic CD8 T Cells Express Protective IL-10 At The Peak Of Coronavirus-induced Encephalitis. J Immunol 2011; 186: 3642–52.

Tretiakoff C. Contribution a l'Etude de l'Anatomiepathologique du Locus Niger de Soemmering Avec Quelques Deductions Relatives a la Pathologenie des Troubles Dutonus Musculaire de Lamaladiede Parkinson. 1919

Tsai CH, Lo SK, See LC, Chen HZ, Chen RS, Weng YH, et al. Environmental risk factors of young onset Parkinson's disease: A case-control study. Clin Neurol Neurosurg 2002; 104: 328–33.

Tupin E, Kinjo Y, Kronenberg M. The unique role of natural killer T cells in the response to microorganisms. Nat Rev Microbiol 2007; 5: 405–17.

Turvey SE, Broide DH. Chapter 2: Innate Immunity. J Allergy Clin Immunol 2010; 125: S24–32.

Uhlén M, Fagerberg L, Hallström BM, Lindskog C, Oksvold P, Mardinoglu A, et al. Tissue-based map of the human proteome. Science (80-) 2015; 347

Ulusoy A, Decressac M, Kirik D, Björklund A. Viral vector-mediated overexpression of alpha-synuclein as a progressive model of Parkinson's disease. Prog Brain Res 2010; 184: 89–111.

Ulvestad E, Williams K, Bø L, Trapp B, Antel J, Mørk S. HLA class II molecules (HLA-DR, -DP, -DQ) on cells in the human CNS studied in situ and in vitro. Immunology 1994; 82: 535–41.

Ünal İ, Emekli-Alturfan E. Fishing for Parkinson's Disease: A review of the literature. J Clin Neurosci 2019; 62: 1–6.

Unger MS, Li E, Scharnagl L, Poupardin R, Altendorfer B, Mrowetz H, et al. CD8+ T-cells infiltrate Alzheimer's disease brains and regulate neuronal- and synapse-related gene expression in APP-PS1 transgenic mice. Brain Behav Immun 2020; 89: 67–86.

Vaccari C, El Dib R, Gomaa H, Lopes LC, de Camargo JL. Paraquat and Parkinson's disease: a systematic review and meta-analysis of observational studies. J Toxicol Environ Heal - Part B Crit Rev 2019; 22: 172–202.

Vandenabeele F, Creemers J, Lambrichts I. Ultrastructure of the human spinal arachnoid mater and dura mater. J Anat 1996; 189 (Pt 2): 417–30.

Varnum MM, Ikezu T. The classification of microglial activation phenotypes on neurodegeneration and regeneration in Alzheimer's disease brain. Arch Immunol Ther Exp 2012; 60: 251–66.

Verkhratsky A, Butt A. Glial Neurobiology. First edit. Chichester: John Wiley & Sons, Ltd; 2007

Vila M, Vukosavic S, Jackson-Lewis V, Neystat M, Jakowec M, Przedborski S. α-synuclein up-regulation in substantia nigra dopaminergic neurons following administration of the parkinsonian toxin MPTP. J Neurochem 2000; 74: 721–9.

Visanji NP, Brotchie JM, Kalia L V., Koprich JB, Tandon A, Watts JC, et al. α-Synuclein-Based Animal Models of Parkinson's Disease: Challenges and Opportunities in a New Era. Trends Neurosci 2016; 39: 750–62.

Vivier E, Artis D, Colonna M, Diefenbach A, Di Santo JP, Eberl G, et al. Innate Lymphoid Cells: 10 Years On. Cell 2018; 174: 1054–66.

Vivier E, Ugolini S. Natural killer cells: From basic research to treatments. Front Immunol 2011; 2: 2–5.

Vlajinac H, Dzoljic E, Maksimovic J, Marinkovic J, Sipetic S, Kostic V. Infections as a risk factor for Parkinson's disease: A case-control study. Int J Neurosci 2013; 123: 329–32.

Volpicelli-Daley LA, Kirik D, Stoyka LE, Standaert DG, Harms AS. How can rAAV-α-synuclein and the fibril α-synuclein models advance our understanding of Parkinson's disease? J Neurochem 2016; 139: 131–55.

Volterra A, Magistretti PJ, Haydon PG. The Tripartite Synapse. First edit. Oxford: Oxford University Press; 2002

de Vos RAI, Jansen ENH, Stam FC, Ravid R, Swaab DF. 'Lewy body disease': clinico-pathological correlations in 18 consecutive cases of Parkinson's disease with and without dementia. Clin Neurol Neurosurg 1995; 97: 13–22.

Voskoboinik I, Whisstock JC, Trapani JA. Perforin and granzymes: Function, dysfunction and human pathology. Nat Rev Immunol 2015; 15: 388–400.

Wahmane SA, Achbani A, Ohaz Z, Elatiqi M, Belmouden A, Nejmeddine M. The possible protective role of α-synuclein against the SARS-CoV-2 infections in patients with Parkinson's disease. Mov Disord 2020; 35: 1293–4.

Wakabayashi K, Tanji K, Mori F, Takahashi H. The Lewy body in Parkinson's disease: Molecules implicated in the formation and degradation of α-synuclein aggregates. Neuropathology 2007; 27: 494–506.

Wakim LM, Woodward-Davis A, Bevan MJ. Memory T cells persisting within the brain after local infection show functional adaptations to their tissue of residence. Proc Natl Acad Sci 2010; 107: 17872–9.

Walker DG, Lue LF, Serrano G, Adler CH, Caviness JN, Sue LI, et al. Altered expression patterns of inflammation-associated and trophic molecules in substantia nigra and striatum brain samples from parkinson's disease, incidental lewy body disease and normal control cases. Front Neurosci 2016; 9: 1–18.

Wallings RL, Tansey MG. LRRK2 regulation of immune-pathways and inflammatory disease. Biochem Soc Trans 2019; 47: 1581–95.

Wang Q, Liu Y, Zhou J. Neuroinflammation in Parkinson's disease and its potential as therapeutic target. Transl Neurodegener 2015; 4: 1–9.

Watson MB, Richter F, Lee SK, Gabby L, Wu J, Masliah E, et al. Regionally-specific microglial activation in young mice over-expressing human wildtype alpha-synuclein. Exp Neurol 2012; 237: 318–34.

Weaver CT, Elson CO, Fouser LA, Kolls JK. The Th17 Pathway and Inflammatory Diseases of the Intestines , Lungs , and Skin. 2013

Wijeyekoon RS, Moore SF, Farrell K, Breen DP, Barker RA, Williams-Gray CH. Cerebrospinal Fluid Cytokines and Neurodegeneration-Associated Proteins in Parkinson's Disease. Mov Disord 2020; 35: 1062–6.

Williams-Gray CH, Wijeyekoon RS, Scott KM, Hayat S, Barker RA, Jones JL. Abnormalities of age-related T cell senescence in Parkinson's disease. J Neuroinflammation 2018; 15: 1–8.

Williams GP, Marmion DJ, Schonhoff AM, Jurkuvenaite A, Won WJ, Standaert DG, et al. T cell infiltration in both human multiple system atrophy and a novel mouse model of the disease. Acta Neuropathol 2020; 139: 855–74.

Wilson HL, O'Neill HC. Murine dendritic cell development: Difficulties associated with subset analysis. Immunol Cell Biol 2003; 81: 239–46.

Wirdefeldt K, Gatz M, Pawitan Y, Pedersen NL. Risk and protective factors for Parkinson's disease: A study in Swedish twins. Ann Neurol 2005; 57: 27–33.

Wissemann WT, Hill-Burns EM, Zabetian CP, Factor SA, Patsopoulos N, Hoglund B, et al. Association of parkinson disease with structural and regulatory variants in the hla region. Am J Hum Genet 2013; 93: 984–93.

Wolf SA, Boddeke HWGM, Kettenmann H. Microglia in Physiology and Disease. Annu Rev Physiol 2017; 79: 619–43.

Wong MT, Ong DEH, Lim FSH, Teng KWW, McGovern N, Narayanan S, et al. A High-Dimensional Atlas of Human T Cell Diversity Reveals Tissue-Specific Trafficking and Cytokine Signatures. Immunity 2016; 45: 442–56.

Woulfe J, Gray MT, Ganesh MS, Middeldorp JM. Human serum antibodies against EBV latent membrane protein 1 cross-react with α-synuclein. Neurol - Neuroimmunol Neuroinflammation 2016; 3: e239.

Woulfe JM, Gray MT, Gray DA, Munoz DG, Middeldorp JM. Hypothesis: A role for EBV-induced molecular mimicry in Parkinson's disease. Park Relat Disord 2014; 20: 685–94.

Wright AK, Miller C, Williams M, Arbuthnott G. Microglial activation is not prevented by tacrolimus but dopamine neuron damage is reduced in a rat model of Parkinson's disease progression. Brain Res 2008; 1216: 78–86.

Xicoy H, Peñuelas N, Vila M, Laguna A. Autophagic- and Lysosomal-Related Biomarkers for Parkinson's Disease: Lights and Shadows. Cells 2019; 8: 1–20.

Xu L, Daly T, Gao C, Flotte TR, Song S, Byrne BJ, et al. CMV-β-actin promoter directs higher expression from an adeno-associated viral vector in the liver than the cytomegalovirus or elongation factor 1α promoter and results in therapeutic levels of human factor X in mice. Hum Gene Ther 2001; 12: 563–73.

Yahr MD, Duvoisin RC, Schear MJ, Barrett RE, Hoehn MM. Treatment of parkinsonism with levodopa. Arch Neurol 1969; 21: 343–54.

Yamada M, Iwatsubo T, Mizuno Y, Mochizuki H. Overexpression of alpha-synuclein in rat substantia nigra results in loss of dopaminergic neurons, phosphorylation of alpha-synuclein and activation of caspase-9: Resemblance to pathogenetic changes in Parkinson's disease. J Neurochem 2004; 91: 451–61.

Yamada T, McGeer PL, McGeer EG. Lewy bodies in Parkinson's disease are recognized by antibodies to complement proteins. Acta Neuropathol 1992; 84: 100–4.

Yang F, Lagerros YT, Bellocco R, Adami HO, Fang F, Pedersen NL, et al. Physical activity and risk of Parkinson's disease in the Swedish National March Cohort. Brain 2015; 138: 269–75.

Yang F, Wolk A, Håkansson N, Pedersen NL, Wirdefeldt K. Dietary antioxidants and risk of Parkinson's disease in two population-based cohorts. Mov Disord 2017; 32: 1631–6.

Yen H-R, Harris TJ, Wada S, Grosso JF, Getnet D, Goldberg M V., et al. Tc17 CD8 T Cells: Functional Plasticity and Subset Diversity. J Immunol 2009; 183: 7161–8.

Yilmaz R, Strafella AP, Bernard A, Schulte C, van den Heuvel L, Schneiderhan-Marra N, et al. Serum Inflammatory Profile for the Discrimination of Clinical Subtypes in Parkinson's Disease. Front Neurol 2018; 9: 1–9.

Yipp BG, Kubes P. NETosis: How vital is it? Blood 2013; 122: 2784–94.

Zeitlin S, Liu JP, Chapman DL, Papaioannou VE, Efstratiadis a. Increased apoptosis and early embryonic lethality in mice nullizygous for the Huntington's disease gene homologue. Nat Genet 1995; 11: 155–63.

Zhang L, Dermawan K, Jin M, Liu R, Zheng H, Xu L, et al. Differential impairment of regulatory T cells rather than effector T cells by paclitaxel-based chemotherapy. Clin Immunol 2008; 129: 219–29.

Zhang N, Bevan MJ. Review CD8 + T Cells : Foot Soldiers of the Immune System. 2020

Zhang XF, Thompson M, Xu YH. Multifactorial theory applied to the neurotoxicity of paraquat and paraquat-induced mechanisms of developing Parkinson's disease. Lab Investig 2016; 96: 496–507.

Zhang Y, Feng S, Nie K, Li Y, Gao Y, Gan R, et al. TREM2 modulates microglia phenotypes in the neuroinflammation of Parkinson's disease. Biochem Biophys Res Commun 2018; 499: 797–802.

Zhao X, Jin T, Zheng C, Ma D, Zhang Y. Imbalance of Circulating Tfh/Tfr Cells in Patients With Parkinson's Disease. Front Neurol 2020; 11: 1–10.

Zhou TT, Zu G, Wang X, Zhang XG, Li S, Liang ZH, et al. Immunomodulatory and neuroprotective effects of ginsenoside Rg1 in the MPTP(1-methyl-4-phenyl-1,2,3,6-tetrahydropyridine) -induced mouse model of Parkinson's disease. Int Immunopharmacol 2015; 29: 334–43.

Zigmond MJ, Smeyne RJ. Exercise: Is it a neuroprotective and if so, how does it work? Park Relat Disord 2014; 20: S123–7.

Zinkernagel RM, Doherty PC. The discovery of MHC restriction. Immunol Today 1997; 18: 14–7.

Zolotukhin S, Byrne BJ, Mason E, Zolotukhin I, Potter M, Chesnut K, et al. Recombinant adeno-associated virus purification using novel methods improves infectious titer and yield. Gene Ther 1999; 6: 973–85.

Zrzavy T, Hametner S, Wimmer I, Butovsky O, Weiner HL, Lassmann H. Loss of 'homeostatic' microglia and patterns of their activation in active multiple sclerosis. Brain 2017; 140: 1900–13.

Zrzavy T, Machado-Santos J, Christine S, Baumgartner C, Weiner HL, Butovsky O, et al. Dominant role of microglial and macrophage innate immune responses in human ischemic infarcts. Brain Pathol 2018; 28: 791–805.

ANNEX I

Annex Table 1. Donor sample information

Case	Sex	Age at death (years)	Disease duration (years)	PMI (hours)	Cause of death	USSLBD
C-1	M	65	-	3,5	Metastatic lung cancer	0
C-2	M	93	-	3	Natural causes	0
C-3	M	79	-	3	Metastatic prostate cancer	0
C-4	F	75	-	2,5	Metastatic colon cancer	0
C-5	M	82	-	3	Sudden death syndrome, aortic stenosis	0
C-6	F	88	-	2,2	Congestive heart failure	0

Case	Sex	Age at death (years)	Disease duration (years)	PMI (hours)	Cause of death	USSLBD
C-7	M	96	-	3	Cardiorespiratory arrest, atrial fibrillation	0
iLBD-1	M	97	-	1,87	Prostate cancer	II
iLBD-2	F	79	-	2,22	Non-Hodgkin cancer	I
iLBD-3	F	91	-	4	Congestive heart failure	II
iLBD-4	M	79	-	5,6	Ventricular fibrillation, coronary artery disease, diabetes mellitus, obesity	III

Case	Sex	Age at death (years)	Disease duration (years)	PMI (hours)	Cause of death	USSLBD
iLBD-5	M	86	-	3,3	Chronic obstructive pulmonary disease	III
iLBD-6	M	81	-	2,25	Renal disease	I
iLBD-7	F	94	-	2,75	Cardiorespiratory arrest	II
iLBD-8	M	64	-	10	Natural causes	I
iLBD-9	M	78	-	6	Pulmonar neoplasia, ischemia	I
PD-1	F	92	10	3,67	Parkinson's disease, pneumonia	II

Case	Sex	Age at death (years)	Disease duration (years)	PMI (hours)	Cause of death	USSLBD
PD-2	M	80	10	2,83	Adult failure to thrive, COPD, Parkinson's disease	III
PD-3	M	90	2	2,25	Diffuse large B-cell lymphoma stage IV	III
PD-4	F	76	9	2,18	Breast cancer stage IV	III
PD-5	M	75	20	2,33	Parkinson's disease, dementia	III
PD-6	M	91	12	2,75	Metastatic cancer	III
PD-7	M	81	20	2,33	Parkinson's disease	IV

Case	Sex	Age at death (years)	Disease duration (years)	PMI (hours)	Cause of death	USSLBD
PD-8	M	75	14	3,97	Cardiorespiratory arrest	III
PD-9	M	80	14	4	Parkinson's disease	III
PD-10	M	76	17	2,42	Parkinson's disease, cardiopulmonary collapse	III
PD-11	M	72	12	3,37	Parkinson's disease	III
PD-12	F	85	18	3,58	Wasting syndrome, Parkinson's disease	IV
PD-13	M	81	14	2,38	Parkinson's disease	IV

Case	Sex	Age at death (years)	Disease duration (years)	PMI (hours)	Cause of death	USSLBD
PD-14	M	80	21	2,6	Mantle cell lymphoma, Parkinson's disease	IV
PD-15	M	83	21	2,47	Parkinson's disease	IV

F Female; *iLBD* incidental Lewy Body disease; *M* Male; PD *Parkinson's disease*; *PMI* post-mortem interval; *USSLBD* unified staging system for Lewy body disorders

Annex Table 2. Clinical and autopsy information

Case	Clinical history	Autopsy
C-1	Restless legs syndrome without other neurological or cognitive condition (4 years bd); metastatic adenocarcinoma; 4 cycles of chemotherapy with Gemzar and Carboplatin without much response; Chemoembolization of the liver (16 months before death); A course of Taxol (last, 5 months bd); Acute thrombocytopenia and idiopathic thrombocytopenic purpura; Developed multi-organ failure.	Adenocarcinoma, poorly differentiated, involving several organs; Calcific atherosclerosis of aorta; Urinary bladder with vascular congestion; Pulmonary congestion; Fibrinous pericarditis; Extensive adhesions, thoracic viscera and colon; Stenosis, descending colon; Cholelithiasis; Lumbar spinal scoliosis; Venous insufficiency, extremities; Onychomycosis, feet.
C-2	Normal cognitive function; Essential tremor; Adult-onset diabetes mellitus; Malignant melanoma resected from his back (14 years bd); Myelodysplastic syndrome; Hypertension; Coronary artery disease; Mitral insufficiency; Aortic stenosis; Congestive heart failure; Pulmonary hypertension; Pulmonary granulomatous disease; Gastroesophageal reflux disease; Gastric peptic ulcer disease; Nephrolithiasis; Benign prostatic hypertrophy; Cataracts; Osteoarthritis.	Cardiac hypertrophy; Pericardial effusion; Calcific atherosclerosis, aorta; Hypercellular bone marrow; Benign renal cortical cysts; Renal calculi; Sigmoid colon diverticulosis; Hepatic atrophy; Splenomegaly; Pancreatic neuroendocrine neoplasm; Benign prostatic hyperplasia with prostatic calculi; Testicular atrophy; Sialoadenitis with sialolithiasis; Emphysema; Osteopenia.
C-3	Restless legs syndrome and essential tremor; Normal cognitive function; Transurethral resection of the prostate for benign hypertrophy (16 years bd); prostate cancer metastatic to the spine and regional lymph nodes, treated with anti-androgen agents cyclophosphamide (4 years bd); Carcinoma treated chemotherapeutic agents cisplatin and gemcitabine (4 years bd); treated with radiation therapy to the	Invasive urothelial carcinoma of bladder with invasion into perivesical fat; Metastatic carcinoma involving several organs; Acute bronchopneumonia with coccoid bacteria; Cardiomegaly; Pleural effusion; Nephrosclerosis; Renal cortical cysts; Testicular atrophy; Colloid nodule, left thyroid lobe; Splenomegaly; Capsular cyst, liver; Status post appendectomy;

	pelvic lymph nodes, bladder and prostate (8 months bd); Asthma; Mastocytosis; Perennial allergic rhinitis; Arthritis; Terminally developed renal insufficiency and anemia.	Inguinal herniorrhaphy; Sigmoid colon resection for diverticulitis.
C-4	Chronic fatigue syndrome; Fibromyalgia; Depression; Restless legs syndrome; Essential tremor; Transient left-sided paralysis after stomach surgery for hiatal hernia (23 years bd); Paresthesias (9 years bd); Two cycles of chemotherapy with a modified FOLFOX protocol to treat colonic adenocarcinoma with pelvic and perhepatic subcapsular metàstasis (14 months bd); Hypertension; Hysterctomy; Type 2 diabetes; Arthritis.	Colonic adenocarcinoma with metastases to several organs; Acute pyelonephritis; Arterial nephrosclerosis; Renal cortical cyst; Emphysema; Hepatic steatosis; Atherosclerotic stenosis, coronary arteries; Calcification, aortic valve; Aortic atherosclerosis; Status post cholecystectomy; Diverticulosis, sigmoid colon; Splenic capsular fibrosis; Status post hysterectomy with bilateral salpingo-oophorectomy; Osteopenia.
C-5	“Mild senile intention tremor" but was otherwise free of neurological illnesses; Aortic stenosis, carotid artery disease; Hypertension; Arthritis; Benign prostatic hypertrophy; Multiple excised benign skin cancers; Cataracts; Benign left lung nodule and left adrenal and renal mass lesions; Persistent normocytic anemia; Malignant melanoma excised from skin (22 months bd); Mild chronic obstructive pulmonary disease; Mild chronic renal insufficiency	Aortic valve calcification; Atherosclerosis involving coronary arteries and aorta; Cardiac hypertrophy; Coccidioidal granuloma, lung; Emphysema with apical pleural blebs; Diverticulosis, sigmoid colon; Benign renal cortical cysts; Glomerular nephrosclerosis; Benign prostatic hypertrophy.
C-6	Sleep disturbance and restless legs syndrome; Depression; Bilateral sensorineural hearing loss; left breast cancer and metastatic carcinoma treated with mastectomy and six cycles of CMF followed by chest wall radiation (9 years bd); Hyperlipidemia; Hypertension; Atrial fibrillation; Hypothyroidism; Gastroesophageal reflux disease;	Solitary skin and soft tissue metastasis, left axilla; No other metastatic disease identified; Generalized atherosclerosis; Coronary artery stenosis; Remote myocardial infarct; Aortic atherosclerosis; Cardiomegaly; Patchy acute bronchopneumonia; Small organized pulmonary embolism; Bilateral apical fibrous

	Colonic polyps; Herniorrhaphy; Osteoporosis; Oateoarthritis; Pulmonary fibrosis; Pelvic fracture (1 year bd).	caps, lungs; Nephrosclerosis; Renal cortical cysts; Chronic thyroiditis; Acute hepatic congestion; Osteopenia.
C-7	Normal limits for cognition and motor function; Hypercholesterolemia; Hypertension; Sick sinus syndrome status post cardiac pacemaker placement; Orthostatic hypotension; Insomnia; Hypothyroidism and prostatic hypertrophy with urethral obstruction; Severe knee arthritis; using an electric wheelchair; Cataract.	Status post cardiac pacemaker placement; Coronary artery disease; Cardiac left ventricular apex scarring suggestive of remote infarct; Aortic valve with calcification; Calcific atherosclerosis of thoracic and abdominal aorta; Pleural blebbing; Pulmonary Coccidioides granuloma; Peribronchial lymph nodes with Coccidioides granulomas; Bilateral renal cortical cysts; Hepatic atrophy with centrilobular congestion; Benign prostatic hyperplasia.
iLBD-1	Normal C in terms of both cognition and movement; Prostate cancer status post prostatectomy and then treated hormonally; Bone metastases (1-2 months bd); Hypertension; Atherosclerotic coronary artery disease; Hyperlipidemia; Paroxysmal atrial fibrillation; Chronic congestive heart failure; Chronic obstructive pulmonary disease; Chronic renal failure; Gout; Glaucoma; Gastroesophageal reflux disease; Nephrolithiasis; Paget's disease of the skull; Lumbar laminectomy; Osteoarthritis; Cataracts.	Metastatic prostatic adenocarcinoma involving bone and bladder; Acute bronchopneumonia; Atelectasis; Cardiomegaly; Aorta, thoracic and abdominal, moderate calcific atherosclerosis; Bilateral lungs, adhesions; Liver, chronic passive congestion and steatosis; Nephrosclerosis; Chronic pyelonephritis; Kidney calculus; Duodenum, spindle cell nodule consistent with leiomyoma; Thyroid, nodular hyperplasia; Abdominal obesity; Status post remote lumbar laminectomy.
iLBD-2	Cognitively normal C; Myelodsyplastic syndrome and pancytopenia; Splenomegaly; Chronic obstructive pulmonary disease; Congestive heart failure; Colitis; CHOP chemotherapy to treat diffuse large B-cell lymphoma (3 weeks bd); Hypertension; Dyslipidemia; Hiatal hernia;	Dyspoietic changes of bone marrow; Splenomegaly; Depletion of splenic white pulp with necrosis; Ischemic change with pseudomembranes, ascending and transverse colon; Ascites, abdominal cavity; Atherosclerosis, coronary arteries and aorta; Calcifications, aortic valve;

	Gastroesophageal reflux disease; Degenerative joint and disc disease (arthritis); Lumbar laminectomy.	Cardiomegaly; Pleural adhesions; Acute hepatic congestion; Right ovary not identified.
iLBD-3	Modest senile intention tremor; Ischemic attack with expressive aphasia (5 years bd); Hypertension; Thoracic aortic aneurysm; Primary atrioventricular block; Aortic stenosis with valve replacement (22 years bd); Cardiac pacemaker placed for sick sinus syndrome; Peripheral vascular disease; Pulmonary hypertension and chronic obstructive pulmonary disease; "Old granulomatous disease" involving several organs; Fibrocystic breast disease; Hypothyroidism; Glaucoma; Cataracts; Osteoarthritia; Osteoporosis; Hip fracture with some episodic disorientation (1 month bd).	
iLBD-4	Essential tremor and symptoms consistent with restless legs syndrome; Poorly Cled adult onset diabetes; hypertension; Hyperlipidemia; Adenocarcinoma of the prostate, treated with radioactive seed implants (11 years bd).	Status post cardiopulmonary resuscitation; Hemopericardium; Severe atherosclerotic stenosis, coronary arteries; Moderate calcification, mitral and aortic valves; Cardiomegaly; Focal subendothelial scarring and myocyte hypertrophy; Calcific atherosclerosis, aorta; Hepatosplenomegaly: liver and spleen with congestion; Kidney cortex pattern consistent with persistent fetal lobulation; Hydrocele; Thyroid with focal adenomatous hyperplasia; Atrophic prostate with focal osseous metaplasia; Lungs with patchy emphysematous changes; Benign arteriolar nephrosclerosis.
iLBD-5	Mild cognitive impairment; Adult-onset diabetes mellitus; Gout; Arthritis; Obstructive sleep apnea; Chronic obstructive lung disease;	

	Hyperlipidemia; Hypertension; Coronary artery disease with angina pectoris; Congestive heart failure; Atrial fibrillation status post cardiac pacemaker placement; Abdominal aortic aneurysm; Gastroesophageal reflux disease; Benign prostatic hypertrophy status post transurethral resection.	
iLBD-6	Essential tremor and cognitively normal; Sleep apnea; Hyperlipidemia; Hypertension; Coronary artery disease; Atrial fibrillation; Congestive heart failure; Carotid artery disease; Aortic stenosis; Peripheral vascular disease; Chronic renal failure with nephrotic syndrome and focal segmental glomerulonephritis (on dialysis); Status post bilateral renal artery stent placement (9 years bd); Severe chronic obstructive pulmonary disease; Non-malignant colonic polyps (2 year bd).	Atherosclerotic vascular disease of left coronary artery and aorta; Calcific degeneration, aortic valve; Cardiomegaly; Centrilobular congestion and necrosis, liver; Melanosis coli with diverticulosis of sigmoid colon; Nephrosclerosis with findings consistent with focal segmental glomerulosclerosis; Nodular hyperplasia, prostate.
iLBD-7	Reduced ability for recalling the names of people and places (starting 2 years bd); Radical right mastectomy for breast cancer (23 years bd); Hysterectomy with bilateral salpingo-oophorectomy; Type II diabetes; Coronary artery disease; Congestive heart failure; Peripheral vascular disease; Hypertension; Hyperlipidemia; Gastroesophageal reflux disease; Blind due to glaucoma and macular degeneration; Osteoporosis; Arthritis.	
iLBD-8	Cognitively normal C; Dyslipidemia; Hyperglycemia (probable diabetes mellitus); replacement of mitral valve with mechanical prosthesis due to papillary muscle rupture after	

	myocardium infarct; Atheroma plate in the aortic arch.	
iLBD-9	Cognitively normal C; Lung neoplasm spread to respiratory and digestive system (not treated with chemotherapy); Heart attack; Ischemic heart disease; Cardiac arrhythmia due to atrial fibrillation; Chronic heart failure; Chronic obstructive pulmonary disease; Fibrothorax; Hypertension; Dyslipidemia; Hyperglycemia; Psoriasis; Leg edema; Cataract.	
PD-1	Clinical diagnosis of Parkinson's disease; Restless legs syndrome; Breast cancer status post right modified radical mastectomy (15 years bd); Peripheral vascular disease; Asthma; Gastroesophageal reflux disease; Esophageal stricture; Irritable bowel syndrome; Macular degeneration; Cataracts; Osteoporosis and osteoarthritis with knee replacement surgery.	Mild atherosclerotic stenosis, coronary arteries; Calcification, mitral and aortic valves; Cardiomegaly; Severe aortic atherosclerosis; Arterionephrosclerosis; Acute and chronic bronchial inflammation; Pleural fibrosis; Candida esophagitis; Mild superficial chronic gastritis; Acute proctitis with focal pseudomembrane formation; Acute hepatic congestion with early ischemia; Patchy atrophy of pancreas; Incidental renal papilloma; Benign endometrial polyp; Uterine leiomyomata; Chronic inflammation of vagina.
PD-2	Clinical diagnosis of Parkinson's disease; Prostate cancer status post radical prostatectomy (14 years bd); Hypertension; Hyperlipidemia; Coronary artery disease status post angioplasty (3 years bd); Atrial fibrillation and paroxysmal atrial tachycardia; Constrictive pericarditis status post pericardial stripping (3 years bd); Aortic valvular sclerosis; Congestive heart failure; Chronic obstructive	Acute bronchopneumonia; Generalized atherosclerosis; Severe pericardial adhesions; Emphysema; Bilateral severe pleural adhesions; Arterionephrosclerosis with renal atrophy; Benign right renal cortical cyst; Hepatic atrophy; Status post midline thoracotomy; Status post radical prostatectomy, no evidence of recurrent or metastatic disease; Status post appendectomy;

	pulmonary disease; Pneumonia (1 and 3 years bd); Barrett's esophagus; Hypothyroidism; Small fiber peripheral neuropathy.	Osteopenia; Mild testicular atrophy.
PD-3	Mildly decreased extremity agility; essential tremor; bradykinesia; Diffuse large B-cell lymphoma; Hypertension; Hyperlipidemia; Hypothyroidism; Obstructive sleep apnea; Chronic normocytic anemia; Prostatic hypertrophy, high-grade prostatic intraepithelial neoplasia; Cataract extraction with lens implantations; Glucose intolerance.	Chronic periportal hepatitis with bridging fibrosis; Residual lymphoma not identified; Mild cardiomegaly; Calcification of mitral and aortic valves; Atherosclerosis involving aorta and coronary arteries; Diverticulosis, sigmoid colon; Chronic cholecystitis with cholelithiasis; Mild thyroidal goiter; Testicular atrophy; Benign prostatic hypertrophy; Emphysema; Arteriolar nephrosclerosis; Chronic esophagitis; Chronic cystitis.
PD-4	Clinical diagnoses of Parkinson's disease and mild cognitive impairment; left breast adenocarcinoma treated with mastectomy and tamoxifen (14 years bd); Rheumatoid arthritis; Hypothyroidism; Suspected left apical lung granuloma; Gastroesophageal reflux disease, Cataract; Spinal osteoarthritis; Osteopenia.	Old myocardial infarction; Atherosclerotic stenosis, coronary arteries; Calcification, tricuspid and pulmonary valves; Calcification, mitral and aortic valves; Cardiomegaly; Moderate aortic atherosclerosis; Adenocarcinoma, morphologically consistent with mammary (ductal) carcinoma, metastatic to lungs, peribronchial lymph node and rib; Pleural effusion; Ascites; Clear cell adenocarcinoma; Hypercoagulable state with organizing thrombi in several organs; Nodular hyperplasia, thyroid; Status post left mastectomy; Status post cardiac monitor placement; Status post appendectomy.
PD-5	Clinical diagnosis of Parkinson's disease; Bilateral subthalamic nucleus placement of deep brain stimulators (2 years bd); REM sleep disorder; Unstable angina pectoris with aortocoronary triple bypass	Acute bronchopneumonia; Chronic ischemic heart disease; Severe coronary atherosclerosis, status post coronary artery bypass graft; Pericardial adhesions; Atherosclerotic abdominal aortic

	surgery (11 bd); Transient ischemic attack (3 and 5 years bd).	aneurysm, distal aorta; Aortic atherosclerosis; Mild portal hepatitis without fibrosis; Macrovesicular steatosis of liver; Acute hepatic congestion; Right renal atrophy; Mucosal hemorrhage; Splenomegaly; Colloid nodule, left superior lobe thyroid; Nodular cortical hyperplasia, right adrenal gland; Atrophy, testis; Stenosis, terminal ileum; Mucosal hemorrhage, rectum.
PD-6	Clinical diagnosis of Parkinson's disease; Atherosclerotic coronary artery disease; Paroxysmal atrial fibrillation; Chronic obstructive pulmonary disease and congestive heart failure; Cataracts; Cholecystectomy; Gastroesophageal reflux; Right-sided colectomy to treat adenocarcinoma of the ascending colon (4 years bd); Metastatic deposits in the lungs and liver (1 year bd).	Status post right hemicolectomy; Metastatic colorectal carcinoma involving lungs, liver and soft tissue of lower chest wall/upper abdominal wall; Ventricular hypertrophy; Aortic atherosclerosis; Bilateral renal atrophy; Acute sialadenitis, submandibular gland; Chronic gastritis with focal atrophy and intestinal metaplasia; Colloid nodule, thyroid; Osteopenia; Status post cholecystectomy; Status post resection of prostate gland.
PD-7	Clinical diagnosis of Parkinson's disease; Recurrent aspiration pneumonia; Dysphagia; Hyponatremia due to idiopathic syndrome of inappropriate anti-diuretic hormone secretion; Hypothyroidism; Pyloric valve stenosis; Gastroesophageal reflux disease; Peptic ulcer disease status post Billroth II surgery with vagotomy (30 years bd); Osteoporosis; Cataracts; Post-mortem serology positive for hepatitis B surface and core antibodies.	Urothelial carcinoma with squamous differentiation involving urinary bladder and replacing prostate gland; Acute pyelonephritis; Nephrosclerosis; Nodular fibrosis with calcification and osseous metaplasia, heart, left ventricle; Aorta atherosclerosis; Calcification of mitral valve; Pericardial adhesions; Pleural adhesions; Patchy lymphoid interstitial infiltrates, lungs; Active esophagitis with epithelial denudation; Chronic gastritis without atrophy; Perivascular fibrosis with dystrophic calcification, spleen; Testicular

		atrophy; Cachexia; Cholelithiasis; Status post partial gastrectomy.
PD-8	Clinical diagnoses of Parkinson's disease and dementia; non-Hodgkins lymphoma treated with chemotherapy, in remission for 11 years bd; Hypertension; Atrial fibrillation; Chronic renal insufficiency and urinary obstruction due to prostatic hypertrophy; Skull fracture, subdural and subarachnoid hemorrhage and numerous small hemorrhagic contusions bilaterally in the frontal and occipital lobes (5 years bd).	Cardiac hypertrophy; Atherosclerotic stenosis, coronary arteries; Calcification, mitral and aortic valves; Calcific atherosclerosis, aorta; Renal cortical cysts; Benign prostatic hypertrophy; Prostatic calculi; Papillary carcinoma of thyroid, follicular variant; Testicular atrophy; Arteriolar nephrosclerosis; Chronic cystitis.
PD-9	Clinical diagnosis of Parkinson's disease and dementia; Seizures, causing falls; Coronary artery stenting for occlusive disease (10 years bd); Obesity, Hypertension; Hyperlipidemia; Gout; Gastroesophageal reflux disease; Depression; Cataracts; Thrombocytopenia; Osteoporosis; Pernicious anemia; Pneumonia and pleuritic chest pains and cough for three or four years (few years bd); Sleep apnea; Centrilobular emphysema.	Heart, cardiomegaly with left ventricular myocardial hypertrophy; Pleural adhesions; Bilateral lungs, consolidation, emphysematous change, chronic interstitial inflammation; Bilateral kidneys, cortical cysts, chronic interstitial inflammation, Mild nephrosclerosis; Bladder, chronic cystitis; Aorta, mild atherosclerosis; Splenomegaly; Liver, mild congestion; Obesity.
PD-10	Clinical diagnosis of Parkinson's disease and dementia; REM sleep behavior disorder; Restless legs syndrome; Hypertension; Atrial fibrillation; Congestive heart failure; Benign prostatic hypertrophy; Gastritis and diverticulosis.	Cardiomegaly; Atherosclerotic stenosis, coronary arteries; Aortic atherosclerosis; Calcification of aortic and mitral valves; Acute hemorrhagic bronchopneumonia; Mild pleural adhesions; Pleural blebbing, bilateral; Chronic cholecystitis with cholelithiasis; Chronic inactive gastritis; Benign nodular hyperplasia, prostate; Diverticulosis, sigmoid colon; Incidental bile duct hamartomas;

		Status post cardiac pacemaker placement.
PD-11	Clinical diagnoses of Parkinson's disease and dementia; soft speech; Prostate cancer status post radical prostatectomy (3 years bd); Ventricular tachycardia; Idiopathic thrombocytopenic purpura; Osteoporosis.	Atherosclerotic stenosis of coronary arteries; Old myocardial infarction, left ventricle; Aortic atherosclerosis; Mild benign nephrosclerosis; Status post radical prostatectomy.
PD-12	Clinical diagnoses of Parkinson's disease and dementia; REM behavior sleep disorder; Periodic limb movements of sleep and restless legs syndrome; Bilateral deep brain stimulating electrodes placed in the globus pallidus interna (7 years bd); Longstanding left-sided Bell's palsy; Obstructive sleep apnea; Neurogenic bladder; Benign breast biopsy; Thyroid nodules; Endometrial cancer status post hysterectomy with bilateral salpingo-oophorectomy (11 years bd).	Cachexia; Atherosclerotic stenosis, coronary arteries; Calcification, mitral and aortic valves; Atherosclerosis, abdominal and thoracic aorta; Pleural adhesion; Emphysema with pleural blebbing; Acute laryngeal mucosal inflammation; Hepatic atrophy with acute hepatic congestion; Patchyacute esophagitis; Adhesions, small bowel; Incidental submucosal lymphangioma of jejunum; Melanosis coli; Bilateral renal atrophy; Nodular hyperplasia with focal calcification, thyroid; Osteopenia; Status post hysterectomy with bilateral salpingo-oophorectomy; No evidence of recurrence or metastatic disease.
PD-13	Clinical diagnosis of Parkinson's disease; Essential tremor; REM sleep behavior disorder; Paroxysmal atrial fibrillation; Melanoma (past); Colonic polyps (past); Cataracts; Aspiration pneumonia with empyema (5 years bd); Prostate resection to treat urinary retention (1 year bd).	Acute bronchopneumonia and patchy emphysematous changes; Pleural adhesions; Atherosclerotic stenosis, coronary arteries; atherosclerosis, abdominal and thoracic aorta; Calcification, heart valves; Cardiomegaly; Intraluminal bladder mass, favor infarcted benign prostatic hyperplasia; Enlarged prostate gland, consistent with benign prostatic hyperplasia; Multinodular goiter, thyroid gland; Chronic gastritis; Pancreas with focal and mild

		nonspecific inflammation and fibrosis, cannot exclude pancreatitis; Liver with agonal congestion and mild acute inflammation; Mild acute laryngitis; Benign renal arteriolar nephrosclerosis.
PD-14	Clinical diagnoses of Parkinson's disease; Essential tremor; REM sleep behavior disorder; Stage IV mantle cell lymphoma treated with 6 cycles of rituxan, Cytoxan, adriamycin and vincristine with maintenance rituximab (4 years bd); Recurrence and tonsillar tumor (3 years bd) and started with bendamustine and rituximab (3 years bd; duration of the treatment not reported); Recurrent mass at the ileocecal valve, treated with right hemicolectomy (2 years bd); IgM kappa monoclonal gammopathy; Hyperlipidemia, Coronary artery disease; Cardiac arrhythmia with pacemaker placement (21 years bd); Stable pulmonary nodule; Chronic renal insufficiency; Diverticulosis; Benign prostatic hypertrophy; Sleep apnea; Hypothyroidism; cataracts; Rotator cuff surgical repair.	Lymphoma, inguinal lymph node; Acute pyelonephritis in background cystic renal dysplasia; Cytomegalovirus enteritis with serosal adhesions, ileum; Cystitis, urinary bladder; Atherosclerotic stenosis, coronary arteries; Calcification, aortic valve and in other heart valves; Atherosclerosis, aorta; Status post cardiac pacemaker placement.
PD-15	Clinical diagnoses of Parkinson's disease and dementia; Cervical laminectomy for spinal stenosis (3 years bd); Aspiration pneumonia (2 years bd); Depression; Type II diabetes; Hypercholesterolemia; Hypertension; Coronary artery disease; Chronic kidney disease; Pernicious anemia; Glaucoma; Macular degeneration; Melanoma on the left shoulder (40 years bd); Thyroid nodules; Benign prostatic hypertrophy; Hernia surgery; Bilateral knee replacement.	Severe acute bronchopneumonia; Ehmphysematous changes of lungs; Peribronchial lymph node with necrotizing granulomatous lymphadenitis and associated Coccidioides organisms; Focal pleural fibrosis; Cardiac myocyte hypertrophy; Calcification of aortic, pulmonary and tricuspid valves; Atherosclerosis of coronary arteries; Mesenteric artery atherosclerosis; Bland submucosal spindle cell nodule, lower esophagus, favor schwannoma; Bladder diverticuli; acute and

	chronic cystitis; Kidneys with arteriolar nephrosclerosis, scattered sclerotic glomeruli; Thyroid cyst and multinodular goiter; Hepatic atrophy; Hepatic congestion; Testicular atrophy.

bd before death; *C* Control, *CHOP* cyclophosphamide, hydroxydaunorubicin, oncovin, prednisone, *CMF* cyclophosphamide, methotrexate, 5-fluorouracil, *FOLFOX* folinic acid, 5-fluorouracil, oxaliplatin; *iLBD* incidental Lewy Body disease; *PD* Parkinson's disease; *REM* Rapid eye movement

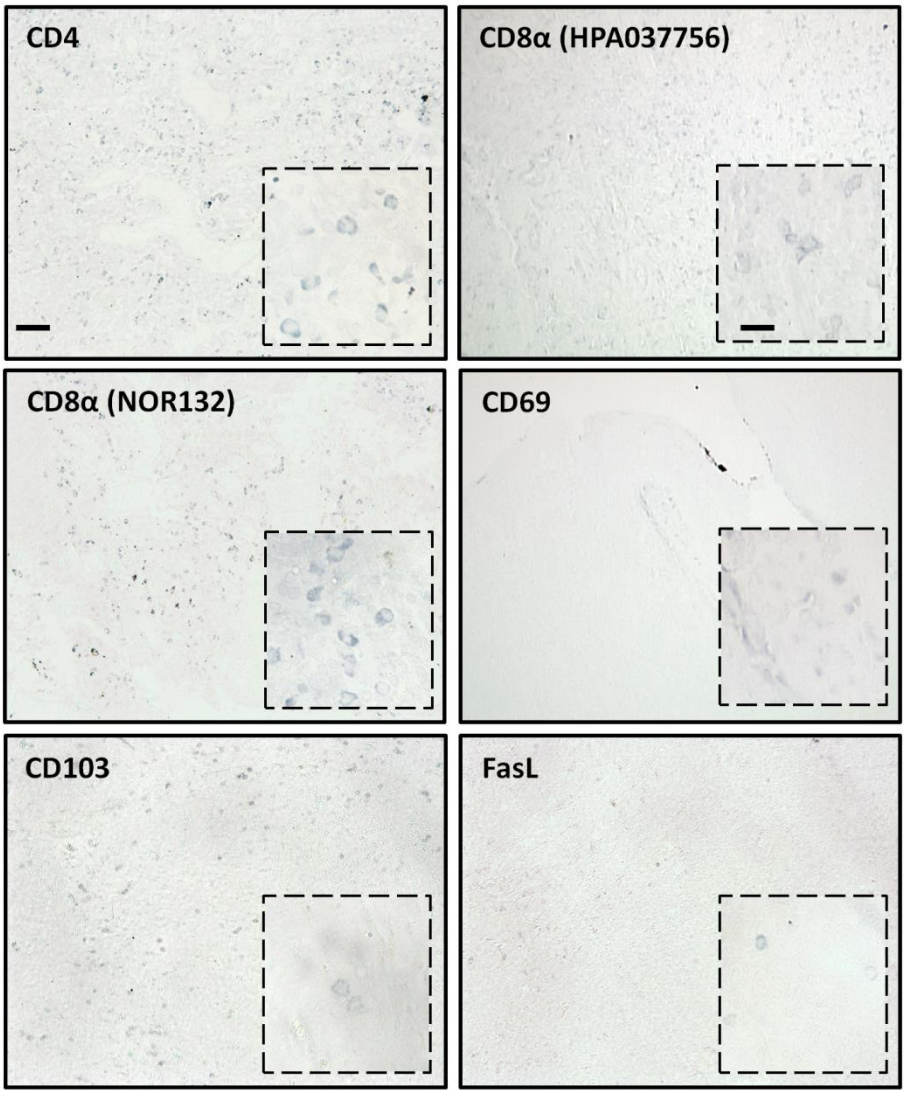

Annex Figure 1. Immunohistochemical images of human positive control tissues to detect T cell markers. Representative photomicrographs of human tonsil/lymph node sections for CD4, CD8α, CD69, CD103 and FasL. Positive staining for each antibody was compared with the staining reported by the company and/or www.proteinatlas.org repository (Uhlén *et al.,* 2015) in order to validate them. Low magnification picture scale bar = 60μm. Inset scale bar = 15μm.

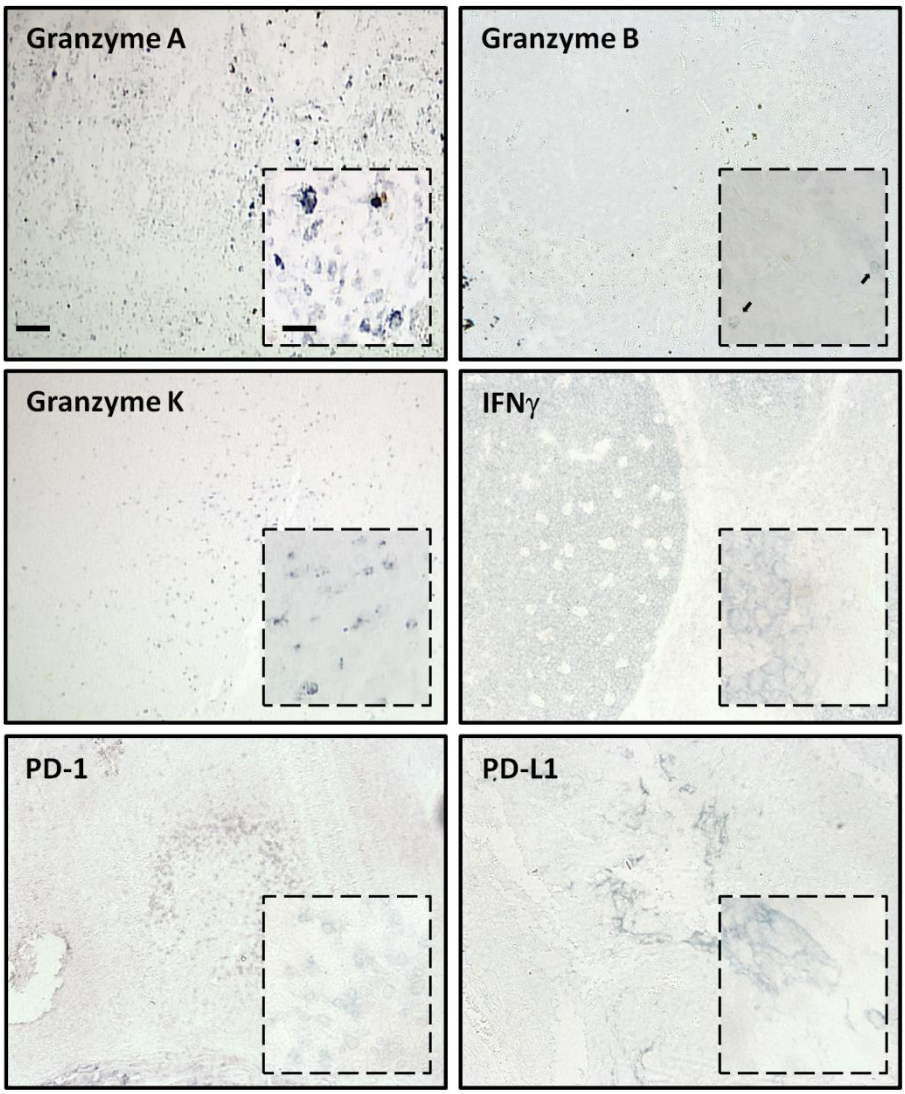

Annex Figure 1 (Continuation number 1). Immunohistochemical images of human positive control tissues to detect T cell markers. Representative photomicrographs of human tonsil/lymph node sections for Granzyme A, Granzyme B (arrows), Granzyme K, IFNγ, PD-1 and PD-L1. Positive staining for each antibody was compared with the staining reported by the company and/or www.proteinatlas.org repository (Uhlén *et al.,* 2015) in order to validate them. Low magnification picture scale bar = 60µm. Inset scale bar = 15µm.

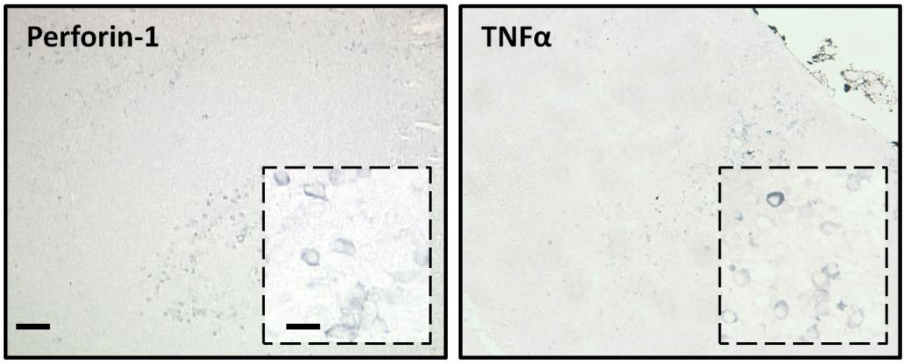

Annex Figure 1 (Continuation number 2). Immunohistochemical images of human positive control tissues to detect T cell markers. Representative photomicrographs of human tonsil/lymph node sections for Perforin-1 and TNFα. Positive staining for each antibody was compared with the staining reported by the company and/or www.proteinatlas.org repository (Uhlén *et al.,* 2015) in order to validate them. Low magnification picture scale bar = 60μm. Inset scale bar = 15μm.

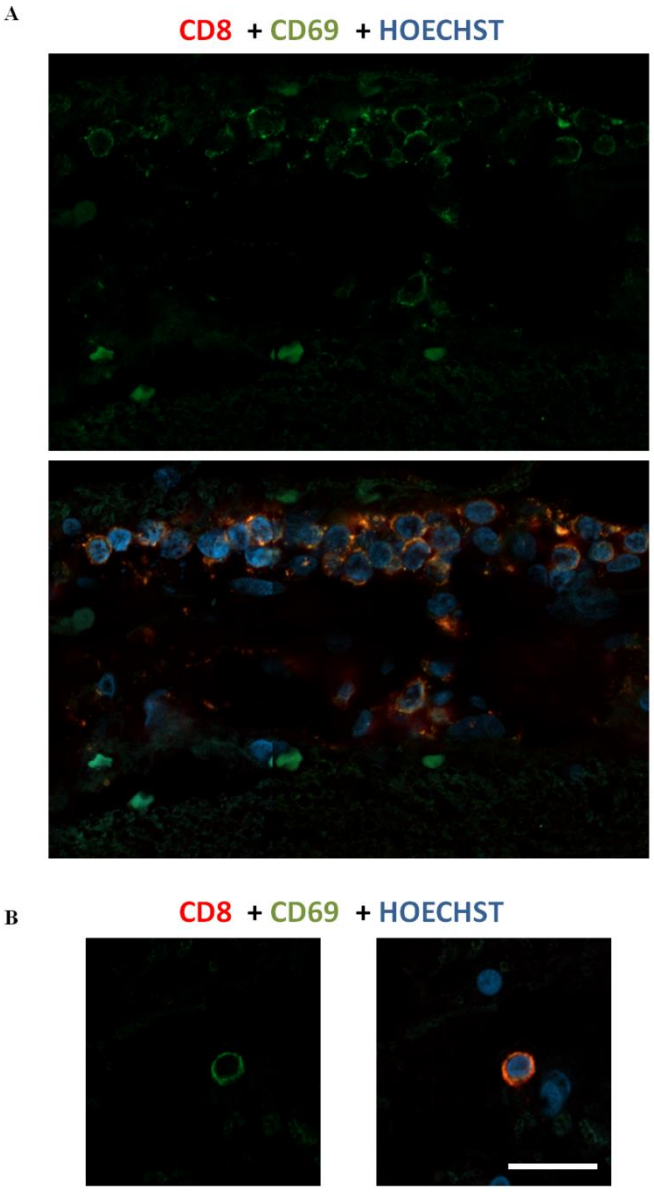

Annex Figure 2. Representative immunofluorescence images of perivascular and parenchymal CD8+ CD69+ T cells in the SN*pc*. High percentage of CD8+ (red) T cells in both perivascular spaces (**A**) and brain parenchyma (**B**) are CD69+ (green). Nuclei were stained with HOECHST (blue). Scale bar = 20µm.

ANNEX II

8. Annex II

1. Scientific articles belonging to my PhD thesis

CD8 T cell nigral infiltration precedes synucleinopathy in early stages of Parkinson's disease

Galiano-Landeira J., Torra A., Vila M., Bové J.

Brain, 2020 Oct 29; 143(12):3717-3733

DOI: https://doi.org/10.1093/brain/awaa269

Elucidating the role of both innate and adaptive immune responses in Parkinson's disease etiopathogenesis (In prep.)

Galiano-Landeira J., Torra A., Bové J.

2. Participation in other published articles

Validation of a reversed phase UPLC-MS/MS method to determine dopamine metabolites and oxidation intermediates in neuronal differentiated SH-SY5Y cells and brain tissue

González-Sepúlveda M., Laguna A., Carballo-Carbajal I., **Galiano-Landeira J.**, Romero-Gímenez J., Cuadros T., Parent A., Peñuelas N., Compte J., Nicolau A., Guillard-Sirieix C., Xicoy H., Kobayashi J., Vila M.

ACS Chemical Neuroscience, 2020 Sep 2; 11(17):2679-2687

DOI: https://doi.org/10.1038/s41467-019-08858-y

TFEB overexpression regulates mitochondrial phenotype and blocks mitochondria-mediated cell death in mice (In prep.)

Torra A., **Galiano-Landeira J.**, Vila M., Bové J.

3. Participation in congresses as a first and presenting author

Cytotoxic T cell nigral infiltration precedes synucleinopathy and neuronal death in Parkinson's disease.

Galiano-Landeira J., Torra A., Vila M., Bové J.

13 Jornades Científiques, Vall d'Hebron Institut de Recerca (VHIR), Barcelona, Spain, 2019. POSTER

Cytotoxic T cell nigral infiltration precedes synucleinopathy and neuronal death in Parkinson's disease.

Galiano-Landeira J., Torra A., Vila M., Bové J.

Translational Medicine explained (TMex), Training in Translational Research. Barcelona, Spain, 2019. POSTER

Adaptive immune response mediated by cytotoxic T lymphocytes is an early and progressive event in Parkinson's disease.

Galiano-Landeira J., Torra A., Pariente C., Vila M., Bové J.

49th Congress of the Society for Neuroscience (SfN). Chicaco, IL, USA, 2019. ORAL

Cytotoxic T cell nigral infiltration precedes synucleinopathy and neuronal death in Parkinson's disease.

Galiano-Landeira J., Torra A., Pariente C., Vila M., Bové J.

VII Scientific Conference, Institut de Neurociències, Universitat Autònoma de Barcelona (UAB), Sant Feliu de Guíxols, Spain, 2019. POSTER

Adaptive immune response mediated by cytotoxic T lymphocytes is an early and progressive event in Parkinson's disease.

Galiano-Landeira J., Torra A., Pariente C., Vila M., Bové J.

XI Simposi de Neurobiologia Experimental, Societat Catalana de Biologia, Barcelona, Spain, 2018. POSTER

Adaptive immune system in Parkinson's disease: the latent foe.

Galiano-Landeira J., Torra A., Barranco A., Melià M., Vila M., Bové J.

VI Scientific Conference, Institut de Neurociències, Universitat Autònoma de Barcelona (UAB), Sant Feliu de Guíxols, Spain, 2018. ORAL

4. Participation in other studies presented in congresses

Transcription Factor EB overexpression drives a neurotrophic effect that neuroprotects and neurorestores dopaminergic neurons in a mouse Parkinson's disease model.

Torra A., **Galiano-Landeira J.**, Parent A., Cuadros T., Rodríguez-Galván B., Ruiz-Bronchal E., Bortolozzi A., Vila M., Bové J.

XI Simposi de Neurobiologia Experimental, Societat Catalana de Biologia. Barcelona, Spain, 2018. ORAL

Activation of Transcription Factor EB as a neuroprotective strategy for Parkinson's disease.

Torra A., **Galiano-Landeira J.**, Parent A., Cuadros T., Rodríguez-Galván B., Ruiz-Bronchal E., Bortolozzi A., Vila M., Bové J.

II Congress of Biology, Societat Catalana de Biologia, Barcelona, Spain, 2018. ORAL

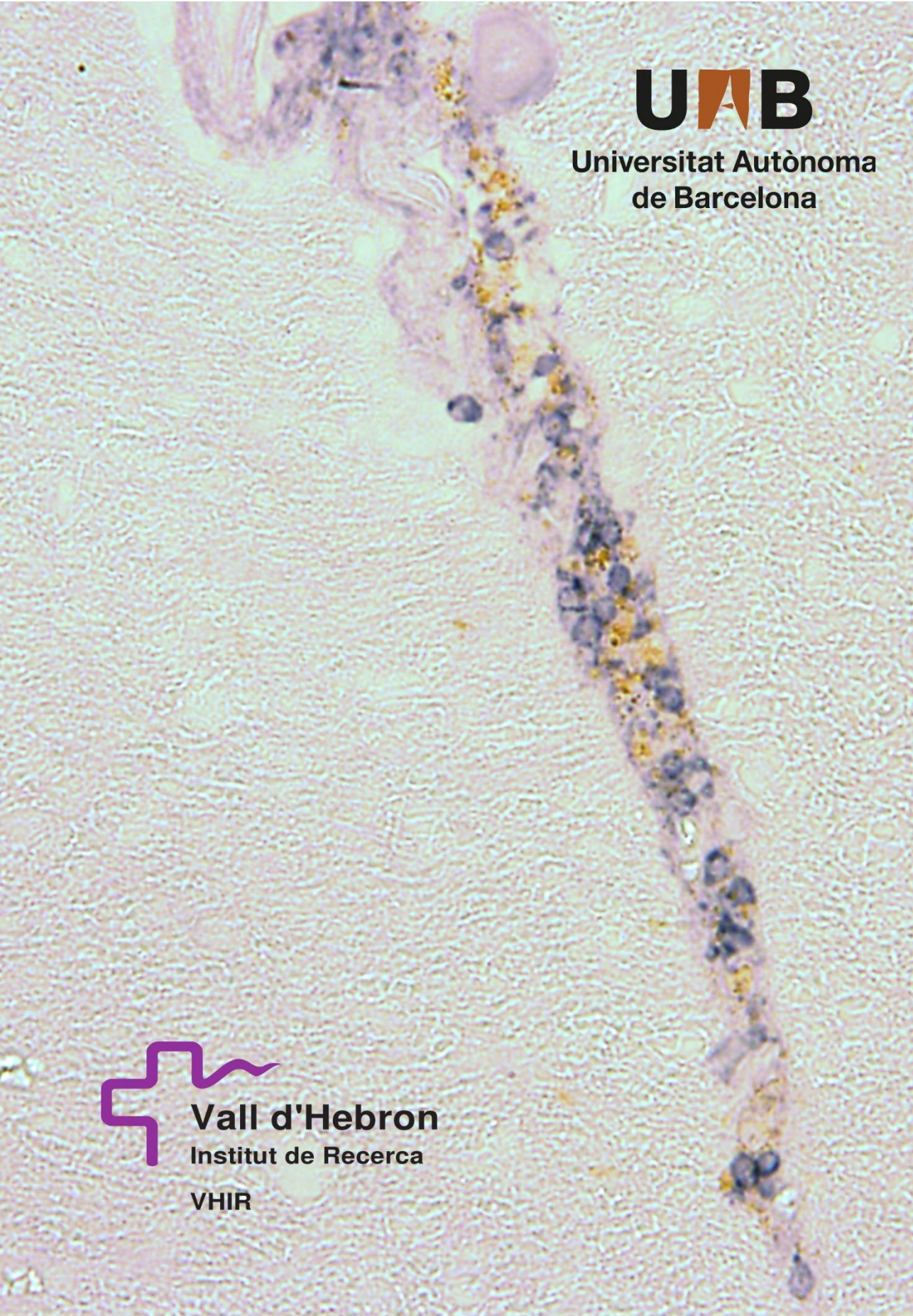

Universitat Autònoma de Barcelona

Vall d'Hebron
Institut de Recerca
VHIR